学位論文（要約）

Development of Organic Reactions in Water Utilizing Innovative Reaction Environments

（革新的反応場を活用した水中での有機反応の開発）

平成 28 年 12 月博士（理学）申請

東京大学大学院理学系研究科
化学専攻
徐　鵬宇 (XU Pengyu)

論文内容の要旨
(Abstract)

Development of Organic Reactions in Water Utilizing Innovative Reaction Environments

（革新的反応場を活用した水中での有機反応の開発）

氏名：徐　鵬宇

Introduction

Water is the most abundant liquid in the earth and it plays an important role in nurturing all the creatures. In chemistry, water, as one of solvents, is known to be safe, benign, environmentally friendly, and inexpensive compared with organic solvents. Organic reactions in water have been investigated because enzymatic reactions are carried out in water, and because unique reactivity and selectivity that are not observed in organic solvents have been found in aqueous media. On the other hand, chemists have devoted their efforts toward efficient catalysis. In particular, catalytic reactions in water have been regarded to be attractive from a viewpoint of green sustainable chemistry. Despite its usability and uniqueness, water has been rarely employed as a reaction medium due to two major obstacles. First, many catalysts may be decomposed or deactivated in water. Second, most organic substances are insoluble in water, resulting in aggregation and unfavorable side reactions in some

cases.

On the other hand, catalysts occupied a pivotal position in most of biochemical and chemical processes. An ideal catalysis is considered to possess three major factors: 1. A choice of green solvent such as water to satisfy requirements of green sustainable chemistry; 2. A dispersed and stable environment with an exquisite assemblage of all components in water that inhibits self-aggregation of organic materials; and 3. A tunable electrochemical property that produces higher reactivity and selectivity.

Here I report my efforts on constructing innovative reaction environment to overcome the disadvantages of using water as solvent, and to satisfy the requests of efficient catalysis.

1. Utilization of Insoluble Cu(II) Salts as Catalysts

Cu(II)-catalyzed enantioselective boron and silicon conjugate additions to α,β-unsaturated carbonyl compounds and α,β,γ,δ-unsaturated carbonyl compounds in water were developed. In boron conjugate addition reactions, substrate scope were further expanded with three optimized catalyst conditions: 1. Heterogeneous $Cu(OH)_2$ system, 2. Heterogeneous $Cu(OH)_2$ + AcOH system, and 3. Homogeneous $Cu(OAc)_2$ system. By choosing the suitable catalysts for each substrate, the corresponding products were obtained in good yields with excellent enantioselectivities, including both α,β-unsaturated imines and nitriles bearing either electron-donating or -withdrawing groups. In silicon conjugate addition reactions, chiral Cu(II) complexes with fixed coordination geometry from Cu(II) salts and chiral 2,2'-bipyridine **L** were prepared. After examining several conditions, it was found that acicular purplish crystals obtained from $Cu(acac)_2$ and **L** could promote the Michael addition reaction of $PhMe_2SiB(pin)$ toward chalcone in water in excellent yield with high enantioselectivity. The scope of the reaction was examined under the optimized reaction conditions. Various chalcone derivatives reacted smoothly with $PhMe_2SiB(pin)$ to afford the desired products in high yields with high enantioselectivities. The silyl group could be transferred to a crowded position to generate a quaternary carbon center bearing a C–Si bond. Cyclic ketones were also applicable without significant loss of enantioselectivity. Similarly, nitroolefins, acyclic α,β-unsaturated esters, lactones, and nitriles were also reacted with $PhMe_2SiB(pin)$ in a highly stereoselective manner. It is noted that in both borylation and silylation reactions, δ-addition products

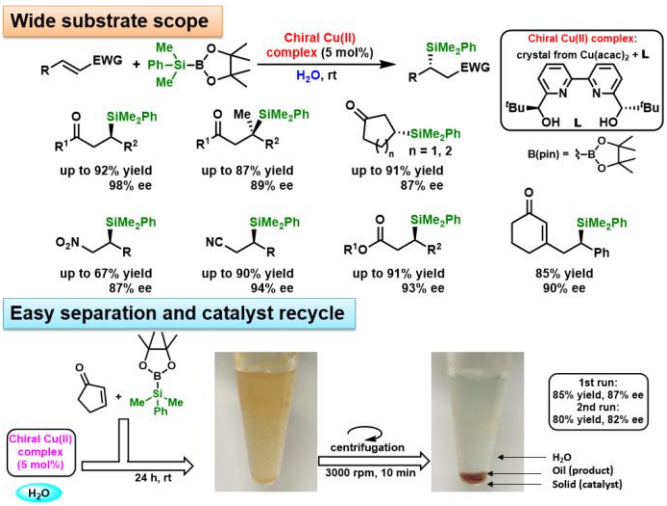

Figure 1. Cu(II)-catalyzed enantioselective silicon conjugate additions

were obtained exclusively when cyclic α,β,γ,δ-unsaturated carbonyl compounds were employed. The catalyst was also applicable to a gram-scale reaction without any loss of enantioselectivity. Catalyst reusability was also evaluated in the reaction of cyclopentenone with $PhMe_2SiB(pin)$. It was found that after the completion of the reaction, the separation of the product from the crude mixture and catalyst reuse were achieved through centrifugation (Figure. 1).

These results exhibited that the solubilities of neither catalysts nor reactants were necessary toward high yield and enantioselectivity. The approach is also in line with the concepts of green sustainable chemistry because it leads to reduction in the amount of organic solvents used and is amenable to catalyst recovery and reuse.

2. Asymmetric Lewis Acid –Single-walled Carbon Nanotube Integrated Catalysts

5 年以内に雑誌等で刊行予定のため非公開

3. Development of New Light-induced Catalysts and Its Application toward Hydration Reactions in Water

5 年以内に雑誌等で刊行予定のため非公開

Conclusion

During my PhD course, several new catalysts were designed. These discoveries, improvement of various Lewis acid catalysts and their applications to several reactions are believed to open new opportunities in the development of designed catalysis in water.

Contents

Acronyms and Abbreviations 6

Chapter 0. General Introduction 7

0-1 The Water 7

0-2 Organic Chemistry in Water - Development of Lewis Acid Catalysts in Water as an Example 19

0-3 The Prospect 28

References 29

Chapter 1. Utilization of Insoluble Cu(II) Salts as Catalysts 35

1-1 Introduction 35

1-2 Optimization of Reaction Conditions 44

1-3 Effect of Water 47

1-4 Effects of Copper Salts 48

1-5 Substrate Scope 53

1-6 Conjugate Additions to Unsaturated Di- and Trienones 63

1-7 Catalyst Recycle 67

1-8 Mechanism Elucidation 68

1-9 Conclusion 82

References 83

Chapter 2. Lewis Acid-Single Walled Carbon Nanotube Integrated Catalysts 87

5 年以内に雑誌等で刊行予定のため非公開

Chapter 3. Development of New Light-Induced Catalysts and Their Application Toward Hydration Reactions in Water 88

5 年以内に雑誌等で刊行予定のため非公開

Recapitulation 90

Experimental Section 92

General 92

Chapter 1: Utilization of Insoluble Cu(II) salts as Catalysts 94

Chapter 2: Lewis Acid –Single-Walled Carbon Nanotube Integrated Catalysts 167

Chapter 3: Development of New Light-Induced Catalysts and Their Application Toward Hydration Reactions in Water 168

Acknowledgement 169

Acronyms and Abbreviations

In order to avoid redundancy, several acronyms and abbreviations are defined as below:

Acronyms & Abbreviations	Full spelling	Structures
AS	Anionic surfactant	$C_xH_yOSO_z^-$
DS	Dodecyl sulfate (lauryl sulfate)	$C_{12}H_{25}OSO_3^-$
LS	Lauryl sulfonate	$C_{12}H_{25}OSO_2^-$
C_N-US	Sulfate surfactant with carbon number N	$C_NH_{2N+1}OSO_3^-$
C_N-OS	Sulfonate surfactant with carbon number N	$C_NH_{2N+1}OSO_2^-$
LO-type	Long-sulfonate type LASC-SWNT	
SO-type	Short-sulfonate type LASC-SWNT	
LU-type	Long-sulfate type LASC-SWNT	
SU-type	Short-sulfate type LASC-SWNT	
N.D.	Not determined	
N.R.	No reaction	
N.T.	Not tried	
SDS	Sodium dodecyl sulfate	$C_{12}H_{25}OSO_3Na$

Chapter 0. General Introduction

"You cannot take away any feature of water without destroying life"

Stoneham, M., *Philos. Trans. R. Soc. Lond. B*, 2004.

0-1 The Water

Water is one of the most crucial factors in nurturing all the life on this planet. NASA even sets the existence of water as guideline for the alien life search.[1] Water seems to be unique compared with other liquid. However, when looking at single water molecule, it really has no peculiar properties despite it being very small (hard sphere diameter 2.75 Å, *c.f.* Ne; 2.79 Å).[2] On the other hand, water as a bulk liquid, contains three-dimensional networks of hydrogen bonding (H-bonding), leading to many unusual properties. Indeed, each of these properties can be observed in other liquid. But no solvent except for water incorporates all of them, which makes bulk water peerless. The significance of these properties for supporting life processes has been intensively investigated, though our understanding toward water is still far from complete.

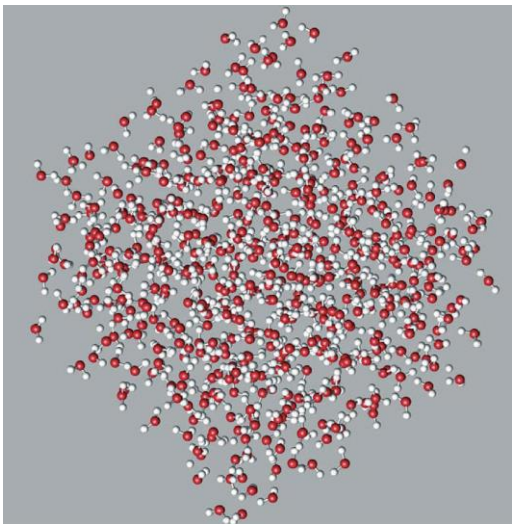

Figure 0.1. A snapshot of liquid water at 298K (Reprinted with permission from Finney, J. L. *Philos. Trans. R. Soc. Lond. B* 2004, *359*, 1145–1165. Copyright 2004, The Royal Society).[2]

In the following sections, I would summarize the properties of liquid water that are adequate and useful for rationalizing the kinetics and thermodynamics of organic reactions in water.

0-1-1 Molecular Water

In a H_2O molecule, the length of O-H bond is 0.9572 Å and the average H-O-H bond angle is 104.52°. The hard sphere diameter of H_2O molecule is only 2.75 Å, which is even smaller than that of Neon (2.79 Å). The tiny size of water molecule plays an imperative role in the hydration (*vide infra*). The structure of single water molecule is shown as below:

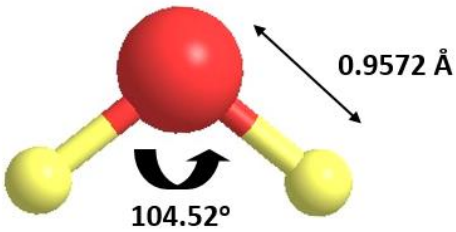

Figure 0.2. The average geometry of the water molecule.

Classically, H_2O molecule is considered to have two positive-charged centers located near the hydrogen nuclei, and two negative-charged regions centered on the electron lone pairs, depicting a tetrahedral symmetry. However, such view is probably an oversimplification.[3] Indeed, in small molecules, not only dipole moment which is only the first term in the multipole expansion, but higher terms in the expansion of the charge distribution such as quadrupole moment is obviously ineligible when considering their polarizability. High-quality molecular dynamics (MD) simulations have revealed that the charge distribution might be more realistically a trigonal structure rather than tetrahedral as shown in Figure 0.3.[4]

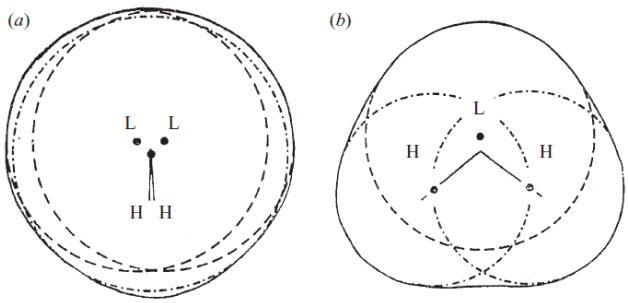

Figure 0.3. Centers of charge in the isolated water molecule through calculation (Reprinted with permission from Finney, J. L. *Philos. Trans. R. Soc. Lond. B* 2004, *359*, 1145–1165. Copyright 2004, The Royal Society).[2] (*a*) Normal to and (*b*) parallel to the HOH plane. The outer solid circles approximate to the outline of the molecule. The dashed lines are centered on the negative (L) charges and dash–dot circles are centered on the positive (H) charge.

In summary, an isolated water molecule is predicted to have, and indeed possesses no exceptional properties compared with the other organic solvents,[2] "*it is apparently an unremarkable*

small molecule". However, on the macroscopic scale, there is a completely different story (Table 0.1).

Table 0.1. Selected properties of bulk and molecular water.[5]

Property	Bulk	Molecular
Density ($g \cdot cm^{-3}$)	1.00	0.97
Specific heat ($kcal \cdot kg^{-1} \cdot {}^{o}C^{-1}$)	1.00	1.25 ± 0.05
Thermal expansion coefficient ($^{o}C^{-1}$)	250 x 10^{-6} (25°C)	(300-700)x 10^{-6}
(Adiabatic) compressibility coefficient (atm^{-1})	45 x 10^{-6}	(60-100)x 10^{-6}
Heat conductivity ($cal \cdot s^{-1}$)	0.0014	~0.01-0.05
Viscosity (cP)	0.089	2-10
Energy of activation ionic conduction ($kcal \cdot mol^{-1}$)	~4	5-8
Dielectric relaxation frequency (Hz)	19 x 109	2 x 109

It is noted that the number of H_2O molecules within the reaction centers of organic reactions in water and within active site of the protein is quite limited (There are only about 5-6 water molecules between protein surfaces).[6] The limited number as well as their restricted translational and rotational freedom made the behaviors of involved H_2O molecules quite different from the bulk water.[7] Therefore, when discussing the effects of water on organic reactions, a careful consideration is required to distinguish the bulk water and the molecular water. The detailed properties of bulk water are discussed in the following section.

0-1-2 Hydrogen Bonding in Liquid Water

It is widely known that water molecules are strongly ensnarled each other through hydrogen bonding. Liquid water constitutes a three-dimensional (3D) network, affording localized H_2O clusters.[8] Therefore, the microphobic liquid structure is mainly determined by intermolecular and directional hydrogen bondings, but not a simple hard-core repulsion. The average strength of hydrogen bonding is approximately 20 kJ/mol. The 3D hydrogen bonding network of water would lead to many unusual natures of water, including high specific heat capacity, the fact that highest density is observed at 4 °C and so on.[9] The properties of the 3D hydrogen bonding network of water are also at the heart of hydrophobic interaction, which is particularly associated with organic chemistry in water. Yet there are a lot of controversy on the sizes and preferable structures of the H_2O clusters which are considered to be a crucial factor in both chemistry and biochemistry.[10]

Advanced neutron diffraction measurements revealed the actual 3D hydrogen bonding network structure is quite chaotic.[11] Apart from the four-coordinating structure of H_2O molecule, trigonal coordinative H_2O molecules possess a dominant role in the network, consistent with the simulated electron density distribution of water. Interestingly, the presence of bifurcated, threefold hydrogen

bonding interactions have been proposed in early studies, suggesting the existence of H_2O molecules with five neighboring H_2O molecules (Figure 0.4). It was confirmed both computationally[12] and experimentally[13] through Raman scattering measurements. This special hydrogen bonding is considered as 'defect' in the network, offering the hopping ability of protons that would explain the anomalously high diffusion rate observed in liquid water.[14] Through the decreasing Gibbs energy of the whole network, each individual of H-O-H angle can be rather easily distorted, affording a significant amount of five-, six-, seven-, and even eightfold rings with three-coordinated structures (Figure 0.5).

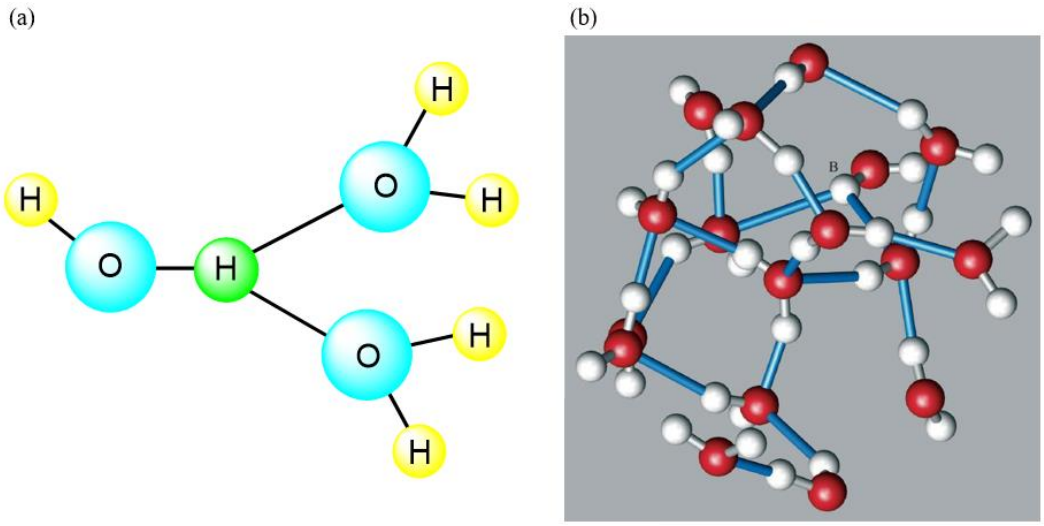

Figure 0.4. Bifurcated, threefold hydrogen bonding interactions (Reprinted and modified with permission from Finney, J. L. *Philos. Trans. R. Soc. Lond. B* 2004, *359*, 1145–1165. Copyright 2004, The Royal Society).[2] (a) A simplified view of bifurcated, threefold hydrogen bonding; (b) Monte Carlo simulation results indicating the existence of bifurcated, threefold hydrogen bonding (Position B).

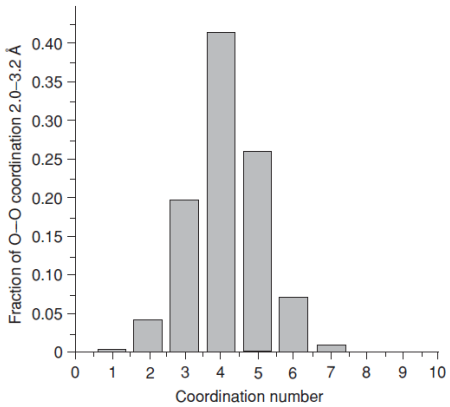

Figure 0.5. Graph of the coordination number vs the fraction of O-O coordination 2.0–3.2 Å (Reprinted with permission from Finney, J. L. *Philos. Trans. R. Soc. Lond. B* 2004, *359*, 1145–1165. Copyright 2004, The Royal Society).[2]

It is important to recognize that due to large amount of intermolecular interactions between H_2O molecules, each H_2O molecule in the liquid water experiences a substantial fluctuating electric field from neighbors, leading to an interactive self-enhancement of the dipole moment.[15] Computer simulation indicated that the distribution of dipole moments in liquid water ranges from ca. 2 D to ca. 4 D, which is significant compared with isolated molecule value of 1.85 D.[16]

Despite its strong mutual interactions, the hydrogen bonding network is also found highly dynamic; it takes *ca.* 2ps[17] for water molecule to reorientate and *ca.* 7ps[18] to move over one molecular distance. Considering the typical hydrogen bonding energy is ca. 20 kJ/mol, which is equivalent to only $10kT_{room}$, it seems that the amputation of the hydrogen bonding is not involved, resulting a corporative motions of water clusters in liquid water.[19]

To understand reactivity and selectivity on organic reactions in water, the behaviors of water molecules and the hydrogen bonding surrounding both the reactants and the activated species are of great importance.

0-1-3 Properties of Liquid Water

The kinetic data correlated with solvent parameters are often used to understand solvent effects on organic reactions. Although this approach cannot distinguish solvent effects of reactants from those of activated states, it still affords many convenient insights into kinetic and thermodynamic factors, which are intricate for computational studies to be characterized. Several representative parameters of water are summarized (Table 0.2). Parameters of four characteristic organic solvents were also listed for comparison.

Table 0.2. Selected solvent properties.[20]

Solvent	ε_r	μ	E_T^N	CED	π	γ
^{n}Hexane	1.88	0.00	0.009	225	239	17.9
Et_2O	4.20	1.14	0.117	251	264	20.1
MeCN	35.94	3.54	0.460	590	379	19.1
EtOH	24.55	1.74	0.654	703	291	22.4
H_2O	78.30	1.8[a] 2.8[b]	1.000	2302	151	72.9

[a] Value of molecular water. [b] Value of bulk water.

■ *Dielectric Constant (ε_r)*

The dielectric constant of a solvent (ε_r) is one of the most common macroscopic parameters to identify the polarity of mediums and it controls ionic dissociation of salts. Water possesses a high dielectric constant, making itself a highly polar solvent. However, the dielectric constant is not a

reliable parameter in water-organic solvent mixture solvent due to its inability to reflect the solute-water interactions.[21]

It is noted that the polarity of water decreases with temperature and/or pressure increasing due to the break-down of hydrogen bonding network. The successful synthesis of benzimidazole at 350 °C and 20.9 MPa can in part attribute to the improved solubility of organic compounds in water (Table 0.3).[22]

Table 0.3. Synthesis of benzimidazoles in water.[22]

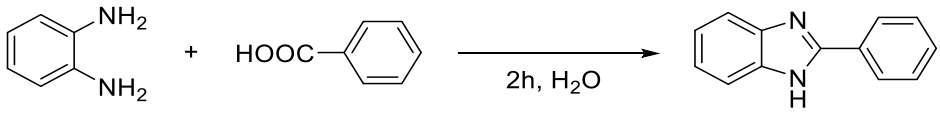

Entry	Temperature (°C)	Pressure (MPa)	Yield (%)
1	100	0.1	0
2	200	1.7	18
3	350	17.8	71
4[a]	350	20.9	91

[a] stirred for 14 h.

■ *Dipole Moment (μ)*

Dipole moment can be obtained through the measurement of the dielectric constant. For a neutral molecule with an asymmetric charge distribution, the dipole moment is described as below

$$\mu = q \cdot l$$

where q is the magnitude of charges and l is the distance of charge separation. The small difference of dipole moment between a water molecule (1.8) and ethanol (1.74) shows the ethyl group contributes little to charge separation. Also as discussed in 0-1-1 , dipole moment is not enough to discuss the charge distribution of small molecules.

■ *Solvatochromic Solvent Parameters (E_T^N)*

As microscopic, empirical polarity parameters, several solvatochromic solvent parameters provide an alternative and more attractive approach to identify the polarity of a solvent due to unsatisfactory correlation between relative permittivities and dipole moments. Among these solvatochromic solvent parameters, Reichardt's $E_T(30)$ is one of the most successful parameters. $E_T(30)$ is based on the theory that the longest wavelength UV/vis absorption band of the betaine dye pyridinium-*N*-phenoxide[23] exhibits highly solvatochromic behavior.[22] The value is defined as below.

$$E_T(30) = hcvN_A = 2.859 \times 10^{-3} \times v \quad \text{kcal/mol} = 1.196 \times 10^{-2} \times v \quad \text{kJ/mol}$$

Due to the limited solubility of betaine dye in water, $E_T(30)$ value of water cannot be directly obtained. Therefore in later years, Reichardt *et al*. then developed the normalized E_T^N values as shown below:

$$\mathrm{E_T^N} = \frac{[E_T(\text{solvent}) - E_T(\text{TMS})]}{[E_T(\text{water}) - E_T(\text{TMS})]} = \frac{[E_T(\text{solvent}) - 30]}{32.4}$$

in which water (E_T^N = 1.00) and tetramethylsilane (E_T^N = 0) were defined as extreme reference solvents.[24]

Although $E_T(30)$ is measurable and therefore more adequate and practical, several drawbacks still exist. For example, $E_T(30)$ cannot be measured in acidic condition due to the disruption of the long-wavelength solvatochromic absorption of the dye.

■ *Cohesive Energy Density*

The cohesive energy density (CED, in MPa = 1 J·cm^{-3}) is a measure of energy required to completely remove unit volume of molecules from their neighbors to infinite separation (an ideal gas) and is defined as below:

$$\mathrm{CED} = \frac{\Delta \mathrm{U_v}}{\mathrm{V_m}} = \frac{[\Delta \mathrm{H_v} - \mathrm{RT}]}{\mathrm{V_m}}$$

in which ΔU_v is the energy of vaporization and ΔH_v is the enthalpy of vaporization of the solvent. V_m represents the molar volume of the solvent. Compared with other organic solvent, water possesses an extremely high CED value, which is consistent with the strong 3D hydrogen bonding interactions in liquid water.[27]

■ *Internal Pressure*

The internal pressure is a measure of how the internal energy of a system changes upon a tiny isothermal volume expansion at constant temperature:

$$\pi = \left[\frac{\partial U}{\partial T_m}\right]_{\mathrm{T}}$$

where U is the molar internal energy.[25] The value could also be approximated into

$$\pi = \frac{\alpha T}{\beta}$$

in which α stands for the thermal expansion coefficient and β stands for the isothermal compressibility of the liquid.[26] It is noted that the internal pressure does not represent a complete disruption of all intermolecular interactions in the solvent. It mainly responds to the collapse of London dispersion and dipole-dipole interactions, while the CED responds to the amputation of hydrogen bondings. The difference between the CED value and the internal pressure can be taken to be the strength of hydrogen bonding. The fact that water possesses an extremely high CED value and a low internal

pressure value can validate the powerful hydrogen bonding in liquid water.[27]

■ *Surface Tension*

The surface tension represents the internal cohesive forces within a solvent. It is defined as

$$\gamma = \frac{\partial \omega}{\partial \sigma}$$

in which $\partial \omega$ represents an energy increment enough to change the surface area and $\partial \sigma$ represents an increment of surface area. Hydrogen bonding is responsible for a quite high surface tension of water and it tends to expose much less surface area to air compared with most of the organic solvents. Interestingly, though both salting-in and salting-out ions could further enhance the surface tension of aqueous solution, they exhibited opposite tendency on cavity formation. While salting-in ions such as $LiClO_4$ and SDS directly hydrate the hydrophobic compounds through the increased Gibbs energy of solvation, salting-out ions such as LiCl increase the size of cavity in water due to electrostriction caused by increased Gibbs energy of cavitation. Therefore, the utilization of SDS to solubilize hydrophobic organic compounds does not necessarily involve the destruction of massive hydrogen bonding in water. Meanwhile, addition of organic solvents would decrease the surface tension of the mixed solvent significantly, leading to surface/interfaces with much weaker hydrogen bonding.

■ *H_2O and D_2O*

Kinetic Isotope Effects (KIEs, k_H/k_D) furnish important information to understand organic reactions. Aside from the KIE experiments which mainly rely on the mass difference between H and D, thereby affecting the activation energy of the reactions, H_2O and D_2O possess far more numbers of different properties other than weights (Table 0.4).[22a]

Table 0.4. Properties of H_2O and D_2O.[22a]

Property	H_2O	D_2O
Molecular mass ($g \cdot mol^{-1}$)	18.015	20.028
Melting point (°C)	0.00	3.81
Boiling point (°C)	100.00	101.42
Temperature of maximum density (°C)	3.98	11.23
Density ($g \cdot cm^{-3}$)	0.9970	1.1045
Molar volume ($cm^3 \cdot mol^{-1}$)	18.069	18.133
Viscosity (Pa·s)	8.9×10^{-4}	11.0×10^{-4}
Heat of vaporization ($kJ \cdot mol^{-1}$)	44.04	45.46
CED ($J \cdot cm^{-3}$)	2365	2297
Dipole moment (D)	1.83	1.84
Ionization constant ($mol \cdot L^{-1}$)	1.81×10^{-16}	0.354×10^{-16}

While several differences such as the dipole moment and boiling point are insignificant, the other differences including the temperature of maximum density, viscosity, and even the molar volume, could result in substantial outcomes in organic reactions. The lower ionization constant of D_2O suggested its stronger intermolecular association than H_2O, which is consistent with the higher value of [ced-π] of D_2O.[28] Also, larger void volume of D_2O leads to more favorable cavity formation, affording slightly improved solubility of noble gases and organic compounds in D_2O.[29]

■ *The Self-Dissociation of Water*

Water is amphoteric. Its ionization constant is 14.004 at 298.15 K and 1 atm, affording a quite low concentration of both proton and hydroxide.[30] Several data are given as below:

Table 0.5. Several data involving the self-dissociation of water.

Standard enthalpy[31]	Heat capacity[32]	Standard volume[33]
55.81 kJ/mol	-215 J/K	-20 cm^3/mol

Recent ultrafast mid-infrared spectroscopic measurements suggested that the first step of the self-dissociation of water undergoes an excited vibrational state of the O-H bond with v = 2 probably.[34] Both proton (36.23) and hydroxide ion (20.64) possess high ionic mobilities (unit: 10^{-4} $cm^2/s{\cdot}V$) in water (Na^+: 5.19, Cl^-: 7.19).[35] The high mobility of proton is well studied and attributes to hopping protons along arrays of hydrogen bondings instead of the actual movement of single protons (Grotthuss mechanism).[36] The high proton mobility is important in enzymatic reactions for transferring protons to their active sites. In organic chemistry in water, the proton mobility is also a crucial point especially for acid-base-mediated reactions.

On the other hand, the high mobility of hydroxide ions received much less attention. Similar hopping mechanisms were also proposed for hydroxide mobility. However, recent computational simulations suggest the formation of specific hydrated complexes through nuclear quantum effects.[37]

0-1-4 Hydration

■ *Ion Hydration*

The hydration of ions has been intensively studied over the last decades.[38] The smallness of the water molecule enables itself to approach the interaction sites of both cations and anions with more than one molecule. The strong hydration of ions has immediate and significant influence on the reactions in water. For example, in a S_N2 process in water, hydrated water molecules coordinating to anionic nucleophiles have to be mostly sifted out to afford the new covalent bond, therefore the Gibbs energy of transition state is strongly determined by the dehydration effect.

Neutron scattering is utilized to evaluate the structure of hydration shells. Two hydration spheres, the primary hydration sphere (PHS) and the secondary hydration sphere (SHS) are generally taken into consideration. In PHS, the strong electrostatic attraction is the main interaction between H_2O molecules and ion center. Together with the strong hydrogen bonding, up to 16 H_2O molecules in PHS are normally positioned in a well-defined structure, which can be observed through X-ray analysis. H_2O molecules in SHS, which are also experiencing dipole polarization effect from the ion center, are mainly bonded toward PHS through hydrogen bonding.

As anticipated, both contact and water-separated ion-pair formations do not occur easily in water and the ion-pair association constants are usually small (ca. 1~10). Two types of ions are normally defined in water: (1) small salting-out ions which have higher charge density (kosmotropes) and stronger ion-water interactions than water-water interactions, thereby decreasing the solubility of apolar solutes and strengthening the hydrophobic interactions; and (2) large salting-in ions which have lower charge density (chaotropes) and weaker ion-water interactions than water-water interactions, thereby increasing the solubility of apolar solutes and weakening the hydrophobic interactions.[39] A series of ordered ions that are able to salt out or salt in proteins is called the Hofmeister series or lyotropic series.[40]

The hydration spheres of 'hydrophobic ions' such as $(C_nH_{2n+1})_4N^+$ have gained prominence.[41] Due to the existence of apolar groups, the ion center is inhibited from the direct interaction with water, resulting in much weaker hydration ability. Computational studies on Me_4N^+-Cl^- demonstrated that the interaction between cation center and water molecule is mainly based on London dispersion. Unlike the Cl^-, Me_4N^+ ion behaves as a hydrophobic solute. Similar phenomena are expected in aqueous cationic surfactant system as well, where anionic surfactant behaves as hydrophobic solutes rather than as hydrated anions.

■ *Hydration of Apolar Compounds*

It is well known that oil and water does not mix and traditionally, apolar compounds is called hydrophobic in water.[42] The reason of the limited solubility of apolar molecules has been intensively studied through thermodynamics.

Indeed, all Gibbs energies of hydration of both hydrocarbons and noble gases are positive. It is noted that ΔG_{tr} decreases when the size of noble gas increases, while hydrocarbons do in an opposite manner. It should be emphasized that even though none of these molecules can participate in the hydrogen bonding in water, the ΔH_{tr} of water is more favorable than those of organic solvents, making theΔH_{tr} value of water negative. One of the explanation is that the apolar surface area is covered by several water molecules through London dispersion interactions, avoiding the direct interactions between apolar solute and outside bulk water. Since the transfer from gas phase to liquid phase is highly unfavorable, all ΔS_{tr} values are highly negative.[43] Therefore, as noted by Haymet *et al.*, 'hydrophobicity is entropic in cold water and enthalpy in hot water'.[44]

On the other hand, most of the organic molecules have one or more hydrophilic functional groups that can interact with the water in PHS, decreasing the overall hydrophobicity and even leading to 'dissolution'.[45] Moreover, although both aromatic group and aliphatic group are hydrophobic, their thermodynamic hydration parameters are quite different. The thermodynamic data comparison between benzene and toluene revealed a definite tendency of hydrogen bonding interactions of the H_2O molecules on the π-electron system of the aromatic compounds (Table 0.6).[46] A recent theoretical study rationalized the quadrupole moment of benzene affected the interactions between π-structures and water.[47]

Table 0.6. Thermodynamic hydration parameters of benzene and toluene.[46]

Property	ΔH^o (kJ/mol)	ΔS^o (J/K·mol)	ΔG^o (kJ/mol)
Benzene	-29.6	-87.2	-3.6
Toluene	-33.9	-101.4	-3.7

■ *Hydrolysis of metal ions*

Hydrolysis is an important component when treating metal ions in water. The hydrolysis of a metal ion is not only dependent on its physical properties including ionic charges and ionic radius, but also affected by the surrounding water environment such as its concentration, the hydrogen bonding strength and the pH value. Indeed, the tendency of hydrolysis of a metal cations is in inverse with their concentration.

Hydrolysis of a metal ion can be understood as a loss of proton(s) from the solvation shell, which is mainly determined by the thermodynamic stabilization of proton(s) when hydrated with another water molecule.[48] When the surrounding water molecules are insufficient, the hydration of proton then becomes thermodynamically unfavorable to suppress hydrolysis of metal ions. Recent calculation studies even revealed that the surrounding water molecules supplied hydrogen bonding to stabilize the hydrolyzed metal cation species in water.[49] The polarization of adjacent cluster water molecules enhances the stability of metal cations in M•••OH species and OH^- groups are stabilized through hydrogen bonding. When isolated water molecules were taken into consideration, these interactions became notably weaker. Moreover, large differences were observed between isolated and clustered hydrogen bonding in the coordination geometry.

0-1-5 Hydrophobic Interactions

In the section of 0-1-4 Hydration, how the formation of hydrophobic hydration spheres would help the dissolution of apolar compounds in water has been discussed. In this section, the hydrophobic interactions in water are focused on. Indeed, hydrophobic interactions are one of the most significant

non-covalent interactions. In biochemistry, the hydrophobic interactions are key to protein folding,[50] the formation of enzyme-substrate,[51] enzyme-inhibitor complexes,[52] and the formation and function of cell membranes,[53] etc. In chemical society and especially in industry, hydrophobic interactions also contribute to detergency,[54] coagulation,[55] and mineral flotation[56] and so on.

The hydrophobicity of water derives from the small size of water, leading to massive entropic cost to create a cavity for solute.

In organic chemistry, recent studies revealed that, unlike the case of aliphatic molecules, enthalpy effects rather than entropy effects dominate hydrophobic interactions between aromatic molecules. Indeed, London dispersion interactions play a much more significant role by involving the polarizable π electrons of aromatic solutes. Recent Monte Carlo simulations also indicated two types of hydrophobic interactions in water: (1) direct contact hydrophobic interaction, and (2) pairwise hydrophobic interactions that form a complex apart from a single water layer.[57] Large solutes prefer the direct contact hydrophobic interaction while smaller solutes tend to form water-separated dimers.

It should be emphasized that hydrophobic interactions do not necessarily involve the precipitation. Depending on the nature of the hydrophobic molecules, three types of non-precipitated hydrophobic interactions can be classified: (1) pairwise interactions, (2) movable small aggregations (e.g. hydrotropes), and (3) movable large aggregations (e.g. micelles or vesicles).[57] Of course with increased concentration and/or size of solutes, the hydrophobic hydration shells of aggregates begin to largely overlap at critical concentration, leading to breakdown of a large amount of hydrogen bondings. As a result, driven by the entropy gain that comes from the release of water from the hydration shell to bulk water environment and the van der Waals interactions due to the contact between the two apolar molecules, immediate precipitation of bulk apolar compounds (phase separation) occurs.[46]

Another significant effects of hydrophobic interactions on organic reactions in water are the ‘enforced’ hydrophobic interactions.[58] Normally, the reaction in liquid phase is much slower than in gas phase due to the close contact between molecules. The close contact leads to a small diffusion rate of the reactants and more importantly, a mutual orbital overlap, which needs partial desolvation before contacts (reactions). In terms of Gibbs energies, the desolvation is costly in all solvents. However in water, hydrophobic interactions make the molecules contact under a more favorable thermodynamics, leading to rate enhancements compared with the reaction in organic solvents.

0-2 Organic Chemistry in Water - Development of Lewis Acid Catalysts in Water as an Example

In organic chemistry, water has two different destinies in synthetic organic chemistry and physical organic chemistry. In physical organic chemistry, water is one of the favorable solvents especially in reaction mechanistic studies.[39] The high dielectric constant of water inhibits kinetic complexities through ion pair formation and more importantly, many mechanistic parameters (pKa, substituent constants, etc) are available for water as the solvent. On the contrary, in synthetic organic chemistry, water was rarely welcome as the solvent due to (1) stability issue which may de-functionalize many catalysts, and (2) solubility issue which may cause the aggregation and unfavorable side-reactions of organic reactants.

0-2-1 Organic Reactions in Water

Organic reactions in water are predicated on the quest for the deep comprehension toward the role of water in biochemistry. It has been revealed over 60 years that the hydrophobic effect in water was always the dominant power; substrate binding with enzyme pocket, the association of antibodies with antigens, and protein folding.[59] However, the detail of hydrophobic interactions remained controversial and the earliest studies on organic chemistry in water were mainly focused on the enzyme models and mimics in aqueous medium.[60]

Studies on behavior of cyclodextrin structures in water are one of the pioneer examples.[61] Water has been identified as the *only* solvent that could bind small hydrophobic molecules into the cavity of macrocyclic rings composed of glucose units, the α-, β-, and γ-cyclodextrins. Taken cyclodextrins as components of artificial enzymes, Breslow *et al.* were inspired to examine organic reactions within cyclodextrin structures in water.[62] It was revealed that in the chlorination of anisole by HOCl in water, *para*- and *ortho*-chlorinated products were obtained in mixture without the addition of cyclodextrin, while when 9 mM α-cyclodextrin (cyclohexaamylose) was added, *para*-chloroanisole was obtained as a major product. Kinetic studies exhibited the para position became 5.3 times more reactive within the cyclodextrin complex than in homogeneous solution. Interestingly, the chemical kinetics revealed the chlorination process as a second-order reaction in water while it was a first-order reaction within the cyclodextrin structure in water. This result suggested that the binding of anisole with cyclodextrins not only blocked the *ortho* positions, but it also accelerated the chlorination through the formation of cyclodextrin-hypochlorite intermediate, making the *para* position accessible to reaction (Figure 0.6).[63] Successive studies involved the utilization of cyclodextrin dimers, the integration of metal ions with cyclodextrin catalysts, and extended applications on other reactions.[64] Further enzyme-mimiced catalysts such as ribonuclease mimics,[65] transaminase mimics,[66] cytochrome P-450

mimics,[67] have stimulated the development of organic reactions in water in the early stages and significantly deepened our knowledge on the effect of hydrophobic interactions.

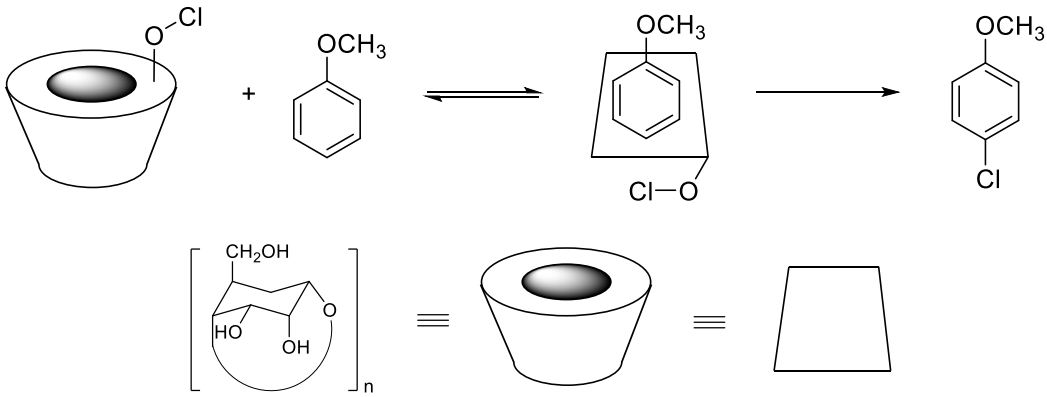

Figure 0.6. Selective chlorination of anisole catalyzed by cyclodextrins in water.[62]

It was also found that the hydrophobic interactions in water could show significant selectivity and rate effects on reactions in water.[68] Diels-Alder reaction is one of typical examples. Diels-Alder reaction is thought not to be sensitive to solvents when considering the reaction mechanism. Indeed, the observed small solvent effects in organic solvents do support. Yet Breslow *et al.* reported the rate-accelerations of Diels-Alder reactions in water despite no diene-dienophile macrophobic aggregation (Table 0.7).[69]

Table 0.7. Rate acceleration observed in Diels-Alder reaction in water.[69]

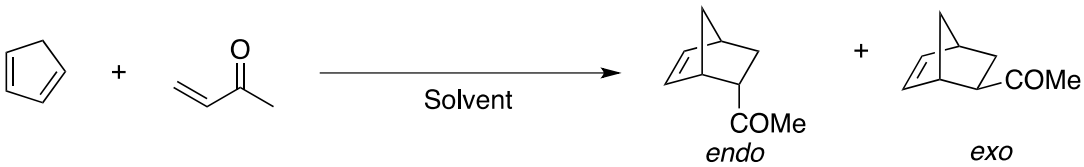

Solvent	10^5 k_2 (M^{-1} s^{-1})
Isooctane	5.94
MeCN	15.2
MeOH	75.5
H_2O	**4400**
LiCl in H_2O (4.86 M)	**10800**
$(NH_2)_3CCl$ in H_2O (4.86 M)	4300

The authors said the addition of salting-out ions (LiCl) further enhanced the hydrophobic interactions and thereby accelerated the reaction while the addition of salting-in ions ($(NH_2)_3CCl$) resulted in slightly decreased reaction rate. The detail of these correlations between hydrophobic

interactions and salting-in/out ions has been investigated computationally and was found in good accordance with experimental results.[70]

Hydrophobic interactions also influence the conformational preferences of organic compounds in water. For example, *n*-butane usually preferred *trans* conformation in gas phase or in organic solvent while in water, it prefers more compact *gauche* conformation.[71] Another example is Diels-Alder reactions, which also exhibited a significantly enhanced *endo/exo* ratio in water (Table 0.8). Considering the solubility of CpH in water (ca. 0.01 M),[72] stronger preference toward *endo*-product was observed along with the rate acceleration when the reactants were distributed homogeneously in the solution.

Table 0.8. Enhanced endo/exo ratio observed in Diels-Alder reaction.[72]

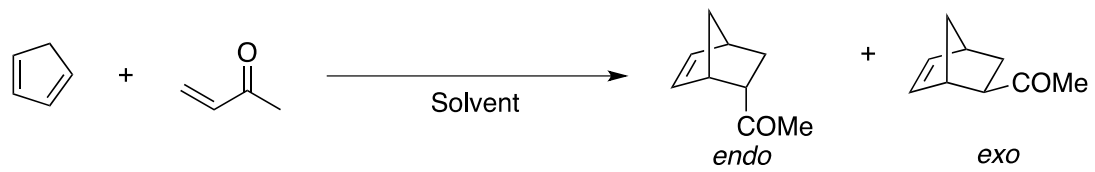

Solvent	*endo/exo*
Cyclopentadiene	3.85
EtOH	8.5
0.15 M CpH in **H_2O**	21.4
0.007 M CpH in **H_2O**	**22.5**

Table 0.9. Effect of hydrophobic interactions on regioselective reduction in water.[73]

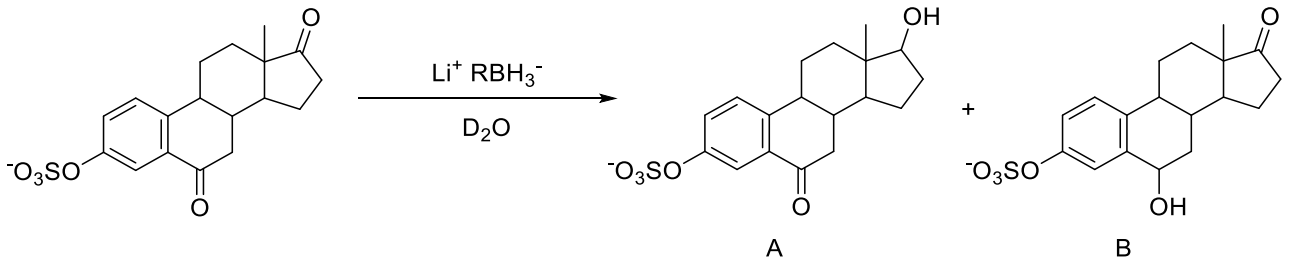

R	A:B ratio	
	D_2O	4M LiCl in D_2O
H	13:87	14:86
Ph	60:40	69:31
C_6F_5	78:22	85:15

Regioselective reduction also exemplifies the effects of hydrophobic interactions between reactants (Table 0.9). The increasing hydrophobicity of reducing agents makes reaction point more hydrophobic to afford A as a major product, while the naked BH_4^- ion is used, B is obtained as a major

product. Similarly, the salting-out ions can further enhance the hydrophobic interactions, affording even higher A/B ratio.[73]

Although the quantification of hydrophobic interactions on molecules with both apolar and polar functional groups remains difficult, when conducting organic reactions in water, hydrophobic interactions should be taken into consideration on the reactivities and selectivities.

0-2-2 Lewis Acid Catalysis in Water

■ *Water-Compatible Lewis Acid Catalysts*

Lewis acid catalysis is one of the most useful methods in modern organic synthesis. Lewis acid catalyst could act as an electron pair acceptor and form a complexation with a lone-pair of electronegative atoms in the substrate. It could activate the substrates with enhanced nucleophilicity and/or electrophile activity. Numerous examples have demonstrated that sufficient activation of the substrates could not only accelerate the reaction, but it also could affect the regio- and stereoselectivity.

Despite the broad applicability of Lewis acid catalysts in modern organic chemistry, they were believed to be incompatible with water for a long time. Indeed, traditional Lewis acids such as BF_3, Al(III), Ti(IV), and Sn(IV) catalysts undergo rapid hydrolysis to form the precipitation of corresponding hydroxide or oxide in water. However, it was discovered in 1991 that rare earth trifluoromethanesulfonates (triflates)[74] such as $Sc(OTf)_3$, $Y(OTf)_3$ and $Ln(OTf)_3$ can work as water-compatible Lewis acids to promote the Mukaiyama aldol reaction in aqueous media (water/organic solvents).[75]

Scheme 0.1. $Yb(OTf)_3$-catalyzed Mukaiyama aldol reaction in aqueous media.[75a]

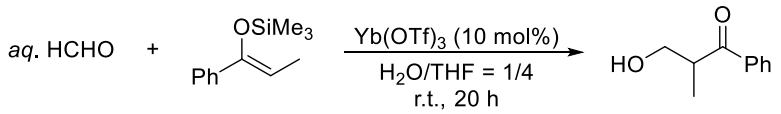

These water-compatible Lewis acid catalysts possessed several inherent advantages over traditional Lewis acid catalysts. For instance, water-compatible Lewis acid catalysts enables the use of aqueous aldehyde, especially formaldehyde, as a reactant. Even though the formaldehyde gas or paraformaldehyde (which is toxic) can be employed in anhydrous conditions, the procedures are more harmful and complicated. In this sense, water-compatible Lewis acid-mediated hydroxymethylation reactions with formaldehyde in aqueous media have become one of the most valuable C1 elongation reactions[76], and have been applied to many total syntheses including diazonamide A[77], (-)-strychnine[78], and acutifolone A[79]. It was also revealed that water-compatible Lewis acid catalysts exhibited superior performance, and even unique reactivity in many reactions. For example, by using

$Gd(OTf)_3$ in water-ethanol-toluene co-solvent system, Baran *et al.* successfully obtained the desired Taxadienone intermediate through Mukaiyama aldol reactions while none of the catalysts afforded undesired products under anhydrous conditions (Scheme 0.2).[80]

Scheme 0.2. Baran's example applying the aqueous Mukaiyama aldol reactions.[80]

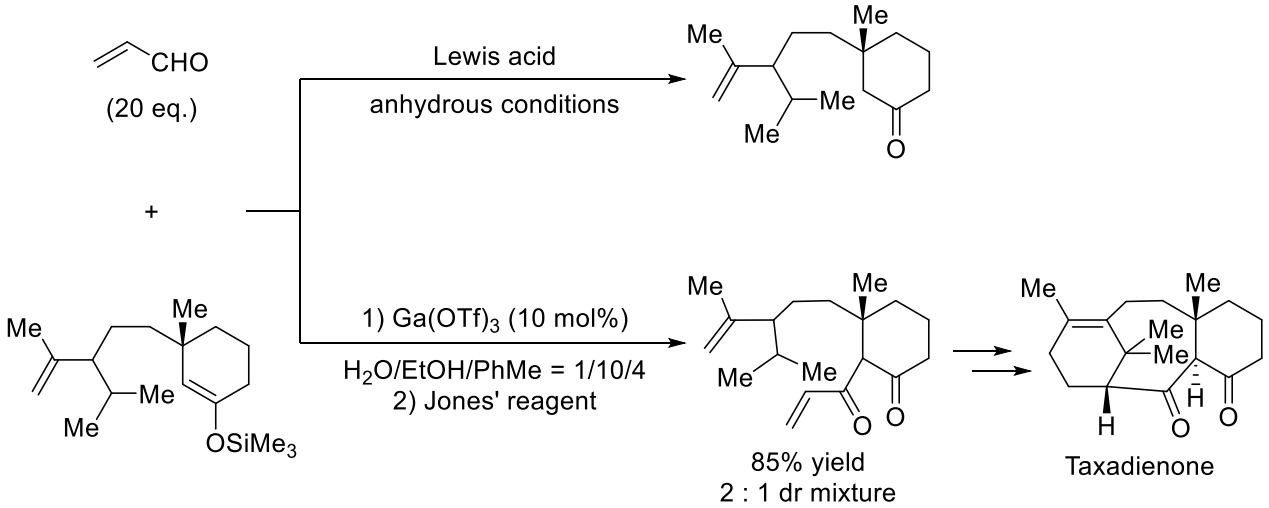

The Lewis acidity of an aqua-metal species is determined by its hydrolysis ability in principle: the higher hydrolysis constant (pK_h), which afford more OH^- as the coordinative ligand toward metal center, results in higher splitting of d-orbitals of the metal center, thereby the higher Lewis acidity. On the other hand, as discussed above, a metal cation species in aqueous solution constitutes a naked metal cation center, a strict primary hydration sphere, and a relatively loose second hydration sphere. Therefore, the rate of releasing hydrated protons, which can be determined through water exchange rate constants (WERCs), is another crucial factor to determine the Lewis acidity of a metal species in aqueous solution. Based on these consideration, a metal cation with smaller pK_h value and larger WERC should work as a good Lewis acid in water theoretically (Scheme 0.3).[81]

Scheme 0.3. Hydrolysis constants and exchange rate constants for substitution of inner-sphere water.[82]

M^{+n} pK_h [a] WERC [b]															
Li^{+1} 13.64 4.7×10^{7}	Be — —											B $^{+3}$ — —	C — —	N — —	
Na^{+1} 14.18 1.9×10^{8}	Mg^{+2} 11.44 5.3×10^{5}											Al^{+3} 4.97 1.6×10^{0}	Si^{+4} — —	P^{+5} — —	
K^{+1} 14.46 1.5×10^{8}	Ca^{+2} 12.85 5×10^{7}	Sc^{+3} 4.3 4.8×10^{7}	Ti^{+4} ≤ 2.3 —	V^{+3} 2.26 1×10^{3}	Cr^{+3} 4.0 5.8×10^{-7}	Mn^{+2} 10.59 3.1×10^{7}	Fe^{+2} 9.5 3.2×10^{6}	Co^{+2} 9.65 2×10^{5}	Ni^{+2} 9.86 2.7×10^{4}	Cu^{+2} 7.53 2×10^{8}	Zn^{+2} 8.96 5×10^{8}	Ga^{+3} 2.6 7.6×10^{2}	Ge^{+4} — —	As — —	
Rb — —	Sr — —	Y^{+3} 7.7 1.3×10^{7}	Zr^{+4} 0.22 —	Nb^{+5} (0.6) —	Mo^{+5} — —	Tc — —	Ru^{+3} — —	Rh^{+3} 3.4 3×10^{-8}	Pd^{+2} 2.3 —	Ag^{+1} 12 $>5\times10^{6}$	Cd^{+2} 10.08 $>1\times10^{8}$	In^{+3} 4.00 4.0×10^{4}	Sn^{+4} — —	Sb^{+5} — —	
Cs — —	Ba^{+2} 13.47 $>6\times10^{7}$	Ln^{+3} 7.6-8.5 10^{6}-10^{8}	Hf^{+4} 0.25 —	Ta^{+5} (-1) —	W^{+6} — —	Re^{+5} — —	Os^{+3} — —	Ir^{+3} — —	Pt^{+2} 4.8 —	Au^{+1} — —	Hg^{+2} 3.40 2×10^{9}	Tl^{+3} 0.62 7×10^{5}	Pb^{+2} 7.71 7.5×10^{9}	Bi^{+3} 1.09 —	

La^{+3} 8.5 2.1×10^{8}	Ce^{+3} 8.3 2.7×10^{8}	Pr^{+3} 8.1 3.1×10^{8}	Nd^{+3} 8.0 3.9×10^{8}	Pm — —	Sm^{+3} 7.9 5.9×10^{8}	Eu^{+3} 7.8 6.5×10^{8}	Gd^{+3} 8.0 6.3×10^{7}	Tb^{+3} 7.9 7.8×10^{7}	Dy^{+3} 8.0 6.3×10^{7}	Ho^{+3} 8.0 6.1×10^{7}	Er^{+3} 7.9 1.4×10^{8}	Tm^{+3} 7.7 6.4×10^{6}	Yb^{+3} 7.7 8×10^{7}	Lu^{+3} 7.6 6×10^{7}

[a] $pK_h = -\log K_h$.[81a,b] [b] Exchange rate constants for substitution of inner-sphere water ligands.[81c]

In accordance with the experimental facts, all the rare-earth metal cations indeed possess smaller pK_h values and larger WERCs. Other than rare-earth metals, Fe(II), Cu(II), Zn(II), Cd(II) and Pb(II) were predicted, and later were proved as efficient Lewis acids in aqueous solution. Particularly, in the Lewis acid catalyzed Mukaiyama aldol reactions in water, metal species whose pK_h values in the range from about 4.3 (for Sc(III)) to 10.08 (for Cd(II)) and WERC values greater than 3.2×10^6 $M^{-1}s^{-1}$ were found to catalyze the reaction efficiently. When pK_h values are less than 4.3, metal cations are hydrolyzed to produce protons in over-sufficient number, resulting in rapid decomposition of silicon enolates. On the other hand, when pK_h values are higher than 10, Lewis acidities of the cations were too low to catalyze the aldol reaction.

The metal cations whose pK_h and/or WERC values are close to the criteria limits, could be assumed that generally a higher K_h with lower WERC finally gave a product in lower yield but higher initial reaction rate. It should always be in mind that the K_h values and WERCs are not the whole factors, but representative factors.

Another momentous factor of Lewis acidity in aqueous solution is the hydrated coordination number of the metal center. The water molecules in primary hydration sphere not only hydrolyze the metal center, but also hydrate to the metal center rather powerfully as ligands. The decrease of water molecule numbers would eliminate the hydrolysis, resulting in weaker Lewis acidity, and significantly make the coordination geometry of the metal center change, resulting in even reversed selectivity (Table 0.10).[83]

Table 0.10. Effect of Yb salts and the correlation between product stereochemistry and the amount of water (Reprinted with permission from Kobayashi, S.; Hachiya, I. *J. Org. Chem.* 1994, *59*, 3590-3596. Copyright 1994, American Chemical Society).[83]

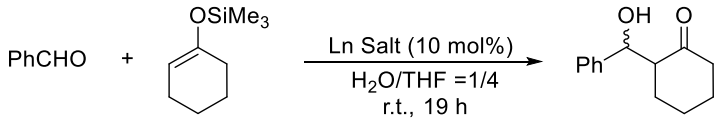

Ln salt	Yield (%)	Ln salt	Yield (%)
$Yb(OTf)_3$	**91**	$Yb(OAc)_3$	14
$Yb(ClO_4)_3$	**88**	$Yb(NO_3)_3$	7
$YbCl_3$	3	$Yb_2(SO_4)_3$	Trace

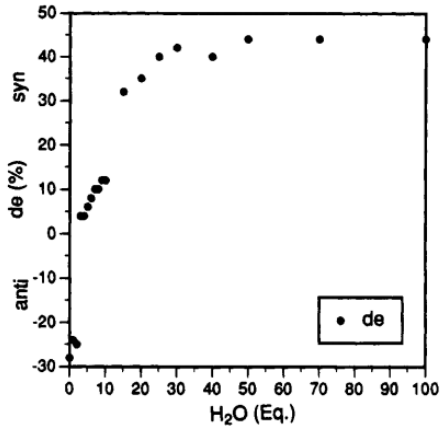

■ *Heterogeneous Chiral Lewis Acid Catalysts in Water*

In the early days, the interest toward heterogeneous Lewis acid catalysts in water mainly comes from the need for green chemistry. It derives from the fact that after completion of the reaction, the reuse of catalyst is almost impossible and moreover, undesired wastes including inorganic salts and coordinated ligands are produced in homogeneous reactions. Therefore there is a necessity to develop heterogeneous solid Lewis acid catalysts for industrial processes.

L-Proline immobilized ZnS nanoparticle catalyst represents one of chiral heterogeneous Lewis acid catalysts.[84] It becomes possible to conduct direct asymmetric aldol reactions. The catalyst was recovered and reused for up to 10 times without any significant lost in activity (Scheme 0.4).

Scheme 0.4. Chiral ZnS nanoparticles for asymmetric aldol condensation reactions in water.[84]

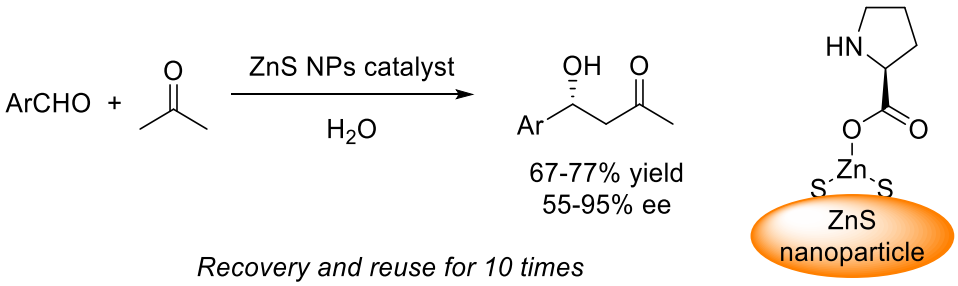

Remarkable advances in heterogeneous Lewis acid catalysts have been achieved using immobilized catalysts, while some other studies focused on direct use of water-insoluble metal salts as Lewis acid sources. An unprecedented catalytic use of In(0) for asymmetric allylation reactions demonstrated the great possibility of metal zero species as chiral heterogeneous Lewis acid catalysts (Scheme 0.5).[85]

Scheme 0.5. Asymmetric allylation reactions catalyzed by chiral In(0) complex in water.[85]

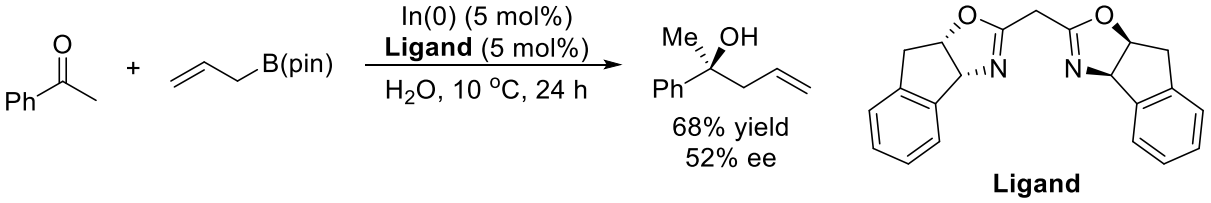

Likewise, the potential of insoluble metal oxide as heterogeneous Lewis acids also received extensive attention. Metal oxides including Nb_2O_5,[86] TiO_2,[87] and ZrO_2[88] were found suitable as Lewis acid catalysts in aqueous medium. Recent studies on Ag_2O also demonstrated unique reactivity and selectivity in water (Scheme 0.6).[89] The allylation reactions of benzaldehyde and allylmethylpinacolsilane achieved the TON of up to 7680 in the presence of 0.005 mol% of Ag_2O as a catalyst. With the combination of chiral phosphine ligand, Ag_2O afforded the desired product in 89% yield with 53% ee. These results further reinforced the ability of metal oxides as heterogeneous Lewis acid catalysts.

Scheme 0.6. Asymmetric allylation reactions catalyzed by chiral silver oxide complex in water.[89]

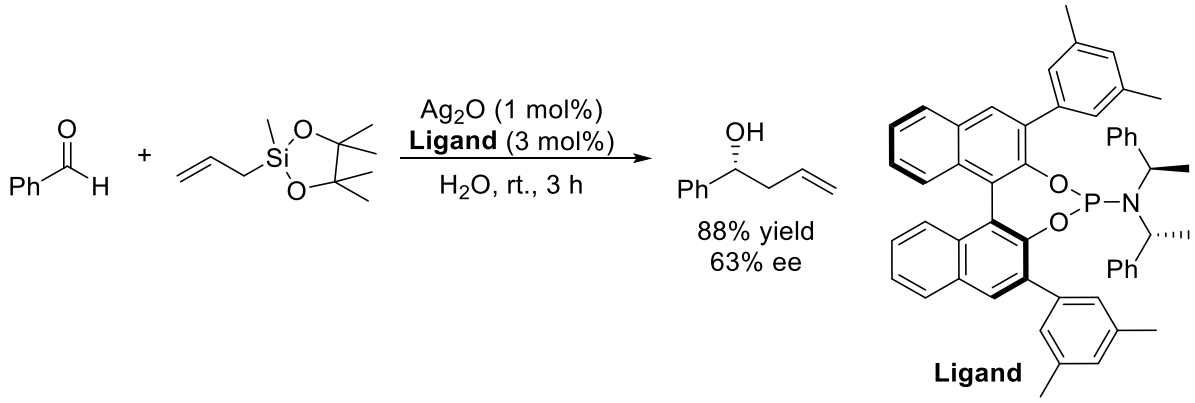

On the other hand, exploration of insoluble metal salts as heterogeneous Lewis acids was limited. Traditionally, fluorides and hydroxides of transitional metals are considered as poor Lewis acid catalysts in water due to their amorphous surface structure and poor solubility in aqueous medium. It

was not until the discovery of insoluble ZnF_2, which actually affords ZnF(OH), that the metal fluoride and metal hydroxide could work as Lewis acids (Scheme 0.7).[90]

Scheme 0.7. ZnF_2-mediated asymmetric allylation reaction in aqueous media.[90b]

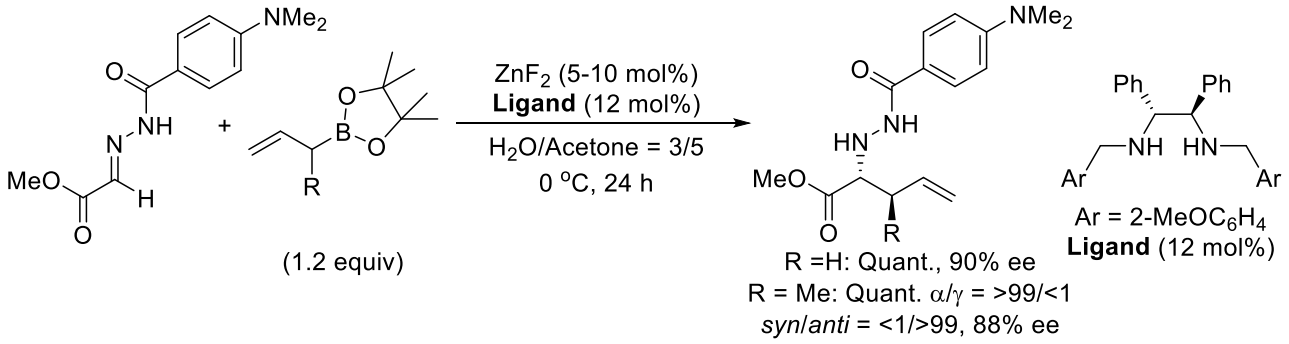

Despite these recent inspiring advances in developing catalysts, especially the Lewis acid catalysts in water, the overall examples are still far from sufficient. Further explorations are eagerly awaited.

0-3 The Prospect

Catalysts occupied a pivotal position in most of the biochemical and the chemical processes. Chemists have sustained their efforts toward efficient catalysis. An ideal catalysis is considered to possess three major advantages: 1. A choice of green solvent, namely water, to satisfy the criteria of green sustainable chemistry; 2. A dispersed and stable environment in water that can inhibit self-aggregation of organic materials yet with an exquisite assemblage of all components into the reaction centers; and 3. A tunable electrochemical property that can furnish higher reactivity and selectivity.

Since the reveal of surprising rate acceleration observed in Diels-Alder reactions in water, organic chemistry in water has experienced a great leap over the last 40 years. Indeed, organic reactions in water have been investigated from a standpoint that the most ideal reactions, enzymatic reactions in vivo, are carried out under aqueous conditions.[91] In some reactions, unique reactivity[92] and selectivity[93], which are not observed in organic solvent, have been found. Despite its usability and uniqueness, water is still rarely employed as a reaction medium due to two major obstacles: the insolubility of many organic reactants and the deactivation of metal catalysts in aqueous media. In this dissertation, some new findings on the reaction in water were presented along with my efforts to create better catalyst environments in water: utilization of both amorphous and well-defined insoluble metal surfaces (Chapter 1); construction of hydrophobic surface environment utilizing Lewis Acid-Surfactant–Combined catalysts (LASCs) and single-walled carbon nanotube (SWNT) (Chapter 2); and creation of a photo-harvesting environment for further extension of organic chemistry in water (Chapter 3). It is noteworthy that water is always a prerequisite to these distinguishing environments. These results would open up new opportunities in the development of new catalysts and organic reactions.

References

(1) https://www.nasa.gov/content/goddard/nasa-research-gives-guideline-for-future-alien-life-search (Visited on Dec. 16th, 2016)

(2) Finney, J. L. *Philos. Trans. R. Soc. Lond. B* **2004**, *359*, 1145–1165.

(3) Buckingham, A. D., The structure and properties of a water molecule, In: Neilson, G.W.E.J.E. (Ed.), *Water and Aqueous Solutions*, Adam Hilger, Bristol, 1986, pp. 1–13.

(4) Hermansson, K. The electron distribution in the bound water molecule. PhD thesis, University of Uppsala, Sweden, **1984**.

(5) Pollack, G. H. *Cells, Gels and the Engines of Life*, Ebner Publishers, Seattle, **2001**.

(6) For organic reactions in water, numerous computational calculations and simulations were conducted: (a) Hinton, J. F.; Amis, E. S. *Chem. Rev.* **1971**, *71* , 627–674; (b) Habenschuss, A.; Spedding, F. H. *J. Chem. Phys.* **1979**, *70*, 3758-3763; (c) Ohtaki, H.; Radnai, T. *Chem. Rev.* **1993**, *93* , 1157-1204; (d) Pavlov, M.; Siegbahn, P. E. M.; Sandström. *J. Phys. Chem. A* **1998**, *102*, 219-228. For biological proteins: Carugo, O.; Bordo, D. *Acta Crystallogr. D Biol. Crystallogr.* **1999**, *55*, 479-483.

(7) Bonn, M.; Nagata, Y.; Backus, E. H. G. *Angew. Chem. Int. Ed.* **2015**, *54*, 5560-5576.

(8) Paul, J. B.; Collier, C. P.; Saykally, R. J.; Scherer, J. J.; O'Keefe, A. *J. Phys. Chem. A* **1997**, *101*, 5211–5214.

(9) Daniel, R. M., Finney, J. L. and Stoneham, M. (Eds.), *Philos. Trans. R. Soc. Lond. B* **2004**, 1141–1328.

(10) Bartels, D. M. *J. Chem. Phys.* **2001**, *115*, 4404–4405.

(11) Soper, A. K. *Mol. Phys.* **2001**, *99*, 1503–1516; For review of water structure analyses, see: Head-Gordon, T.; Hura, G. *Chem. Rev.* **2002**, *102*, 2651-2670.

(12) Alagona, G.; Ghio, C.; Kollman, P. *J. Am. Chem. Soc.* **1983**, *105*, 5226-5230

(13) Giguère, P. A. *J. Raman Spectrosc.* **1984**, *15*, 354-359.

(14) Laage, D. and Hynes, J. *Science* **2006**, *311*, 832-835.

(15) Gregory, J. K.; Clary, D. C.; Brown, M. G.; Saykally, R. J. *Science* **1997**, *275*, 814-827.

(16) Silvestrelli, P. L. and Parrinello, M. *Phys. Rev. Lett.* **1999**, *82*, 3308–3311.

(17) Teixeiro, J.; Bellisent-Funel, J. C. M. -C.; Dianoux, A. J. *Phys. Rev. A* **1985**, *31*, 1913–1917.

(18) Denisov, V. P. and Halle, B. *Faraday Discuss.* **1996**, *103*, 227–244.

(19) (a) Ohmine, I. *J. Phys. Chem.* **1995**, *99*, 6767–6776; (b) Liu, K.; Cruzan, J. D.; Saykally, R. J. *Science* **1996**, *271*, 5251-5255; (c) Keutsch, F. N.; Saykally, R. J. *Proc. Natl. Acad. Sci. U. S. A.* **2001**, *98*, 10533–10540.

(20) Smallwood, I. *Handbook of organic solvent properties*. Butterworth-Heinemann, **2012**.

(21) (a) Franks, F.; Ives, D. J. G. *Q. Rev. Chem. Soc.* **1966**, *20*, 1-44; (b) Rubino, J. T.; Yalkowsky, S. H. *Pharm. Res.* **1987**, *4*, 220-230; (c) Millard, J. W.; Alvarez- Núñezb, F. A.; Yalkowsky, S. H. *Int. J. Pharm.* **2002**, *245*, 153-166.

(22) (a) Reichardt, Ch. *Solvents and Solvent Effects in Organic Chemistry*, 4nd edn., VCH,Weinheim, **2010**; (b) Dudd, L.M., Venardou, E., Garcia-Verdugo, E.; Licence, A.J.; Blake, A. J. *Green Chem.* **2003**, *5*, 187–192.
(23) Dimroth, K.; Reichardt, Ch.; Siepmann, T.; Bohlmann, F. *Liebigs Ann. Chem.* **1963**, *661*, 1–37.
(24) Reichardt, Ch. and Schafer, G. *Liebigs Ann. Chem.* 1995, 1579–1582.
(25) (a) Israelachvili, J., *Intermolecular and Surface Forces*, 2nd edn., Academic Press, London, 1992; (b) Dack, M.R.J. *Chem. Soc. Rev.* **1975**, *4*, 211–229.
(26) Allen, G.; Gee, G.; Wilson, G. J. *Polymer*, **1960**, *1*, 456–466.
(27) Dack, M. R. J. *Aust. J. Chem.*, **1975**, *28*, 1643–1648.
(28) Whalley, E. *Trans. Faraday Soc.* **1957**, *53*, 1578-1585.
(29) (a) Crovetto, R.; Prini, R. F.; Japas, M. L. *J. Chem. Phys.* **1982**, *76*, 1077-1086; (b) Graziano, G. *J. Phys. Chem. B* **2000**, *104*, 9249–9254.
(30) Eigen, M.; De Maeyer, L. *Proc. Royal Soc. A* **1958**, *247*, 505-533.
(31) Olofsson, G.; Olofsson, I. *J. Chem. Thermodynamics* **1977**, *9*, 65-69.
(32) Enea, O.; Singh, P. P.; Woolley, E. M.; McCurdy, K. G.; Hepler, L. G. *J. Chem. Thermodynamics* **1977**, *9*, 731-734.
(33) (a) Christensen, J.; Kimball, G. L.; Johnston, H. D.; Izatt, R. M. *Thermochim. Acta* **1972**, *4*, 141-150; (b) Lown, D. A.; Thirsk, H. R.; Wynne-Jones, L. *Trans. Faraday Soc.* **1968**, *64*, 2073-2080.
(34) Bakker, H. J. and Nienhuys, H. -K. *Science* **2002**, *297*, 587–590.
(35) (a) P. Atkins and J. de Paula, Atkins' Physical Chemistry, 7th Ed. (OUP, Oxford, 2002); (b) Ryding, M. J.; Andersson, P. U.; Zatula, A. S.; Uggerud, E. *Eur. J. Mass Spectrom* **2012**, *18*, 215-222.
(36) Agmon, N. *Chem. Phys. Lett.* **1995**, *244*, 456–462.
(37) Tuckerman, M. E.; Marx, D.; Parrinello, M. *Nature* **2002**, *417*, 925–929.
(38) (a) Friedman, H. L. and Krishnan, C. V., Thermodynamics of ion hydration, In: Franks, F. (Ed.), *Water, A Comprehensive Treatise*, Vol. 3, 1st edn., Plenum Press, New York, 1973, pp. 1–118; (b) Enderby, J. E. and Neilson, G.W., X-ray and neutron scattering by aqueous solutions of electrolytes, In: Franks, F. (Ed.),*Water: A Comprehensive Treatise*, Vol. 6, 1st edn., Plenum Press, New York, 1979, pp. 1–46.
(39) Anslyn, E.V. and Dougherty, D. A. *Modern Physical Organic Chemistry*, University Science Books, Sausalito, CA, 2006.
(40) Jencks, W. P. *Catalysis in Chemistry and Enzymology*, McGraw-Hill, New York, 1969.
(41) Saielli, G.; Scorrano, G.; Bagno, A.; Wakisaka, A. *Chem. Phys. Chem.* **2005**, *6*, 1307-1315.
(42) (a) Graziano, G. *J. Phys. Chem. B*, **2002**, *106*, 7713–7716; (b) Graziano, G. *J. Phys. Chem. B* **2001**, *105*, 2079-2081.
(43) (a) Lee, B. *Biopolymers* **1985**, *24*, 813–823; (b) Graziano, G. *J. Phys. Soc. Jpn.* **2000**, *69*, 1566-1569.
(44) Southall, N. T.; Dill, K. A.; Haymet, A. D. J. *J. Phys. Chem. B* **2002**, *106*, 521-533.
(45) Guo, J. -H.; Luo, Y.; Augustsson, A.; Kashtanov, S.; Rubensson, J. -E.; Shuh, D. K.; Agren, H.;

Nordgren, J. *Phys. Rev. Lett.* **2003**, *91*, 157401-1–157401-4.
(46) Meyer, E.A.; Castellano, R. K.; Diederich, F. *Angew. Chem. Int. Ed.* **2003**, *42*, 1210–1250.
(47) (a) Raschke, T.M. and Levitt, M. *Proc. Natl. Acad. Sci. U. S. A.* **2005**, *102*, 6777–6782; (b) Dorairaj, S.; Jeon, J.; Kim, H. J. *J. Phys. Chem. B* **2006**, *110*, 429-435.
(48) Baes, C. F.; Mesmer, R. E. *The hydrolysis of Cations*, John Wiley & Sons, Inc., New York. **1976**.
(49) Robertazzi, A.; Platts, J. A. *J. Comput. Chem.* **2004**, *25*, 1060-1067.
(50) Rose, G. D. *Annu. Rev. Biophys. Biomol. Struct.* **1993**, *22*, 381-415.
(51) Fersht, A. R.; Shi, J. P.; Knill-Jones, J.; Lowe, D. M.; Wilkinson, A. J.; Blow, D. M.; Brick, P.; Carter, P.; Waye, M. M.; Winter, G. *Nature* **1985**, *314*, 235-238.
(52) Bartlett, P .A.; Marlowe, C. K. *Science* **1987**, *235*, 569-571.
(53) (a) Slater, S. J.; Ho, C.; Taddeo, F. J.; Kelly, M. B.; Stubbs, C. D. *Biochemistry* **1993**, *32*, 3714-1721; (b) Zhou, F. X.; Cocco, M. J.; Russ, W. P.; Brunger, A. T.; Engelman, D. M. *Nat. Struct. Biol.* **2000**, *7*, 154-160.
(54) Pautsch, A.; Schulz, G. E. *Nat. Struct. Biol.* **1998**, *5*, 1013-1017.
(55) Yee, V. C.; Pedersen, L. C.; Trong, I. Le.; Bishop, P. D.; Stenkamp, R. E.; Teller, D. C. *Proc. Nat. Acad. Sci. U. S. A.* **1994**, *91*, 7296-7300.
(56) Good, R. J.; Srivatsa, N. R.; Islam, M.; Huang, H. T. L.; Van Oss, C. J. *J. Adhesion Sci. Technol.* **1990**, *4*, 1-617.
(57) Southall, N.T. and Dill, K.A. *Biophys. Chem.* **2002**, *101–102*, 295–307.
(58) (a) Blokzijl, W. and Engberts, J. B. F. N. *J. Am. Chem. Soc.* **1991**, *113*, 4241–4246; (b) Blokzijl,W. and Engberts, J. B. F. N. *J. Am. Chem. Soc.* **1992**, *114*, 5440–5442.
(59) Kauzmann, W. *Adv. Protein Chem.* **1959**, *14*, 1-63. For review, see: Chandler, D. *Nature* **2005**, *437*, 640-647.
(60) (a) Breslow, R. *J. Am. Chem. Soc.* **1957**, *79*, 1762; (b) Breslow, R. *Chem. Ind.* **1957**, 893–894; (c) Breslow, R. *J. Am. Chem. Soc.* **1958**, *80*, 3719–3726; (d) Breslow, R.; McNelis, E. *J. Am. Chem. Soc.* **1959**, *81*, 3080–3082; (e) Breslow, R.; McNelis, E. *J. Am. Chem. Soc.* **1960**, *82*, 2394; (f) Breslow, R. *CIBA Foundation Study Group II*, J.A. Churchill Ltd., London, **1961**.
(61) (a) Cramer, F.; Mackensen, G. *Chem. Ber.*, **1970**, *103*, 2138–2147; (b) D'Souza, V. T.; Bender, M. L. *Acc. Chem. Res.* **1987**, *20*, 146–152; (c) Siegel, B.; Breslow, R. *J. Am. Chem. Soc.* **1975**, *97*, 6869–6870; (d) VanEtten, R. L.; Sebastian, J. F.; Clowes, G. A.; Bender, M. L. *J. Am. Chem. Soc.* **1967**, *89*, 3242–3253.
(62) (a) Breslow, R.; Campbell, P. *J. Am. Chem. Soc.*, **1969**, *91*, 3085; (b) Breslow, R.; Campbell, P. *Bioorg. Chem.* **1971**, *1*, 140–156.
(63) Breslow, R.; Kohn, H.; Siegel, B. *Tetrahedron Lett.* **1976**, *17*, 1645–1646.
(64) For early examples of combination of cyclodextrins with metal ions, see: (a) Breslow, R.; Overman, L. E. *J. Am. Chem. Soc.* **1970**, *92*, 1075–1077; (b) Breslow, R.; Zhang, B. *J. Am. Chem. Soc.* **1992**, *114*, 5882–5883; (c) Breslow, R.; Schmir, M. *J. Am. Chem. Soc.* **1971**, *93*, 4960–4961; (d) Breslow, R.; Mcallister, C. *J. Am. Chem. Soc.* **1971**, *93*, 7096–7097; (e) Tang, C. C.; Davalian, D.;

Huang, P.; Breslow, R. *J. Am. Chem. Soc.* **1978**, *100*, 3918–3922; (f) Chin, J.; Breslow, R. *Tetrahedron Lett.* **1982**, *23*, 4221–4224; (g) Breslow, R.; Hunt, J.; Smiley, R.; Tarnowski, T. *J. Am. Chem. Soc.* **l983**, *105*, 5337–5342; (h) Gellman, S.; Petter, R.; Breslow, R. *J. Am. Chem. Soc.* **1986**, *108*, 2388–2394; (i) Schepartz, A.; Breslow, R. *J. Am. Chem. Soc.* **1987**, *109*, 1814–1826; (j) Breslow, R.; Singh, S. *Bioorg. Chem.* **1988**, *16*, 408–417; (k) Light, J.; Breslow, R. *Bioorg. Chem.* **1990**, *18*, 63–77; (l) Breslow, R.; Berger, D.; Huang, D. –L. *J. Am. Chem. Soc.* **1990**, *112*, 3686–3687; (m) Breslow, R.; Duggan, P. J.; Light, J. P. *J. Am. Chem. Soc.* **1992**, *114*, 3982–3983; (n) Breslow, R.; Huang, D. -L. *Proc. Natl. Acad. Sci. U. S. A.* **1991**, *88*, 4080–4083. For early examples of cyclodextrin dimers, see: (a) Breslow, R.; Greenspoon, N.; Guo, T.; Zarzycki, R. *J. Am. Chem. Soc.* **1989**, *111*, 8296-8297; (b) Zhang, B.; Breslow, R. *J. Am. Chem. Soc.* **1993**, *115*, 9353-9354; (c) Breslow, R.; Zhang, B. *J. Am. Chem. Soc.* **1996**, *118*, 8495 – 8496; (d) Breslow, R.; Chung, S. *J. Am. Chem. Soc.* **1990**, *112*, 9659-9660; (e) Breslow, R.; Halfon, S.; Zhang, B. *Tetrahedron* **1995**, *51*, 377-388; (f) Leung, D. K.; Atkins, J. H.; Breslow, R. *Tetrahedron Lett.* **2001**, *42*, 6255-6258; (g) Breslow, R.; Yang, Z.; Ching, R.; Trojandt, G.; Odobel, F. *J. Am. Chem. Soc.* **1998**, *120*, 3536-3537; (h) Maletic, M.; Wennemers, H.; McDonald, D. Q.; Breslow, R.; Still, W. C. *Angew. Chem. Int. Ed. Engl.* **1996**, *35*, 1490-1492; (i) Breslow, R.; Duggan, P. J.; Wiedenfeld, D.; Waddell, S. T. *Tetrahedron Lett.* **1995**, *36*, 2707-2710.

(65) For preliminary works, see: (a) Siegel, B.; Pinter, A.; Breslow, R. *J. Am. Chem. Soc.* **1977**, *99*, 2309–2312; (b) Ueno, A.; Breslow, R. *Tetrahedron Lett.* **1982**, *23*, 3451–3454;(c) Breslow, R.; Labelle, M. *J. Am. Chem. Soc.* **1986**, *108*, 2655–2659; (d) Anslyn, E.; Breslow, R. *J. Am. Chem. Soc.* **1989**, *111*, 4473–4482.

(66) For preliminary works, see: (a) Breslow, R.; Hammond, M.; Lauer, M. *J. Am. Chem. Soc.* **1980**, *102*, 421–422; (b) Winkler, J.; Coutouli-Argyropoulou, E.; Leppkes, R.; Breslow, R. *J. Am. Chem. Soc.* **1983**, *105*, 7198–7199; (c) Breslow, R.; Czarnik, A. W.; Lauer, M.; Leppkes, R.;Winkler, J.; Zimmerman, S. *J. Am. Chem. Soc.* **1986**, *l08*, 1969-1979.

(67) For preliminary work, see: Breslow, R., Brown, A. B.; McCullough, R. D.; White, P. W. *J. Am. Chem. Soc.* **1989**, *111*, 4517–4518.

(68) Breslow, R. Hydrophobic and antihydrophobic effects on organic reactions in aqueous solution, In: Cramer, C. J.; Truhlar, D.G. (Eds.), *Structure and Reactivity in Aqueous Solution*, American Chemical Society, Washington, DC, **1994**, pp. 291–302.

(69) Rideout, D. C.; Breslow, R. *J. Am. Chem. Soc.* **1980**, *102*, 7816-7817. For a review, see: Li, C.-J. *Chem. Rev.* **2005**, *105*, 3095–3165.

(70) Chandrasekhar, J.; Shariffskul, S.; Jorgensen, W. L. *J. Phys. Chem. B* **2002**, *106*, 8078–8085.

(71) Jorgensen, W.L. and Buckner, J.K. *J. Phys. Chem.* **1987**, *91*, 6083–6085.

(72) Streitwieser Jr., A.; Nebenzahl, L. L. *J. Am. Chem. Soc.* **1976**, *98*, 2188-2190.

(73) Biscoe, M. R.; Uyeda, C.; Breslow, R. *Org. Lett.* **2004**, *6*, 4331-4334.

(74) Rare earth triflates were reported to be prepared in aqueous solution: (a) Thom, K. F. U.S. Patent 3615169, **1971**; CA 1972, 76, 5436a; (b) Forsberg, J. H.; Spaziano, V. T.; Balasubramanian, T. M.; Liu, G. K.; Kinsley, S. A.; Duckworth, C. A.; Poteruca, J. J.; Brown, P. S.; Miller, J. L. *J. Org. Chem.*

1987, *52*, 1017-1021.
(75) (a) Kobayashi, S. *Chem. Lett*. **1991**, 2187-2190; (b) Kobayashi, S. Lanthanide Triflate-Catalyzed Carbon–Carbon Bond-Forming Reactions in Organic Synthesis. In *Lanthanides: Chemistry and Use in Organic Synthesis*; S. Kobayashi, Ed.; Springer: Heidelberg, **1999**; (c) Kobayashi, S. *Eur. J. Org. Chem.* **1999,** 15-27; (d) Kobayashi, S. *Synlett* **1994**, 689-701; (e) Kobayashi, S.; Sugiura, M.; Kitagawa, H.; Lam, W. W.-L. *Chem. Rev*. **2002**, *102*, 2227-2302; (f) Kobayashi, S.; Ogawa, C. *Chem. Eur. J*. **2006**, *12*, 5954-5960.
(76) (a) Geissman, T. A. *Org. React*. **1944**, *2*, 94-113; (b) Neilsen, T.; Houlihan, A. T. *Org. React*. **1968**, *16*, 1-438.
(77) (a) Nicolaou, K. C.; Huang, X.; Giuseppone, N.; Rao, P. B.; Bella, M.; Reddy, M. V.; Snyder, S. A. *Angew. Chem. Int. Ed.* **2001**, *40*, 4705-4709; (b) Nicolaou, K. C.; Hao, J.; Reddy, M. V.; Rao, P. B.; Rassias, G.; Synder, S. A.; Huang, X.; Chen, D. Y. –K.; Brenzovich, W. E.; Giuseppone, N.; Giannakakou, P.; O'Brate, A. *J. Am. Chem. Soc.* **2004**, *126*, 12897-12906.
(78) Ohshima, T.; Xu, Y.; Takita, R.; Shimizu, S.; Zhong, D.; Shibasaki, M. *J. Am. Chem. Soc.* **2002**, *124*, 14546-14547.
(79) Shiina, J.; Oikawa, M.; Nakamura, K.; Obata, R.; Nishiyama, S. *Eur. J. Org. Chem.* **2007**, 5190-5197.
(80) Mendoza, A.; Ishihara, Y.; Baran, P. S. *Nature Chem.* **2012**, *4*, 21-25.
(81) (a) Baes, Jr., C. F.; Mesmer, R. E. *The Hydrolysis of Cations*, John Wiley & Sons: New York, **1976**; (b) Yatsimirksii, K. B.; Vasil'ev, V. P. *Instability Constants of Complex Compounds*; Pergamon: New York, **1960**; (c) Martell, A. E. Ed.; *Coordination Chemistry*; ACS Monograph 168; American Chemical Society: Washington, DC, **1978**; Vol. 2.
(82) Kobayashi, S.; Nagayama, S.; Busujima, T. *J. Am. Chem. Soc*. **1998**, *120*, 8287–8288.
(83) (a) Kobayashi, S.; Hachiya, I. *Tetrahedron Lett*. **1992**, *33*, 1625-1628; (b) Kobayashi, S.; Hachiya, I. *J. Org. Chem.* **1994,** *59*, 3590-3596; (c) Kobayashi, S. *Synlett* **1994**, 689-699.
(84) Shah, E.; Soni, H. P. *RSC Advance* **2013**, *3*, 17453-17461.
(85) Schneider, U.; Ueno, M.; Kobayashi, S. *J. Am. Chem. Soc.* **2008**, *130*, 13824–13825.
(86) (a) Nakajima, K.; Baba, Y.; Noma, R.; Kitano, M.; Kondo, J. N.; Hayashi, S.; Hara, M. *J. Am. Chem. Soc.* **2011**, *133*, 4224–4227; (b) Tanabe, K. *Mat. Chem. Phys*. **1987**, *17*, 217-225.
(87) (a) Nakajima, K.; Noma, R.; Kitano, M.; Hara, M. *J. Phys. Chem. C* **2013**, *117*, 16028–16033; (b) Shintaku, H.; Nakajima, K.; Kitano, M.; Ichikuni, N.; Hara, M. *ACS Catal.* **2014**, *4*, 1198–1204
(88) Song, S. X.; Kydd, R. A. *J. Chem. Soc., Faraday Trans.* **1998**, *94*, 1333-1338.
(89) Ueno, M.; Tanoue, A.; Kobayashi, S. *Chem. Lett.* **2014**, *43*, 1867-1869.
(90) First report used 50 mol% of ZnF_2 as catalyst: (a) Kobayashi, S.; Hamada, T.; Manabe, K. *J. Am. Chem. Soc.* **2002**, *124*, 5640-5641; (b) Hamada, T.; Manabe, K.; Kobayashi, S. *Chem. Eur. J.* **2006**, *12*, 1205 – 1215.
(91) Matějů, V.; Čižinská, S.; Krejčí, J.; Janoch, T. *Enzyme and Microbial Tech.* **1992**, *14*, 170-183.
(92) Kobayashi, S.; Xu, P.; Endo, T.; Ueno, M.; Kitanosono, T. *Angew. Chem. Int. Ed.* **2012**, *51*,

12763-12766.
(93) Kobayashi, S.; Endo, T.; Ueno, M. *Angew. Chem. Int. Ed.* **2011**, *50*, 12262–12265.

Chapter 1. Utilization of Insoluble Cu(II) Salts as Catalysts

"The greatest and most important problems of life are all in a certain sense insoluble"

Carl Jung., *[1931]*, 1962.

1-1 Introduction

1−1−1 Surface Properties of Insoluble Metal Salts in Water

Traditionally, heterogeneous metal oxides such as Nb_2O_5, TiO_2, and ZrO_2 are considered as excellent Lewis acids for their well-ordered, naked metal cations on the surfaces.[94] In contrast, surfaces of many metal hydroxides or related structures (e.g. $Cu(OH)_2$, $Ni(OH)_2$) are amorphous, and thus considered as uncontrollable Lewis acids. Several successful trials to utilize water-insoluble metal salts include an application to Metal-Organic Frames (MOFs) [95] and the simple recrystallization[96] from other solvents. Nevertheless, the preparation procedure is complicated and the applicable metal species are limited.

On the other hand, recent studies indicated that the surface of insoluble metal salts, especially metal hydroxides, possessed many unparalleled properties in aqueous medium.[97] Particularly, measurements of ζ-potentials of $Ni(OH)_2$ and $Cu(OH)_2$ revealed the pH-dependent charge-switch on their surface.[98] Considering the charge-switch boundary of $Cu(OH)_2$ at pH = 9.0 and that of $Ni(OH)_2$ at pH = 9.5, and the pH values of saturated $Cu(OH)_2$ and $Ni(OH)_2$ solutions (around 9.1 and 8.1, respectively), both hydroxide surfaces are considered positive-charged in water (Figure 1.1).

Meanwhile, the Gouy-Chapman-Stern model[99] defines three water layers nearby the surface of metal oxides/hydroxides (Figure 1.2): the primary water layer (PWL), in which most water molecules orientate toward the metal oxide/hydroxide positive-charged surface; the secondary layer (SWL), in which water molecule orientations are dominated by the "exuded" metal cations and anions; and the outside bulk water. Interestingly, the dielectric constant of water molecules in PWL is too low ($\varepsilon = 6$) to hydrate the nearby metal cations. As a result, the "exuded" metal cations could participate in the chemical reactions at the surface, affording products that subsequently release into bulk water, and stick back to the surface. This process is enthalpy-driven due to low lipophobicity of water molecules in PWL and SWL.

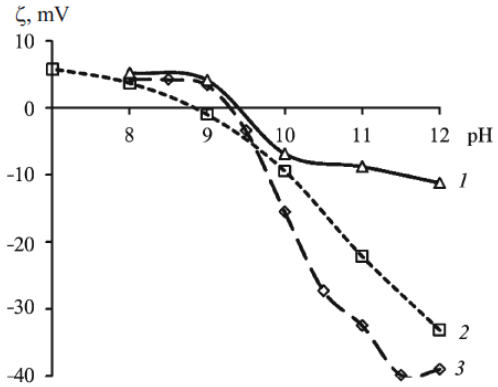

Figure 1.1. Effect of the pH on the ζ-potential of the hydroxides in the 0.001 M Na_2SO_4 solution (Reprinted with permission from Brodskii, V. A.; Gubin, A. F.; Kolesnikov, A. V.; Makarov, N. A. *Glass and Ceramics* 2015, *72*, 220-224. Copyright 2015, Springer).[98] 1) $Ni(OH)_2$; 2) $Cu(OH)_2$; 3) $Mn(OH)_2$.

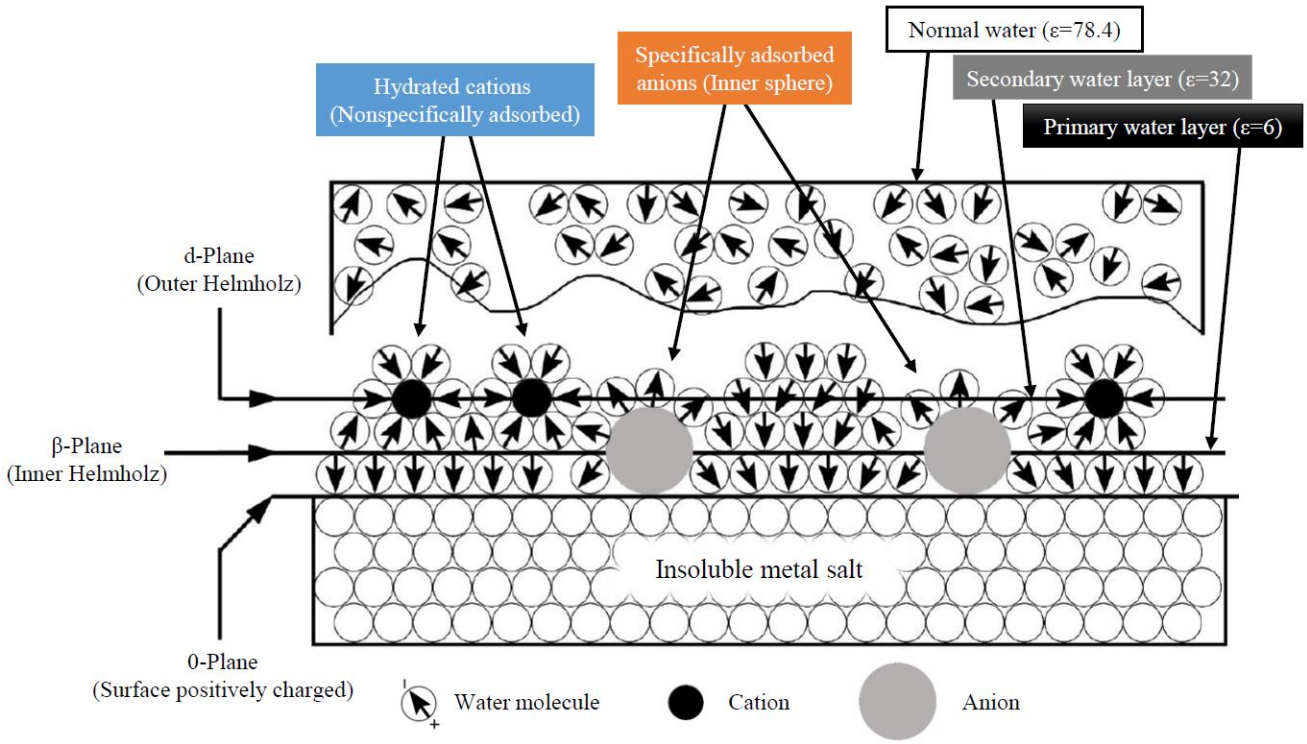

Figure 1.2. Schematic model of the electrical double layer (EDL) at the interface.[99]

It is also important to consider the actual situation of surfaces; most of the metal hydroxides possess amorphous surface structures (a majority of edges contains a few flat surfaces), while surfaces of crystallized metal salts or metal oxides are normally well-defined.[100] Recent calculation confirmed a significant difference in crystal faces of goethite (α-FeOOH) (Figure 1.3).[101] Generally, edge faces such as (021) and (110) appear to be more highly charged than <100> face. It should be noted that even though total charge values of α-FeOOH (021) and (110) are similar, their detailed microscopic

charging behaviors are quite different in binding energies as well as surface hydrogen-bonding network.[102] These results could be rationalized from orbital diagrams (Figure 1.4).

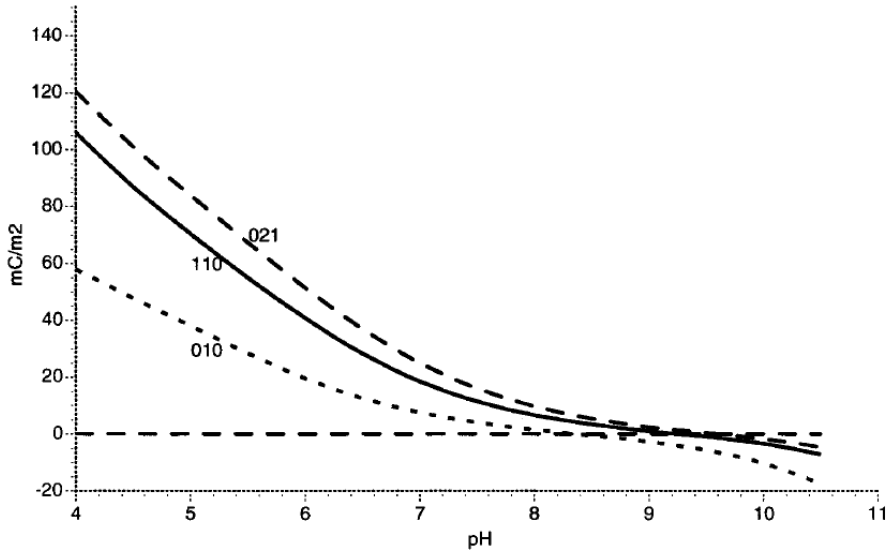

Figure 1.3. Calculated surface charge for different crystal faces of goethite (α-FeOOH) (Reprinted with permission from Brown, G. E.; Henrich, V. E.; Casey, W. H.; Clark, D. L.; Eggleston, C.; Felmy, A.; Goodman, D. W.; Grätzel, M.; Maciel, G.; McCarthy, M. I.; Nealson, K. H.l Sverjensky, D. A.; Toney, M. F.; Zachara, J. M. *Chem. Rev.* 1999, *99*, 77-174. Copyright 1999, American Chemical Society).[103]

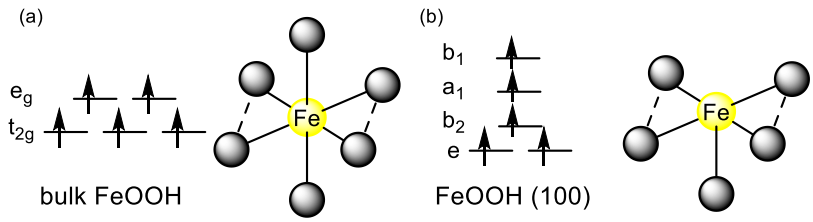

Figure 1.4. Comparison of orbital diagrams for (a) bulk FeOOH and (b) FeOOH (110).

Indeed, the bulk Fe(III) ion is embedded in the symmetric octahedral environment of six nearest oxygen ions or ligands, leading to a splitting of the five d-orbitals into two sets, denoted as t_{2g} and e_g. On the other hand, the surface Fe(III) ion lost one of its oxygen neighbors, leading to a reduction of the symmetry. It also affects the energy of the d electronic levels. Owing to the reduced symmetry of the surface, the t_{2g} and e_g subsets split further into e and b_2, and a_1 and b_1 levels, respectively. Therefore, on these surfaces, the excitation energy for electrons becomes lower at ground state than that of bulk species, affording larger surface charges. Likewise, on the side surface (e.g. (110)), advanced loss of oxygen neighbors of metal center is predictable, resulting in the subsequent further splitting of the orbitals.

Conclusively, metal ion catalysts could be classified into three types: (1) the homogeneous metal ions, (2) the heterogeneous surface metal ions with one defect, and (3) the heterogeneous surface metal ions with two or more defects. Since the coordination structure is at the heart of Lewis acid catalysis. Not only homogeneous and heterogeneous but amorphous and crystalized structures are predicted to have significant differences in reactivity and even selectivity.

1−1−2 Boron and Silicon Conjugate Addition Reactions

Organoboron and organosilicon derivatives are an important class of compounds, and their C–B linkages can be transformed into C–O, C–N, as well as C–C bonds through 1,2-migration of intermediary ate complexes with appropriate nucleophiles.[104] Transformations *via* boron intermediates can provide an ensured route with easy handling, accessible to complicated compounds, which are difficult to obtain by other methods.[105] In the meanwhile, the incorporation of silicon affords compounds with increased robustness under harsh conditions, increased lipophilicity, and significantly modified polarization compared with their carbon analogues, resulting in unique activities and phenomena.[106] More importantly, we can produce a number of chiral structures through well-known couplings of enantioenriched organoboron and organosilicon compounds as one of the most effective methods, especially when the direct introduction of chirality is difficult.[107]

On the other hand, despite the numerous synthetic methods to synthesize organoboron/silicon compounds, it is still difficult to afford the enantiopure products. Enantioselective boron/silicon conjugate addition to α,β-unsaturated carbonyl and related compounds provides one of the most reliable methods to give chiral organoboron/silicon compounds. Pioneering Cu(I)-catalyzed conjugate borylation were reported by Hosomi *et al.*[108] and Miyaura *et al.*[109] independently.

Scheme 1.1. Cu(I)-catalyzed conjugate borylation by Hosomi *et al.*[108]

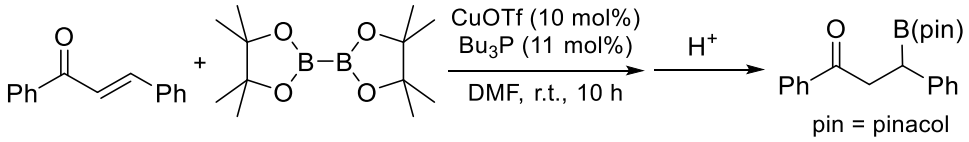

Scheme 1.2. Cu(I)-catalyzed conjugate borylation by Miyaura *et al.*[109]

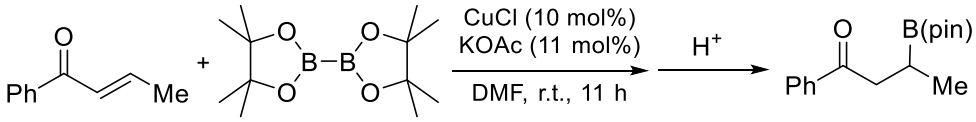

One of the key points were the successful identification of Cu(I)-B species. The discovery of Cu-B intermediate greatly promoted the further investigations on Cu(I)-catalyzed conjugate borylation reactions and development of its silicon version follows boron due to the relative unstability of Cu(I)-Si species under strong basic conditions.

Yun *et al.* initially focused on the effects of additives on Cu(I) catalyzed boron conjugate reactions and established the employment of alcohol as a standard additive.[110] Alcohol additives were found to both accelerate the initial reaction rate and increase the reaction yield in organic solvent. Moreover, Yun *et al.* succeeded in the first enantioselective boron conjugate addition reaction with Josiphos ligand, even though the substrate generality was limited to β-hydroxy nitrile compound.[111] Several following studies focusing on phosphine type ligands indeed lead to the successful enantioselective boron conjugate addition reactions with broader substrate generality (Figure 1.5).[112] Esters, nitriles, and normal unsaturated ketones were converted to the corresponding products in high yields with high enantioselectivities.

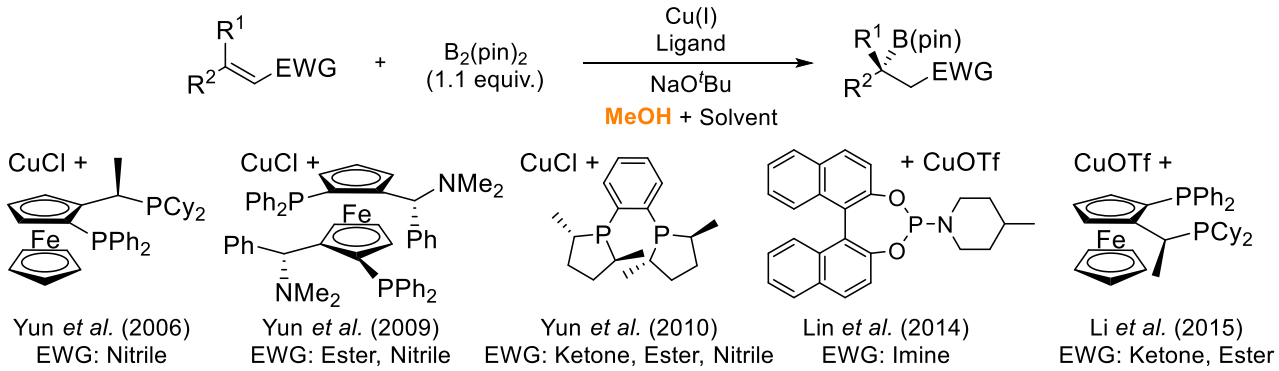

Figure 1.5. Recent developments on Cu(I)-catalyzed enantioselective boron conjugate reactions with alcohol as additive.

Meanwhile, systems using additives except for alcohols were also investigated, mainly by Shibasaki *et al.*[113] It was found that diamine-Cu(I) complex could afford the products in high yield with high enantioselectivity. It is noted that in these examples alcohol additives were not required for the smooth reaction, but would even inhibit the reaction. Yet Cu(I)-diamine complex can only promote the reactions of unsaturated ketones with good results and cannot apply to other type of substrates such as ester and amide.

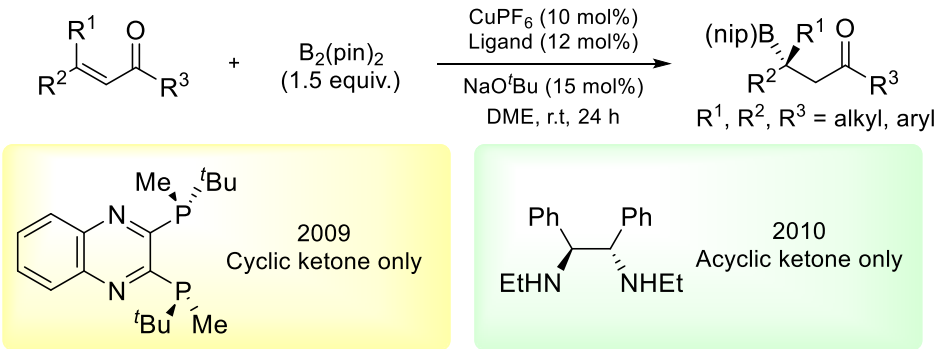

Figure 1.6. Recent developments on Cu(I)-catalyzed enantioselective boron conjugate reactions without alcohol as additive.

Although Cu(I) played a significant role in development of boron conjugated addition reactions, other metals such as Fe,[114] Ni,[115] Zn,[116] Pt,[117] Pd,[118] Ag,[119] and Ir[120] were also found to be practical catalysts for β-borylation. One of the advantages for the employments of transition metals in second or third d block series as catalysts is no need to use strong base for the reactions. Yet several drawbacks such as high temperatures and too complicated solvent systems were obvious. Ni(II) seemed to be a promising metal catalyst instead of Cu(I), which is too sensitive to water. However, the use of stoichiometric amount of strong base and protonic additives restricted the application. In 2010, Fernández successfully achieved another metal-free catalyst using inexpensive phosphine ligand.[121] The employment of phosphine ligand at room temperature is indeed advantageous to applications on industrial scales and is environmental friendly. However, the necessity of large modification on ligand structures to apply to a wide range of substrates diminished the value. Interestingly, only aliphatic substrates were available in high yields and high enantioselectivities (Figure 1.7).

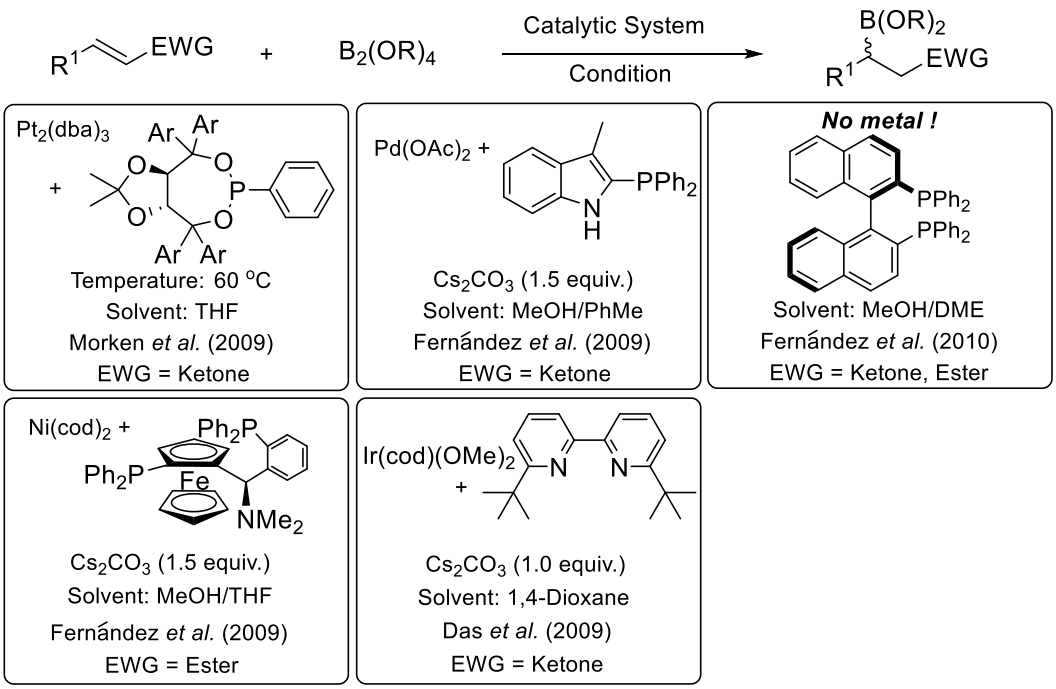

Figure 1.7. Several other examples of asymmetric β-borylation reactions.

On the other hand, it was not surprising that Rh catalysts could catalyze both borylation reactions and silylation reactions. Kabalka *et al.* reported the first Rh(I)-mediated β-borylation reactions with a wide substrate generality including α,β-unsaturated ketones, esters, aldehydes, and nitriles at 80 °C. In 2006, Oestreich *et al.* reported the Rh(I)-catalyzed protocol of silyl conjugate additions of cyclic enones and lactones and the substrate generality was further expanded in 2008.[122] Successively, this protocol was further improved and applied on total syntheses of natural compounds.[123] Afterwards, Rh(II) was found to be applicable to asymmetric borylation reactions in

excellent yield with high enantioselectivity, while the substrate generality was limited to esters and amides (Figure 1.8).[124] Despite the limited number of reports on Rh-mediated borylation/silylation reactions, the general mechanism of rhodium-catalyzed reactions have been well studied even before the discovery of boron/silicon conjugate additions. Similar to Cu(I) catalysts, alkene-rhodium species was proposed as a key intermediate.

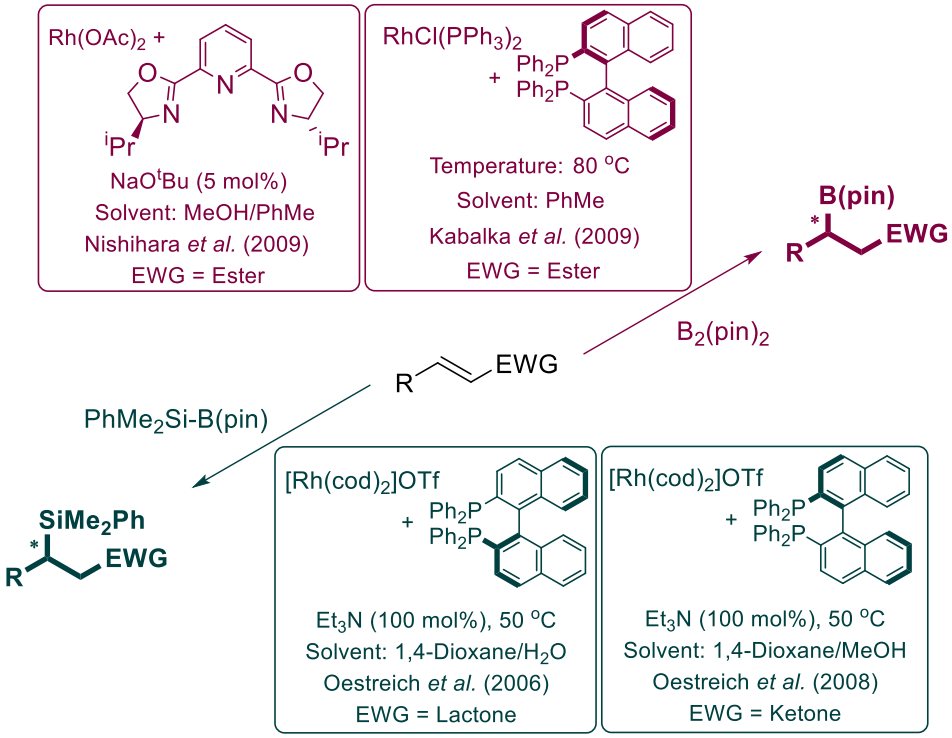

Figure 1.8. Rhodium catalyzed asymmetric β-borylation/silylation reactions.

Another breakthrough in asymmetric β-borylation/silylation reactions is the emergence of N-heterocyclic carbene (NHCs) catalysts.[125] The potential of Cu(I)-based NHC complexes was demonstrated by Hoveyda *et al.* for the first time to generate quaternary stereogenic centers in boron conjugate additions as well as in silicon conjugate additions.[126] In the absence of a protic additive, the corresponding boron/silicon enolate was obtained as an intermediate. In succession of NHC-Cu(I) catalyzed borylation reactions, Hong *et al.* reported the structural modification of NHC precursor to apply to asymmetric α,β-unsaturated *N*,*N*-dialkylated amides.[127] In contrast to 5-membered NHC rings, 6-membered NHC rings are marked by the change of both steric and electronic properties along with increased ring size. The extended N–C–N bond angle is suggested to affect the carbine-metal bond, providing a more restrictive chiral pocket that is constructed by a blocking group on one side. Increased electron-donating ability leads to higher nucleophilicity of NHC, which is confirmed through their IR stretching frequencies.[128] McQuade's is the pioneer of employing 6-membered NHC-Cu(I) catalyst for β−borylation reactions.[129] Their catalyst exhibited superb activity, showing 10,000 catalytic turnover numbers (TONs) at 0.01 mol% of catalyst, the highest value at that time.

Subsequently, 6-membered NHC catalyst bearing chiral 3,4-dihydroquinazolinium core was examined in asymmetric boron conjugate addition toward α,β-unsaturated esters at 1 mol% catalyst loading (Figure 1.9).[130] Successive reports included the chiral imidazolinium zwitterion type NHC catalyst[131] and *pseudo-ortho*-disubstituted [2,2]paracyclophane type NHC catalysts.[132] Curiously, despite the numerous efforts on deceloping NHC-Cu(I) catalyzed borylation reactions, NHC-Cu(I) mediated silylation reactions acquired much less attention and the focus were mainly on the expansion of substrate generality.[133] On the other hand, metal-free NHC catalysts were also found capable for both β-borylation/silylation reactions.[134]

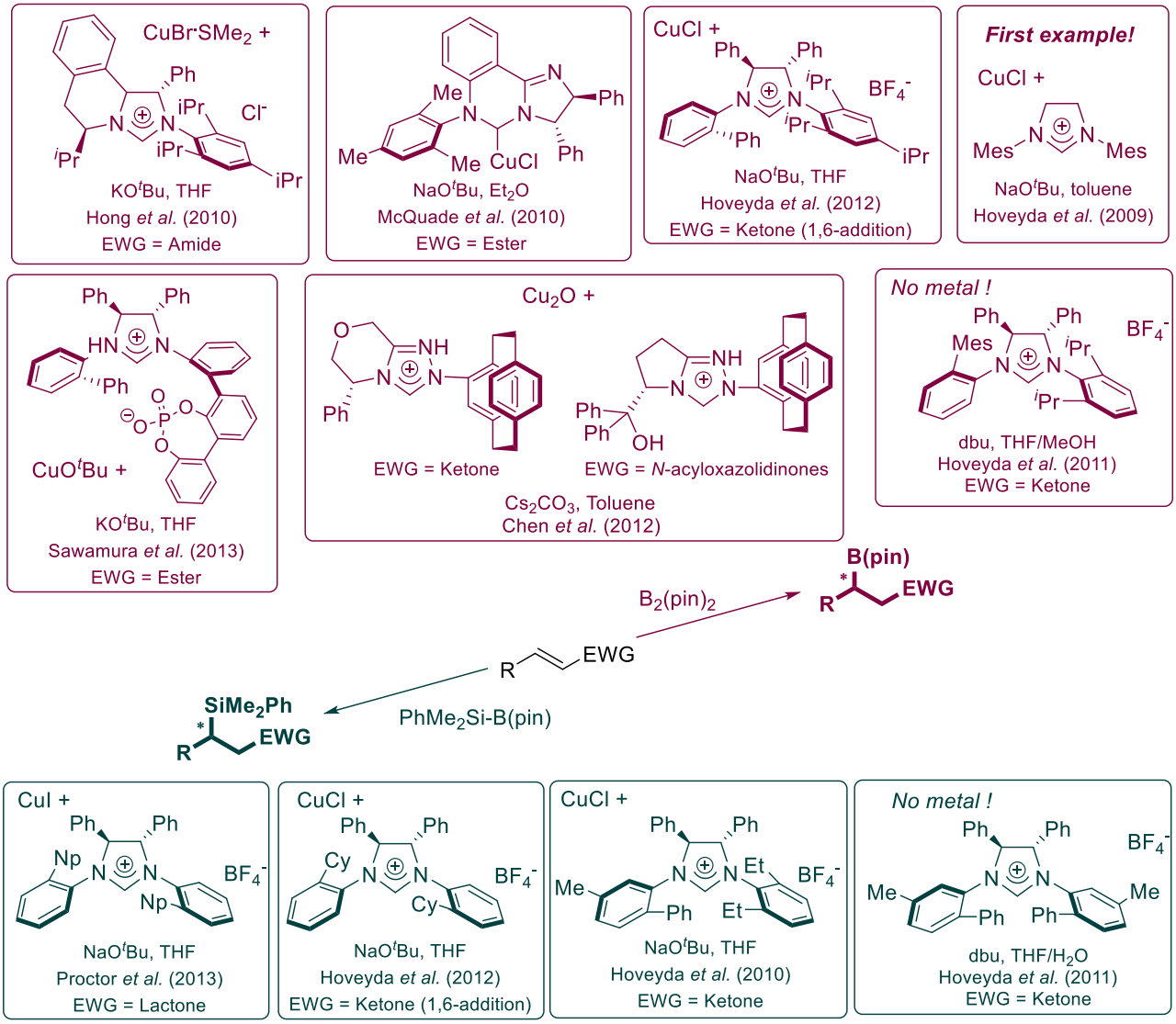

Figure 1.9. Summary of NHC catalysts for asymmetric β-borylation/silylation.

It should be emphasized that although NHC-Cu(I) is found widely applicable to both borylation and silylation, the bothersome reaction conditions including complicated ligand synthesis, ligand structure-dependent substrate scope, and low temperature (-78 °C) have impeded further applications.

Despite the flourish of Cu(I) catalysts in borylation/silylation reactions, Cu(II) catalyst was

rarely explored. Although recently, Santos *et al*. reported both β-borylation reaction and β-silylation reaction under very mild condition using Cu(II) catalyst in water, it was achiral reaction and only limited esters and ketones were available.[135] A new system for asymmetric boron conjugate addition, which can be performed under mild condition with wider substrate generality, is eagerly expected. Moreover, a detailed mechanistic study is required to reveal the behavior of copper catalysts.

In summary, intensive studies had been carried out on asymmetric boron conjugate addition reactions while the reports on asymmetric silicon conjugate addition reactions are limited. NHC-type catalysts as well as Rh catalysts were revealed to be applicable for both reactions. Moreover, Cu(I) catalysts as well as Ni, Pt and several other metal catalysts were found useful in chiral β-borylation. Several metal-free protocols were also investigated as an alternative to improve the result of chiral β-borylation. However, in all of these cases, the strict anhydrous condition, use of strong base and protonic organic solvents are imperative for the smooth progress of the reactions. Moreover, the substrate generalities in all of these cases are moderate. In order to overcome and improve the condition and the result, we continued to develop a new asymmetric boron and silicon conjugate addition system, which can proceed under mild condition with much wider substrate generality.

1-2 Optimization of Reaction Conditions

Inspired by the characteristic performance of metal hydroxides as catalysts in aqueous media, initial investigation was conducted to examine their possibility to catalyze enantioselective boron conjugate additions in water.

First, $B_2(pin)_2$ and chalcone **1a** were chosen as model substrates for the reaction and several promising metal hydroxides as heterogeneous catalysts were examined (Table 1). As a result, it was found that when $Cu(OH)_2$ was combined with dibenzylamine, the desired 1,4-addition product **1aa** was obtained in 88% yield (Entry 1). $Zn(OH)_2$ showed inferior reactivity (Entry 2). Next, several chiral ligands were examined based on the previous knowledge on the combination of water-compatible Lewis acidic metals and ligands. It was revealed that $Cu(OH)_2$-**L1**[136] catalyst showed promising result; the desired product was obtained in 83% yield with 81% ee in the presence of 10 mol% of $Cu(OH)_2$ and 12 mol% of **L1** at room temperature in water for 12 h. The corresponding $Zn(OH)_2$-**L1** catalyst gave low yield and moderate enantioselectivity. The use of **L2** and **L3** with $Cu(OH)_2$ afforded high yields, though the enantioselectivities were moderate. When no ligand was employed, the product was obtained in 22% yield.

Table 1.1. Initial screening for enantioselective borylation reactions.

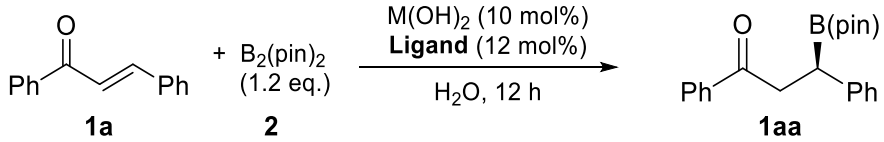

Entry	M	**Ligand**	Yield (%)	Ee (%)
1	Cu	Dibenzylamine	88	-
2	Zn	Dibenzylamine	64	-
3	Cu	**L1**	83	81
4	Zn	**L1**	17	46
5	Cu	**L2**	79	36
6	Cu	**L3**	80	37
7	Cu	-	22	-

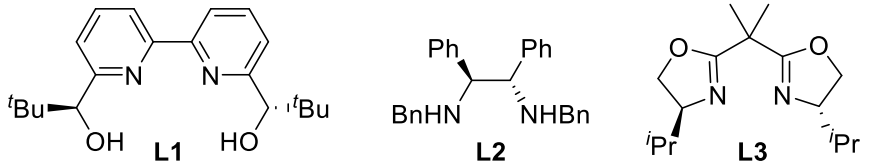

Similarly, enantioselective silicon conjugate additions in water was examined with several insoluble Cu(II) catalysts. While the direct use of $Cu(OH)_2$, $Cu_2(OH)_2CO_3$ or $Cu(acac)_2$ with **L1** only afforded the product in moderate yield with low enantioselectivity, acicular purplish crystals obtained

from $Cu(acac)_2$ and **L1** worked well in the reaction of chalcone with $PhMe_2Si$-B(pin) to provide the desired product **1ab** in good yield with high selectivity (Table 1.2, Entry 4). The recrystallization of $Cu(OH)_2$ or $Cu_2(OH)_2CO_3$ has failed due to their insolubility in any solvent. The reaction did not proceed at all without addition of any ligand.

Table 1.2. Initial screening for enantioselective silylation reactions.

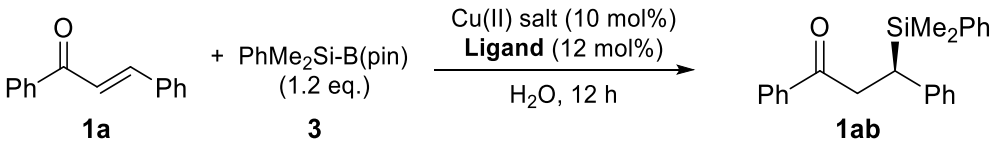

Entry	Cu(II)	**Ligand**	Yield (%)	Ee (%)
1	$Cu(OH)_2$	**L1**	39	12
2	$Cu_2(OH)_2CO_3$	**L1**	50	18
3	$Cu(acac)_2$	**L1**	42	26
4[a]	$Cu(acac)_2$	**L1**	84	93
5	$Cu(acac)_2$	-	N.R.	-

[a] $Cu(acac)_2$ and **L1** were crystalized before use.

Table 1.3. Additive Screening.

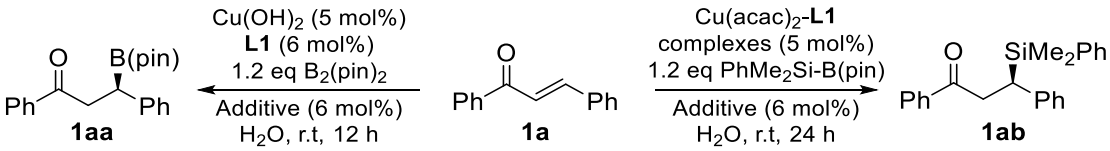

Borylation		Entry		Entry	Silylation	
Yield(%)	Ee(%)		Additive		Yield(%)	Ee(%)
86	81	1A	PhCOOH	1B	76	72
82	83	2A	HCOOH	2B	N.T.	-
93	**89**	3A	CH_3COOH	3B	82	92
89	84	4A	C_2H_5COOH	4B	N.T.	-
93	86	5A	CF_3COOH	5B	87	12
87	86	6A	Ascorbic acid	6B	86	91
94	87	7A	H_3BO_3	7B	84	87
91	77	8A	$PhB(OH)_2$	8B	N.T.	-
72	70	9A	Pyridine	9B	78	62
65	80	10A	KOH	10B	40	59
90	77	11A	CH_3COOK	11B	82	49

On the other hand, the catalyst loading was set to 5 mol% and several reaction conditions were investigated to improve the yield and enantioselectivity. The addition of additives was known to be effective for the improvement of catalyses.[137] Although the actual effects of additives remain unknown in general, additives sometimes possess advantages such as lowering the energy barrier, increasing the Lewis acidity of metal center and strengthening the catalyst-substrate binding. A number of additives were screened (Table 1.3).

As a result, acid additives showed an overall superiority over basic additives in both reactions. In borylation, less water-soluble acid additives such as benzoic acid and propionic acid improved the yield, but hardly affected the enantioselectivity. The addition of acetic acid, trifluoroacetic acid or ascorbic acid had positive effects on both reactivity and enantioselectivity, and using acetic acid as additive has afforded the highest enantioselectivity in $Cu(OH)_2$-mediated borylation reaction. In silylation, weakly acidic additives almost did not affect the reaction while strongly acidic additives such as trifluoroacetic acid have significantly deteriorated the enantioselectivity. In both borylation and silylation reactions, the basic additives, especially those capable of coordinating strongly with copper center (e.g. pyridine), gave decreased enantioselectivity. In summary of additive screening, acetic acid and boronic acid gave the highest yields and enantioselectivities in borylation, while no additive gave improved results in silylation.

1-3 Effect of Water

Next, several solvents and co-solvent systems were screened to demonstrate the positive role of water (Table 1.4). In the previous reports of metal hydroxide mediated asymmetric reactions in aqueous media, the employment of water-organic co-solvent systems showed superior reactivities and selectivities to 100% water systems.[138,139]

It was found that the reaction did not proceed at all in typical organic solvents such as THF, CH_2Cl_2, DMF, and DMSO (Entries 3A/B-7A/B). On the other hand, protic organic solvent such as MeOH and EtOH can somewhat promote the reaction while the enantioselectivities were low (Entries 8A/B, 9A/B). Both reactions failed to give the desired adducts when performed without any solvent (neat conditions) (Entries 2A, 2B). When co-solvent system was used, both enantioselectivity and yield were almost retained in borylation reactions while the enantioselectivity decreased significantly in silylation reactions (Entries 10A/B, 11A/B). Based on these results, the use of water without any organic solvent was confirmed to be indispensable for getting high reactivity and selectivity.

Table 1.4. Solvent Screening.

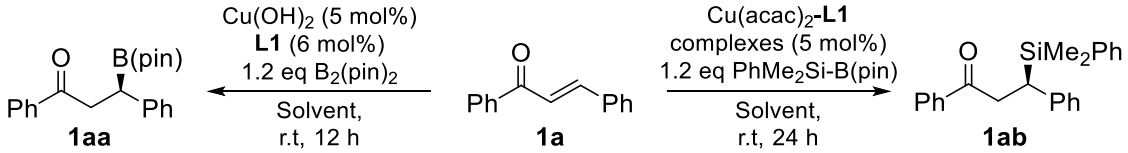

Borylation		Entry		Entry	Silylation	
Yield(%)	Ee(%)		Solvent		Yield(%)	Ee(%)
83	81	1A	H_2O	1B	84	93
N.R.	-	2A	neat	2B	N.R.	-
N.R.	-	3A	CH_2Cl_2	3B	N.R.	-
N.R.	-	4A	THF	4B	N.R.	-
N.R.	-	5A	Et_2O	5B	N.R.	-
N.R.	-	6A	Toluene	6B	N.R.	-
N.R.	-	7A	DMSO	7B	N.R.	-
17	29	8A	MeOH	8B	22	31
1	41	9A	EtOH	9B	4	0
82	34	10A	H_2O/MeOH =1/4	10B	76	37
77	79	11A	H_2O/THF =1/4	11B	73	6

1-4 Effects of Copper Salts

Then several copper salts were screened to demonstrate the difference between heterogeneous and homogeneous conditions, as well as the anion effects.

Table 1.5. Screening of copper salts.

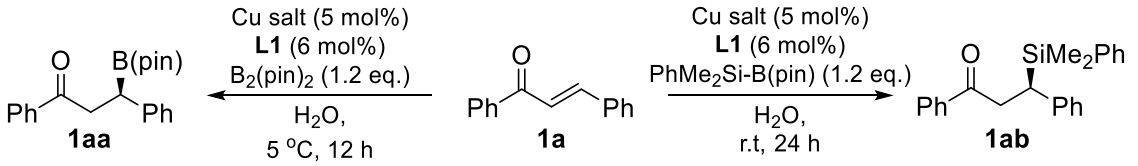

Borylation		Entry		Entry	Silylation	
Yield(%)	Ee(%)		Cu salt		Yield(%)	Ee(%)
83	81	1A	$Cu(OH)_2$	1B	47	8
95	99	2A	[a]$Cu(OH)_2$	2B	57	12
89	87	3A	$Cu_2(OH)_2CO_3$	3B	50	18
90	94	4A	[a]$Cu_2(OH)_2CO_3$	4B	56	24
96	82	5A	$Cu(acac)_2$	5B	42	26
93	81	6A	[b]$Cu(acac)_2$	6B	84	93
90	82	7A	[a,b]$Cu(acac)_2$	7B	82	92
N.R.	-	8A	CuO	8B	N.R.	-
89	69	9A	$Cu(OTf)_2$	9B	39	18
87	68	10A	[b]$Cu(OTf)_2$	10B	49	28
62	65	11A	$CuSO_4$	11B	46	17
71	61	12A	$CuCl_2$	12B	43	37
82	54	13A	$CuBr_2$	13B	37	35
62	54	14A	$Cu(LS)_2$	14B	43	32
95	91	15A	$Cu(OAc)_2$	15B	62	9
94	91	16A	[b]$Cu(OAc)_2$	16B	74	28

[a] 6 mol% of AcOH was added as additive [b] Pre-crystallization was conducted.

Despite the insolubility of all materials (both chalcone (**1a**) and $B_2(pin)_2$ (**2**) or $PhMe_2Si$-B(pin) (**3**), $Cu(OH)_2$ and chiral ligand **L1**) in water, the reactions proceeded smoothly in good yield with good enantioselectivity (Table 1.5, Entries 1A/B-7A/B). The addition of acetic acid to $Cu(OH)_2$ or $Cu_2(OH)_2CO_3$ contributed to better results in both yield and enantioselectivity, while acetic acid did not affect the reaction when $Cu(acac)_2$ was employed (Entries 1A/B, 4A/B, 5A/B, 7A/B). When the purplish crystal obtained from $Cu(acac)_2$ and **L1** was used, a significant improvement of yield and enantioselectivity was observed in silylation reaction while borylation reaction was not affected (Entries 6A, 6B). Heterogeneous CuO catalyzed neither of reactions. Most homogeneous Cu(II) salts

promoted both reactions to afford the products in moderate yield with moderate enantioselectivity. The pre-crystallization of soluble Cu(II) species and **L1** had little influence on activity and selectivity, probably due to dissociation of the crystals in water (Entries 6A/B, 7A/B, 16A/B).

During the screening of the Cu(II) salts, it was noticed that while the reaction mixture was heterogeneous (Entries 1A/B-8A/B), the catalyst systems were almost homogeneous (Entries 9A/B-16A/B). Especially in borylation reactions, the appearance of the reactions was compared between heterogeneous $Cu(OH)_2$ and homogeneous $Cu(OAc)_2$ (Figure 1.10). In the reaction using $Cu(OH)_2$, a light-blue heterogeneous system consisting of $Cu(OH)_2$, **L1** in water was observed (top row, (a)). After the addition of chalcone, the color remained unchanged with yellowish chalcone dispersing heterogeneously in the solution (top row, (b)). The color changed immediately into brown after addition of $B_2(pin)_2$ (top row, (c)), and the brown color became dark after 15 min (top row, (d)); the same color was maintained even after 30 min and 60 min (top row, (e) and (f)). Finally after 12 h, the reaction mixture was obtained with a similar color (top row, (g)). In all stages, the reaction mixture looks heterogeneous. On the other hand, a light-blue homogeneous solution was formed by combining $Cu(OAc)_2$ with **L1** (bottom row, (a)). After addition of **1a** and $B_2(pin)_2$ (both are solid and insoluble in water at the initial stage), the same color was maintained at first (bottom row, (b) and (c)), then gradually became brown (bottom row, 15 min - (d), 30 min - (e), and 60 min - (f)). Because the starting materials and the product (**1aa**) were not soluble in water, some insoluble materials existed in the reaction mixture; however, the catalyst remained soluble even after 12 h (bottom row, (g)).

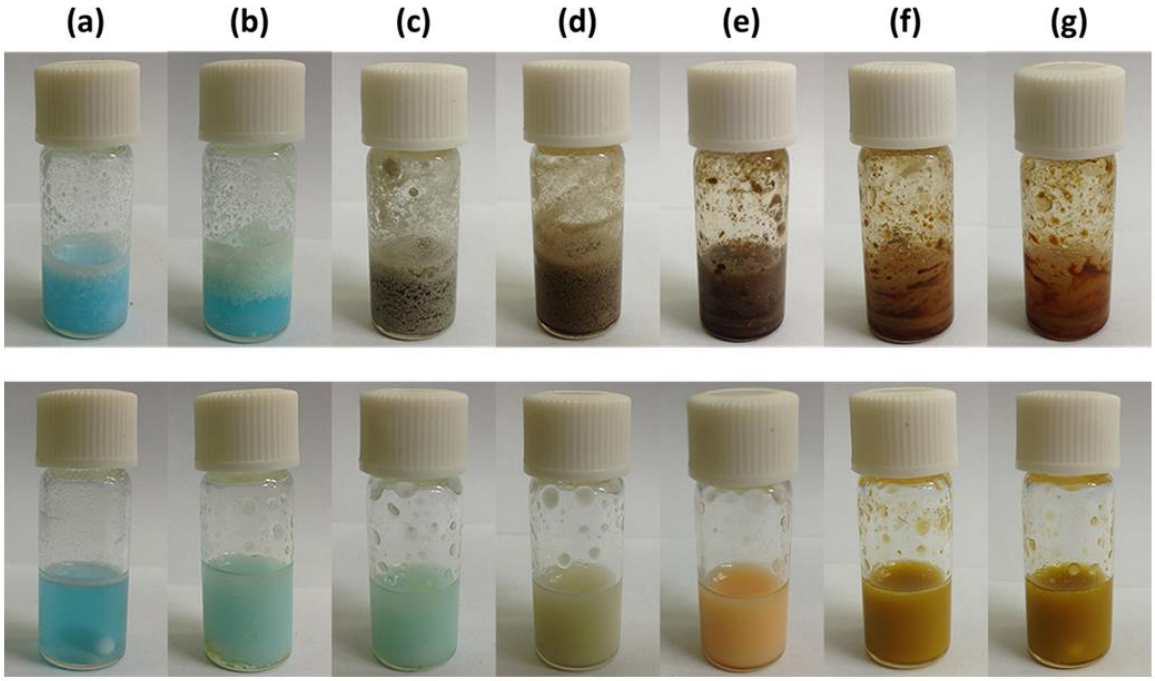

Figure 1.10. Comparison of the appearance of the borylation reactions using $Cu(OH)_2$ (top) and $Cu(OAc)_2$ (bottom). (a) Prepared catalyst solution with L1; (b) just after addition of 1a;

(c) 1 min after addition of $B_2(pin)_2$; (d) 15 min; (e) 30 min; (f) 60 min, (g) 12 h.

Similar phenomena were also observed in silylation reactions. In order to confirm the homogeneity or heterogeneity of both catalysts, filtration tests were then conducted (Scheme 1.3).

Scheme 1.3. Filteration tests.

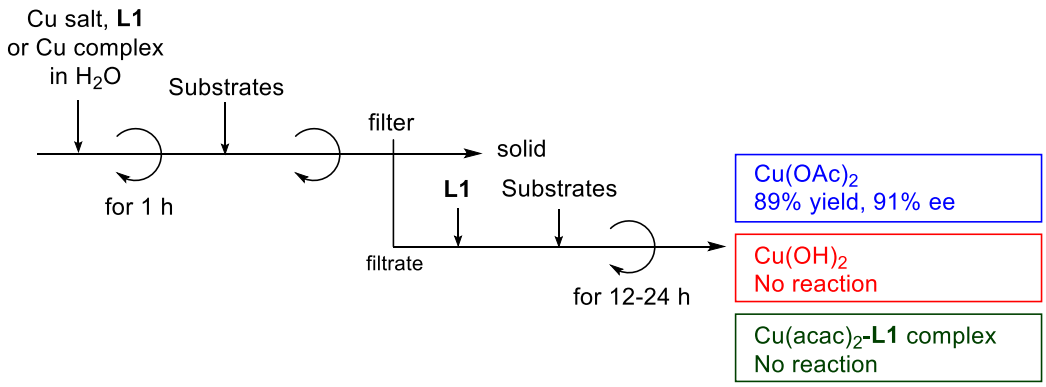

For borylation reactions, in the presence of $Cu(OH)_2$ (5 mol%) and **L1** (6 mol%), chalcone **1a** was combined with $B_2(pin)_2$ in water. After 10 min, the reaction mixture was filtered. The filtrate was analyzed by ICP analysis. It was confirmed that the Cu content in the filtrate was under the detection limit of the ICP equipment (0.005 ppm). Additional chalcone **1a** and $B_2(pin)_2$ in the filtrate could not further produce any product. On the other hand, when $Cu(OAc)_2$ (5 mol%) and **L1** (6 mol%) were combined, a homogeneous solution was formed. These homogeneous systems remained even after the addition of chalcone **1a** and $B_2(pin)_2$. Even after filtration, the filtrate was able to catalyze the reaction to give the product in 89% yield with 91% ee without additional copper source. Similarly, filtration test was conducted to confirm heterogeneous $Cu(acac)_2$-**L1** complex with silylation reactions, and it was confirmed that the Cu leaching of the filtrate is under the detection limit (0.0014 ppm), which did not afford any product. In conclusion, it was confirmed that both $Cu(OH)_2$ and $Cu(acac)_2$-**L1** complex produced heterogeneous catalyst, while $Cu(OAc)_2$ afforded a homogeneous catalyst.

In borylation, it was found that a brown color of the reaction mixture might indicate the formation of the product. Since the color of $Cu(OH)_2$ system changed much faster than that of $Cu(OAc)_2$ system, it seemed that $Cu(OH)_2$-catalyzed reaction was faster than $Cu(OAc)_2$-catalyzed reaction. To confirm this, a preliminary kinetic study on $Cu(OH)_2$- and $Cu(OAc)_2$-catalyzed boron conjugate addition in water was conducted. The profiles of the reactions of chalcone **1a** with $B_2(pin)_2$ in the presence of $Cu(OH)_2$ with **L1** and $Cu(OAc)_2$ with **L1** are shown in Figure 1.11. It was revealed that the reaction using $Cu(OH)_2$ was much faster than that using $Cu(OAc)_2$.

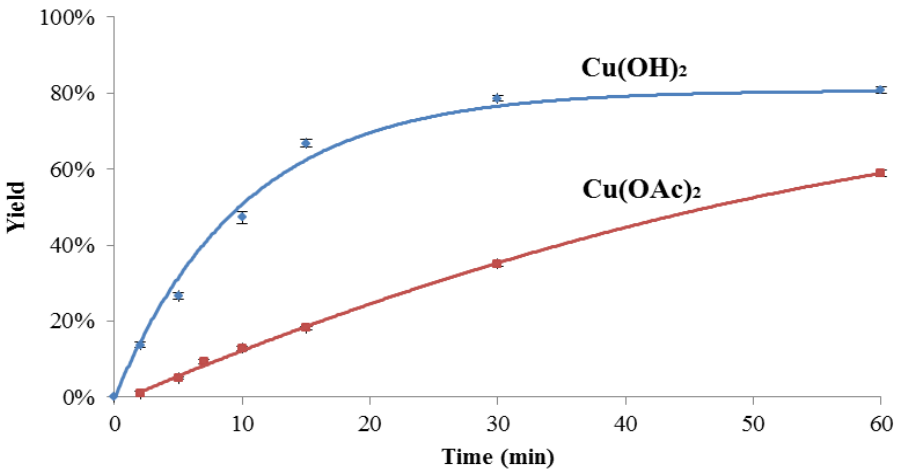

Figure 1.11. Reaction profile on $Cu(OH)_2$- and $Cu(OAc)_2$-catalyzed boron conjugate addition in water.

Turnover frequency (TOF) experiments were also conducted in the reaction of chalcone **1a** with $B_2(pin)_2$ or $PhMe_2Si$-B(pin) (Scheme 1.4). In previous reports, the TOF was less than 50 h^{-1}, except for one report on the borylation reaction where 5580 h^{-1} TOF was attained using a chiral carbene Cu(I) complex in toluene.[129] In borylation reactions, in the presence of 0.005 mol% of three catalyst systems, namely $Cu(OH)_2$-**L1**, $Cu(OH)_2$-CH_3COOH-**L1** and $Cu(OAc)_2$-**L1**, chalcone **1a** was treated with $B_2(pin)_2$ in water for 15 min, and similarly, in the presence of 0.005 mol% of $Cu(acac)_2$-**L1** complex or $Cu(OH)_2$-**L1** system, TOF experiments were conducted. The results are shown in Scheme 1.4. In borylation reactions, TOFs of 17,600 h^{-1} and 12,800 h^{-1} were obtained using $Cu(OH)_2$ with acetic acid as an additive and $Cu(OAc)_2$, respectively, with high enantioselectivities. The TOF reached 43,200 h^{-1} when $Cu(OH)_2$ was used, the highest value in asymmetric boron conjugate addition reactions ever reported, although the enantioselectivity was slightly lower. Similarly, TOF of 15,200 h^{-1} was obtained for silylation reaction in $Cu(OH)_2$-**L1** system with low enantioselectivity. It is noted that 0.005 mol% of heterogeneous $Cu(acac)_2$-**L1** complex did not catalyze at all.

Scheme 1.4. Turnover Frequency.

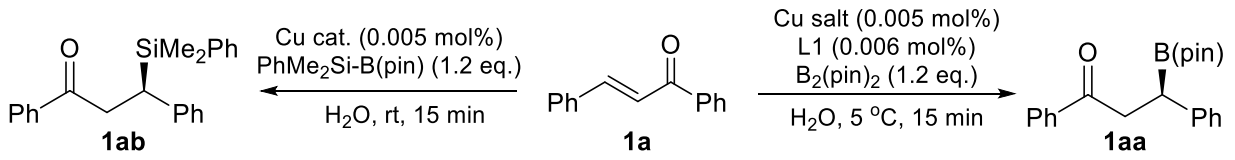

$Cu(OH)_2$ + 0.006 mol% **L1**:
19% yield, 11% ee. TOF: 15,200 h^{-1}

$Cu(acac)_2$-**L1** complex:
Trace. TOF: Not Available

$Cu(OH)_2$:
54% yield, 63% ee. TOF: 43,200 h^{-1}

$Cu(acac)_2$-**L1** complex:
Trace. TOF: Not Available

$Cu(OH)_2$ + CH_3COOH:
22% yield, 85% ee. TOF: 17,600 h^{-1}

$Cu(OH)_2$ + CH_3COOH:
16% yield, 79% ee. TOF: 12,800 h^{-1}

Table 1.6. Turnover Number of $Cu(OH)_2$ with acetic acid as additive in borylation reaction.

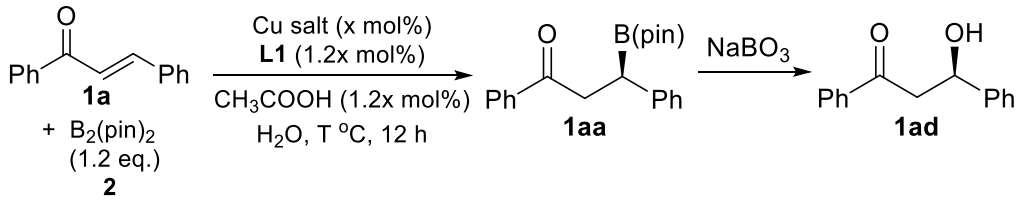

Entry	x	T (°C)	Yield (%)	Ee (%)	TON
1	5	31	94	84	19
2	5	22	95	91	19
3	1	22	87	89	87
4	0.005	22	63	79	12600
5	0.005	5	49	84	9800

Finally, Turnover number (TON) experiments were performed in borylation reaction. The highest TON was achieved when catalyst loading was decreased to 0.005 mol% at room temperature. At 5 °C, the TON decreased slightly while the enantioselectivity recovered to 84% (Table 1.6, Entry 5). High TON was not observed in $Cu(acac)_2$-**L1** complex system either. The detailed elucidation is presented in Section 1-7.

1-5 Substrate Scope

Next three catalyst systems: $Cu(OH)_2$ (5 mol%) and **L1** (6 mol%) (heterogeneous); $Cu(OH)_2$ (5 mol%), acetic acid (6 mol%), and **L1** (6 mol%) (homogeneous); $Cu(OAc)_2$ (5 mol%) and **L1** (6 mol%) (homogeneous), were tested in boron conjugate additions of 28 electrophiles, including acyclic and cyclic α,β-unsaturated ketone, β,β-disubstituted enone, α,β-unsaturated esters, amides, and nitriles. $Cu(acac)_2$-**L1** complex (5 mol%) obtained as purplish crystal from $Cu(acac)_2$ and **L1** was tested in silicon conjugate additions using 24 different substrates. Typically for boron conjugate additions, it was confirmed that the product, isolated as an α-chiral boron derivative **1aa**, was quantitatively converted to β-hydroxy ketone **1ad** or β-amino ketone **1ae** *via* subsequent oxidation or a substitution reaction (Scheme 1.5). Therefore during the substrate scope, most of the borylated products were directly transformed into β-hydroxy form for easier isolation and determination of the enantioselectivity.

Scheme 1.5. Quantitative transformation of β-borylated product 1aa.

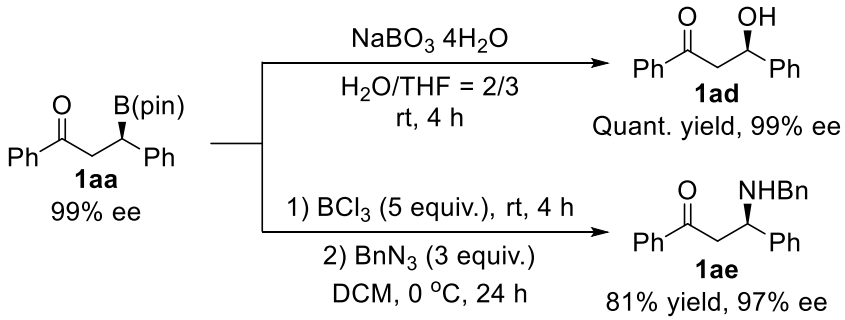

Table 1.7. Summary for substrate scope.

Reaction	Catalyst	Ketone	Ester	Amide	Amine	Nitrile	Nitroolefin	Others
Borylation	$Cu(OH)_2$+**L1**	○	○	×	△	△	×	△
	[a]$Cu(OH)_2$+**L1**	◎	○	○	○	○	×	△
	$Cu(OAc)_2$+**L1**	◎	○	○	○	○	×	△
Silylation	$Cu(acac)_2$-**L1**	◎	○	×	×	○	○	○

[a] 6 mol% of AcOH was added as additive. ◎ represents wide substrate generality with overall >85% yield and 85% ee; ○ represents wide substrate generality with overall >70% yield and 70% ee; △ represents limited substrate generality with overall >70% yield and 70% ee; × represents no reaction or limited substrate generality with low yield and low enantioselectivity.

The detail is summarized in Table 1.7. A wide generality of applicable substrates was realized and no previous catalysts have covered all these substrates with high yields and high enantioselectivities in either boron or silicon conjugate addition reactions. The detailed results and comparisons are shown as below:

1-5-1 Ketone-derived Substrates

In both borylation and silylation reactions, these Cu(II) catalysts were applicable to a wide range of α,β-unsaturated ketones including acyclic and cyclic α,β-unsaturated ketones as well as acyclic and cyclic β,β-disubstituted enones (Scheme 1.6).

Scheme 1.6. Common ketone-type substrates for borylation and silylation. [a] 6 mol% of AcOH was added as additive.

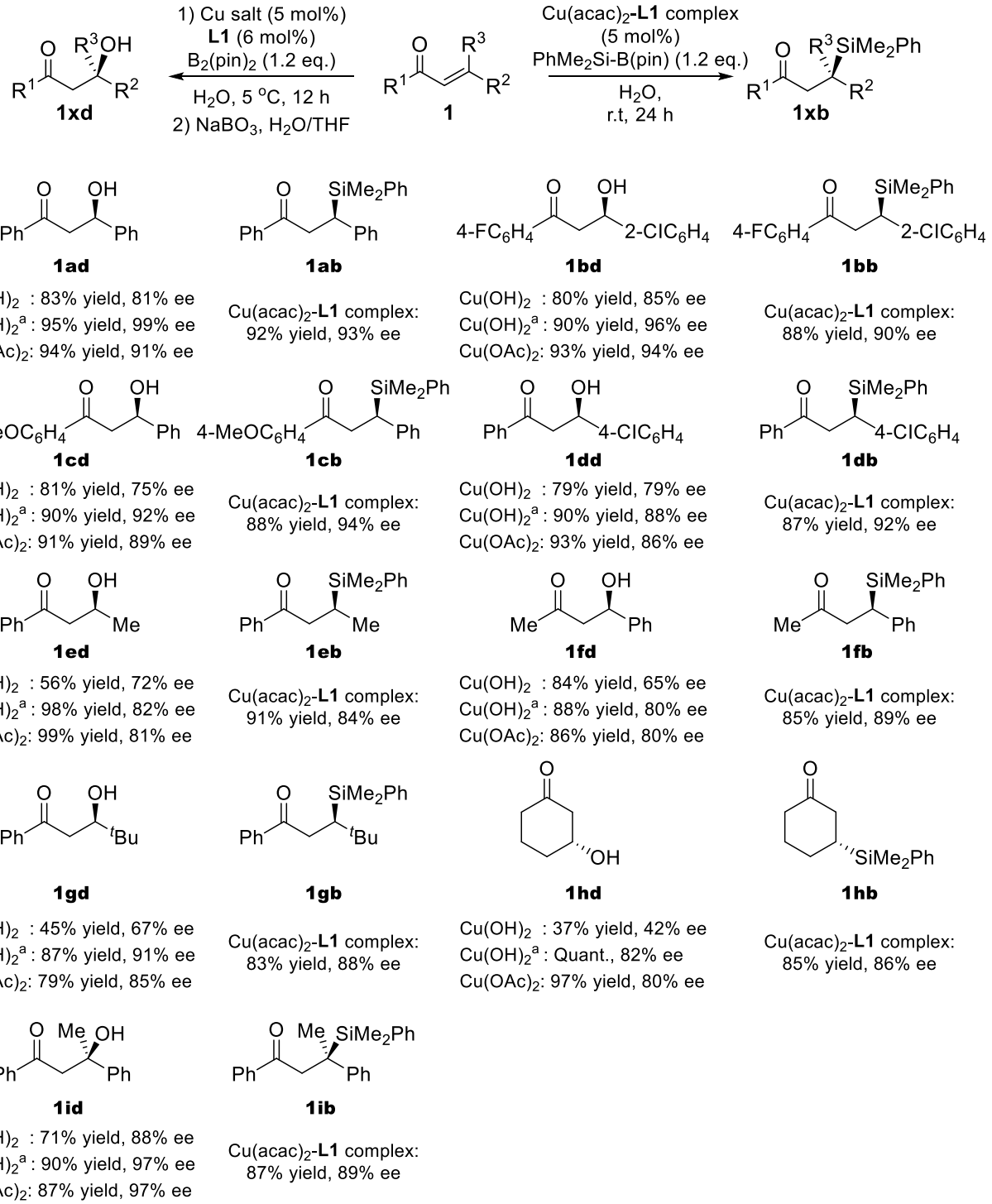

Scheme 1.7. Other ketone-type substrates for borylation.

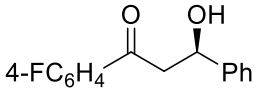

1jd

$Cu(OH)_2$: 81% yield, 72% ee.
$Cu(OH)_2$[a] : 91% yield, 89% ee
$Cu(OAc)_2$: 84% yield, 82% ee

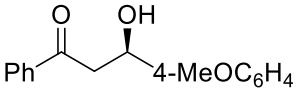

1kd

$Cu(OH)_2$: 81% yield, 84% ee
$Cu(OH)_2$[a] : 95% yield, 89% ee
$Cu(OAc)_2$: 90% yield, 82% ee

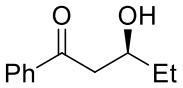

1ld

$Cu(OH)_2$: 59% yield, 76% ee
$Cu(OH)_2$[a] : 92% yield, 92% ee
$Cu(OAc)_2$: 90% yield, 88% ee

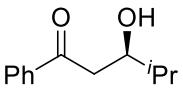

1md

$Cu(OH)_2$: 49% yield, 70% ee
$Cu(OH)_2$[a] : 91% yield, 88% ee
$Cu(OAc)_2$: 79% yield, 82% ee

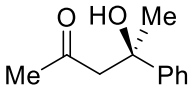

1nd

$Cu(OH)_2$: 68% yield, 78% ee
$Cu(OH)_2$[a] : 91% yield, 93% e
$Cu(OAc)_2$: 91% yield, 92% ee

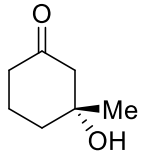

1od

$Cu(OH)_2$: 43% yield, 47% ee
$Cu(OH)_2$[a] : 91% yield, 86% ee
$Cu(OAc)_2$: 90% yield, 82% ee

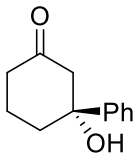

1pd

$Cu(OH)_2$: 21% yield, 63% ee
$Cu(OH)_2$[a] : 83% yield, 89% ee
$Cu(OAc)_2$: 84% yield, 87% ee

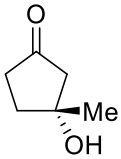

1qd

$Cu(OH)_2$: 57% yield, 24% ee
$Cu(OH)_2$[a] : 89% yield, 85% ee
$Cu(OAc)_2$: 80% yield, 84% ee

[a] 6 mol% of AcOH was added as additive.

Scheme 1.8. Other ketone-type substrates for silylation.

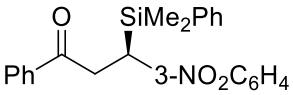

1rb

$Cu(acac)_2$-**L1** complex:
87% yield, 96% ee

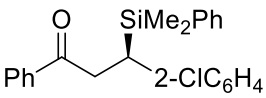

1sb

$Cu(acac)_2$-**L1** complex:
89% yield, 90% ee

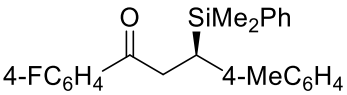

1tb

$Cu(acac)_2$-**L1** complex:
91% yield, 87% ee

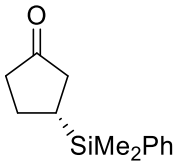

1ub

$Cu(acac)_2$-**L1** complex:
91% yield, 87% ee

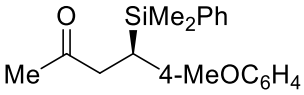

1vb

$Cu(acac)_2$-**L1** complex:
88% yield, 87% ee

For borylation reactions, the heterogeneous $Cu(OH)_2$+**L1** system showed relatively lower yields and enantioselectivities in most cases. In particular, low yields and enantioselectivities were observed for cyclic substrates.

It is noted that while Cu(acac)$_2$-**L1** catalyzed the reaction of NO_2 containing substrate in good yield with excellent enantioselectivity, this substrate was not tolerated with Cu(II)-mediated borylation due to the faster reduction of NO_2 group by $B_2(pin)_2$.

1-5-2 Imine-derived Substrates

Similarly, $Cu(OH)_2$ with **L1** was applied to the reaction of chalcone-derived imines with bis(pinacolato)diboron in water. The reaction proceeded smoothly to afford the desired product in high yield with moderate enantioselectivity after subsequent oxidation. Then several types of imines were examined. Whereas the reactions of α,β-unsaturated imines derived from isopropylamine or aniline gave low yields with low enantioselectivities (Table 1.8, Entries 1, 2), the use of the α,β-unsaturated imines derived from benzylamine resulted in high reactivity and excellent enantioselectivity (Entry 3). The reactions of α,β-unsaturated oxime or hydrazone produced poor results, presumably because of the strong coordination between copper and the substrates (Entries 4, 5).

Table 1.8. Screening of imines and copper salts.

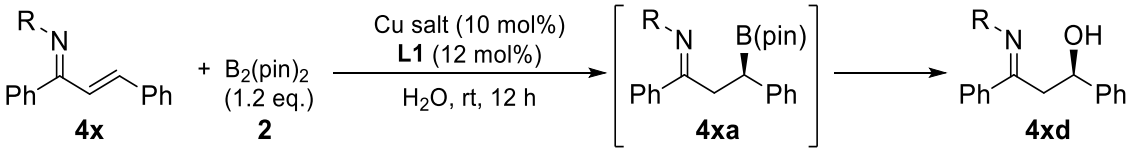

Entry	Cu salt	R	Yield (%)	Ee (%)
1	$Cu(OH)_2$	^{i}Pr	20	32
2	$Cu(OH)_2$	Ph	19	35
3	$Cu(OH)_2$	Bn	65	>99
4	$Cu(OH)_2$	OH	43	17
5	$Cu(OH)_2$	NHPh	Trace	-
6	$Cu(OAc)_2$	Bn	91	>99

Since the catalytic use of Cu(II) acetate resulted in higher yield of the desired product, which was formed with 99% ee (Entry 6), the scope of α,β-unsaturated imines was examined with the homogeneous $Cu(OAc)_2$+**L1** system (Scheme 1.9). It is noteworthy that imines bearing chalcone and benzalacetone backbones gave β-hydroxy imines with outstanding enantioselectivities (>99% ee). The use of a substrate with an electron-withdrawing substituent at the β-position resulted in lower enantioselectivity.

Scheme 1.9. Enantioselective β-borylation of α,β-unsaturated imines.

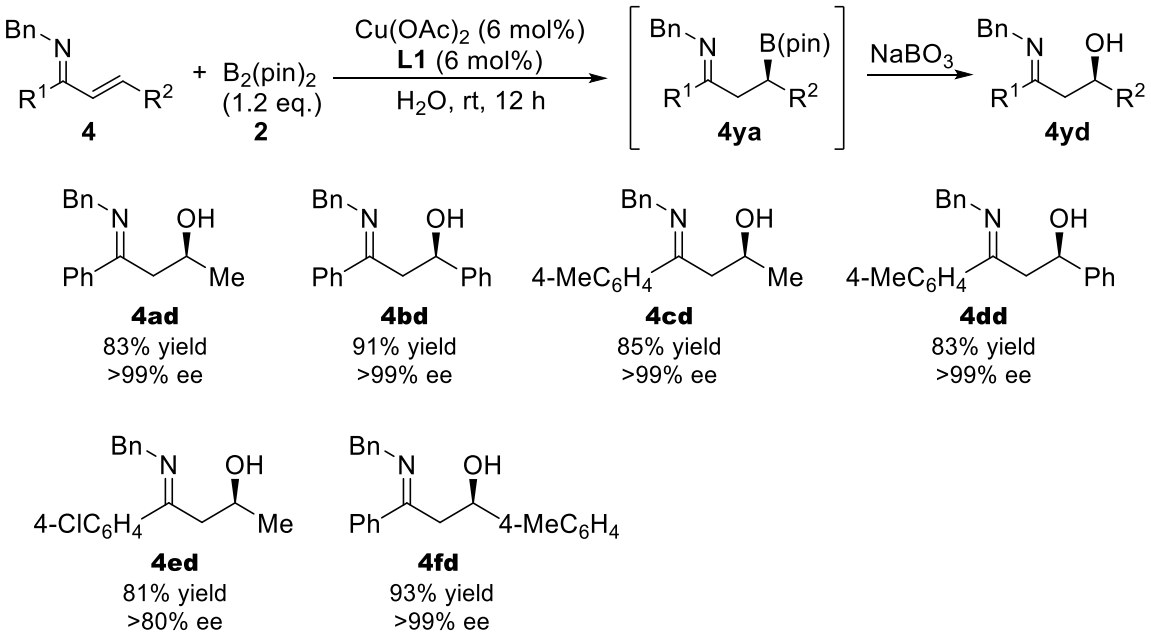

1-5-3 Ester-derived Substrates

Several acyclic and cyclic α,β-unsaturated esters including β,β-disubstituted forms were also examined for borylation and silylation reactions (Scheme 1.10). For borylation reactions, the heterogeneous $Cu(OH)_2$+**L1** system particularly afforded the desired acyclic ester adducts in high yield and enantioselectivity; in the reactions with cinnamyl esters, the yields and enantioselectivities were highest among the three catalyst systems. The $Cu(acac)_2$-**L1** complex catalyzed the silylation reactions of both acyclic and cyclic α,β-unsaturated esters in good yield with good enantioselectivity. It is noted that while both heterogeneous and homogeneous system were applicable to borylation of the β,β-disubstituted ester, the $Cu(acac)_2$-**L1** complex did not catalyze silylation reaction of the β,β-disubstituted ester at all.

Scheme 1.10. Common ester-type substrates for borylation and silylation.

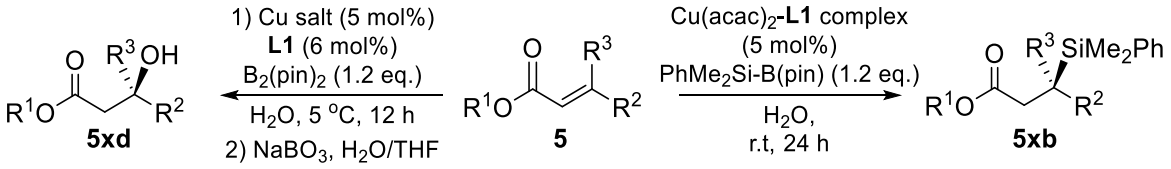

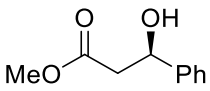

5ad

$Cu(OH)_2$: 85% yield, 82% ee
$Cu(OH)_2$[a] : 58% yield, 40% ee
$Cu(OAc)_2$: 55% yield, 35% ee

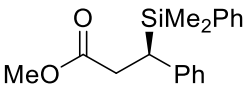

5ab

$Cu(acac)_2$-**L1** complex:
87% yield, 88% ee

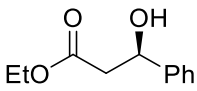

5bd

$Cu(OH)_2$: 73% yield, 82% ee
$Cu(OH)_2$[a] : 49% yield, 53% ee
$Cu(OAc)_2$: 32% yield, 51% ee

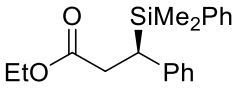

5bb

$Cu(acac)_2$-**L1** complex:
81% yield, 90% ee

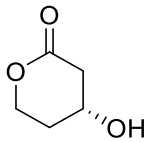

5cd

$Cu(OH)_2$: 42% yield, 59% ee
$Cu(OH)_2$[a] : 81% yield, 87% ee
$Cu(OAc)_2$: 80% yield, 84% ee

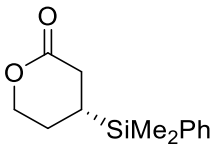

5cb

$Cu(acac)_2$-**L1** complex:
91% yield, 93% ee

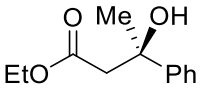

5dd

$Cu(OH)_2$: 70% yield, 81% ee
$Cu(OH)_2$[a] : 77% yield, 86% ee
$Cu(OAc)_2$: 78% yield, 83% ee

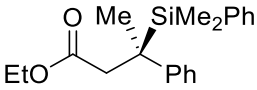

5db

$Cu(acac)_2$-**L1** complex:
NR

Scheme 1.11. Other ester-type substrates for borylation.

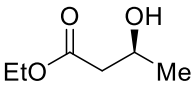

5ed

$Cu(OH)_2$: 80% yield, 84% ee
$Cu(OH)_2$[a] : 80% yield, 86% ee
$Cu(OAc)_2$: 75% yield, 81% ee

Scheme 1.12. Other ester-type substrates for silylation.

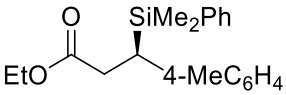

5fb

$Cu(acac)_2$-**L1** complex:
84% yield, 85% ee

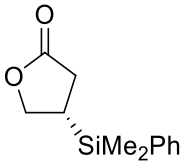

5gb

$Cu(acac)_2$-**L1** complex:
85% yield, 91% ee

[a] 6 mol% of AcOH was added as additive.

1-5-4 Nitrile-derived Substrates

In terms of α,β-unsaturated nitriles, $Cu(OAc)_2$+**L1** system promoted the borylation reactions in good yield with good enantioselectivity. The electronic nature of the double bonds did not affect the chiral induction. On the other hand, copper complex afforded the silylated products in moderate-to-good yield with good enantioselectivity in most cases under 48-hour stirring with 1.5 equivalent of silyl boron reagent (Scheme 1.13).

Scheme 1.13. Common nitrile-type substrates for borylation and silylation.

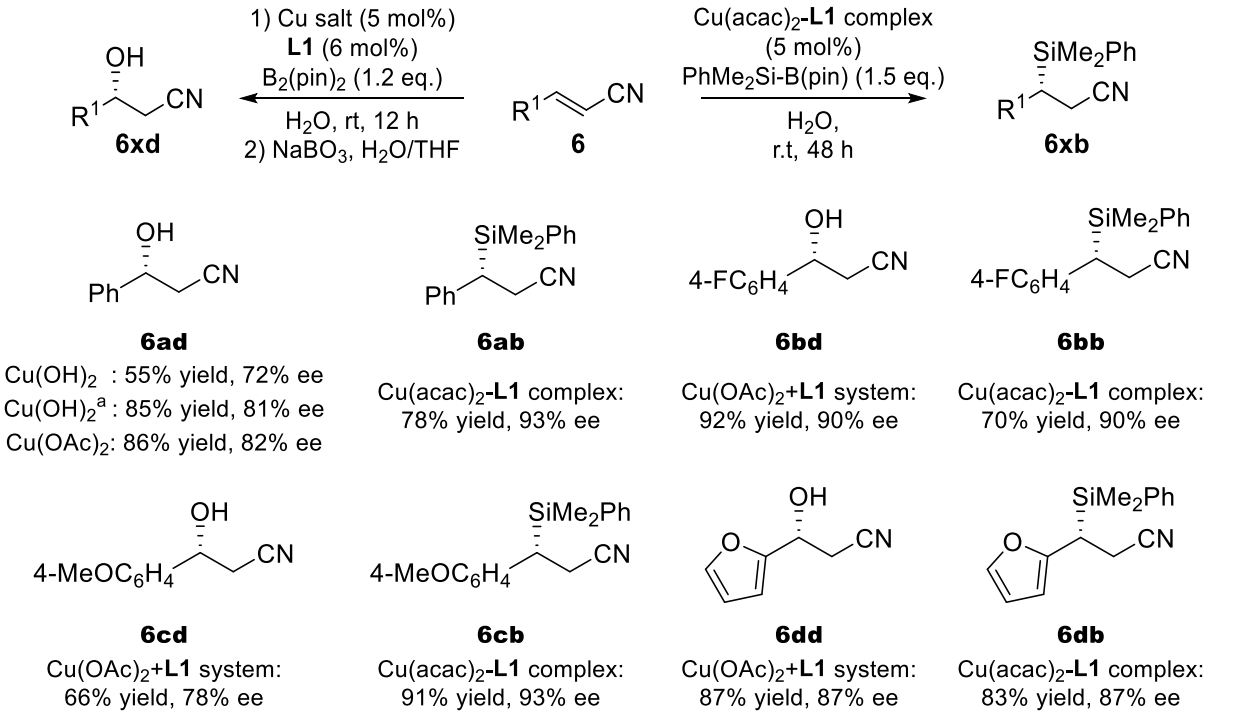

[a] 6 mol% of AcOH was added as additive.

The asymmetric β-borylation and subsequent oxidation of crotonitrile (**6e**) as an aliphatic nitrile were attempted. The obtained β-hydroxynitrile **6ed** was converted into the corresponding benzyl ether **6ef** in the presence of Ag_2O,[140] followed by hydrolysis with $TiCl_4$ in AcOH[141] without loss of enantiopurity of **6eg** (Scheme 1.14).

Scheme 1.14. Formation of aliphatic chiral β-hydroxy nitrile 6ed and its subsequent conversion.

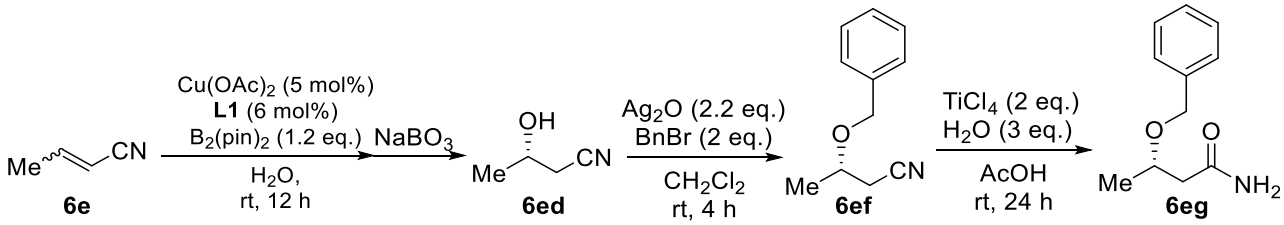

1-5-5 Amide and Amine Derived Substrates

When acyclic α,β-unsaturated amides and amines including β,β-disubstituted forms were used as substrates, only homogeneous $Cu(OAc)_2$+**L1** or $Cu(OH)_2$-AcOH+**L1** systems could catalyze borylation reactions to give the products in good yield with good enantioselectivity (Scheme 1.15). Heterogeneous $Cu(OH)_2$+**L1** afforded the borylated products in low yield with moderate enantioselectivity. The silylation of α,β-unsaturated amides or amines hardly proceeded in the presence of $Cu(acac)_2$-**L1** complex.

Scheme 1.15. Amide and amine-type substrates for borylation.

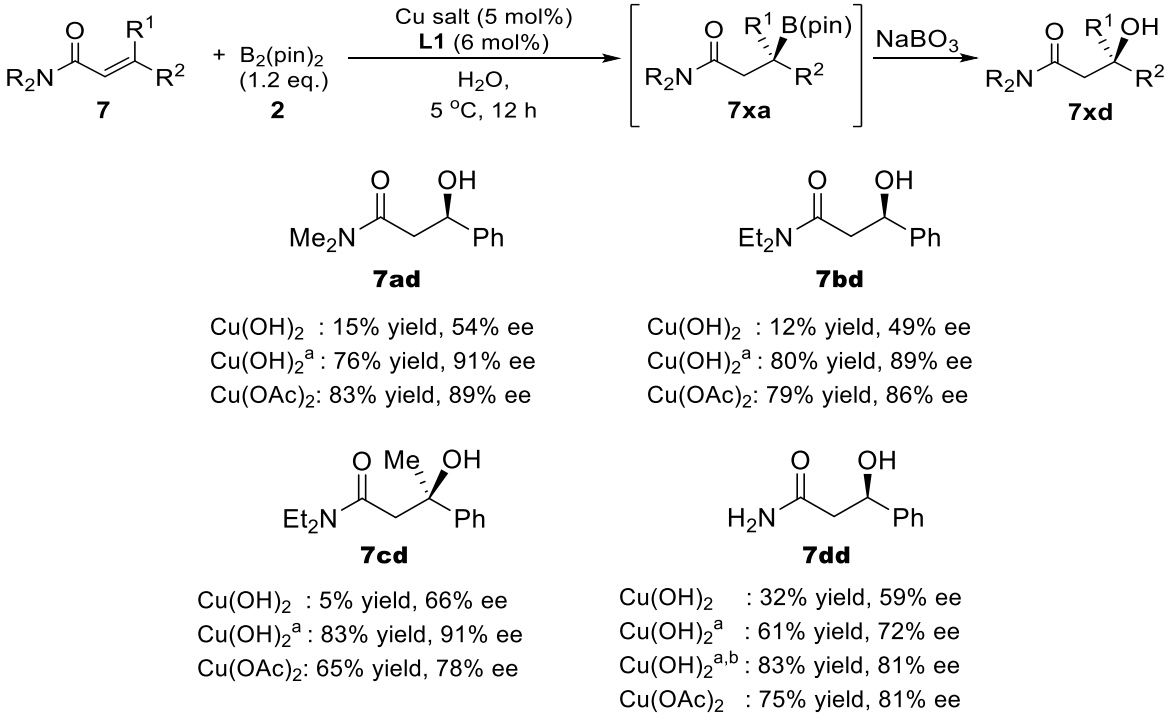

[a] 6 mol% of AcOH was added as additive. [b] 20 mol% of AcOH was added as additive.

1-5-6 Nitroolefin Derived Substrates

Notably, there has been no previous report on asymmetric silicon or boron conjugate addition of β-nitrostyrenes. While in the presence of chiral copper complex, the desired silyl adducts were obtained in moderate yields and good enantioselectivities (Scheme 1.16).

Scheme 1.16. β-Nitrostyrenes for silylation.

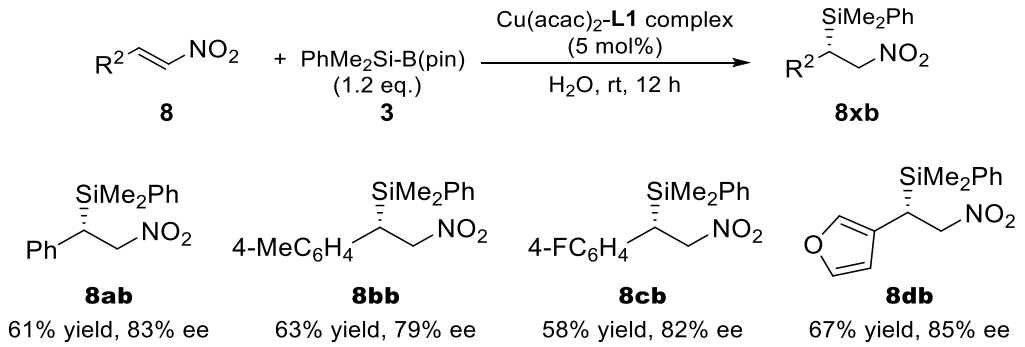

Transformations of the product were conducted to determine the absolute configuration under Tamao-Fleming oxidation (Scheme 1.17).[142]

Scheme 1.17. Tamao-Fleming oxidation.

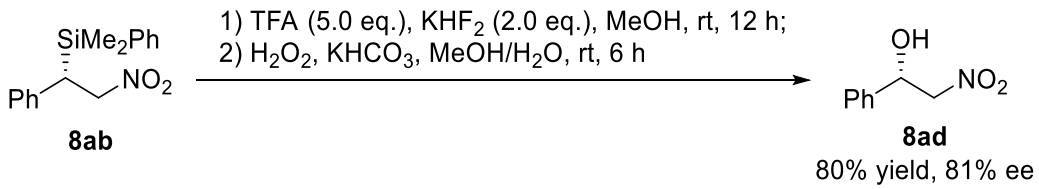

On the other hand, the asymmetric boron conjugate addition of β-nitrostyrenes did not give desired products, mainly due to the competitive reduction of NO_2 group by diboron species.

1-5-7 Other Substrates

Interestingly, the homogeneous $Cu(OAc)_2$ could even catalyze the reaction of a weinreb amide-type substrate, which can be transformed into various useful compounds, in moderate yield with relatively good enantioselectivity. Also, it is noteworthy that $Cu(acac)_2$-**L1** complex was applicable to α,β-unsaturated *N*-acyl oxazolidinone, which can be easily transformed to other potentially bioactive oxazolidinone derivatives (Scheme 1.18).

Scheme 1.18. Borylation of a weinreb amide-type substrate and silylation of α,β-unsaturated *N*-acyl oxazolidinone.

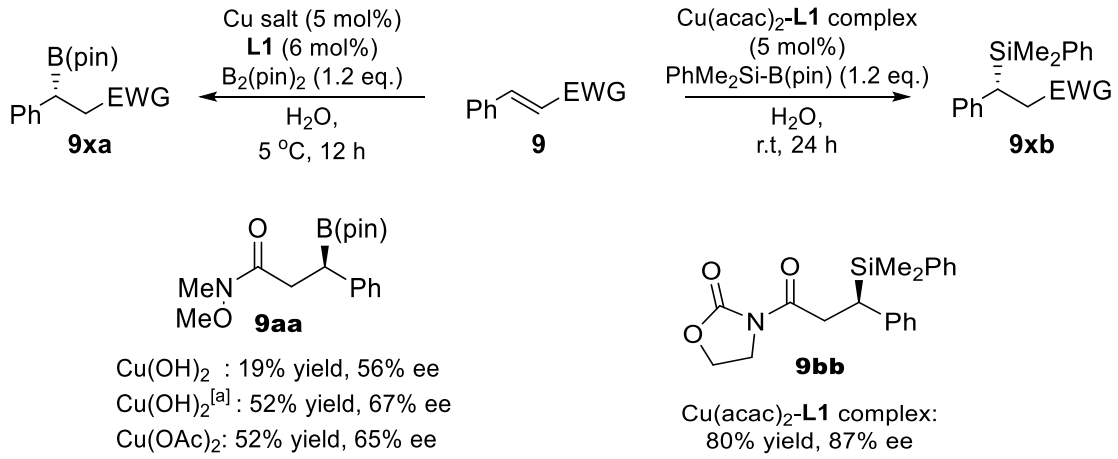

[a] 6 mol% of AcOH was added as additive.

Regretfully, neither of catalysts could catalyze the reactions of α,β-unsaturated thioesters or carboxylic acids due to the strong ionic interactions of sulfur and carboxylic acids with catalyst. Although both borylation and silylation reactions of α,β-unsaturated aldehydes proceeded smoothly, the instability of aldehydes under oxidized condition resulted in poor reproducibility. Similarly, substrates containing phenol moieties can coordinate to Cu(II) catalysts strongly.

1-6 Conjugate Additions to Unsaturated Di- and Trienones

1-6-1 Acyclic α,β,γ,δ-unsaturated dienones

First, the borylation reaction of acyclic α,β,γ,δ-unsaturated dienone 6a with compound 2 was performed in the presence of $Cu(OH)_2$ and **L1** (cat. 1) in water. The yield and the enantioselectivity were improved when the reaction was conducted using $Cu(OH)_2$, acetic acid and **L1** (cat. 2) or $Cu(OAc)_2$ and **L1** (cat. 3). The allylborane was also isolated without any loss of the yield and the enantioselectivity. On the other hand, $CuCl_2$, $CuSO_4$, and $Cu(OTf)_2$ showed much lower enantioselectivity. Although the silylated adduct of α,β,γ,δ-unsaturated dienone was not obtained at all in the presence of $Cu(acac)_2$-**L1** complex, the addition of Triton X-100 was successful to give the product in high yield with high enantioselectivity. The ameliorated dispersity of substrates by Triton X-100 could be the reason of improvement.

It is noted that in both borylation and silylation reactions, only 1,4-addition products were obtained without the observation of any 1,6-addition products. Other acyclic α,β,γ,δ-unsaturated acyclic dienones and dienoates were also tested with borylation reactions and identical tendencies in regioselectivity was observed. Acyclic dienones bearing methyl substituents at the β-position were known to be amenable to 1,6-addition, presumably because of a reluctance to react at the β-position.[143] Notably, the reaction of sterically congested dienone **10c** and dienoate **10g** furnished the corresponding 1,4-adducts **11cd** and **11gd** exclusively with high enantioselectivity. It is noteworthy that 1,4-addition products were obtained exclusively, regardless of heterogeneous and homogeneous catalysts and substituent patterns of acyclic α,β,γ,δ-unsaturated dienones and dienoates, and that no 1,6-addition products were produced (Scheme 1.19).

Scheme 1.19. Boron conjugate addition to acyclic α,β,γ,δ-unsaturated dienones and dienoates.

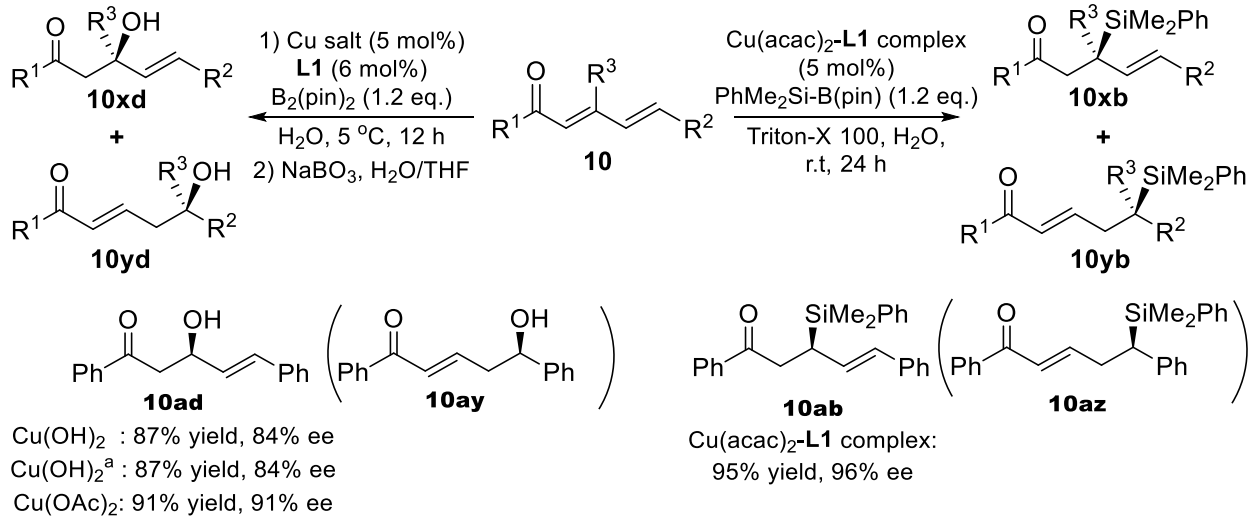

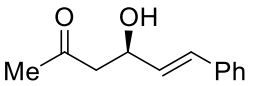

10bd

$Cu(OH)_2$: 81% yield, 77% ee
$Cu(OH)_2$[a] : 87% yield, 84% ee
$Cu(OAc)_2$: 91% yield, 87% ee

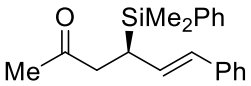

10bb

$Cu(acac)_2$-**L1** complex:
90% yield, 92% ee

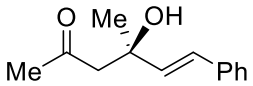

10cd

$Cu(OH)_2$: 75% yield, 83% ee
$Cu(OH)_2$[a] : 87% yield, 84% ee
$Cu(OAc)_2$: 85% yield, 91% ee

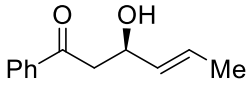

10dd

$Cu(OH)_2$: 73% yield, 75% ee
$Cu(OH)_2$[a] : 87% yield, 84% ee
$Cu(OAc)_2$: 84% yield, 83% ee

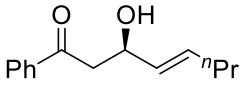

10ed

$Cu(OH)_2$: 67% yield, 72% ee
$Cu(OH)_2$[a] : 87% yield, 84% ee
$Cu(OAc)_2$: 81% yield, 82% ee

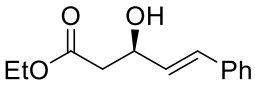

10fd

$Cu(OH)_2$: 83% yield, 85% ee
$Cu(OH)_2$[a] : 87% yield, 84% ee
$Cu(OAc)_2$: 91% yield, 92% ee

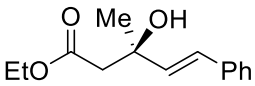

10gd

$Cu(OH)_2$: 86% yield, 90% ee
$Cu(OH)_2$[a] : 87% yield, 84% ee
$Cu(OAc)_2$: 91% yield, 94% ee

[a] 6 mol% of AcOH was added as additive.

1-6-2 Cyclic α,β,γ,δ-unsaturated dienones

Cyclic dienones have also served as acceptors congenial to conjugate additions. While several reports on copper-catalyzed 1,6-conjugate addition of organometallic reagents to cyclic dienones have appeared,[144] not until very recently were 1,6-boron/silicon conjugate additions explored. First, several Cu(II) salts were examined closely in the borylation reaction of six-membered cyclic dienone **11a**. When heterogeneous $Cu(OH)_2$+**L1** system was employed, 1,6-addition product was obtained in good yield with good enantioselectivity (Table 1.9, Entry 1). The E/Z ratio of γ,δ-olefin did not have any influence on the reactivity and selectivity of this reaction. Meanwhile, when homogeneous $Cu(OAc)_2$+**L1** system was employed, in spite of the construction of a quaternary asymmetric carbon, 1,4-addition product was obtained exclusively in good yield with high enantioselectivity (Entries 2, 3). To the best of our knowledge, the dependence of regioselectivity on not nucleophiles or chiral ligands but counteranions has never been reported in asymmetric Michael additions. It was astonishing that a simple swap of counteranions was disclosed to switch the regioselectivity between 1,4- and 1,6-addition. Meanwhile, both 1,4- and 1,6-addition pathways competed with each other in the presence of other copper(II) salts such as $CuCl_2$, $CuSO_4$, and $Cu(OTf)_2$ (Entries 4-6). Similarly, heterogeneous $Cu(acac)_2$-**L1** complex catalyzed the silylation of cyclic dienone in 1,6-mode, providing the product in good yield with excellent enantioselectivity (Scheme 1.20).

Table 1.9. Effect of Cu(II) salts on regioselectivity of cyclic dienone in borylation reaction.

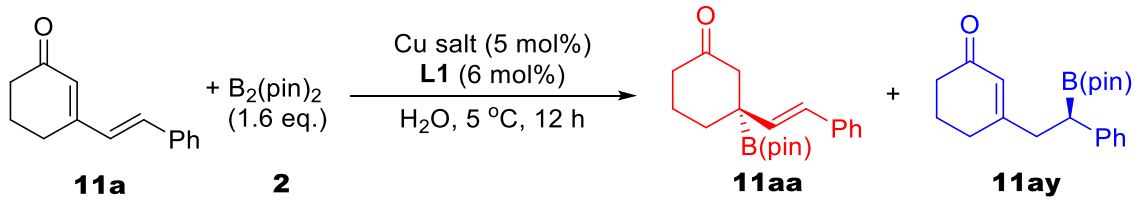

Entry	Cu(II)	**11aa/11ay**	Total yield (%)	Ee (**11aa/11ab**)
1	$Cu(OH)_2$	**<1/>99**	81	ND/76%
2[a]	$Cu(OH)_2$	**>99/<1**	92	87%/ND
3	$Cu(OAc)_2$	**>99/<1**	94	91%/ND
4	$CuCl_2$	**69/31**	49	32%/3%
5	$CuSO_4$	**56/44**	37	6%/1%
6	$Cu(OTf)_2$	**91/9**	81	45%/-1%

[a] 6 mol% of AcOH was added as additive.

Scheme 1.20. $Cu(acac)_2$-L1 complex catalyzed silylation reaction of cyclic dienone.

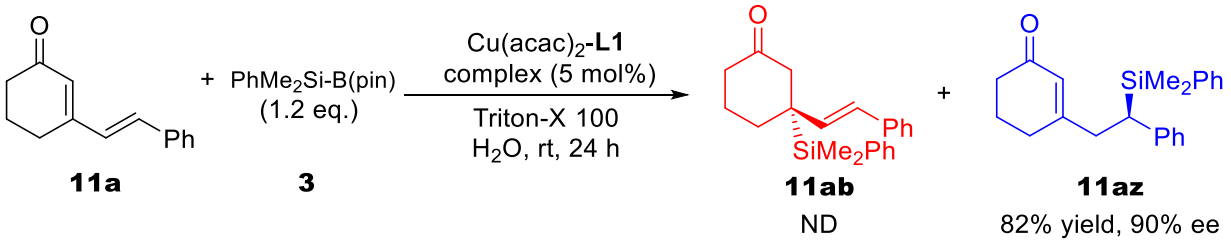

Furthermore, several cyclic dienone derivatives were examined in borylation raction. In the presence of heterogeneous $Cu(OH)_2$ catalyst, 1,6-addition products were obtained exclusively in all cases with good enantioselectivity. It is noted that the sterically congested electrophilic site at the δ-position of **11a** did not shift the preference of $Cu(OH)_2$ system toward 1,4-addition. On the other hand, the 1,4-addition pathway took precedence exclusively with high enantioselectivity when homogeneous $Cu(OAc)_2$ catalyst was used as the catalyst.

1-6-3 Cyclic trienone

Further investigation was conducted with the addition of $B_2(pin)_2$ to trienone **11b** bearing an additional electrophilic site at the terminal position (Table 1.10). While the use of $CuCl_2$ resulted in the formation of a messy mixture that could not be separated, the desired addition products were obtained in the presence of $Cu(OH)_2$ and $Cu(OAc)_2$. The 1,6-adduct **11by** and the 1,8-adduct **11bz** were obtained in the reaction catalyzed by $Cu(OH)_2$ and **L1** with moderate selectivity (Entry 1). No 1,4-adduct **11bx** was obtained. It is noteworthy that the remote ζ-position was functionalized

successfully. On the other hand, homogeneous systems of $Cu(OH)_2$ and acetic acid with **L1** or $Cu(OAc)_2$ with **L1** rendered 1,4-adduct **11bx** exclusively in high yields with high enantioselectivities (Entries 2, 3). Other copper salts such as $CuCl_2$ only afford messy products (Entry 4).

Table 1.10. Conjugate boron addition reaction of cyclic trienone.

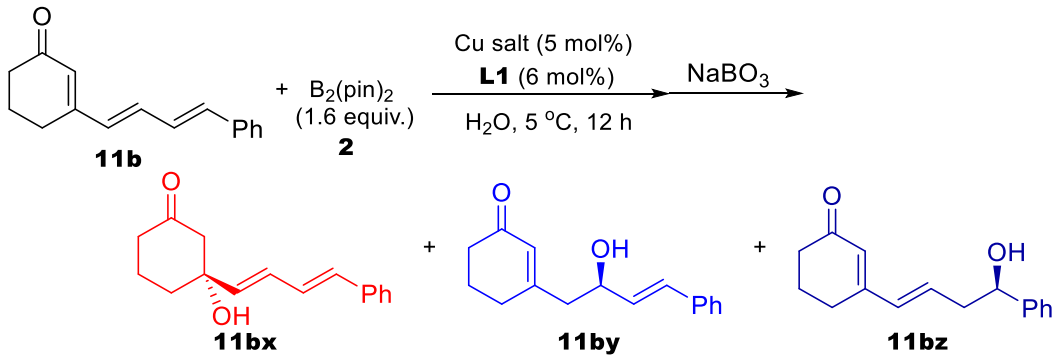

Entry	Cu(II)	**11bx/11by/11bz**	Total yield (%)	Ee (**11bx/11by/11bz**)
1	$Cu(OH)_2$	**<1/74/26**	71	ND/72%/46%
2[a]	$Cu(OH)_2$	**>99/<1/<1**	86	92%/ND/ND
3	$Cu(OAc)_2$	**>99/<1/<1**	87	91%/ND/ND
4	$CuCl_2$		Messy	

[a] 6mol% of of AcOH was added as additive.

Inspired by these results, cyclic tetraenone was synthesized and employed in the reaction with $B_2(pin)_2$. However, due to the long chain of olefins, large amounts of the starting material were polymerized and some cyclized products were obtained (Scheme 1.21).

Scheme 1.21. Conjugate boron addition reaction of cyclic tetraenone.

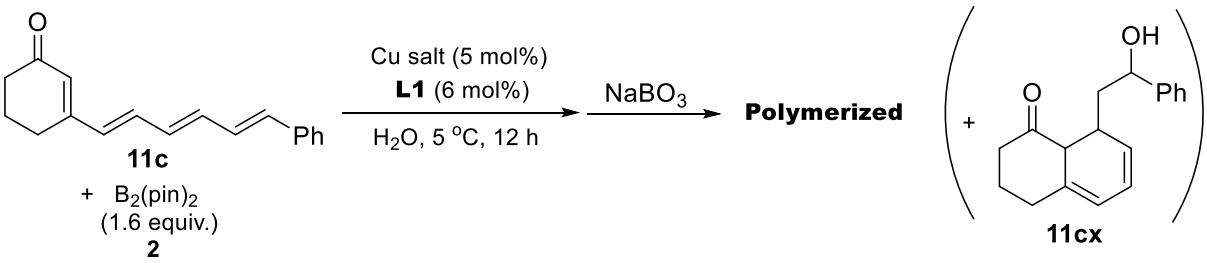

1-7 Catalyst Recycle

Catalyst reusability was evaluated in the silylation reaction of cyclopentenone **1u** with $PhMe_2Si$-B(pin) (Figure 1.12). After the first run, the reaction tube was centrifuged at 3000 rpm to separate the reaction mixture into aqueous, organic, and solid phases. No product, copper, or chiral ligand was detected in the aqueous phase, whereas the product 3m and a trace amount of the chiral ligand were found in the oil phase. The product **1ub** was isolated in 85% yield with 87% ee. The collected solid was then used in a second run, resulting in a comparable result with little erosion of the selectivity (80% yield, 82% ee).

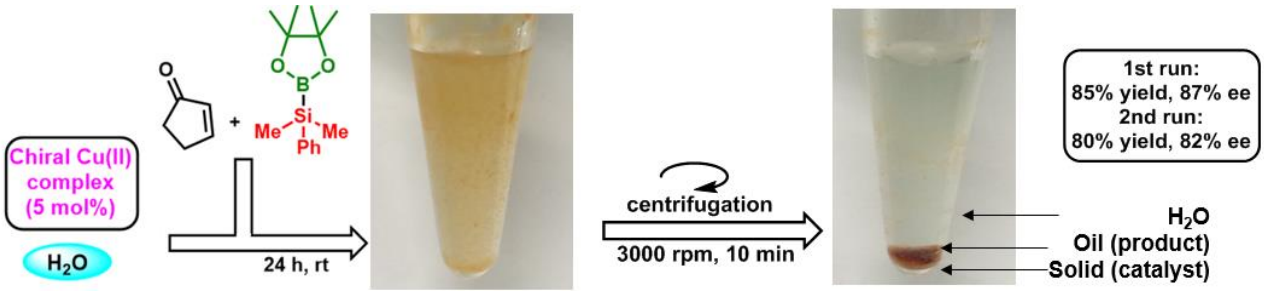

Figure 1.12. Catalyst recycle and reuse.

1-8 Mechanism Elucidation

Based on the experimental results and previous results, the catalytic cycle of the chiral Cu(II)-catalyzed asymmetric boron and silicon conjugate addition to unsaturated carbonyl compounds in water was proposed. The initial formation of (pin)B-Cu(II)•**L1** or $PhMe_2Si$-Cu(II)•**L1** was assumed as a reactive intermediate, which would be produced from Cu(II)-**L1** and $B_2(pin)_2$ or $PhMe_2Si$-B(pin). Based on crystallographic structure of $CuBr_2$-**L1** complex investigated before,[145] the free OH group in the ligand might interact with the boron parter of $B_2(pin)_2$ or $PhMe_2Si$-B(pin) and further promote the formation of Cu(II)-B or Cu(II)-Si. Next, **II-B** or **II-Si** is sufficiently Lewis acidic to form complex **III-B** or **III-Si**, in which the substrate was coordinated and activated by copper center, and boron addition might proceed via six-membered cyclic transition states to afford **IV-B/IV-Si**. Finally, Cu(II) enolate would be immediately protonated by H_2O to give desired compound and Cu(II) -**L1** was regenerated.

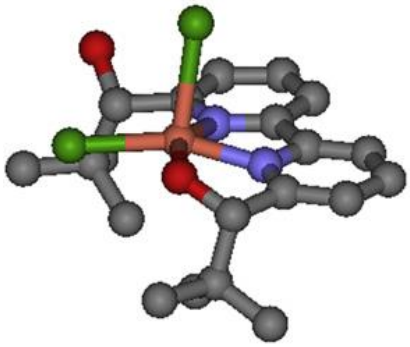

Figure 1.13. X-ray structure of [$CuBr_2$•L1].[145]

It should be emphasized that just proposing a catalyst cycle never fell into difficulties, it is the validation of the mechanism that always becomes knotty. In my M.S. dissertation, through DFT calculations and experimental investigations (See Experimental Section), several answers on borylation reactions have been obtained including the rate determining step in borylation reactions, the exact role of acetic acid as an additive, the coordination pattern of substrate to the Cu(II) center (*O*-enolate formation), and the decisive difference between the previous Cu(I) catalyst in organic solvent and the newly developed Cu(II) catalyst in water.

However, through the comparison between borylation and silylation reactions, several new questions have raised, namely:

1. What makes difference between heterogeneous $Cu(OH)_2$ catalyst and heterogeneous $Cu(acac)_2$-**L1** complex, and how these differences have influenced the asymmetric borylation/silylation reactions?
2. Why are heterogeneous Cu(II) catalysts possess higher reaction rates than homogeneous Cu(II) catalysts do?

In order to resolve these questions and deepen the understanding toward the reactions, further investigations were continued.

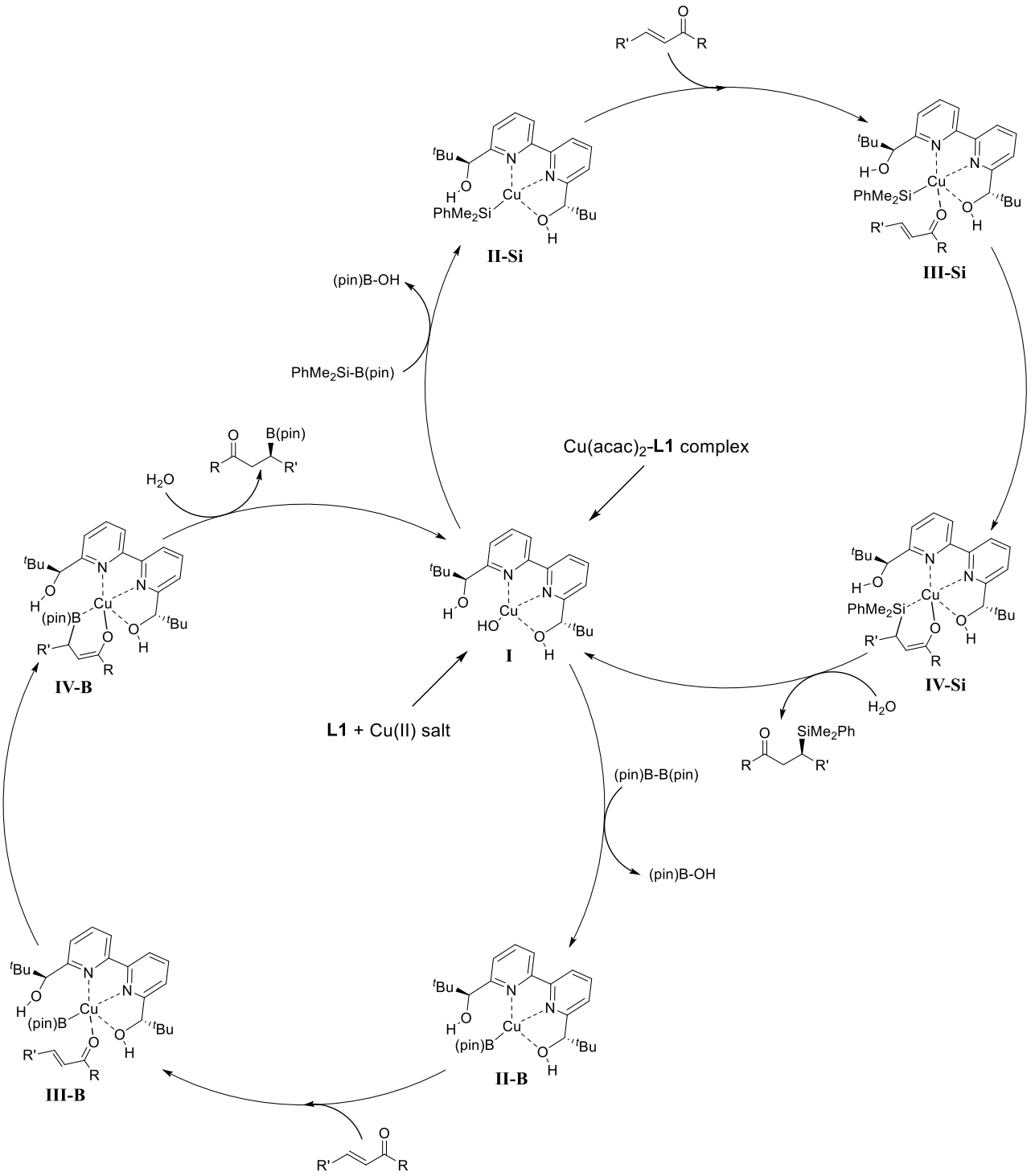

Figure 1.14. Simplified reaction mechanism.

1-8-1 Experimental Studies

■ *Detailed effect of organic solvents*

The catalyst behavior of Cu(acac)$_2$-**L1** complex mediated silylation reactions in the solution state was investigated using aqueous THF solutions. Indeed, the employment of aqueous co-solvent only slightly affected the reactivity and selectivity in borylation reactions while a drastic decrement in enantioselectivity was observed in Cu(acac)$_2$-**L1** complex-mediated silylation reactions.

A sharp increase in enantioselection correlated with a decrease in solubility of the catalyst, whereas the yields of **1ab** were maintained. When the amount of water was equal to or less than the amount of THF, the catalyst solution became transparent. Given that leaching of Cu was not detected in the absence of THF, the catalyst should be entirely heterogeneous in water.

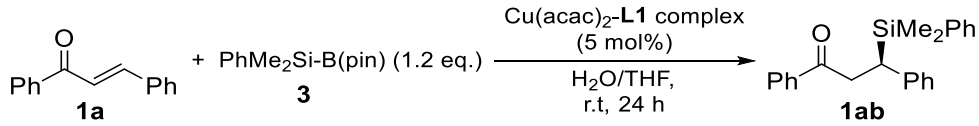

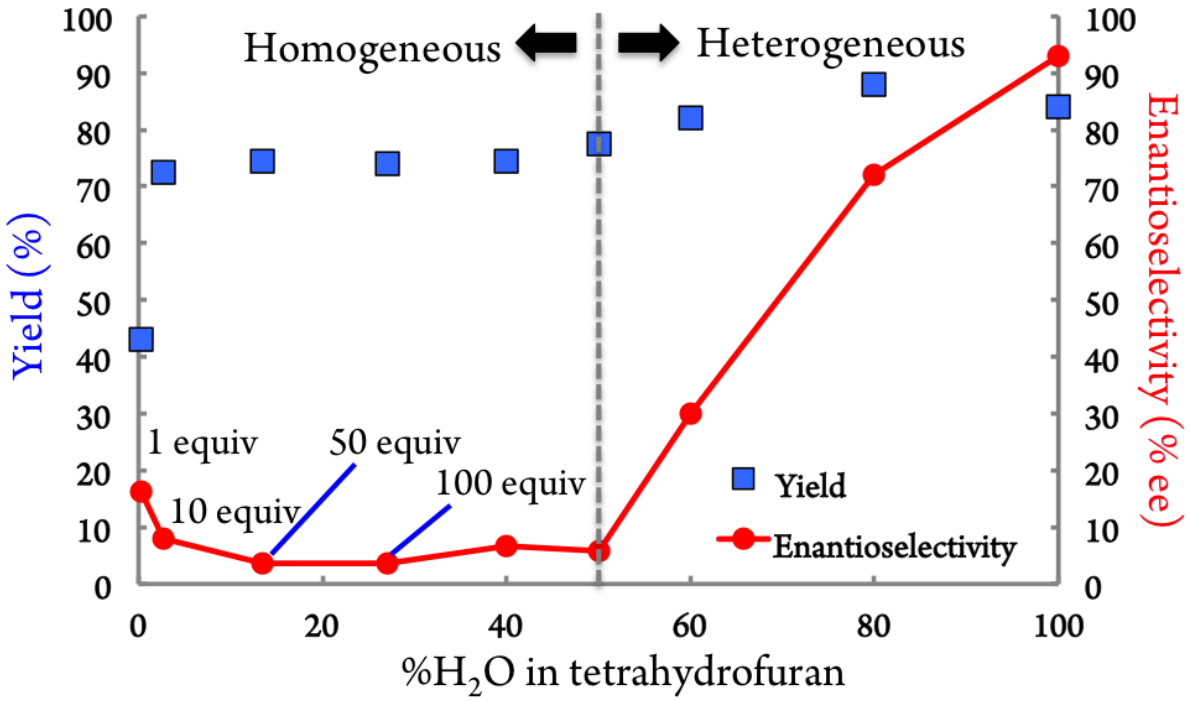

Figure 1.15. Homogeneous versus heterogeneous catalysis.

■ *Reaction comparison*

The reaction profile of $Cu(OAc)_2$-catalyzed β-borylation of an α,β-unsaturated imine was compared with that of the reaction of the corresponding ketone. Although the β-borylation of the α,β-unsaturated imine was slightly slower than that of the corresponding ketone, the relatively rapid completion of the reaction implied sufficient and efficient activation of the α,β-unsaturated imine by $Cu(OAc)_2$.

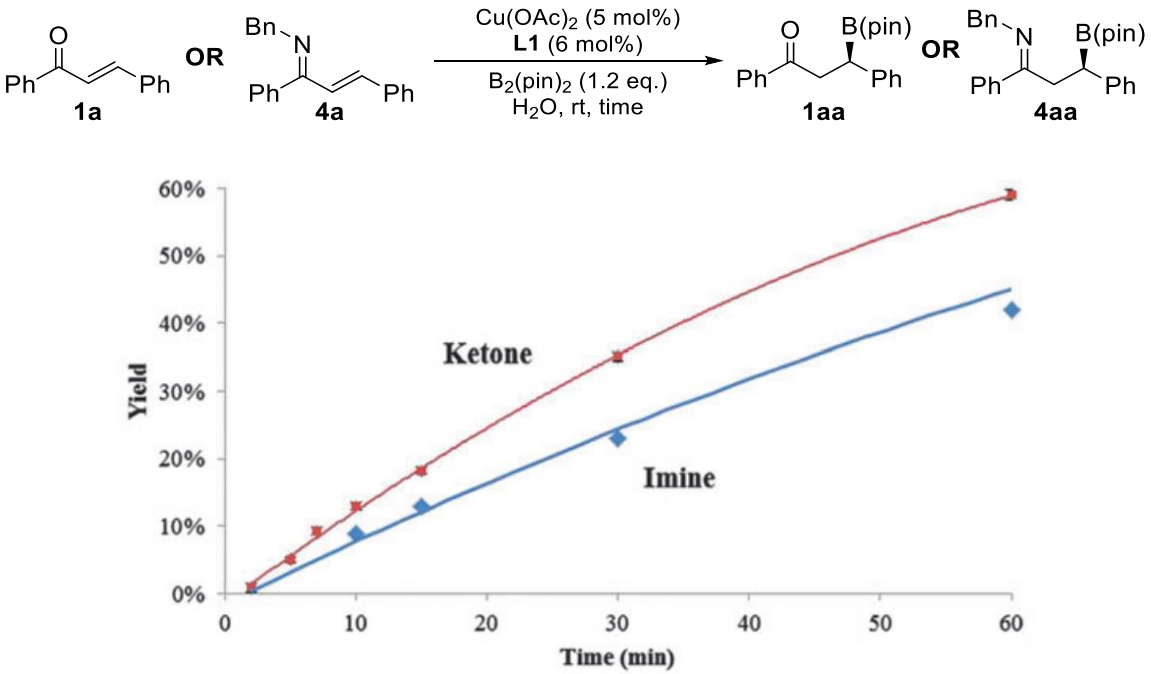

Figure 1.16. Reaction profile on $Cu(OAc)_2$-catalyzed boron conjugate addition to ketone/imine in water.

On the other hand, a simple comparison experiment was proposed to distinguish the *O*-enolate formation from the *C*-enolate formation. The idea derives from the fact that the electronic properties of C=C or C=X double bond should correspond to the reactivity of the *O*-enolate or the *C*-enolate; namely *C*-enolate prefers more electron-rich C=C double bond and *O*-enolate prefers C=O double bond over C=N double bond.

Indeed, when a 1:1 mixture of chalcone **1a** and acrylophenone **1w** was added to the catalyst solution, both substrates reacted and Cu(OAc)2+**L1** system afforded the product from acrylophenone in slightly higher yield than that of chalcone (Scheme 1.22, Left). Considering the rather large difference of electron density across the C=C double bonds between chalcone and acrylophenone and much smaller influence on C=O double bonds of them, the formation of *O*-enolate is more reasonable. Furthermore, when a 1: 1 mixture of chalcone **1a** and the corresponding imine **4a** was added to the catalyst solution, chalcone was consumed almost quantitatively while the competitive β-borylation of the imine was clearly hampered (Scheme 1.22, Right). Considering decomposition of the imine in

water, the amounts of the recovered imine and the ketone are reasonable. The exclusive preference toward chalcone could attribute to the higher stability of C=O···Cu(II) than C=N(R)···Cu(II).

Scheme 1.22. Competitive reactivity against chalcone 1a with acrylophenone 1w and chalcone 1a with the corresponding imine 4a as a mixed system.

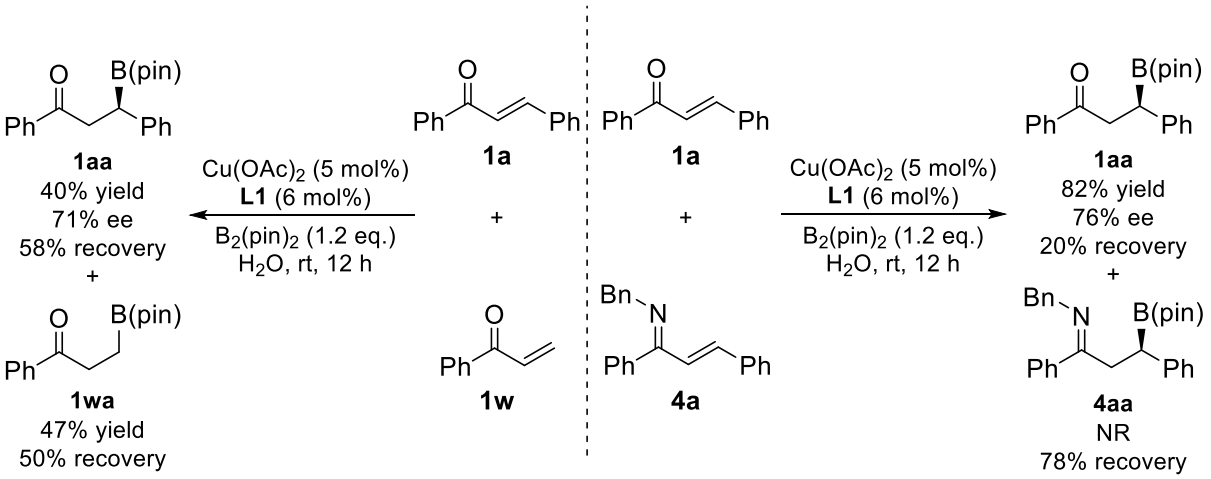

■ *Kinetic Isotope Effect*

Next, deuteration of the dienolate was conducted in both borylation and silylation reactions. In previous reports, most chiral copper catalysts in the reactions of organometallic reagents with cyclic dienones furnished β,γ-unsaturated 1,6-addition adducts *via* kinetic protonation of dienolate intermediates.[146] The isomerization of these deconjugated adducts was known to lead easily to reconjugated adducts.

Nevertheless, it was verified that the $Cu(OH)_2$-mediated borylation reactions furnished a thermodynamically favorable conjugated product in D_2O and deuteration of the dienolate took place exclusively at the δ-position. On the other hand, in Cu(acac)2-**L1** complex-mediated silylation reactions, deuteration took place at both β- and δ-position.

Scheme 1.23. Borylation and silylation reactions of cyclic dienone in D_2O.

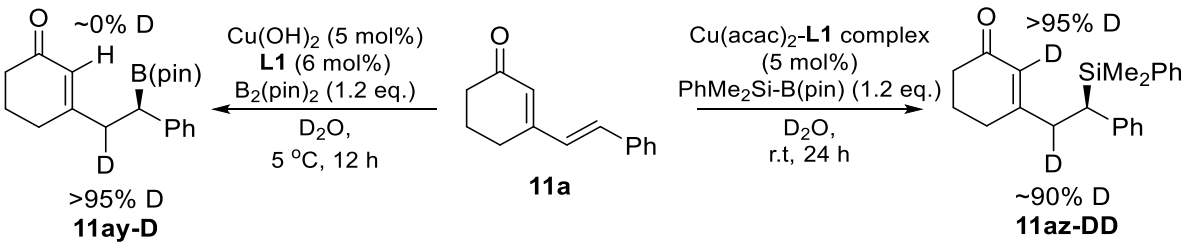

Since H/D exchange of the β-silylated product did not take place as shown below, deuterium would be incorporated during tandem silyl conjugate addition/protonation (deuteration) process.

Scheme 1.24. Deuteration experiment with the product.

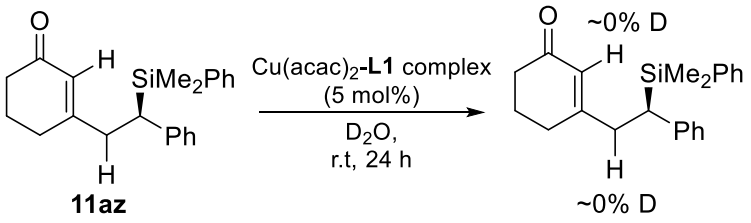

Detailed studies revealed that at the beginning of the silylation reaction, kinetically protonated δ-silylated product **11aw-D**, bearing a β,γ-alkene moiety, was obtained exclusively with almost complete Z-preference. After stirring for 3 h, the reaction furnished γ-protonated isomer **11az-DD** predominantly. Eventually, no **11aw-D** remained, and a significant amount of **11az-DD** was obtained after 24 h. Hoveyda *et al.* reported that by using their NHC-Cu(I) catalyst system, **11aw-D** was obtained that contained 15−20% **11az-DD** as a result of adventitious isomerization.[146b] The Cu(II)-based system ultimately reached thermodynamic convergence with the formation of **11az-DD**.

Scheme 1.25. Proposed di-deuteration mechanism for silylation reaction of cyclic dienone.

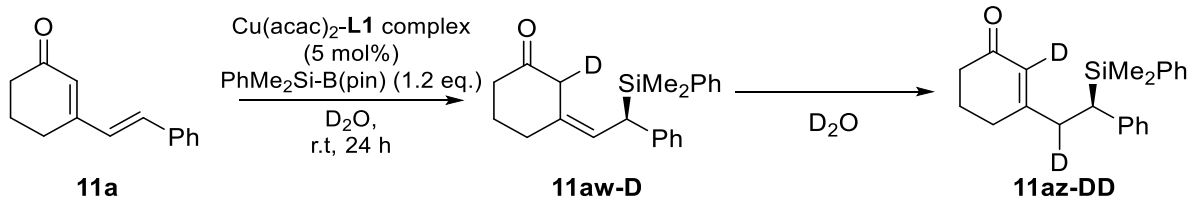

■ *Reactions with typical substrate*

In order to verify the effect of the phenyl group in the Si part, another Si-B substrate without phenyl group was synthesized and applied on the reaction. As a result, the reaction did not proceed at all, suggesting the phenyl group is imperative for the smooth reaction.

Scheme 1.26. Silylation reaction with tri-ethyl silicon boron species.

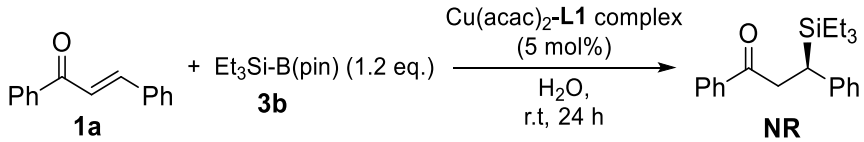

1-8-2 Instrumental Analyses

■ *The pH Analysis*

The pH analysis provides the direct information on the proton environment, which is a crucial factor in both the generation of active catalysts and the protonation step in catalytic cycle.[147] Preliminary measurement indicated pH = 7.829 in heterogeneous $Cu(OH)_2$ solution, which is in satisfactory agreement with the theoretical pH = 7.808 at 25 °C (K_{sp} of $Cu(OH)_2$ is 1.9×10^{-20}). In most cases, the addition of **L1** caused decreasing pH value temporally and it recovered after 1 hr stirring, which suggests the metal-ligand complexation. Interestingly, the addition of $B_2(pin)_2$ caused an immediate decrement of pH values in both heterogeneous $Cu(OH)_2$ (Figure 1.17, Entry 1) and $Cu(acac)_2$ + **L1** systems (Entry 2), while it did not affect the pH value of $Cu(acac)_2$-**L1** complex system (Entry 3) as well as the other homogeneous systems at the initial stage. This phenomena may attribute to the rapid formation of Cu-B intermediate on amorphous heterogeneous surfaces, which led to the rapid release of HO-B(pin) through transmetallation between Cu(II) and $B_2(pin)_2$. Likewise, regarding the immediate decrement of pH value after the addition of $B_2(pin)_2$ in $Cu(OH)_2$ + AcOH + **L1** system, the addition of AcOH is supposed to retain the amorphous surface of $Cu(OH)_2$ rather. Indeed, further observation of $Cu(OH)_2$ + AcOH + **L1** system revealed the tardy precipitation of Cu(II) species (maybe Cu(OH)(OAc)) after three days (Figure 1.18). It is not surprising that the strongly Lewis acidic $Cu(OTf)_2$ has afforded quite acidic environment since the beginning of the reaction, leading to a fast decomposition of $B_2(pin)_2$ and thereby the lower yield and enantioselectivity.

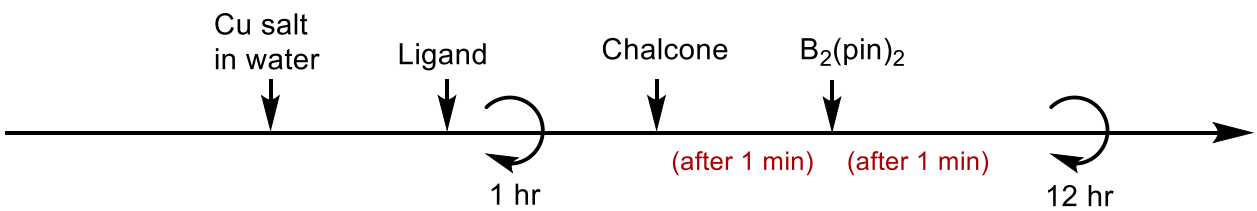

Entry	Cu salt	pH	pH	pH	pH	pH	pH
1	**$Cu(OH)_2$**	7.83	8.12	7.87	7.59	6.62	6.50
2	**$Cu(acac)_2$**	7.87	8.09	7.92	7.50	6.50	6.35
3[a]	**$Cu(acac)_2$**	7.62	-	7.62	7.58	7.48	6.52
4[b]	**$Cu(OH)_2$**	5.26	5.86	5.76	5.73	4.80	4.13
5	**$Cu(OAc)_2$**	5.45	6.04	5.85	5.83	5.79	4.00
6	**$Cu(OTf)_2$**	4.83	4.86	4.85	4.92	4.91	2.28

Figure 1.17. The pH measurement results for β-borylation reactions. [a] $Cu(acac)_2$-L1 complex was employed [b] 6 mol% of AcOH was added as additive.

Figure 1.18. The photo of $Cu(OH)_2$ + AcOH + L1 system left water for three days.

A detailed time course of pH values during the borylation reactions were then measured. Surprisingly, while pH values of the reaction mixture started to decrease immediately at the initial 4 minutes in heterogeneous $Cu(OH)_2$ and $Cu(OH)_2$+AcOH catalyst systems, a relaxation time at the initial stages was identified in homogeneous $Cu(OAc)_2$ and $Cu(OTf)_2$ catalyst systems. DFT calculations conducted during my M.S. studies have already revealed that the formation of boryl copper species is the rate determining step. Therefore, the relaxation time could be explained as the pre-formation time of Cu-B intermediate in homogeneous system. No observation of relaxation time in heterogeneous systems is probably due to the rapid formation of Cu-B intermediates through activated surfaces.

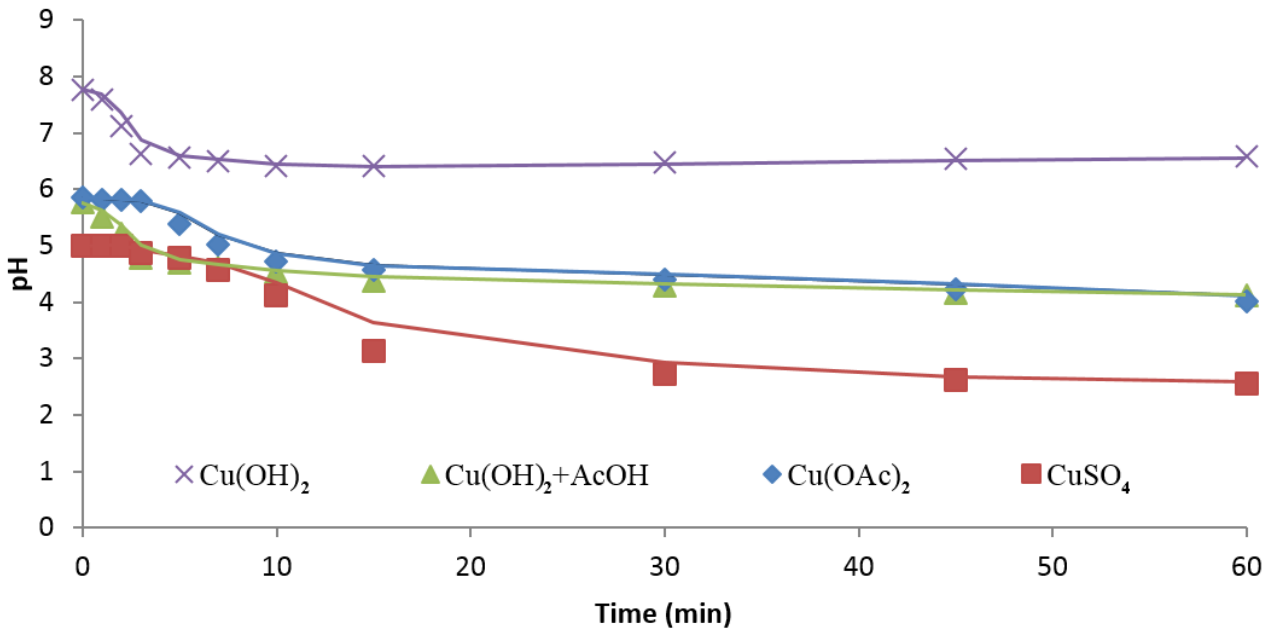

Figure 1.19. Time course of pH values in β-borylation reactions.

Similarly, the pH values were also measured in silylation reactions. Heterogeneous $Cu(OH)_2$ system exhibited the identical tendency on pH values (Figure 1.20, Entry 1). Interestingly, the addition of $PhMe_2Si$-B(pin) to the system caused immediate decrement of pH values in both heterogeneous $Cu(acac)_2$-**L1** complex (Entry 3) and homogeneous $Cu(OAc)_2$ catalyst systems (Entry 4), though after 12 hr stirring, the pH values were the same as those in borylation reactions. Time

course measurement of pH values revealed a significant but temporary decreasing of pH values at the initial 20 min in $Cu(acac)_2$-**L1** complex and $Cu(OAc)_2$ system. Also, it was found that the color of both systems started to change only after around 10 min stirring. On the other hand, no such temporary decreasing of pH values was observed in $Cu(OH)_2$-mediated silylation system with an rapid change of color of the reaction mixture from the beginning.

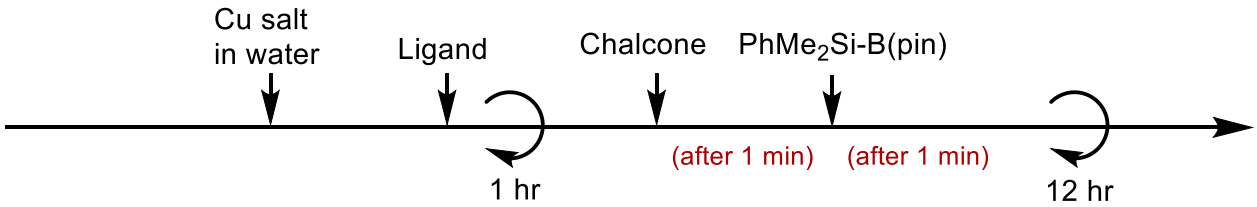

Entry	Cu salt	pH	pH	pH	pH	pH	pH
1	**$Cu(OH)_2$**	7.83	8.12	7.87	7.59	6.78	6.19
2	**$Cu(acac)_2$**	7.87	8.09	7.92	7.50	6.51	6.26
3[a]	**$Cu(acac)_2$**	7.62	-	7.62	7.58	5.59	6.23
4	**$Cu(OAc)_2$**	5.46	6.03	5.84	5.84	3.96	5.86

Figure 1.20. The pH measurement results for β-silylation reactions. [a] $Cu(acac)_2$-L1 complex was employed.

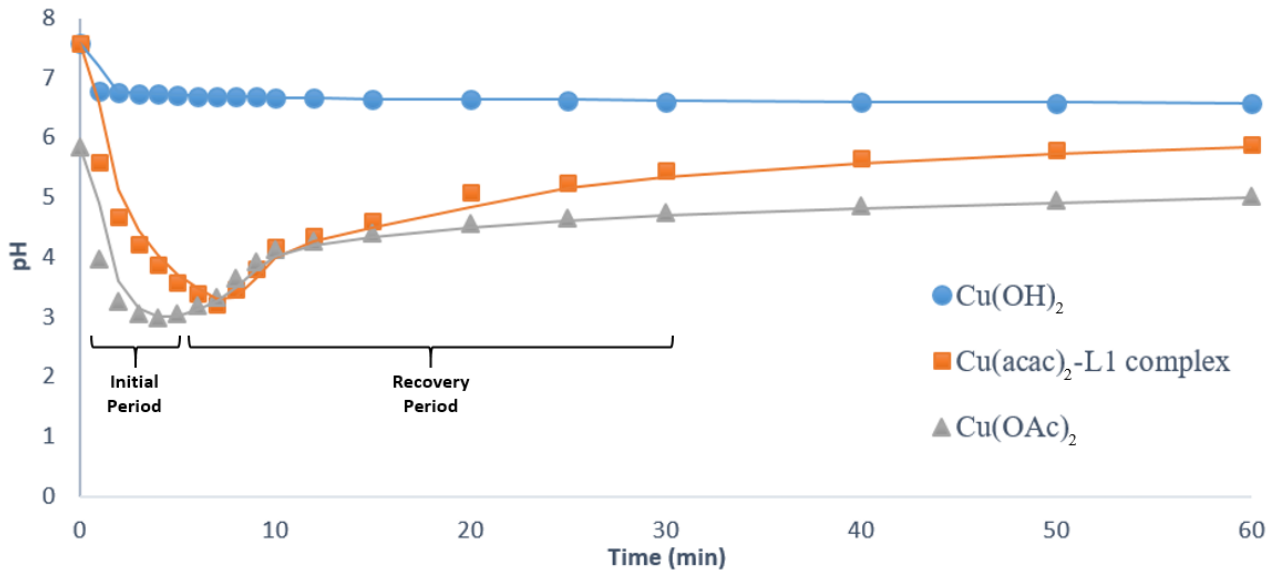

Figure 1.21. Time course of pH values in β-silylation reactions

■ *Mass Spectroscopy Studies*

ESI-MS analysis was then conducted so as to monitor the intermediates. For borylation reactions, chalcone **1a** and $B_2(pin)_2$ were added to a homogeneous solution of $Cu(OAc)_2$ with **L1** in H_2O/THF = 9/1 co-solvent, which can completely dissolve all the components including $Cu(OAc)_2$, **L1**, **1a**, and $B_2(pin)_2$. Minimum addition of organic solvent not only enabled the ESI-MS analysis but also ensured that the observed peaks indeed represented the actual intermediates. An immediate submission to ESI-MS analysis after mixing all the components afforded the detection of a strong peak at m/z 726.3265 corresponding to [**L1** + CuB(pin) + **1a**]$^+$ in the light of the isotope pattern. Besides the intermediate peak, several peaks were also detected including [Cu(OAc) + **L1**] $^+$at m/z 465.9729 and the dimerized catalyst [Cu_2(OH) +2 **L1** - 2H]$^+$ at m/z 434.2066.

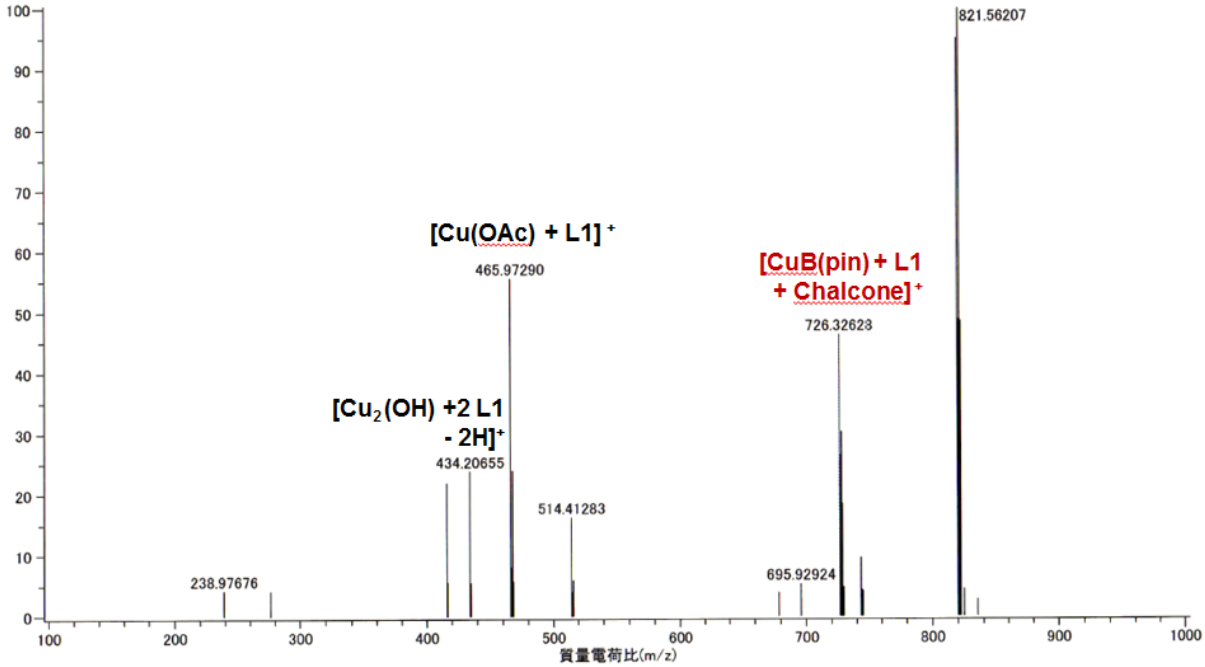

Figure 1.22. ESI-MS analysis for β-borylation in water.

When the amount of H_2O was reduced with a co-solvent system of H_2O/MeCN = 1/25, a peak corresponding to [**L1** + CuB(pin) + **1a**]$^+$ was no longer observed while a new peak at m/z 852.4119 appeared. Taken the isotope pattern into consideration, it was attributed to [**L1** + Cu + B(pin) + B(pin) + **1a** - 1H]$^+$. Since $B_2(pin)_2$ itself was confirmed to decompose under ESI-MS environment, the peak should correspond to $L_nCu[B(pin)]_2$ species. Because the peak of [**L1** + CuB(pin) + **1a**]$^+$ in Figure 1.22 disappeared quickly and the peak of [**L1** + Cu + B(pin) + B(pin) + **1a** - 1H]$^+$ remained for a relatively long time when the reaction started (30-60 sec), it might represent an interim reaction product (Figure 1.23).

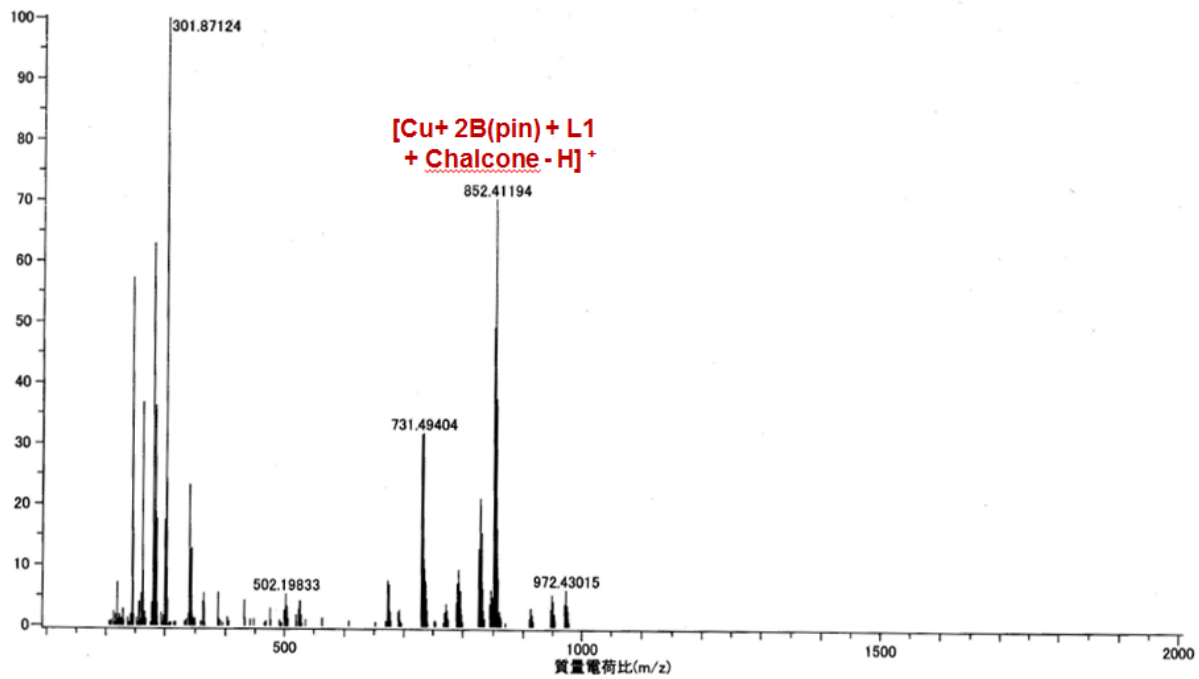

Figure 1.23. ESI-MS analysis for β-borylation under a co-solvent system of H_2O/MeCN = 1/25.

Likewise in silylation reactions, chalcone **1a** and $PhMe_2Si$-B(pin) were added to a homogeneous solution of $Cu(acac)_2$-**L1** complex in H_2O/acetone = 4/1 co-solvent. It was found that $Cu(acac)_2$-**L1** complex existing in a dimer form of [**L1** + 2Cu + acac]$^+$ even under homogeneous condition (Figure 1.24).

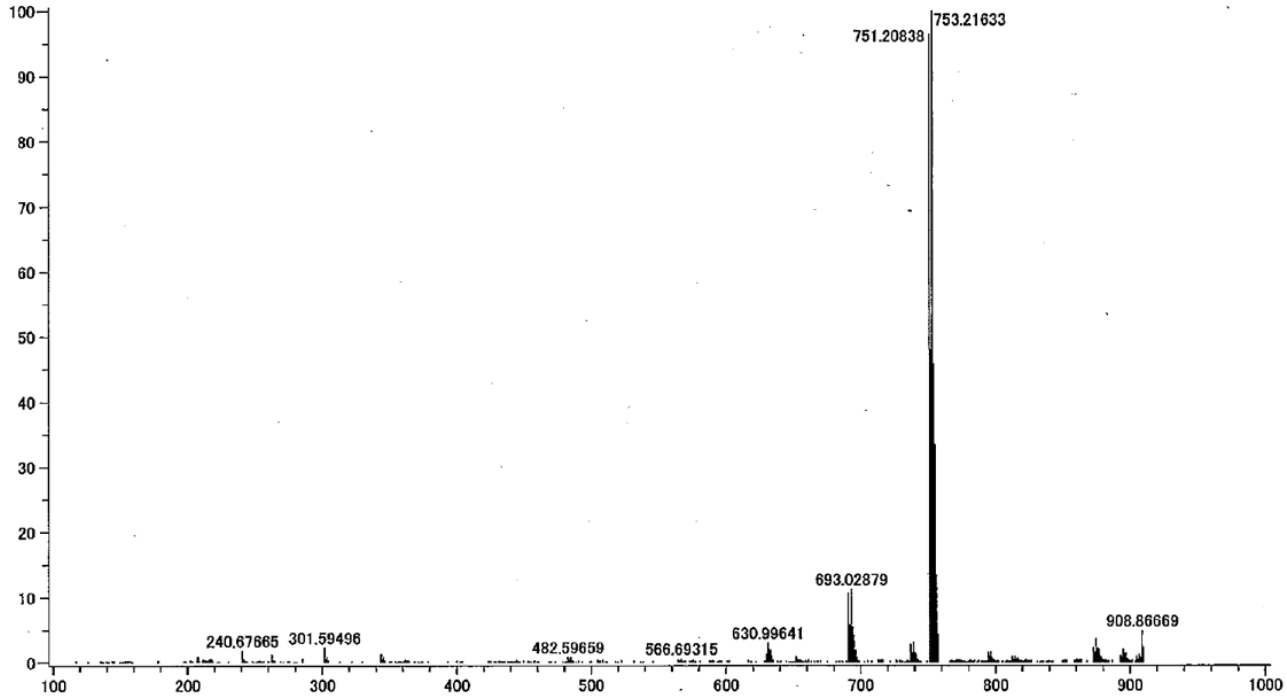

Figure 1.24. ESI-MS analysis for $Cu(acac)_2$-L1 complex in water/acetone = 4/1 co-solvent.

An immediate injection of the reaction mixture after addition of PhMe2Si-B(pin) into the system afforded the detection of a strong peak at m/z 787.2262 corresponding to [**L1** + $Cu_2(SiMe_2Ph)$ + 2acac]$^+$ in the light of the isotope pattern (Figure 1.25). The result is in accordance with the formation of the 1,6-addition product when cyclic α,β,γ,δ-unsaturated ketones were served as substartes even under homogeneous co-solvent condition.

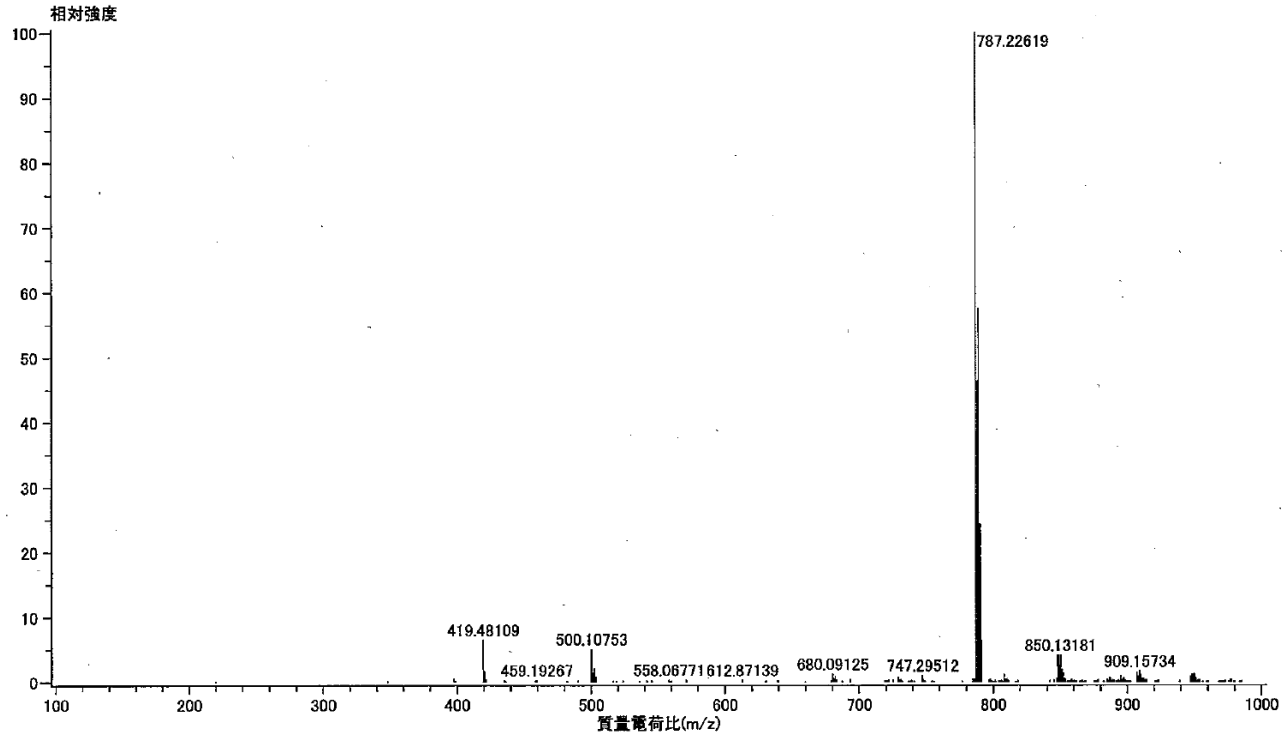

Figure 1.25. ESI-MS analysis for β-silylation in water/acetone = 4/1 co-solvent.

1-8-3 Discussion

Based on these mechanistic studies, it was confirmed that even though both $Cu(OH)_2$ catalyst and $Cu(acac)_2$-**L1** complex were recognized as heterogeneous catalysts, their reactivity and catalytic behaviors are quite different. Indeed, $Cu(OH)_2$ is considered to possess amorphous heterogeneous surface, while crystallization of $Cu(acac)_2$-**L1** complex affords a well-defined surface. It is microscopic differences on surface morphology that make $Cu(OH)_2$ different from $Cu(acac)_2$-**L1** complex. Combined with the hypothesis and the obtained data, the detailed answers for the proposed questions were given.

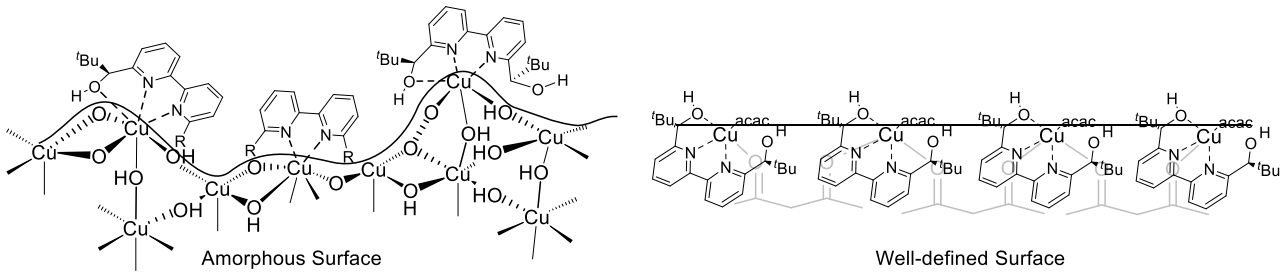

Figure 1.26. Exemplification of amorphous $Cu(OH)_2$ surface and well-defined $Cu(acac)_2$-L1 complex surface.

As just mentioned, microscopic differences on surface morphology is believed to be the origin for these differences (Figure 1.26). On one hand, $Cu(OH)_2$ has a large number of defects at neighboring OH groups on the surface, and the symmetry collapse gives the significant increment of activity. The well-defined heterogeneous $Cu(acac)_2$-**L1** complex surface is constantly losing one axial coordination partner, and therefore, exhibits relatively lower activity. Yet a loss of coordination site improved the activity of $Cu(acac)_2$-**L1** complex over homogeneous Cu(II) species in water, which retains all of its coordination partners with a Jahn-Teller distortion. Conclusively, the reaction rate could be sequenced as follow: amorphous heterogeneous catalyst (e.g. $Cu(OH)_2$, $Cu_2(OH)_2CO_3$) > well-defined heterogeneous catalyst (e.g. $Cu(acac)_2$-**L1** complex) > homogeneous catalyst (e.g. $Cu(OAc)_2$, $Cu(OTf)_2$), which presents the answer of Q2.

On the other hand, the amorphous $Cu(OH)_2$ surface does not necessarily bind the ligand in a strongly coordinative manner. Due to the enhanced activity and exchange rate of the surface, the ligands are always in competitive with other molecules. In borylation, the relatively weaker Cu-B bond, which was even weaker than the coordinative interaction between Cu(II) and **L1**, guaranteed the asymmetric environment surrounding the Cu-B(pin) intermediate. However in silylation, the stronger Cu-Si bond may result in the dissociation between Cu(II) and **L1**, and a loss of chiral information of Cu(II)-$SiMe_2Ph$ intermediate gave low enantioselection of the reaction. Meanwhile, the well-defined surface of $Cu(acac)_2$-**L1** complex prevented the dissociation of chiral ligand by the excessive formation of Cu-Si bond formation. Therefore, in general as for the answer of Q1,

Cu(acac)$_2$-**L1** complex as a heterogeneous catalyst exhibited lower reacvitiy and higher enantioselectivity than Cu(OH)$_2$+**L1** catalyst.

The pH value analysis further supported this idea. The main reaction during the induction period is considered as below:

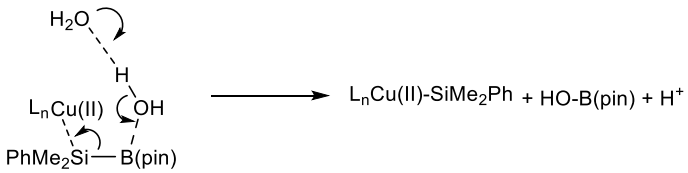

Figure 1.27. Proposed reaction during the induction period.

With the accumulation of Cu-Si intermediates, the 1,4-addition occurs successively. The proposal is also in accordance with the fact that despite the decrement rate at the initial period of Cu(OAc)$_2$ system is faster than Cu(acac)$_2$-**L1** complex, while the recovery period of Cu(acac)$_2$-**L1** complex is shorter. Due to the enhanced reactivity of Cu(OH)$_2$ surface, no induction period was observed.

1-9 Conclusion

Novel Cu(II)-catalyzed enantioselective boron and silicon conjugate additions to α,β-unsaturated compounds and α,β,γ,δ-unsaturated carbonyl compounds in water were developed. In contrast to the Cu(I) catalysis in organic solvents reported previously, a chiral Cu(II) catalysis in water was demonstrated. In borylation reactions, three catalyst systems were developed: $Cu(OH)_2$ with chiral ligand **L1**; Cat 2: $Cu(OH)_2$ and CH_3COOH with **L1**; $Cu(OAc)_2$ with **L1**. It has been shown that while $Cu(OH)_2$-**L1** system is a heterogeneous system, $Cu(OH)_2$-CH_3COOH-**L1** system and $Cu(OAc)_2$-**L1** system are homogeneous systems. Interestingly, the reaction proceeded faster with the heterogeneous system than with the homogeneous systems. Twenty nine α,β-unsaturated carbonyl compounds and an α,β-unsaturated nitrile including acyclic and cyclic α,β-unsaturated ketones, acyclic and cyclic β,β-disubstituted enones, acyclic and cyclic α,β-unsaturated esters including β,β-disubstituted forms, and acyclic α,β-unsaturated amides including β,β-disubstituted forms, were tested. $Cu(OH)_2$-CH_3COOH-**L1** system and $Cu(OAc)_2$-**L1** system showed high yields and high enantioselectivity for almost all the substrates; the TOF reached 17,600 h^{-1} and 12,800 h^{-1}, respectively. In silylation reactions, we have isolated crystals of a chiral heterogeneous Cu(II) catalyst prepared from $Cu(acac)_2$ and **L1**, which, although not soluble in water, nevertheless catalyzes asymmetric silyl conjugate addition of lipophilic substrates in this medium. The catalytic asymmetric reactions proceed in high yield and with high enantioselectivity only in water, despite neither catalysts nor reactants/products are soluble. Neither borylation nor silylation reactions proceeded at all in most organic solvents. Even in mixed water/organic solvents in which the catalyst and substrates dissolved completely, only low-to-moderate yield and low-to-moderate enantioselectivity was observed. These results are in striking contrast to many conventional organic reactions in which solubility is required. As a synthetic methodology, chiral Cu(II) catalysis in water has several advantages over previously reported catalyst systems, such as wide substrate scope and high enantioselectivity. It is noteworthy that an unprecedented TOF (43,200 h^{-1}) was achieved for the borylation reactions with the heterogeneous $Cu(OH)_2$+**L1** system. The approach is also in line with the concepts of green sustainable chemistry because it leads to a reduction in the amount of organic solvents used and is amenable to catalyst recovery and recycling. Moreover, mechanistic studies confirmed the differences between amorphous surface of heterogeneous $Cu(OH)_2$ catalyst and well-defined surface of heterogeneous $Cu(acac)_2$-**L1** complex. The actual active species on the surface of heterogeneous copper catalysts were investigated and proposed. The antagonistic combination of water-insoluble chiral heterogeneous catalyst coupled with the use of water as a solvent may open new avenues in organic chemistry that are not available through the use of conventional homogeneous catalyst systems. Water may play a prominent role in building sterically confined transition states and accelerating subsequent protonation to achieve high yield and high enantioselectivity.

References

(94) Corma, A.; Garcia, H. *Chem. Rev.* **2003**, *103*, 4307-4366.

(95) Zou, R.; Li, P. Z.; Zeng, Y. F.; Liu, J.; Zhao, R.; Duan, H.; Luo, Z.; Wang, J. G.; Zou, R.; Zhao, Y. *Small* **2016**, *12*, 2334-2343.

(96) Noda, Y.; Lee, B.; Domen, K.; Kondo, J. N. *Chem. Mater*. **2008**, *20*, 5361-5367.

(97) Biesinger, M. C.; Payne, B. P.; Grosvenor, A. P.; Lao, L. W. M.; Gerson, A. R.; Smart, R. St. C. *Appl. Surf. Sci*. **2011**, *257*, 2717-2730.

(98) Brodskii, V. A.; Gubin, A. F.; Kolesnikov, A. V.; Makarov, N. A. *Glass and Ceramics* **2015**, *72*, 220-224.

(99) Adamson, A. W.; Gast, A. P. *Physical Chemistry of Surfaces*, 6th ed.; New York, **1997**.

(100) Hubbard, A. T. *Encyclopedia of Surface and Colloid Science*, 1st ed.; Crc Pr I Llc, **2002**.

(101) (a) Rustad, J. R.; Hay, B. P.; Halley, J. W. *J. Chem. Phys.* **1995**, *102*, 427-431; (b) Rustad, J. R.; Hay, B. P. *Geochim. Cosmochim. Acta* **1995**, *59*, 1251-1257; (c) Rustad, J. R.; Felmy, A. R.; Hay, B. P. *Geochim. Cosmochim. Acta* **1996**, *60*, 1553-1562.

(102) (a) Felmy, A. R.; Rustad, J. R. *Geochim. Cosmochim. Acta* **1998**, *62*, 25-31; (b) Halley, J. W.; Rustad, J. R.; Rahman, A. *J. Chem. Phys.* **1993**, *98*, 4110-4119; (c) Curtiss, L. A.; Halley, J. W.; Hautman, J.; Rahman, A. *J. Chem. Phys*. **1987**, *86*, 2319-2327.

(103) Brown, G. E.; Henrich, V. E.; Casey, W. H.; Clark, D. L.; Eggleston, C.; Felmy, A.; Goodman, D. W.; Grätzel, M.; Maciel, G.; McCarthy, M. I.; Nealson, K. H.l Sverjensky, D. A.; Toney, M. F.; Zachara, J. M. *Chem. Rev.* **1999**, *99*, 77-174.

(104) For boron, see: (a) Lee, J. C. H.; McDonald, R.; Hall, D. G. *Nature Chem.* **2011**, *3*, 894–899; (b) Solé, C.; Tatla, A.; Mata, J. A.; Whiting, A.; Gulyás, H.; Fernández, E. *Chem. Eur. J.* **2011**, *17*, 14248–14257; (c) Scott, H. K.; Aggarwal, V. K. *Chem. Eur. J.* **2011**, *17*, 13124–13132; (d) Ohmura, T.; Awano, T.; Suginome, M. *J. Am. Chem. Soc.* **2010**, *132*, 13191–13193; (e) Imao, D.; Glasspoole, B. W.; Laberge, V. S.; Crudden, C. M. *J. Am. Chem. Soc.* **2009**, *131*, 5024–5025; (f) Stymiest, J. L.; Bagutski, V.; French, R. M.; Aggarwal, V. K. *Nature* **2008**, *456*, 778–782. For silicon, see: (a) Franz, A. K.; Wilson, S. O. *J. Med. Chem.* **2013**, *56*, 388-405; (b) Bo, Y.; Singh, S.; Duong, H. Q.; Cao, C.; Sieburth, S. M. *Org. Lett.* **2011**, *13*, 1787-1789; (c) Nielsen, L.; Skrydstrup, T. *J. Am. Chem. Soc.* **2008**, *130*, 13145-13151; (d) Sieburth, S. M.; Chen, C.-A. *Eur. J. Org. Chem.* **2006**, *2006*, 311-322; (e) Kim, J.; Hewitt, G.; Carroll, P.; Sieburth, S. M. *J. Org. Chem.* **2005**, *70*, 5781-5789; (f) Showell, G. A.; Mills, J. S. *Drug Discovery Today* **2003**, *8*, 551-556; (g) Wakahara, T.; Maeda, Y.; Kako, M.; Akasaka, T.; Kobayashi, K.; Nagase, S. *J. Organomet. Chem.* **2003**, *685*, 177-188.

(105) Suzuki, A. *Pure & Appl. Chem.* **1994**, *66*, 213-222.

(106) (a) Min, G. K.; Hernández, D.; Skrydstrup, T. *Acc. Chem. Res.* **2013**, 46, 457-470; (b) Shintani, R.; Ichikawa, Y.; Hayashi, T.; Chen, J.; Nakao, Y.; Hiyama, T. *Org. Lett.* **2007**, *9*, 4643-4645; (c) Thomas, S. E. *Organic Synthesis: The Roles of Boron and Silicon*; Oxford University

Press: Oxford, **1991**.
(107) The initial discovery of utilizing transition metals with a diboron reagent: Nguyen, P.; Lesley, G.; Taylor, N. J.; Marder, T. B.; Pickett, N. L.; Clegg, W.; Elsegood, M. R. J.; Norman, N. C. *Inorg. Chem.* **1994**, *33*, 4623–4624.
(108) Ito, H.; Yamanaka, H.; Tateiwa, J.; Hosomi, A. *Tetrahedron Lett.* **2000**, *41*, 6821–6825.
(109) (a) Takahashi, K.; Takagi, J.; Ishiyama, T.; Miyaura, N. *Chem. Lett.* **2000**, *29*, 126–127; (b) Takahashi, K.; Ishiyama, T.; Miyaura, N. *J. Organomet. Chem.* **2001**, *625*, 47–53.
(110) Kim, D.; Park, B. –M.; Yun, J. *Chem. Commun.* **2005**, 1755-1757.
(111) Mun, S.; Lee, J.-E.; Yun, J. *Org. Lett.* **2006**, *8*, 4887–4889.
(112) (a) Feng, X.; Yun, J. *Chem. Eur. J.* **2010**, *16*, 13609–13612; (b) Chea, H.; Sim, H.-S.; Yun, J. *Adv. Synth. Catal.* **2009**, *351*, 855–858; (c) Sim, H.; Feng, X.; Yun, J. *Chem. Eur. J.* **2009**, *15*, 1939–1943; (d) Lee, J.-E.; Yun, J. *Angew. Chem. Int. Ed.* **2008**, *47*, 145–147.
(113) Works by Shibasaki *et al.*: (a) Chen, I. -H.; Yin, L.; Itano, W.; Kanai, M.; Shibasaki, M. *J. Am. Chem. Soc.* **2009**, *131*, 11664-11665; (b) Chen, I. –H.; Kanai, M.; Shibasaki, M. *Org. Lett.* **2010**, *12*, 4098-4101. Work by Fernández *et al.*; Fleming, W. J.; Müller-Bunz, H.; Lillo, V.; Fernández, E.; Guiry, P. J. *Org. Biomol. Chem.* **2009**, *7*, 2520-2524.
(114) Bonet, A.; Solé, C.; Gulyás, H.; Fernández, E. *Chem. Asian J.* **2011**, *6*, 1011-1014.
(115) (a) Hirano, K.; Yorimitsu, H.; Oshima, K. *Org. Lett.* **2007**, *9*, 5031-5033; (b) Lillo, V.; Geier, M. J.; Westcott, S. A.; Fernández, E. *Org. Biomol. Chem.* **2009**, *7*, 4674-4676.
(116) Kajiwara, T.; Terabayashi, T.; Yamashita, M.; Nozaki, K. *Angew. Chem. Int. Ed.* **2008**, *47*, 6606-6610.
(117) (a) Liu, B.; Gao, M.; Dang, L.; Zhao, H.; Marder, T. B.; Lin, Z. *Organometallics* **2012**, *31*, 3410-3425; (b) Bell, N. J.; Cox, A. J.; Cameron, N. R.; Evans, J. S. O.; Marder, T. B.; Duin, M. A.; Elsevier, C. J.; Baucherel, X.; Tulloch, A. A. D.; Tooze, R. P. *Chem. Commun.* **2004**, 1854-1855; (c) Ali, H. A.; Goldberg, I.; Srebnik, M. *Organometallics* **2001**, *20*, 3962-3965; (d) Lawson, Y. G.; Lesley, M. J. G.; Marder, T. B.; Norman, N. C.; Rice, C. R. *Chem. Commun.* **1997**, 2051-2052.
(118) (a) Lillo, V.; Geier, M. J.; Westcott, S. A.; Fernández, E. *Org. Biomol. Chem.* **2009**, *7*, 4674–4676; (b) Pubill-Ulldemolins, C.; Bonet, A.; Bo, C.; Gulyás, H.; Fernández, E. *Org. Biomol. Chem.* **2011**, *8*, 2667-2682; (c) Bonet, A.; Gulyás, H.; Koshevoy, I. O.; Estevan, F.; Sanaú, M.;Úbeda, M. A.; Fernandéz, E. *Chem. Eur. J.* **2010**, *16*, 6382-6390.
(119) Ramírez, J.; Corberán, R.; Sanaú, M.; Peris, E.; Fernández, E. *Chem. Commun.* **2005**, 3056-3058.
(120) Hata, H.; Shinokubo, H.; Osuka, A. *J. Am. Chem. Soc.* **2005**, *127*, 8264-8265.
(121) Bonet, A.; Gulyás, H.; Fernández, E. *Angew. Chem. Int. Ed.* **2010**, *49*, 5130-5134.
(122) (a) Walter, C.; Auer, G.; Oestreich, M. *Angew. Chem. Int. Ed.* **2006**, *45*, 5675-5677; (b) Walter, C.; Oestreich, M. *Angew. Chem. Int. Ed.* **2008**, *47*, 3818-3820.
(123) (a) Walter, C.; Fröhlich, R.; Oestreich, M. *Tetrahedron* **2009**, *65*, 5513-5520; (b) Hartmann, E.; Oestreich, M. *Angew. Chem., Int. Ed.* **2010**, *49*, 6195-6198; (c) Hartmann, E.; Oestreich, M. *Org. Lett.*

2012, 14, 2406-2409.
(124) (a) Toribatake, K.; Zhou, L.; Tsuruta, A.; Nishiyama, H. *Tetrahedron* **2013**, *69*, 3551-3560; (b) Shiomi, T.; Adachi, T.; Toribatake, K.; Zhou, L.; Nishiyama, H. *Chem. Commun.* **2009**, 5987-5989.
(125) First achiral example of NHC-Cu(I) catalyzed borylation reactions toward alkene: Laitar, D. S.; Müller, P.; Sadighi, J. P. *J. Am. Chem. Soc.* **2005**, *127*, 17196-17197; First asymmetric example of NHC-Cu(I) catalyzed borylation reactions: Bonet, A.; Díaz-Requejo, M. M.; Fernández, E.; Lillo, V.; Pérez, P. J.; Prieto, A.; Ramírez, J. *Organometallics* **2009**, *28*, 659-662.
(126) For boron, see: (a) O'Brien, J. M.; Lee, K. -S.; Hoveyda, A. H. *J. Am. Chem. Soc.* **2010**, *132*, 10630-10633; (b) Lee, K. -S.; Zhugralin, A. R.; Hoveyda, A. H. *J. Am. Chem. Soc.* **2009**, *131*, 7253–7255. For silicon, see: (a) Lee, K. -S.; Hoveyda, A. H. *J. Am. Chem. Soc.* **2010**, *132*, 2898-2900; (b) O'Brien, J. M.; Hoveyda, A. H. *J. Am. Chem. Soc.* **2011**, *133*, 7712-7715; (c) Lee, K. -S.; Wu, H.; Haeffner, F.; Hoveyda, A. H. *Organometallics* **2012**, *31*, 7823-7826.
(127) Hirsch-Weil, D.; Abboud, K. A.; Hong, S. *Chem. Commun.* **2010**, *46*, 7525-7527.
(128) Iglesias, M.; Beetstra, D. J.; Stasch, A.; Horton, P. N.; Hursthouse, M. B.; Coles, S. J.; Cavell, K. J.; Dervisi, A.; Fallis, I. A. *Organometallics* **2007**, *26*, 4800-4809.
(129) Park, J. K.; Lackey, H. H.; Rexford, M. D.; Kovnir, K.; Shatruk, M.; McQuade, D. T. *Org. Lett.* **2010**, *12*, 5008-5011.
(130) Huang, L.; Cao, Y.; Zhao, M.; Tang, Z.; Sun, Z. *Org. Biomol. Chem.* **2014**, *12*, 6554-6556.
(131) Iwai, T.; Akiyama, Y.; Sawamura, M. *Tetrahedron: Asymmetry* **2013**, *24*, 729-735.
(132) (a) Bolm, C.; Focken, T.; Raabe, G. *Tetrahedron: Asymmetry* **2003**, *14*, 1733-1746; (b) Hong, B.; Ma, Y.; Zhao, L.; Duan, W.; He, F.; Song, C. *Tetrahedron: Asymmetry* **2011**, *22*, 1055-1062; (c) Zhao, L.; Ma, Y.; Duan, W.; He, F.; Chen, J.; Song, C. *Org. Lett.* **2012**, *14*, 5780-5783; (d) Zhao, L.; Ma, Y.; He, F.; Duan, W.; Chen, J. C. Song, *J. Org. Chem.* **2013**, *78*, 1677-1681.
(133) (a) Pace, V.; Rae, J. P.; Harb, H. Y.; Procter, D. J. *Chem. Commun.* **2013**, 5150-5152; (b) Pace, V.; Rae, J. P.; Procter, D. J. *Org. Lett.* **2014**, *16*, 476-479.
(134) (a) Lee, K. S.; Zhugralin, A. R.; Hoveyda, A. H. *J. Am. Chem. Soc.* **2009**, *131*, 7253-7255 (Correction: *J. Am. Chem. Soc.* **2010**, *132*, 12766); (b) Radomkit, S.; Hoveyda, A. H. *Angew. Chem. Int. Ed.* **2014**, *53*, 3387-3391; (c) Wu, H.; Garcia, J. M.; Radomkit, S.; Zhugralin, A. R.; Hoveyda, A. H. *J. Am. Chem. Soc.* **2015**, *137*, 10585-10602.
(135) For borylation: Thorpe, S. B.; Calderone, J. A.; Santos, W. L. *Org. Lett.* **2012**, *14*, 1918–1921; For silylation: Calderone, J. A.; Santos, W. L. *Angew. Chem. Int. Ed.* **2014**, *53*, 4154-4158.
(136) (a) Ishikawa, S.; Hamada, T.; Manabe, K.; Kobayashi, S. *Synthesis* **2005**, 2176–2182; (b) Bolm, C.; Ewald, M.; Felder, M.; Schlingloff, G. *Chem. Ber.* **1992**, *125*, 1169–1190; (c) Bolm, C.; Zehnder, M.; Bur, D. *Angew. Chem. Int. Ed.* **1990**, *29*, 205–207.
(137) Dai, W.; Guo, D.; Sun, L. *Tetrahedron Lett.* **2001**, *42*, 5275-5278.
(138) Fujita, M.; Nagano, T.; Schneider, U.; Hamada, T.; Ogawa, C.; Kobayashi, S. *J. Am. Chem. Soc.* **2008**, *130*, 2914-1915.
(139) Kobayashi, S.; Endo, T.; Ueno, M. *Angew. Chem. Int. Ed.* **2011**, *50*, 20262-20265.

(140) Ma, D.-Y.; Wang, D.-X.; Pan, J.; Huang, Z.-T.; Wang, M.-X. *J. Org. Chem.* **2008**, *73*, 4087–4091.

(141). Mukaiyama, T.; Kamio, K.; Kobayashi, S.; Takei, H. *Chem. Lett.* **1973**, 357–358.

(142) Tamao, K.; Ishida, N. *J. Organomet. Chem*. **1984**, *269*, c37-c39.

(143) Lee, K.-S.; Wu, H.; Haeffner, F.; Hoveyda, A. H. *Organometallics* **2012**, *31*, 7823–7826.

(144) (a) Tissot, M.; Poggiali, D.; Hénon, H.; Müller, D.; Guénée, L.; Mauduit, M.; Alexakis, A. *Chem. Eur. J.* **2012**, *18*, 8731–8747; (b) Wencel-Delord, J.; Alexakis, A.; Crévisy, C.; Mauduit, M. *Org. Lett.* **2010**, *12*, 4335–4337; (c) Hénon, H.; Mauduit, M.; Alexakis, A. *Angew. Chem. Int. Ed.* **2008**, *47*, 9122–9124; (d) den Hartog, T.; Harutyunyan, S. R.; Font, D.; Minnaard, A. J.; Feringa, B. L. *Angew. Chem. Int. Ed.* **2008***, 47*, 398–401; (e) Hayashi, T.; Yamamoto, S.; Tokunaga, N. *Angew. Chem. Int. Ed.* **2005**, *44*, 4224–4227; (f) Cesati, R. R.; de Armas, J.; Hoveyda, A. H. *J. Am. Chem. Soc.* **2004**, *126*, 96–101.

(145) Kokubo, M.; Naito, T.; Kobayashi, S. *Tetrahedron* **2010**, *66*, 1111–1118.

(146) (a) Tissot, M.; Poggiali, D.; Hénon, H.; Müller, D.; Guénée, L.; Mauduit, M.; Alexakis, A. *Chem. Eur. J.* **2012**, *18*, 8731–8747; (b) Lee, K. -S.; Wu, H.; Haeffner, F.; Hoveyda, A. H. *Organometallics* **2012**, *31*, 7823–7826.

(147) Scorrano, G.; O'Ferrall, R. M. *J. Phys. Org. Chem.* **2013**, *26*, 1009-1015.

Chapter 2. Lewis Acid-Single Walled Carbon Nanotube Integrated Catalysts

5年以内に雑誌等で刊行予定のため非公開

Chapter 3. Development of New Light-Induced Catalysts and Their Application Toward Hydration Reactions in Water

5年以内に雑誌等で刊行予定のため非公開

Recapitulation

Water has occupied a pivotal place in (bio)organic synthesis, and will continue to be imperative to develop organic chemistry with undiscovered reactivity and regio-/stereo- selectivity. The primary objective of the present dissertation is to deepen our understanding toward organic chemistry in water, *acting as a brick to attract jade*.

In Chapter 1, I presented enantioselective boron/silicon conjugate additions to α,β-unsaturated carbonyl compounds and α,β,γ,δ-unsaturated carbonyl compounds in water. In contrast to the Cu(I) catalysis reported previously in organic solvents, chiral Cu(II) catalysis was found to work efficiently in water. In silylation reactions, crystalline Cu(acac)-**L1** complex was identified as the best catalyst. In borylation reactions, three catalyst systems have been exploited: Cat 1: $Cu(OH)_2$ with chiral ligand **L1**; Cat 2: $Cu(OH)_2$ and acetic acid with **L1**; Cat 3: $Cu(OAc)_2$ with **L1**. While Cat 1 is a heterogeneous system, Cat 2 and Cat 3 are homogeneous systems. For both reactions, more than 30 kinds of substrates were tested, including α,β-unsaturated carbonyl compounds, α,β-unsaturated nitriles and nitroolefins, acyclic and cyclic α,β-unsaturated ketones, acyclic and cyclic β,β-disubstituted enones, acyclic and cyclic α,β-unsaturated esters including β,β-disubstituted forms, and acyclic α,β-unsaturated amides including β,β-disubstituted forms. It is noted that no catalysts that cover all these substrates with high yields and high enantioselectivities have ever been reported for both boron and silicon conjugate addition reactions. In borylation reactions, while Cat 2 and Cat 3 afforded better results in most cases, the heterogeneous Cat 1 sometimes gave high yields and high enantioselectivities for some substrates, and also gave the highest TOF (43,200 h^{-1}). In addition, the Cu(II)-catalyst systems were also applicable to boron/silicon conjugate additions to α,β,γ,δ-unsaturated carbonyl compounds, although conventional methods have been very limited even in organic solvents. 1,4-Addition products were obtained exclusively in high yield with high enantioselectivity in the reactions of acyclic α,β,γ,δ-unsaturated carbonyl compounds with diboron **2** or boron-silicon **3**. It is noteworthy that in the borylation reactions of cyclic α,β,γ,δ-unsaturated carbonyl compounds with diboron **2**, while 1,4-addition products were obtained exclusively using Cat 2 or Cat 3, 1,6-addition products were exclusively produced using Cat 1. Similar unique reactivities and selectivities were also shown in the reactions of cyclic trienones. Finally, the reaction mechanisms were investigated both experimentally and computationally. The differences between amorphous heterogeneous $Cu(OH)_2$ catalyst and heterogeneous $Cu(acac)_2$-**L1** complex with well-defined surface were interpreted. Water is expected to be effective in the activation of a borylcopper(II) intermediate and a protonation event subsequent to a nucleophilic addition, leading to overwhelmingly high catalytic turnover.

Scheme 4.1. Cu(II)-mediated enantioselective boron/silicon conjugate additions.

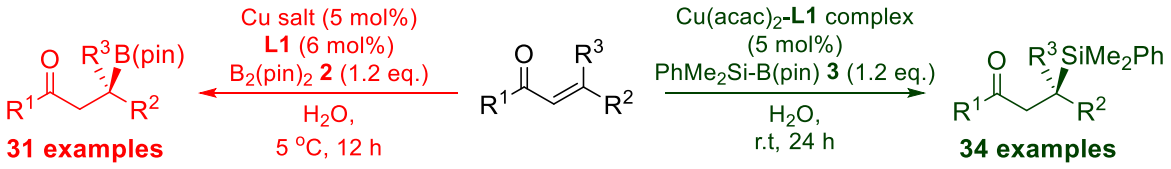

On a final note, I hope that this dissertation will provide expedient, environmentally benign, and highly efficient synthetic methodologies to synthesize optically active compounds and open up new opportunities in organic chemistry.

Experimental Section

General

Nuclear magnetic resonance (NMR) spectra were recorded on a JEOL ECX-600 or ECX-500 spectrometer, operating at 600 or 500 MHz for ^{1}H and 150 or 125 MHz for ^{13}C NMR in $CDCl_3$ unless otherwise noted. Trimethylsilane (TMS) served as the internal standard ($\delta = 0$) for ^{1}H NMR and $CDCl_3$ was used as the internal standard ($\delta = 77.0$) for ^{13}C NMR. Infrared (IR) spectra were obtained using a JASCO FT/IR-4200 spectrometer. Data are represented as frequency of absorption (cm^{-1}). High-performance liquid chromatography was carried out using following apparatuses; SHIMADZU LC-10ATvp (liquid chromatograph), SHIMADZU SPD-10A (UV detector) and SHIMADZU C-R8A (Chromatopac) using Daicel chiralpak® or chiralcel® columns. Dynamic laser light scattering (DLS) analysis was performed to measure the particle size distribution and average particle sizes using a Zetasizer Nano ZS machine (Malvern Instruments Ltd.). Preparative thin-layer chromatography (PTLC) was carried out using Wakogel B-5F from Wako Pure Chemical Industries, Ltd. High Resolution Mass Spectra (HRMS) were recorded using a JEOL JMS-T100TD (DART) spectrometer or Brucker Daltonics BioTOF II (ESI) spectrometer. Optical Rotations were measured on a JASCO P1010 polarimeter using a 2 mL cell with 1 dm path length. Data are reported as follows: $[\alpha]_D^T$ (*c* in g/100 mL, solvent). STEM/EDS images were obtained using a JEOL JEM-2100F instrument operated at 200 kV. Optical Microscope studies were conducted using BX53 instrument (Olympus). Inductively Coupled Plasma (ICP) analysis was performed on Shimadzu ICPS-7510 equipment. 0.45 μm PTFE membrane filter (Whatman™ cat. No. 6784-2504) or 0.20 μm PTFE membrane filter (Whatman™ cat. No. 6784-2502) was used for filtration experiment. Cyclic voltammetry was carried out in a standard one-compartment cell under an argon atmosphere using a Pt-wire counter electrode and an Ag/Ag^+ reference electrode with a HZ-5000 voltammetric analyzer (HOKUTO DENKO). A glassy carbon rod was embedded in Pyrex glass, and the cross section was used as a working electrode.Raman spectroscopy was recorded using Horiba HR-800 Raman spectrometer. The Raman signal was collected with a long working distance lens, with the excitation wavelength of 488, 514, 633, and 785 nm. Centrifugation was performed by using KOKUSAN H-36 centrifuge. Deionized water from a MILLIPORE MilliQ machine (Gradient A 10) was used as solvent without further treatment. Deuterium oxide (99.8% atom% D) was purchased from ACROS and used without further treatment. All organic solvents used were commercially available dry solvents,

which were distilled appropriately under an argon atmosphere or were stored over molecular sieves prior to use. All reagents used as additives were either distilled or recrystallized before use.

Chapter 1: Utilization of Insoluble Cu(II) salts as Catalysts

1.1 For Cu(II)-mediated borylation reactions:

1.1-1 <Reagents>

Unless stated otherwise, commercially available reagents were used as received with the exception of the following substrates, which were prepared through reported methods. Analytical data for these compounds are in full agreement with reported data.

(*E*)-1-(4'-methoxyphenyl)-3-phenylprop-2-en-1-one (**1c**)[1]

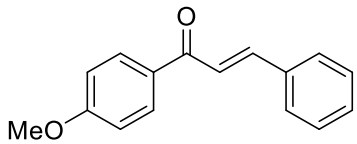

White solid

^{1}H NMR (500 MHz); δ = 3.90 (s, 3H), 6.98 (dd, *J* = 1.7, 5.2 Hz, 2H), 7.40-7.43 (m, 3H), 7.48 (d, *J* = 48.7 Hz, 1H), 7.56-7.65 (m, 2H), 7.80 (d, *J* = 8.7 Hz, 1H), 8.03-8.05 (t, *J* = 2.3 Hz, 2H)

^{13}C NMR (125 MHz); δ = 56.7, 115.3, 120.2, 122.2, 123.5, 126.6, 128.1, 129.9, 138.8, 147.3, 166.0, 199.6.

(*E*)-4,4-Dimethyl-1-phenylpent-2-en-1-one (**1g**)[3]

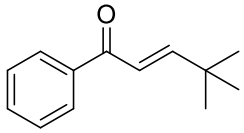

Pale yellow liquid

^{1}H NMR (500 MHz); δ = 1.15 (s, 9H), 6.76 (d, *J* = 13.8 Hz, 1H), 7.04 (d, *J* = 13.8 Hz, 1H), 7.44-7.48 (m, 2H), 7.52-7.56 (m, 1H), 7.90 (d, *J* = 8.4 Hz, 2H).

^{13}C NMR (125 MHz); δ = 26.1, 28.8, 34.1, 121.0, 128.5, 132.5, 138.3, 159.6, 191.6.

(*E*)-1,3-Diphenyl-2-buten-1-one (**1i**)[4]

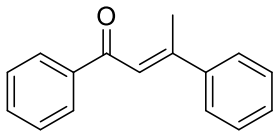

Orange oil

^{1}H NMR (500 MHz); δ = 2.62 (s, 3H), 7.15 (s, 1H), 7.42-7.89 (m, 8H), 8.02-8.05 (m, 2H).

^{13}C NMR (125 MHz); δ = 18.9, 122.2, 125.9, 128.0, 128.3, 128.4, 129.9, 132.0, 139.0, 142.3, 155.2, 199.2.

(*E*)-4-Methyl-1-phenylpent-2-en-1-one (**1m**)[2]

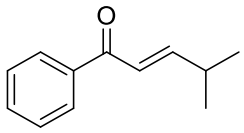

Pale yellow liquid

^{1}H NMR (500 MHz); δ = 1.11 (d, *J* = 6.9 Hz, 6H), 2.54-2.56 (m, 1H), 6.79 (dd, *J* = 6.4, 9.2 Hz, 1H), 7.04 (dd, *J* = 6.4, 9.2 Hz, 1H), 7.42-7.52 (m, 3H), 7.89 (d, *J* = 7.6 Hz, 2H).

^{13}C NMR (125 MHz); δ = 21.4, 31.5, 123.1, 128.5, 129.6, 132.5, 138.1, 156.0, 191.3.

(*E*)-4-Phenylpent-3-en-2one (**1n**)[5]

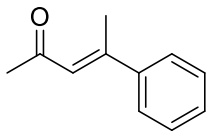

Yellow oil

^{1}H NMR (500 MHz); δ = 2.30 (d, *J* = 1.1 Hz, 3H), 2.54 (s, 3H), 6.50 (s, 1H), 7.36-7.39 (m, 3H), 7.45-7.50 (m, 2H).

^{13}C NMR (125 MHz); δ = 18.9, 31.9, 125.0, 126.4, 128.6, 129.1, 142.4, 154.0, 199.1.

Ethyl (*E*)-3-phenylbut-2-enoate (**5d**)[6]

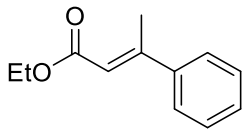

Pale yellow liquid

^{1}H NMR (500 MHz); δ = 1.06 (t, *J* = 7.3 Hz, 3H), 2.16 (s, 3H), 3.96-4.01 (m, 2H), 5.88-5.90 (m, 1H),

7.15-7.38 (m, 5H).

^{13}C NMR (125 MHz); δ = 14.1, 26.5, 59.5, 119.2, 126.4, 127.5, 128.0, 138.2, 154.3, 169.9.

(*E*)- and (*Z*)-4-Fluorocinnamonitrile (**6b**)[49]

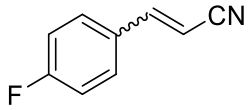

Wet white solid (*E/Z* = 5.3/1).

^{1}H NMR (600 MHz); δ = 5.77 (d, J = 16.5 Hz, 1H), 7.06-7.12 (m, 2H), 7.33 (d, J = 16.5 Hz, 1H), 7.41-7.44 (m, 2H).

^{13}C NMR (150 MHz); δ = 96.1, 116.0 (d), 117.9, 129.3 (d), 131.1 (d), 149.2, 163.5 (d).

(*E*)- and *(Z*)-2-(2-Furyl)acrylonitrile (**6d**)[49]

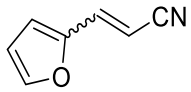

Wet white solid (*E/Z* = 5.3/1).

^{1}H NMR (600 MHz); δ = 5.73 (d, J = 16.3 Hz, 1H), 6.51 (d, *J* = 3.4 Hz, 1H), 6.60 (d, *J* = 3.4 Hz, 1H), 7.10-7.18 (m, 1H), 7.47-7.50 (m, 1H).

^{13}C NMR (150 MHz); δ = 93.4, 112.6, 115.5, 118.2, 136.1, 145.4, 149.8.

(*E*)-*N*,*N*-Diethyl-3-phenylbut-2-enamide (**7c**)[7]

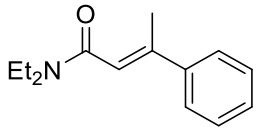

White Solid

^{1}H NMR (500 MHz); δ = 1.07 (t, *J* = 5.3 Hz, 6H), 2.19 (s, 3H), 2.59-2.62 (m, 4H), 5.75.73 (s, 1H), 7.19-7.41 (m, 5H).

^{13}C NMR (125 MHz); δ = 13.9, 35.2, 59.1, 117.2, 127.1, 127.6, 128.0, 140.2, 155.3, 172.1.

(3*E*, 5*E*)-4-methyl-6-phenylhexa-3,5-dien-2-one (**10c**)[9]

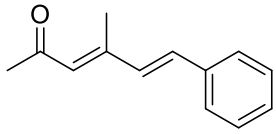

Pale yellow solid

^{1}H NMR (500 MHz); δ = 2.24 (s, 3H), 2.36 (s, 3H), 6.24 (s, 1H), 6.75 (d, *J* = 13.4 Hz, 1H), 6.98 (d, *J* = 13.4 Hz, 1H), 7.26–7.35 (m, 3H), 7.44–7.46 (m, 2H).

^{13}C NMR (125 MHz); δ = 14.1, 32.2, 127.1, 127.4, 128.7, 128.9, 132.8, 135.4, 136.4, 151.3, 200.1

Ethyl (2*E*, 4*E*)-5-Phenylpenta-2,4-dienoate (**10f**)[8]

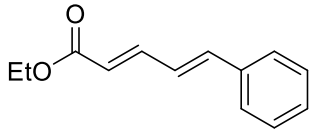

Pale yellow liquid

^{1}H NMR (500 MHz); δ = 1.07 (t, *J* = 5.6 Hz, 3H), 3.87-3.93 (m, 2H), 6.01-6.02 (m, 1H), 6.31-6.31 (m, 1H), 6.65-6.67 (m, 1H), 6.91-6.93 (m, 1H), 7.22-7.43 (m, 5H).

^{13}C NMR (125 MHz); δ = 14.3, 26.5, 126.8, 127.4, 127.9, 129.1, 130.4, 133.2, 136.1, 148.7, 169.1.

Ethyl (2*E*, 4*E*)-3-methyl-5-phenylpenta-2,4-dienoate (**10g**)[10]

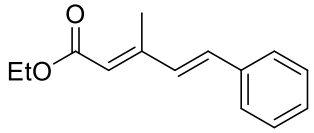

Yellow liquid

^{1}H NMR (500 MHz); δ = 1.12 (t, *J* = 5.4 Hz, 3H), 2.42 (s, 3H), 3.84-3.92 (m, 2H), 5.89-5.91 (m, 1H), 6.61-6.62 (m, 1H), 6.78-6.80 (m, 1H), 7.19-7.43 (m, 5H).

^{13}C NMR (125 MHz); δ = 14.3, 17.2, 26.5, 121.2, 126.7, 127.9, 128.4, 130.1, 134.7, 138.2, 152.3, 174.1.

(*E*)-3-Styrylcyclohex-2-en-1-one (**11a**)[11]

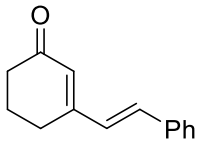

Yellow solid

^{1}H NMR (500 MHz); δ = 1.99-2.08 (m, 2H), 2.42-2.54 (m, 4H), 6.02 (s, 1H), 6.69 (d, *J* = 15.6 Hz, 1H), 6.92 (d, *J* = 15.6 Hz, 1H), 7.24-7.41 (m, 5H).

^{13}C NMR (125 MHz); δ = 23.1, 25.2, 38.0, 126.2, 127.9, 128.2, 128.6, 130.1, 134.5, 137.7, 160.2,

200.7.

(*E*)-3-(2-Phenylprop-1-en-1-yl)cyclohex-2-en-1-one (**11d**)[12]

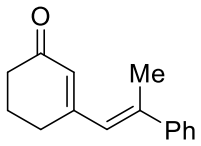

Yellow solid

^{1}H NMR (500 MHz); δ = 1.89-2.01 (m, 2H), 2.32-2.56 (m, 7H), 6.02 (s, 1H), 6.87 (s, 1H), 7.25-7.42 (m, 5H).

^{13}C NMR (125 MHz); δ = 16.7, 22.4, 24.7, 38.2, 127.1, 127.8, 128.4, 128.8, 128.9, 134.5, 137.7, 157.8, 199.9.

(*E*)-3-Styrylcyclopent-2-en-1-one (**11e**)[11]

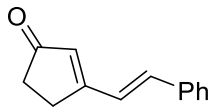

A liitle bit yellow solid

^{1}H NMR (500 MHz); δ = 2.48-2.54 (m, 2H), 2.85-2.88 (m, 2H), 6.09 (s, 1H), 7.06 (d, *J* = 17.8 Hz, 1H), 7.19 (d, *J* = 17.6 Hz, 1H), 7.29-7.41 (m, 3H), 7.48-7.53 (m, 2H).

^{13}C NMR (125 MHz); δ = 29.7, 36.5, 125.5, 126.3, 127.7, 128.3, 128.9, 131.0, 133.6, 159.2, 207.2.

(*E*)-3-Styrylcyclohept-2-en-1-one (**11f**)[11]

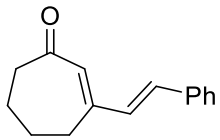

Pale yellow solid

^{1}H NMR (500 MHz); δ = 1.78-1.91 (m, 4H), 2.59-2.63 (m, 2H), 2.70-2.72 (m, 2H), 6.13 (s, 1H), 6.81 (d, *J* = 15.6 Hz, 1H), 6.92 (d, *J* = 15.6 Hz, 1H), 7.24-7.46 (m, 5H).

^{13}C NMR (125 MHz); δ = 21.5, 25.7, 28.7, 42.3, 127.7, 128.9, 129.3, 132.1, 134.0, 134.7, 137.3, 155.6, 206.2.

(*Z*)-4-Benzylidenecyclohex-2-en-1-one (**11g**)

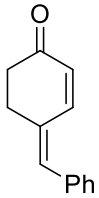

Pale yellow solid; mp 127-130 ºC.

IR (neat) = 1189, 1607, 1664, 2762 cm^{-1}.

^{1}H NMR (500 MHz); δ = 1.69-1.79 (m, 2H), 2.65-2.68 (m, 2H), 6.06 (d, *J* = 13.4 Hz, 1H), 6.39 (d, *J* = 13.4 Hz, 1H), 7.09 (s, 1H), 7.29-7.53 (m, 5H).

^{13}C NMR (125 MHz); δ = 28.7, 39.2, 126.5, 127.2, 127.5, 128.2, 129.5, 131.2, 134.1, 150.2, 200.3.

HRMS (ESI) calcd for $C_{13}H_{12}O$ $[M+H]^+$ 184.0888, found 184.0886.

Cyclohexa-2,4-dien-1-one (**11h**)[13]

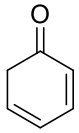

Yellow liquid

^{1}H NMR (500 MHz); δ = 3.02 (d, *J* = 8.2 Hz, 2H), 6.28-6.30 (m, 1H), 6.77-6.79 (m, 1H), 7.01-7.04 (m, 1H), 7.12-7.14 (m, 1H).

^{13}C NMR (125 MHz); δ = 39.9, 126.7, 129.2, 133.2, 137.9, 194.5.

7-Phenyl-4,4a,5,6-tetrahydronaphthalen-2(3H)-one (**11i**)[14]

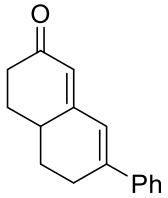

Yellow solid

^{1}H NMR (500 MHz); δ = 1.57-1.87 (m, 4H), 2.56-2.91 (m, 5H), 6.26 (s, 1H), 6.96 (s, 1H), 7.16-7.35 (m, 5H).

^{13}C NMR (125 MHz); δ = 28.0, 29.2, 29.6, 36.7, 37.6, 121.9, 123.7, 126.9, 127.7, 127.9, 136.4, 140.9, 158.6, 200.9.

3-((1*E*, 3*E*)-4-Phenylbuta-1,3-dien-1-yl)cyclohex-2-en-1-one (**11b**)[15]

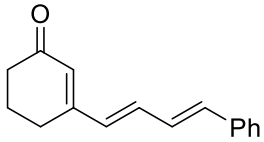

Orange solid

^{1}H NMR (500 MHz); δ = 2.06-2.09 (m, 2H), 2.44(t, *J* = 7.6 Hz, 2H), 2.54 (t, *J* = 7.6 Hz, 2H), 6.02 (s, 1H), 6.42 (d, *J* = 16.3 Hz, 1H), 6.72 (d, *J* = 16.7 Hz, 1H), 6.82 -6.84 (m, 1H), 6.92-6.95 (m, 1H), 7.29-7.43 (m, 5H).

^{13}C NMR (125 MHz); δ = 22.5, 25.0, 37.6, 127.0, 127.8, 128.5, 128.7, 129.4, 133.5, 136.0, 136.9, 137.2, 158.7, 199.9.

(2*E*, 3*E*)-*N*-isopropyl-4-phenylbut-3-en-2-imine

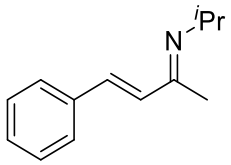

Followed Method A (*vide infra*)

Yellow oil.

^{1}H NMR (400 MHz, $CDCl_3$); δ = 1.00 (d, *J* = 5.6 Hz, 6H), 2.05 (s, 3H), 2.49-2.57 (m, 1H), 6.83 (d, *J* = 16.6 Hz, 1H), 7.32-7.59 (m, 6H).

^{13}C NMR (100 MHz, $CDCl_3$); δ = 11.6, 23.4, 67.3, 119.9, 127.8, 128.8, 128.9, 129.8, 136.2, 165.0.

HRMS (ESI) calcd for $C_{13}H_{18}N$ $[M+H]^+$ 188.1439, found 188.1426.

(2*E*, 3*E*)-N,4-Diphenylbut-3-en-2-imine[1]

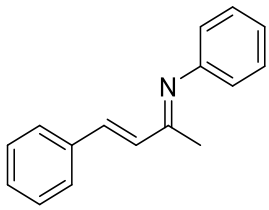

Followed Method B (*vide infra*)

White solid; mp 47-53 ºC.

^{1}H NMR (500 MHz, $CDCl_3$); δ = 2.28 (s, 3H), 6.69 (d, *J* = 15.9 Hz, 1H), 7.18-7.53 (m, 11H).

^{13}C NMR (125 MHz, $CDCl_3$); δ = 13.7, 115.8, 116.6, 119.5, 120.1, 122.3, 128.1, 130.9, 136.3, 145.4,

149.1, 161.2.

(2*E*, 3*E*)-*N*-Benzyl-4-phenylbut-3-en-2-imine [1]

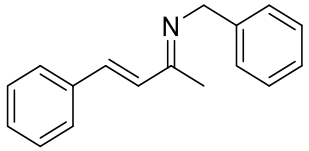

Followed Method B (*vide infra*)

Pale yellow solid; mp 61-66 ºC.

^{1}H NMR (500 MHz, $CDCl_3$); δ = 2.19 (s, 3H), 4.67 (s, 1H), 4.74 (s, 1H), 6.99 (d, 1H, *J* = 16.4 Hz), 7.03 (d, 1H, *J* = 8.5 Hz), 7.26-7.53 (m, 10H).

^{13}C NMR (125 MHz, $CDCl_3$); δ = 12.2, 50.1, 120.6, 124.5, 125.4, 126.0, 126.3, 126.9, 128.5, 133.4, 137.1, 139.9, 162.8.

(2*E*, 3*E)*-4-Phenylbut-3-en-2-one oxime

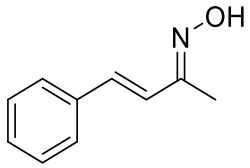

To a solution of (*E*)-4-phenylbut-3-en-2-one (1.46 g, 10 mmol) and pyridine (2.0 mL, 25 mmol) in EtOH (20 mL) was added NH_2OH•HCl (1.04 g, 15 mmol) in one portion and the reaction mixture was stirred at 60 °C for 12 h. The reaction was quenched with water and extracted twice with AcOEt. The combined organic layers was washed with 1N aqueous HCl and brine, and dried over $MgSO_4$. Volatile materials were removed under reduced pressure.

White solid; mp 122-124 ºC.

^{1}H NMR (500 MHz, $CDCl_3$); δ = 2.15 (s, 3H), 6.87-6.93 (m, 2H), 7.28-7.35 (m, 3H), 7.46 (d, 2H, *J* = 7.9 Hz).

^{13}C NMR (125 MHz, $CDCl_3$); δ = 9.7, 125.7, 126.9, 128.4, 128.7, 133.4, 136.3, 156.8.

(*E*)-1-Phenyl-2-((*E*)-4-phenylbut-3-en-2-ylidene)hydrazine[1]

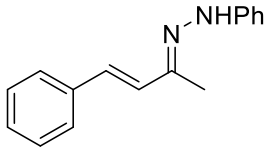

Benzalacetone (1.46 g, 10 mmol) and phenylhydrazine (1.16 g, 11 mmol) were dissolved in MeOH and AcOH (1mL) was added. The reaction solution was stirred at room temperature. After the completion of the reaction, the solid was collected by filtration and washed with cooled MeOH. Then the solid was dissolved in dichloromethane, and the organic layer was washed with saturated aqueous NaHCO3, brine. After dried over Na_2SO_4, the mixture was filtered and evaporated to give the solid, which was further purified by recrystallization from AcOEt/MeOH.

Yellow solid; mp 132-135 ºC.

^{1}H NMR (500 MHz, $CDCl_3$); δ = 1.96 (s, 3H), 5.40 (br s, 1H), 6.64 (d, 1H, *J* = 8.2 Hz), 6.89 (d, 1H, *J* = 8.0 Hz), 7.24-7.37 (m, 8H), 7.47-7.50 (d, 2H, *J* = 8.8 Hz).

^{13}C NMR (125 MHz, $CDCl_3$); δ = 14.5, 113.5, 120.5, 126.5, 127.6, 128.4, 129.3, 129.4, 130.1, 138.7, 143.0, 147.1.

(1*Z*, 2*E*)-*N*-Benzyl-1,3-diphenylprop-2-en-1-imine [1]

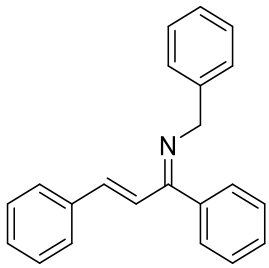

Followed Method B (*vide infra*)

White solid.

^{1}H NMR (500 MHz, $CDCl_3$); δ = 4.48 (s, 2H), 6.48 (d, 1H, *J* = 16.4 Hz), 7.20-7.24 (m, 3H), 7.24-7.29 (m, 4H), 7.30-7.40 (m, 6H), 7.46-7.51 (m, 3H).

^{13}C NMR (125 MHz, $CDCl_3$); δ = 57.6, 121.2, 126.6, 127.3, 127.6, 127.9, 128.5, 128.6, 128.7, 128.9, 132.4, 135.8, 136.0, 139.9, 140.2, 170.4.

(1*Z*, 2*E*)-*N*-Benzyl-1-phenyl-3-(*p*-tolyl)prop-2-en-1-imine

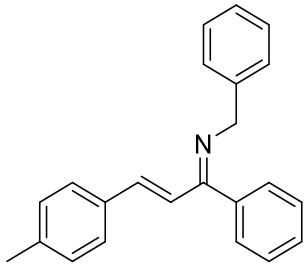

Followed Method B (*vide infra*), then recrystallized from ^{n}pentane/THF = 4/1.

^{1}H NMR (500 MHz, $CDCl_3$); δ = 2.28 (s, 3H), 4.62 (s, 1H), 4.78 (s, 1H), 6.29 (d, 1H, *J* =16.4 Hz), 6.57 (d, 1H, *J* = 16.4 Hz), 7.04-7.32 (m, 14H).

^{13}C NMR (125 MHz, $CDCl_3$); δ = 17.6, 22.5, 55.7, 57.5, 126.4, 126.8, 127.3, 127.6, 128.1, 128.7, 128.8, 132.2, 135.9, 136.0, 140.1, 140.6, 169.9.

HRMS (ESI) calcd for $C_{23}H_{21}N$ $[M+H]^+$ 312.1752, found 312.1744.

(1*Z*, 2*E*)-*N*-Benzyl-3-phenyl-1-(*p*-tolyl)prop-2-en-1-imine

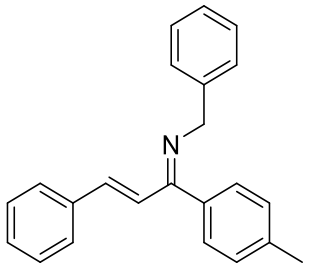

Followed Method B, then recrystallized from ^{n}hexane/1,4-dioxane = 4/1.

^{1}H NMR (500 MHz, $CDCl_3$); δ = 2.40 (s, 3H), 4.29-4.61 (m, 2H), 6.39 (d, 1H, *J* =16.0 Hz), 6.61 (d, 1H, *J* = 16.0 Hz), 7.07-7.39 (m, 14H).

^{13}C NMR (125 MHz, $CDCl_3$); δ = 18.7, 24.1, 56.1, 59.2, 126.5, 126.8, 127.3, 127.4, 128.1, 128.5, 129.3, 131.9, 136.2, 136.4, 139.9, 140.2, 170.8.

HRMS (ESI) calcd for $C_{23}H_{21}N$ $[M+H]^+$ 312.1752, found 312.1761.

(1*Z*, 2*E*)-*N*-Benzyl-3-(4-chlorophenyl)-1-phenylprop-2-en-1-imine

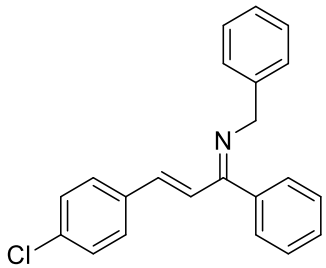

Followed Method B (*vide infra*).

^{1}H NMR (500 MHz, $CDCl_3$); δ = 4.57 (s, 1H), 4.73(s, 1H), 6.44 (d, 1H, *J* =14.5 Hz), 6.91 (d, 1H, *J* = 14.6 Hz), 7.07-7.39 (m, 14H).

^{13}C NMR (125 MHz, $CDCl_3$); δ = 60.5, 120.6, 124.5, 127.6, 127.9, 128.4, 128.7, 128.9, 129.1, 129.3, 129.7, 130.2, 132.1, 134.7, 140.3, 167.9.

HRMS (ESI) calcd for $C_{22}H_{18}NCl$ $[M+H]^+$ 332.1206, found 332.1202.

(2*E*, 3*E*)-*N*-Benzyl-4-(*p*-tolyl)but-3-en-2-imine

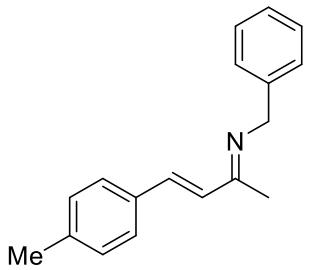

Method B

^{1}H NMR (500 MHz, $CDCl_3$); δ = 2.15 (s, 3H), 2.41 (s, 3H), 4.65 (s, 1H), 4.75 (s, 1H), 6.92 (d, 1H, *J* = 17.2 Hz), 7.21-7.47 (m, 10H).

^{13}C NMR (125 MHz, $CDCl_3$); δ = 12.1, 23.5, 50.0, 120.0, 120.4, 127.5, 127.6, 128.7, 130.3, 130.5, 136.2, 137.8, 139.8, 159.9.

HRMS (ESI) calcd for $C_{22}H_{18}NCl$ $[M+H]^+$ 250.1596, found 250.1604.

Bis(pinacolato)diboron ($B_2(pin)_2$)[16]

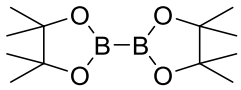

White solid

^{1}H NMR (500 MHz); δ = 1.26 (s, 24H).

^{13}C NMR (125 MHz); δ = 25.0, 83.5.

^{11}B NMR (160 MHz); δ = 30.6 [lit[17] 30.6 ppm].

<Metal Salts>

$Cu(OH)_2$ was purchased from Kojundo Chemical Lab. Co., Ltd (99.0% min. purity).

$Cu(OAc)_2$ anhydrous was purchased from Kanto Chemical Co., Inc (95.0% min. purity).

<Preparation of Ligands>

Chiral 2,2'-bipyridine L1 was synthesized using protocols described in literatures.

(*S*, *S*)-6,6'-Bis(1-hydroxy-2,2-dimethylpropyl)-2,2'-bipyridine (**L1**)[18]

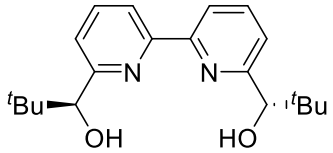

White solid

^{1}H NMR (400 MHz); δ= 0.98 (s, 18H), 4.43 (m, 2H), 7.22 (d, *J* = 7.6 Hz, 2H), 7.79 (dd, *J* = 7.6, 8.0 Hz, 2H), 8.30 (d, *J* = 8.0 Hz, 2H).

^{13}C NMR (100 MHz); δ= 25.9, 36.3, 80.2, 119.6, 123.1, 136.6, 153.8, 159.3.

HPLC (Dialcel Chiralcel OD, ^{n}hexane/ ^{i}PrOH = 19/1, flow rate 1.0 mL/min); t_R = 40.2 min (*R*, *R*), t_R = 48.7 min (*S*, *S*), t_R = 19.9 min (*meso* isomer). >99.5% *ee*

(*S*)-1-(6'-((*S*)-1-Methoxy-2,2-dimethylpropyl)-[2,2'-bipyridin]-6-yl)-2,2-dimethylpro pan-1-ol (**L14**)[19]

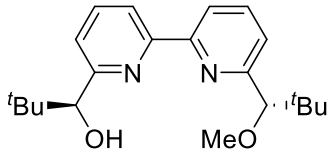

White solid; mp 116-119 ˚C.

^{1}H NMR (400 MHz, $CDCl_3$): δ= 1.00 (s, 18H), 3.32 (s, 3H), 4.42 (s, 1H), 4.45 (d, *J* = 7.3 Hz, 1H), 4.53 (d, *J* = 7.3 Hz, 1H), 7.23 (d, *J* = 7.3 Hz, 1H), 7.43 (d, *J* = 7.8 Hz, 1H), 7.77-7.86 (m, 2H), 8.29 (d, *J* = 7.8 Hz, 1H), 8.37 (d, *J* = 7.8 Hz, 1H).

^{13}C NMR (100 MHz, $CDCl_3$): δ= 25.9, 26.2, 35.5, 36.2, 57.8, 80.1, 92.8, 119.1, 119.8, 121.9, 122.6, 136.5, 136.6, 154.2, 154.6, 158.9, 159.9.

1.1-2 Analytical Data for Borylated Compounds

(*R*)-1,3-Diphenyl-3-(4,4,5,5-tetramethyl-1,3,2-dioxaborolan-2-yl)propan-1-one (**1aa**)[20]

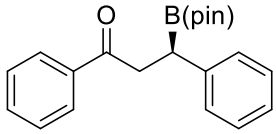

^{1}H NMR (500 MHz); δ = 1.06 (s, 6H), 1.14 (s, 6H), 2.80 (t, *J* = 6.0 Hz, 1H), 3.39 (d, *J* = 2.9 Hz, *J* = 5.8 Hz, 1H), 3.54 (d, *J* = 2.9 Hz, *J* = 5.8 Hz, 1H), 7.28-7.48 (m, 7H), 7.56-7.59 (m, 1H), 7.95 (d, *J* = 7.0 Hz, 2H).

^{13}C NMR (125 MHz); δ = 25.1, 44.4, 70.0, 83.6, 120.7, 127.5, 128.0, 128.3, 128.4, 133.6, 136.6, 143.0, 200.1.

HPLC (Dialcel Chiralpak IA, ^{n}hexane/ ^{i}PrOH = 90/10, flow rate 0.5 mL/min); t_R = 9.2 min (*S*, minor), t_R = 12.5 min (*R*, major).

$[\alpha]_D^{26}$ = –36.5 (*c* = 0.76, $CDCl_3$).

1-Phenyl-3-(4,4,5,5-tetramethyl-1,3,2-dioxaborolan-2-yl)propan-1-one (**1wa**)[50]

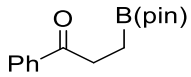

Colorless oil

^{1}H NMR (500 MHz); δ = 1.05 (t, *J* = 5.8 Hz, 2H), 1.22 (s, 6H), 1.24 (s, 6H), 3.14 (t, *J* = 5.8 Hz, 2H), 7.28-7.48 (m, 3H), 7.95 (d, *J* = 8.0 Hz, 2H).

^{13}C NMR (125 MHz); δ = 21.7, 25.4, 34.3, 84.1, 128.2, 129.2, 132.1, 200.3.

(*R*, *E*)- 6-Phenyl-4-(4,4,5,5-tetramethyl-1,3,2-dioxaborolan-2-yl)hex-5-en-2-one (**10ba**)

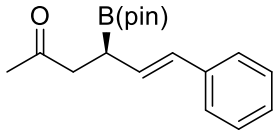

Colorless oil

^{1}H NMR (500 MHz); δ = 1.06 (s, 6H), 1.15 (s, 6H), 2.07-2.13 (m, 3H), 2.71-2.79 (m, 3H), 6.21 (d, *J* = 15.1 Hz, 1H), 6.64 (d, *J* = 15.1 Hz, 1H), 7.26-7.41 (m, 3H), 7.47 (d, *J* = 5.6 Hz, 2H).

^{13}C NMR (125 MHz); δ = 23.7, 30.6, 40.2, 49.8, 88.7, 127.2, 128.2, 128.9, 129.4, 130.3, 135.1, 209.4.

HPLC (Dialcel Chiralpak IA, ^{n}hexane/ ^{i}PrOH = 90/10, flow rate 0.5 mL/min); t_R = 13.2 min (*S*, minor),

t_R = 14.4 min (*R*, major).

$[\alpha]_D^{25}$ = –31.3 (*c* = 0.78, $CDCl_3$).

(*R*)-3-(2-Phenyl-2-(4,4,5,5-tetramethyl-1,3,2-dioxaborolan-2-yl)ethyl)cyclohex-2-en-1-one (**11ay**)

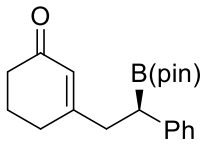

Colorless oil

^{1}H NMR (500 MHz); δ = 1.08 (s, 6H), 1.15 (s, 6H), 1.85-1.90 (m, 2H), 2.21-2.26 (m, 4H), 2.46 (dd, *J* = 5.4, 9.2 Hz, 1H), 2.55 (dd, *J* = 4.9, 8.7 Hz, 1H), 2.79-2.83 (m, 1H), 5.86 (s, 1H), 7.22-7.30 (m, 5H).

^{13}C NMR (125 MHz); δ = 22.5, 24.1, 30.0, 37.0, 37.6, 47.6, 84.2, 125.6, 127.7, 127.8, 128.5, 143.7, 163.0, 200.0.

HPLC (Dialcel Chiralpak IA, ^{n}hexane/ ^{i}PrOH = 90/10, flow rate 0.5 mL/min); t_R = 32.5 min (*S*, minor), t_R = 41.2 min (*R*, major).

$[\alpha]_D^{26}$ = –17.3 (*c* = 0.31, $CDCl_3$).

(*S*, *E*)-3-Styryl-3-(4,4,5,5-tetramethyl-1,3,2-dioxaborolan-2-yl)cyclohexan-1-one (**11aa**)

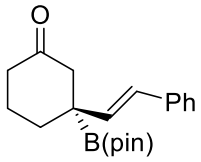

Colorless oil

^{1}H NMR (500 MHz); δ = 1.16 (s, 6H), 1.23 (s, 6H), 2.42-2.68 (m, 4H), 3.13-3.15 (m, 2H), 4.19 (dd, *J* = 6.4, 8.5 Hz, 2H), 6.07 (dd, *J* = 4.6, 9.4 Hz, 1H), 6.49 (d, *J* = 13.2 Hz, 1H), 7.24-7.42 (m, 5H).

^{13}C NMR (125 MHz); δ = 14.1, 23.2, 28.5, 39.6, 45.5, 60.8, 85.2, 126.5, 127.5, 127.8, 128.5, 134.7, 136.7, 172.6.

HPLC (Dialcel Chiralpak IA, ^{n}hexane/ ^{i}PrOH = 90/10, flow rate 1.0 mL/min); t_R = 14.2 min (*S*, minor), t_R = 19.3 min (*R*, major).

$[\alpha]_D^{29}$ = –16.5 (*c* = 0.27, $CDCl_3$).

<Analytical Data for Oxidized or Substituted Compounds>

Almost all adducts are literature-known; obtained analytical data for these compounds are in full agreement with reported data. The absolute configurations of optically active compounds were determined by comparison of the order of retention time in the chiral HPLC analyses.

<Typical Experimental Procedure for Oxidation Step>

After the reaction of 1a with 2 completed, the reaction mixture was filtered and rinsed with THF (3 mL). The excess amount of $NaBO_3 \cdot 4H_2O$ (488 mg) was then added and the mixture was stirred at room temperature for 4 h. The aqueous layer was extracted with AcOEt (20 mL) three times, and the combined organic layers were dried over anhydrous Na_2SO_4. After concentrated under reduced pressure, the crude mixture was purified by preparative TLC (^{n}hexane/AcOEt = 4/1) to afford the desired product 4a (84.6 mg, Quant.) as a colorless oil.

(*R*)-3-Hydroxy-1,3-diphenylpropan-1-one (**1ad**)[21]

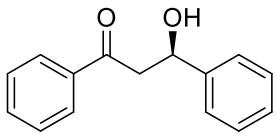

Colorless oil

^{1}H NMR (500 MHz); δ = 3.37 (d, *J* = 5.8 Hz, 2H), 5.35 (t, *J* = 6.0 Hz, 1H), 7.28-7.48 (m, 7H), 7.56-7.59 (m, 1H), 7.95 (d, *J* = 7.0 Hz, 2H).

^{13}C NMR (125 MHz); δ = 47.4, 70.0, 120.7, 127.5, 128.0, 128.3, 128.4, 133.6, 136.6, 143.0, 200.1.

HPLC (Dialcel Chiralcel OD-H, ^{n}hexane/ ^{i}PrOH = 85/15, flow rate 0.7 mL/min); t_R = 14.4 min (*S*, minor), t_R = 16.3 min (*R*, major).

$[\alpha]_D^{27}$ = + 69.3 (*c* = 0.84, $CHCl_3$).

<Typical Experimental Procedure for Substitution Step>[22]

After the reaction of **1ad** with $B_2(pin)_2$ completed, the reaction mixture was filtered and the crude was purified by flash column chromatography and dissolved in 5 mL of DCM. Then BCl_3 (1.0 mmol) was added slowly to the solution. The reaction mixture was stirred for 4 h at room temperature. After removal of the solvent and pumped off the volatiles (0.4 kPa, 1 h), 5 mL of DCM was added and the solution was cooled to 0 °C. Benzyl azide was added and the reaction mixture was warmed up slowly to room temperature and continued stirring for 30 min. Finally, Et_2O and NaOH (1 M in H_2O) were added to the solution to quench the reaction. The crude was purified by PTLC

(^{n}hexane/AcOEt = 1/2) to afford the desired product 5a (95.5 mg, 81% yield) as a colorless oil.

(*R*)-3-(Benzylamino)-1,3-diphenylpropan-1-one (**1ae**)[23]

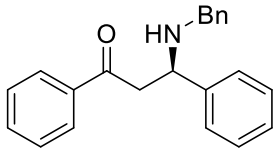

Colorless oil

^{1}H NMR (500 MHz); δ = 1.77 (s, 1H), 3.28-3.40 (m, 2H), 3.57-3.66 (m, 2H), 4.30-4.32 (m, 1H), 7.19-7.52 (m, 13H), 7.90 (d, *J* = 7.0 Hz, 2H).

^{13}C NMR (125 MHz); δ = 45.6, 47.1, 58.7, 127.2, 127.2, 127.3, 127.4, 127.7, 127.9, 128.1, 128.3, 133.4, 137.8, 140.1, 143.2, 198.6.

HPLC (Dialcel Chiralcel OD-H, ^{n}hexane/ ^{i}PrOH = 90/10, flow rate 1.0 mL/min); t_R = 14.7 min (*S*, minor), t_R = 18.9 min (*R*, major).

$[\alpha]_D^{28}$ = + 26.3 (*c* = 0.42, MeOH).

(*R*)-3-Phenyl-3-hydroxy-1-(4'-fluorophenyl)propan-1-one (**1jd**)[24]

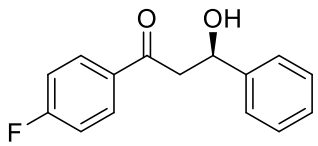

Colorless oil

^{1}H NMR (500 MHz); δ = 3.33-3.36 (m, 2H), 3.46 (d, *J* = 2.6 Hz, 1H), 5.33-5.35 (m, 1H), 7.10-7.14 (m, 2H), 7.28-7.44 (m, 5H), 7.99 (d, *J* = 7.0 Hz, 2H).

^{13}C NMR (125 MHz); δ = 47.2, 70.1, 115.8 (d, *J* = 4.2 Hz), 121.5, 125.7, 128.2 (d, *J* = 107.5 Hz), 130.9 (d, *J* = 9.6 Hz), 132.9, 142.9, 157.2 (d, *J* = 256 Hz), 198.4.

HPLC (Dialcel Chiralpak AS-H, ^{n}hexane/ ^{i}PrOH = 90/10, flow rate 1.0 mL/min); t_R = 13.2 min (*S*, minor), t_R = 14.2 min (*R*, major).

$[\alpha]_D^{28}$ = + 53.3 (*c* = 0.86, $CHCl_3$).

(*R*)-3-(2'-Chlorophenyl)-3-hydroxy-1-(4'-fluorophenyl)propan-1-one (**1bd**)[24]

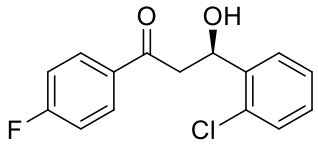

Colorless oil

^{1}H NMR (500 MHz); δ = 3.13 (dd, *J* = 8.7, 11.5 Hz, 1H), 3.51 (d, *J* = 16.3 Hz, 1H), 3.73 (s, 1H), 5.32 (d, *J* = 9.6 Hz, 1H), 7.10-7.15 (m, 2H), 7.22-7.26 (m, 1H), 7.31-7.36 (m, 2H), 7.70 (d, *J* = 7.7 Hz, 1H), 7.99-8.00 (m, 2H).

^{13}C NMR (125 MHz); δ = 45.3, 66.8, 115.8 (d, *J* = 4.2 Hz), 127.3 (d, *J* = 4.7 Hz), 128.6, 129.4, 130.9 (d, *J* = 9.6 Hz), 131.0, 131.2, 133.0, 140.3, 167.1, 198.5.

HPLC (Dialcel Chiralcel OD-H, ^{n}hexane/ ^{i}PrOH = 85/15, flow rate 0.7 mL/min); t_R = 13.9 min (*S*, minor), t_R = 16.2 min (*R*, major).

$[\alpha]_D^{27}$ = + 58.2 (*c* = 0.85, $CHCl_3$).

(*R*)-3-Hydroxy-1-(4'-methoxylphenyl)-3-phenylpropan-1-one (**1cd**)[24]

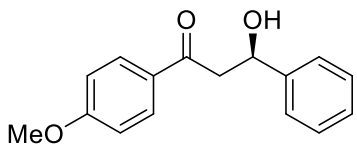

Colorless oil

^{1}H NMR (500 MHz); δ = 3.31 (d, *J* = 7.6 Hz, 2H), 3.72 (s, 1H), 3.86 (s, 3H), 5.32 (m, 1H), 6.91(d, *J* = 9.0 Hz, 2H), 7.27-7.30 (m, 1H), 7.37 (t, *J* = 6.0 Hz, 2H), 7.44 (d, *J* = 7.7 Hz, 2H), 7.93 (d, *J* = 9.0 Hz, 2H).

^{13}C NMR (125 MHz); δ = 46.9, 55.5, 70.2, 113.8, 113.9, 121.3, 125.7, 127.6, 128.5, 129.7, 130.5, 164.3, 198.7.

HPLC (Dialcel Chiralcel OD-H, ^{n}hexane/ ^{i}PrOH = 85/15, flow rate 1.0 mL/min); t_R = 11.2 min (*S*, minor), t_R = 12.8 min (*R*, major).

$[\alpha]_D^{25}$ = + 37.2 (*c* = 0.80, $CHCl_3$).

(*R*)-3-(4'-Chlorophenyl)-3-hydroxy-1-phenylpropan-1-one (**1dd**)[21]

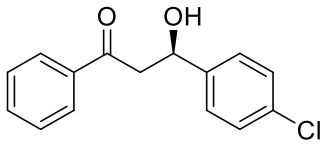

Colorless oil

^{1}H NMR (500 MHz); δ = 3.34 (d, *J* = 5.8 Hz, 2H), 3.61 (d, *J* = 8.5 Hz, 1H), 5.33 (t, *J* = 6.0 Hz, 1H), 7.33-7.39 (m, 4H), 7.47 (t, *J* = 8.1 Hz, 2H), 7.58-7.61 (m, 1H), 7.95 (d, *J* = 7.0 Hz, 2H).

^{13}C NMR (125 MHz); δ = 47.2, 69.5, 127.2, 128.1, 128.7, 128.8, 133.8, 136.5, 140.1, 141.5, 200.0.

HPLC (Dialcel Chiralpak AD-H, ^{n}hexane/ ^{i}PrOH = 90/10, flow rate 1.0 mL/min); t_R = 13.6 min (*S*, minor), t_R = 14.3 min (*R*, major).

$[\alpha]_D^{26}$ = + 43.3 (*c* = 0.81, $CHCl_3$).

(*R*)-3-(4'-Methoxyphenyl)-3-hydroxy-1-phenylpropan-1-one (**1kd**)[21]

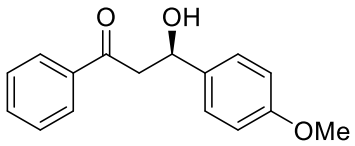

Colorless oil

^{1}H NMR (500 MHz); δ = 3.34-3.37 (m, 2H), 3.50 (d, *J* = 2.9 Hz, 1H), 3.80 (s, 3H), 5.28-5.30 (m, 1H), 6.89-6.92 (m, 2H), 7.34-7.37 (m, 2H), 7.44-7.47 (m, 2H), 7.56-7.59 (m, 1H), 7.95 (dd, *J* = 1.8, 5.2 Hz, 2H).

^{13}C NMR (125 MHz); δ = 55.3, 67.1, 74.3, 114.0, 127.0, 128.1, 128.7, 133.6, 135.2, 136.7, 159.2, 200.2.

HPLC (Dialcel Chiralpak AS-H, ^{n}hexane/ ^{i}PrOH = 80/20, flow rate 1.0 mL/min); t_R = 15.2 min (*S*, minor), t_R = 16.2 min (*R*, major).

$[\alpha]_D^{25}$ = + 46.5 (*c* = 0.92, $CHCl_3$).

(*S*)-3-Hydroxy-1-phenylbutan-1-one (**1ed**)[25]

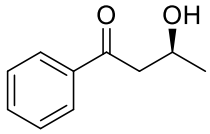

Colorless oil

^{1}H NMR (500 MHz); δ = 1.30 (d, *J* = 6.9 Hz, 3H), 3.04 (dd, *J* = 8.6, 9.2 Hz, 1H), 3.16 (dd, *J* = 3.4,

14.9 Hz, 1H), 3.30 (s, 1H), 4.41 (d, *J* = 2.3 Hz, 1H), 7.47 (t, *J* = 8.0 Hz, 2H), 7.56-7.60 (m, 1H), 7.94-7.96 (m, 2H).

^{13}C NMR (125 MHz); δ = 22.4, 46.5, 64.0, 128.0, 128.7, 133.5, 136.8, 200.8.

HPLC (Dialcel Chiralcel OD-H, ^{n}hexane/ ^{i}PrOH = 90/10, flow rate 0.7 mL/min); t_R = 5.3 min (*R*, minor), t_R = 7.1 min (*S*, major).

$[\alpha]_D^{29}$ = + 68.2 (*c* = 0.93, $CHCl_3$).

(*S*)-3-Hydroxy-1-phenylpentan-1-one (**1ld**)[25]

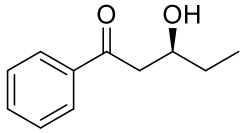

Colorless oil

^{1}H NMR (500 MHz); δ = 1.00-1.03 (m, 3H), 1.57-1.66 (m, 2H), 3.01-3.06 (m, 1H), 3.19 (dd, *J* = 2.3, 16.5 Hz, 1H), 3.28 (s, 1H), 4.15 (d, *J* = 7.5 Hz, 1H), 7.47 (t, *J* = 8.0 Hz, 2H), 7.58-7.61 (m, 1H), 7.95-7.97 (m, 2H).

^{13}C NMR (125 MHz); δ = 9.9, 29.3, 44.5, 69.1, 128.0, 128.7, 133.5, 136.7, 201.0.

HPLC (Dialcel Chiralcel OD-H, ^{n}hexane/ ^{i}PrOH = 90/10, flow rate 0.7 mL/min); t_R = 10.0 min (*R*, minor), t_R = 13.1 min (*S*, major).

$[\alpha]_D^{27}$ = + 62.2 (*c* = 0.79, $CHCl_3$).

(*R*)-3-Hydroxy-4-methyl-1-phenylpentan-1-one (**1md**)[26]

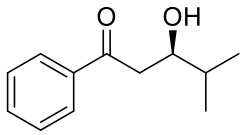

Colorless oil

^{1}H NMR (500 MHz); δ = 0.99-1.02 (m, 6H), 1.79-1.83 (m, 1H), 3.03 (dd, *J* = 8.0, 9.8 Hz, 1H), 3.14-3.18 (m, 1H), 4.00 (t, *J* = 2.5 Hz, 1H), 7.47 (t, *J* = 8.1 Hz, 2H), 7.56-7.59 (m, 1H), 7.96 (dd, *J* = 1.2, 7.5 Hz, 2H).

^{13}C NMR (125 MHz); δ = 17.8, 18.5, 33.1, 42.0, 72.4, 128.1, 128.6, 133.4, 137.0, 195.7.

HPLC (Dialcel Chiralcel OD-H, ^{n}hexane/ ^{i}PrOH = 90/10, flow rate 0.5 mL/min); t_R = 12.4 min (*S*, minor), t_R = 13.2 min (*R*, major).

$[\alpha]_D^{28}$ = + 69.9 (*c* = 0.98, $CHCl_3$).

(*R*)-3-Hydroxy-4,4-dimethyl-1-phenylpentan-1-one (**1gd**)[27]

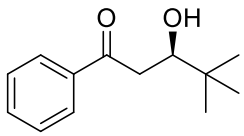

Colorless oil

^{1}H NMR (500 MHz); δ = 0.98 (s, 9H), 2.98 (dd, *J* = 7.5, 10.3 Hz, 1H), 3.07 (s, 1H), 3.18 (d, *J* = 17.2 Hz, 1H), 3.88 (d, *J* = 10.1 Hz, 1H), 7.45-7.48 (m, 2H), 7.56-7.59 (m, 1H), 7.96 (d, *J* = 8.4 Hz, 2H).

^{13}C NMR (125 MHz); δ = 25.8, 27.7, 34.4, 40.1, 75.1, 123.5, 128.1, 128.6, 133.4, 201.6.

HPLC (Dialcel Chiralcel OD-H, ^{n}hexane/ ^{i}PrOH = 85/15, flow rate 0.7 mL/min); t_R = 11.2 min (*S*, minor), t_R = 13.1 min (*R*, major).

$[\alpha]_D^{29}$ = + 70.2 (*c* = 0.87, $CHCl_3$).

(*R*)-4-Hydroxy-4-phenylbutan-2-one (**1fd**)[24]

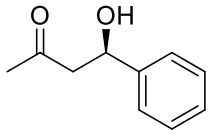

Colorless oil

^{1}H NMR (500 MHz); δ = 1.63 (s, 3H), 2.79-2.91 (m, 2H), 3.26 (d, *J* = 3.5 Hz, 1H), 5.15 (t, *J* = 2.8 Hz, 1H), 7.26-7.35 (m, 5H).

^{13}C NMR (125 MHz); δ = 30.7, 52.0, 69.9, 125.6, 127.7, 128.5, 142.8, 209.0.

HPLC (Dialcel Chiralcel AS-H, ^{n}hexane/ ^{i}PrOH = 90/10, flow rate 1.0 mL/min); t_R = 10.1 min (*S*, minor), t_R = 11.1 min (*R*, major).

$[\alpha]_D^{28}$ = + 55.5 (*c* = 1.06, $CHCl_3$).

(*R*)-3-Hydroxycyclohexanone (**1hd**)[28]

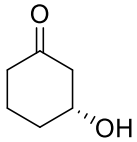

Colorless oil

^{1}H NMR (500 MHz); δ = 1.69-1.79 (m, 2H), 1.89-2.07 (m, 2H), 2.30 (dd, *J* = 7.0, 6.2 Hz, 2H), 2.38 (dd, *J* = 7.6, 14.0 Hz, 1H), 2.59 (dd, *J* = 4.1, 14.0 Hz, 1H), 4.07-4.19 (m, 1H).

^{13}C NMR (125 MHz); δ = 21.2, 33.4, 40.8, 50.2, 69.4, 210.2.

$[\alpha]_D^{29}$ = + 37.3 (*c* = 0.80, $CHCl_3$).

The er value was determined as benzoylated compound;

To the oxidized product (ca. 0.2 mmol) in dichloromethane (2 mL) was added pyridine (31.6 mg, 0.4 mmol) and benzoyl chloride (140.6 mg, 1.0 mmol). The mixture was stirred for 1 h at 0 °C. The resulting mixture was quenched with water. The obtained organic layer was extracted with brine and dried over anhydrous Na_2SO_4. After removal of the solvent, the residue was purified by preparative TLC (^{n}hexane/AcOEt = 3/1) to afford benzoylated product (41.9 mg, 96% yield in 3 steps) as a colorless oil.

(*R*)-3-Oxocyclohexyl benzoate (**1he**)

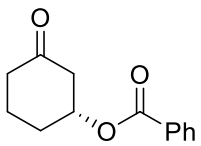

Colorless oil

^{1}H NMR (500 MHz); δ = 1.69-1.79 (m, 2H), 1.99-2.07 (m, 2H), 2.28-2.32 (m, 2H), 2.37-2.42 (m 1H), 2.60-2.66 (m, 1H), 4.83-4.87 (m, 1H), 7.45-7.48 (m, 2H), 7.56-7.59 (m, 1H), 7.96-7.99 (m, 2H).

^{13}C NMR (125 MHz); δ = 21.2, 32.4, 40.8, 50.2, 68.4, 128.0, 128.7, 133.6, 136.9, 207.3, 212.2.

HPLC (Dialcel Chiralcel OD-H, ^{n}hexane/ ^{i}PrOH = 90/10, flow rate 0.5 mL/min); t_R = 16.9 min (*S*, major), t_R = 18.5 min (*R*, minor).

(*S*)-3-Hydroxy-1,3-diphenylbutan-1-one (**1id**)[29]

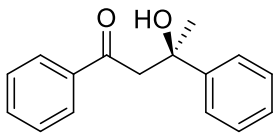

Colorless oil

^{1}H NMR (500 MHz); δ = 1.62 (s, 3H), 3.34 (d, *J* = 17.0 Hz, 1H), 3.79 (d, *J* = 17.0 Hz, 1H), 4.87 (s, 1H), 7.21 (t, *J* = 7.0 Hz, 1H), 7.31 (t, *J* = 8.0 Hz, 2H), 7.44-7.49 (m, 4H), 7.57 (t, *J* = 7.0 Hz, 1H), 7.95 (d, *J* = 8.0 Hz, 2H).

^{13}C NMR (125 MHz); δ = 30.9, 49.1, 71.2, 124.3, 126.6, 128.0, 128.2, 128.6, 133.6, 136.6, 147.5, 200.6.

HPLC (Dialcel Chiralcel OD-H, ^{n}hexane/ ^{i}PrOH = 90/10, flow rate 0.7 mL/min); t_R = 18.5 min (*R*, minor), t_R = 21.7 min (*S*, major).

$[\alpha]_D^{29}$ = + 51.2 (*c* = 1.21, $CHCl_3$).

(*R*)-4-Hydroxy-4-phenylpentan-2-one (**1nd**)[30]

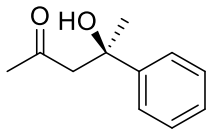

Colorless oil

^{1}H NMR (500 MHz); δ = 1.51 (s, 3H), 2.06 (s, 3H), 2.83 (d, *J* = 17.0 Hz, 1H), 3.10 (d, *J* = 17.0 Hz, 1H), 4.31 (s, 1H), 7.23-7.43 (m, 5H).

^{13}C NMR (125 MHz); δ = 30.2, 33.6, 53.9, 72.8, 124.1, 126.3, 128.4, 147.2, 208.7.

HPLC (Dialcel Chiralcel OD-H, ^{n}hexane/ ^{i}PrOH = 90/10, flow rate 0.8 mL/min); t_R = 15.0 min (*R*, major), t_R = 16.8 min (*S*, minor).

$[\alpha]_D^{28}$ = + 27.3 (*c* = 0.93, $CHCl_3$).

(*R*)-3-Hydroxy-3-methylcyclohexan-1-one (**1od**)[31]

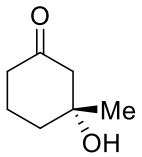

Colorless oil

^{1}H NMR (500 MHz); δ = 1.32 (s, 3H), 1.89-1.99 (m, 2H), 2.34-2.48 (m, 4H), 3.98 (m, 1H), 5.31 (s, 1H).

^{13}C NMR (125 MHz); δ = 13.8, 20.4, 29.8, 37.6, 47.9, 54.1, 64.7, 208.0.

The er value was determined as benzoylated compound;

To the oxidized product (ca. 0.2 mmol) in dichloromethane (2 mL) was added pyridine (31.6 mg, 0.4 mmol) and benzoyl chloride (140.6 mg, 1.0 mmol). The mixture was stirred for 1 h at 0 °C. The resulting mixture was quenched with water. The obtained organic layer was extracted with brine and dried over anhydrous Na_2SO_4. After removal of the solvent, the residue was purified by preparative TLC (^{n}hexane/AcOEt = 3/1) to afford benzoylated product (42.2 mg, 91% yield in 3 steps)

as a colorless oil.

(*R*)-1-Methyl-3-oxocyclohexyl benzoate (**1oe**)

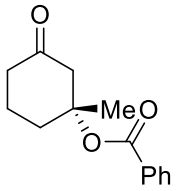

Colorless oil

^{1}H NMR (500 MHz); δ = 1.35 (s, 3H), 1.89-2.02 (m, 2H), 2.34-2.48 (m, 4H), 3.98 (m, 1H), 5.31 (s, 1H), 7.45-7.96 (m, 5H).

^{13}C NMR (125 MHz); δ = 13.8, 20.4, 29.8, 37.6, 47.9, 54.1, 64.7, 128.0, 128.7, 133.6, 136.9, 178.2, 208.2.

HPLC (Dialcel Chiralcel OD-H, ^{n}hexane/ ^{i}PrOH = 90/10, flow rate 0.5 mL/min); t_R = 5.1 min (*S*, minor), t_R = 6.5 min (*R*, major).

(*R*)-3-Hydroxy-3-phenylcyclohexan-1-one (**1pd**)[32]

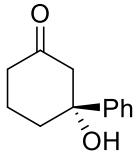

White Powder; mp 134-136 ºC.

^{1}H NMR (500 MHz); δ = 1.59-1.89 (m, 2H), 2.20-2.48 (m, 5H), 2.61 (m, 1H), 2.92 (s, 1H), 7.26-7.46 (m, 5H).

^{13}C NMR (125 MHz); δ = 21.7, 36.5, 47.9, 54.1, 68.7, 124.7, 128.2, 128.2, 131.9, 131.9, 147.5, 210.0.

HPLC (Dialcel Chiralcel AD-H, ^{n}hexane/ ^{i}PrOH = 90/10, flow rate 1.0 mL/min); t_R = 10.0 min (*R*, major), t_R = 13.7 min (*S*, minor).

$[\alpha]_D^{27}$ = + 12.2 (*c* = 0.85, $CHCl_3$).

(*R*)-3-Hydroxy-3-methylcyclopentan-1-one (**1qd**)[33]

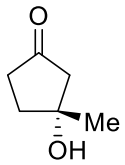

Colorless oil

^{1}H NMR (500 MHz); δ =1.55 (s, 3H), 2.21-2.23 (m, 2H), 2.68-2.69 (m, 2H), 3.01 (s, 3H), 4.17 (s, 1H).

^{13}C NMR (125 MHz); δ = 29.6, 33.7, 37.6, 52.1, 69.8, 213.9.

$[\alpha]_D^{30}$ = + 19.1 (*c* = 0.93, $CHCl_3$).

The e.r. value was determined as benzoylated compound;

To the oxidized product (ca. 0.2 mmol) in dichloromethane (2 mL) was added pyridine (31.6 mg, 0.4 mmol) and benzoyl chloride (140.6 mg, 1.0 mmol). The mixture was stirred for 1 h at 0 °C. The resulting mixture was quenched with water. The obtained organic layer was extracted with brine and dried over anhydrous Na_2SO_4. After removal of the solvent, the residue was purified by preparative TLC (^{n}hexane/AcOEt = 3/1) to afford benzoylated product (38.8 mg, 89% yield in 3 steps) as a colorless oil.

(*R*)-1-Methyl-3-oxocyclohexyl benzoate (**1qe**)

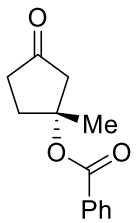

Colorless oil

^{1}H NMR (500 MHz); δ = 1.55 (s, 3H), 2.21-2.23 (m, 2H), 2.68-2.69 (m, 2H), 3.01 (s, 3H), 7.41-7.89 (m, 5H).

^{13}C NMR (125 MHz); δ = 29.6, 33.7, 37.6, 52.1, 69.8, 128.0, 128.7, 133.6, 136.9, 175.4, 205.9.

HPLC (Dialcel Chiralcel OD-H, ^{n}hexane/ ^{i}PrOH = 90/10, flow rate 0.5 mL/min); t_R = 13.9 min (*S*, minor), t_R = 16.9 min (*R*, major).

(*R*, *E*)-3-(Benzylimino)-1-phenylbutan-1-ol (**4ad**)[1]

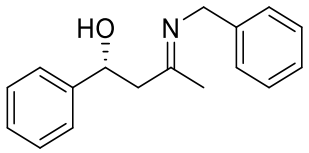

Colorless oil

^{1}H NMR (500 MHz, $CDCl_3$); δ = 1.63 (s, 3H), 2.66 (s, 2H), 2.79-2.91 (m, 2H), 3.46 (d, 1H, *J* = 3.3 Hz), 5.11 (t, 1H, *J* = 3.2 Hz), 7.35-7.24 (m, 10H).

^{13}C NMR (125 MHz, $CDCl_3$); δ = 27.9, 30.7, 53.4, 70.1, 125.6, 126.5, 126.9, 127.7, 128.1, 128.5, 129.0, 139.9, 189.1.

HPLC; (Dialcel Chiralcel OD, ^{n}hexane/ ^{i}PrOH = 85/15, flow rate 0.7 mL/min); t_R = 12.9 min (*S*, minor), t_R = 14.3 min (*R*, major).

$[\alpha]_D^{23}$ = + 35.3 (*c* = 0.63, $CDCl_3$).

(*R*, *Z*)-3-(Benzylimino)-1,3-diphenylpropan-1-ol (**4bd**)[1]

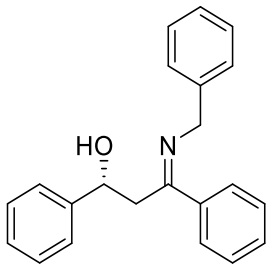

Colorless oil

^{1}H NMR (500 MHz, $CDCl_3$); δ = 3.41 (d, 2H, *J* = 5.8 Hz) , 4.32 (s, 2H), 5.39 (t, 1H, *J* = 6.5 Hz), 7.28-7.48 (m, 7H), 7.56-7.82 (m, 6H), 7.95 (d, 2H, *J* = 7.0 Hz).

^{13}C NMR (125 MHz, $CDCl_3$); δ = 47.4, 59.2, 70.2, 123.7, 127.5, 128.0, 128.3, 128.4, 128.5, 128.6, 129.1, 129.7, 133.9, 136.6, 143.2, 167.2.

HPLC; (Dialcel Chiralcel OD, ^{n}hexane/ ^{i}PrOH = 85/15, flow rate 0.7 mL/min); t_R = 14.4 min (*S,* minor), t_R = 16.3 min (*R,* major).

$[\alpha]_D^{21}$ = + 39.9 (*c* = 0.42, $CDCl_3$).

(*R*, *Z*)-3-(Benzylimino)-3-phenyl-1-(*p*-tolyl)propan-1-ol (**4cd**)

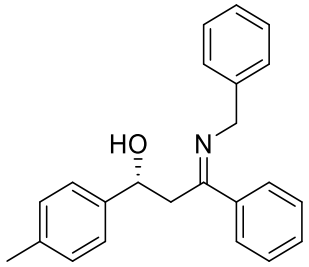

Colorless oil.

IR (KBr) ν = 1037, 1178, 1648, 2936, 3421 cm^{-1}.

^{1}H NMR (500 MHz, $CDCl_3$); δ = 3.41(d, 2H, *J* = 5.8 Hz), 4.32 (s, 2H), 5.39 (t, 1H, *J* = 6.5 Hz), 7.28-7.48 (m, 7H), 7.56-7.82 (m, 6H), 7.95 (d, 2H, *J* = 7.0 Hz).

^{13}C NMR (125 MHz, $CDCl_3$); δ = 47.4, 59.2, 70.2, 123.7, 127.5, 128.0, 128.3, 128.4, 128.5, 128.6, 129.1, 129.7, 133.9, 136.6, 143.2, 167.2.

HPLC; (Dialcel Chiralcel OD-H, ^{n}hexane/ ^{i}PrOH = 90/10, flow rate 1.0 mL/min); t_R = 9.0 min (*S*, minor), t_R = 10.2 min (*R*, major).

HRMS (ESI) calcd for $C_{23}H_{24}NO$ $[M+H]^+$ 330.1858, found 330.1859.

$[\alpha]_D^{19}$ = + 54.2 (*c* = 0.35, $CDCl_3$).

(*R*, *Z*)-3-(Benzylimino)-1-phenyl-3-(*p*-tolyl)propan-1-ol (**4dd**)

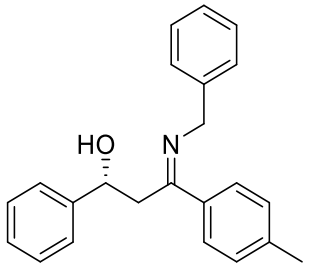

Yellow oil.

IR (KBr) ν = 1041, 1154, 1646, 2899, 3394 cm^{-1}.

^{1}H NMR (500 MHz, $CDCl_3$); δ = 3.34 (d, 2H, *J* = 7.6 Hz), 3.67 (s, 1H), 3.86 (s, 3H), 4.37 (s, 2H), 5.33-5.37 (m, 1H), 6.91 (d, 2H, *J* = 9.0 Hz), 7.27-7.30 (m, 1H), 7.37 (t, 2H, *J* = 6.0 Hz), 7.44-7.73 (m, 7H), 7.93 (d, 2H, *J* = 9.0 Hz).

^{13}C NMR (125 MHz, $CDCl_3$); δ = 26.9, 55.9, 61.2, 71.1, 113.8, 121.3, 125.7, 127.6, 128.4, 128.5, 129.1, 129.5, 129.7, 130.5, 171.7.

HPLC; (Dialcel Chiralcel OD-H, ^{n}hexane/ ^{i}PrOH = 90/10, flow rate 1.0 mL/min); t_R = 9.8 min (*S*, minor), t_R = 11.3 min (*R*, major).

HRMS (ESI) calcd for $C_{23}H_{24}NO$ $[M+H]^+$ 330.1858, found 330.1853.

$[\alpha]_D^{20}$ = + 39.8 (*c* = 0.47, $CDCl_3$).

(*R*, *Z*)-3-(Benzylimino)-1-(4-chlorophenyl)-3-phenylpropan-1-ol (**4ed**)

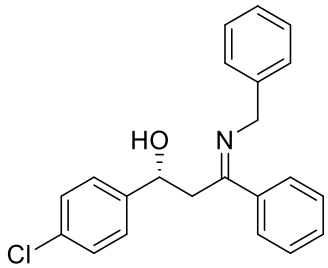

Yellow oil.

^{1}H NMR (500 MHz, $CDCl_3$); δ = 2.92 (s, 2H), 2.79-2.92 (m, 2H), 3.65 (d, 1H, *J* = 7.8 Hz), 5.37 (t, 1H, *J* = 7.8 Hz), 7.21-7.59 (m, 14H).

^{13}C NMR (125 MHz, $CDCl_3$); δ = 31.7, 53.5, 70.0, 124.9, 125.7, 126.3, 126.6, 127.7, 127.9, 128.0, 128.5, 130.0, 131.2, 133.9, 137.5, 170.3.

HPLC; (Dialcel Chiralcel OD, ^{n}hexane/ ^{i}PrOH = 90/10, flow rate 1.0 mL/min); t_R = 11.7 min (*S*, minor), t_R = 13.5 min (*R*, major).

HRMS (ESI) calcd for $C_{22}H_{21}ClNO$ $[M+H]^+$ 350.1312, found 350.1332.

$[\alpha]_D^{22}$ = + 38.6 (*c* = 0.53, $CHCl_3$).

(*R*, *E*)-3-(Benzylimino)-1-(p-tolyl)butan-1-ol (**4fd**)

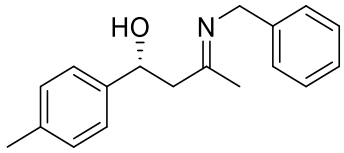

Colorless oil.

^{1}H NMR (500 MHz, $CDCl_3$); δ = 1.59 (s, 3H), 2.12 (s, 1H), 2.59 (s, 1H), 2.69-2.89 (m, 2H), 3.46 (d, 1H, *J* = 3.8 Hz), 5.12 (t, 1H, *J* = 4.0 Hz), 7.21-7.41 (m, 9H).

^{13}C NMR (125 MHz, $CDCl_3$); δ = 23.4, 28.6, 31.7, 53.5, 70.0, 123.1, 126.5, 126.8, 127.2, 128.4, 129.0, 138.7, 176.2.

HPLC; (Dialcel Chiralcel OD, ^{n}hexane/ ^{i}PrOH = 90/10, flow rate 1.0 mL/min); t_R = 11.7 min (*S*, minor), t_R = 13.5 min (*R*, major).

HRMS (ESI) calcd for $C_{18}H_{22}NO$ $[M+H]^+$ 268.1701, found 268.1697.

$[\alpha]_D^{20}$ = + 21.6 (*c* = 0.23, $CDCl_3$).

(*R*)-Methyl 3-hydroxy-3-phenylpropanoate (**5ad**)[34]

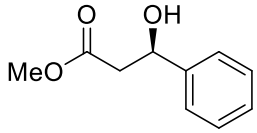

Colorless oil

^{1}H NMR (500 MHz); δ = 2.66-2.77 (m, 2H), 3.38 (s, 1H), 3.68 (s, 3H), 5.11 (d, *J* = 9.1 Hz, 1H), 7.25-7.37 (m, 5H).

^{13}C NMR (125 MHz); δ = 43.2, 51.7, 70.2, 125.6, 127.7, 128.4, 142.6, 172.6.

HPLC (Dialcel Chiralcel OD-H, ^{n}hexane/ ^{i}PrOH = 90/10, flow rate 1.0 mL/min); t_R = 12.0 min (*S*, minor), t_R = 13.3 min (*R*, major).

$[\alpha]_D^{28}$ = + 37.9 (*c* = 0.92, $CHCl_3$).

(*R*)-Ethyl-3-hydroxy-3-phenylpropanoate (**5bd**)[35]

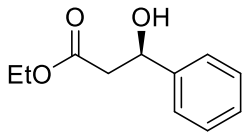

Colorless oil

^{1}H NMR (500 MHz); δ = 1.23 (t, *J* = 6.3 Hz, 3H), 2.66-2.75 (m, 2H), 3.30 (d, *J* = 2.9 Hz, 1H), 4.15 (q, *J* = 5.7 Hz, 1H), 5.09-5.12 (m, 1H), 7.23-7.36 (m, 5H).

^{13}C NMR (125 MHz); δ = 14.1, 43.3, 60.8, 70.3, 125.6, 127.7, 128.5, 142.5, 173.3.

HPLC (Dialcel Chiralcel OD-H, ^{n}hexane/ ^{i}PrOH = 90/10, flow rate 1.0 mL/min); t_R = 11.2 min (*S*, minor), t_R = 12.9 min (*R*, major).

$[\alpha]_D^{28}$ = + 48.9 (*c* = 0.84, $CHCl_3$).

(*S*)-Ethyl-3-hydroxybutanoate (**5ed**)[36]

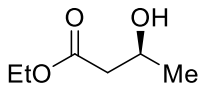

Colorless oil

^{1}H NMR (500 MHz); δ = 1.20-1.29 (m, 6H), 2.39-2.51 (m, 2H), 3.05 (s, 1H), 4.15-4.23 (m, 3H).

^{13}C NMR (125 MHz); δ = 22.4, 42.8, 60.6, 64.2, 172.8, 212.2.

$[\alpha]_D^{28}$ = + 36.2 (*c* = 0.96, $CHCl_3$).

The er value was determined as benzoylated compound;

To the oxidized product (ca. 0.2 mmol) in dichloromethane (2 mL) was added pyridine (31.6 mg, 0.4 mmol) and benzoyl chloride (140.6 mg, 1.0 mmol). The mixture was stirred for 1 h at 0 °C. The resulting mixture was quenched with water. The obtained organic layer was extracted with brine and dried over anhydrous Na_2SO_4. After removal of the solvent, the residue was purified by preparative TLC (^{n}hexane/AcOEt = 3/1) to afford benzoylated product (37.8 mg, 80% yield in 3 steps) as a colorless oil.

(*S*)-4-Ethoxy-4-oxobutan-2-yl benzoate (**5ee**)

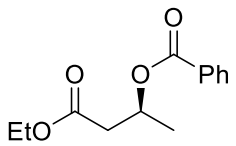

Colorless oil

^{1}H NMR (500 MHz); δ = 1.20-1.29 (m, 6H), 2.39-2.51 (m, 2H), 4.19-4.23 (m, 3H), 4.98 (s, 1H), 7.45-7.48 (m, 2H), 7.56-7.59 (m, 1H), 7.95-7.99 (m, 2H).

^{13}C NMR (125 MHz); δ = 14.0, 22.4, 42.8, 60.6, 64.2, 128.0, 128.7, 133.6, 136.9, 172.8, 212.2.

HPLC (Dialcel Chiralcel OD-H, ^{n}hexane/ ^{i}PrOH = 85/15, flow rate 0.7 mL/min); t_R = 10.8 min (*S*, major), t_R = 12.2 min (*R*, minor).

(*S*)-4-Hydroxytetrahydro-2H-pyran-2-one (**5cd**)[37]

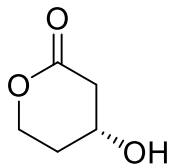

Colorless oil

^{1}H NMR (500 MHz); δ= 1.81-1.88 (m, 2H), 2.61-2.78 (m, 2H), 3.56 (m, 1H), 4.29 (m, 1H), 4.36 (m, 1H), 4.64 (m, 1H).

^{13}C NMR (125 MHz); δ = 27.1, 42.5, 59.5, 68.3, 178.2.

$[\alpha]_D^{33}$ = + 9.1 (*c* = 0.93, $CHCl_3$).

The e.r. value was determined as benzoylated compound;

To the oxidized product (ca. 0.2 mmol) in dichloromethane (2 mL) was added pyridine (31.6 mg, 0.4 mmol) and benzoyl chloride (140.6 mg, 1.0 mmol). The mixture was stirred for 1 h at 0 °C. The resulting mixture was quenched with water. The obtained organic layer was extracted with brine and dried over anhydrous Na_2SO_4. After removal of the solvent, the residue was purified by preparative TLC (^{n}hexane/AcOEt = 3/1) to afford benzoylated product (35.7 mg, 81% yield in 3 steps) as a colorless oil.

(*S*)-3-Oxocyclohexyl benzoate (**5ce**)

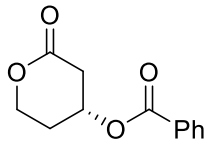

Colorless oil

^{1}H NMR (500 MHz); δ = 1.81-1.88 (m, 2H), 2.61-2.78 (m, 2H), 3.56 (m, 1H), 4.29 (m, 1H), 4.53 (m, 1H), 7.45-7.48 (m, 2H), 7.56-7.59 (m, 1H), 7.96-7.99 (m, 2H).

^{13}C NMR (125 MHz); δ = 27.1, 42.5, 59.5, 64.3, 127.6, 127.9, 128.1, 129.4, 178.2, 181.6.

HPLC (Dialcel Chiralcel OD-H, ^{n}hexane/ ^{i}PrOH = 90/10, flow rate 0.5 mL/min); t_R = 16.9 min (*R*, minor), t_R = 18.5 min (*S*, major).

Ethyl (*R*)-3-hydroxy-3-phenylbutanoate (**5dd**)[38]

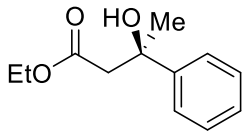

Yellow oil

^{1}H NMR (500 MHz); δ =1.18 (t, *J* = 6.8 Hz, 3H), 1.62-1.68 (m, 3H), 2.32-2.39 (m, 2H), 2.73 (d, *J* = 13.4 Hz, 1H), 3.00 (d, *J* = 13.4 Hz, 1H), 4.73 (s, 1H), 7.24 (t, *J* = 6.9 Hz, 1H), 7.32 (t, *J* = 7.5 Hz, 2H), 7.43 (d, *J* = 8.0 Hz, 2H).

^{13}C NMR (125 MHz); δ = 14.1, 28.5, 45.6, 60.8, 72.3, 127.5, 127.8, 128.5, 129.6, 182.9.

HPLC (Dialcel Chiralcel OD-H, ^{n}hexane/ ^{i}PrOH = 90/10, flow rate 0.7 mL/min); t_R = 8.8 min (*S*, minor), t_R = 13.2 min (*R*, major).

$[\alpha]_D^{21}$ = + 27.9 (*c* = 0.82, $CHCl_3$).

(*R*)-3-Hydroxy-*N,N*-dimethyl-3-phenylpropanamide (**7ad**)[39]

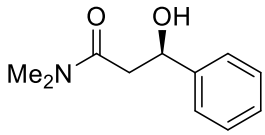

Pale yellow oil

^{1}H NMR (500 MHz); δ = 2.59-2.71 (m, 2H), 2.90 (s, 3H), 2.94 (s, 3H), 5.12-5.15 (m, 1H), 7.28-7.29 (m, 1H), 7.34-7.40 (m, 4H).

^{13}C NMR (125 MHz); δ = 34.9, 36.8, 70.1, 125.5, 127.1, 128.1, 143.0, 172.0.

HPLC (Dialcel Chiralcel OD-H, ^{n}hexane/ ^{i}PrOH = 90/10, flow rate 1.0 mL/min); t_R = 13.0 min (*S*, minor), t_R = 14.6 min (*R*, major).

$[\alpha]_D^{26}$ = + 91.5 (*c* = 0.62, $CHCl_3$).

(*R*)-3-Hydroxy-*N,N*-diethyl-3-phenylpropanamide (**7bd**)[40]

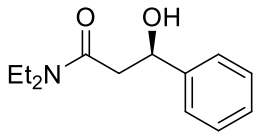

Pale yellow oil

^{1}H NMR (500 MHz); δ = 1.07-1.12 (m, 6H), 2.55-2.67 (m, 4H), 3.15-3.24 (m, 1H), 3.31-3.42 (m, 1H), 4.99 (s, 1H), 5.34 (d, *J* = 9.3 Hz, 1H), 7.24-7.38 (m, 5H).

^{13}C NMR (125 MHz); δ = 12.9, 13.9, 40.1, 41.4, 41.8, 70.5, 125.6, 127.3, 128.3, 143.2, 171.3.

HPLC (Dialcel Chiralcel OD-H, ^{n}hexane/ ^{i}PrOH = 90/10, flow rate 1.0 mL/min); t_R = 13.7 min (*S*, minor), t_R = 14.4 min (*R*, major).

$[\alpha]_D^{27}$ = + 89.9 (*c* = 0.73, $CHCl_3$).

(*R*)-*N,N*-Diethyl-3-hydroxy-3-phenylbutanamide (**7cd**)[41]

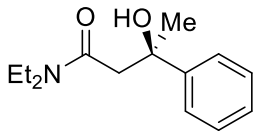

Colorless oil

^{1}H NMR (500 MHz); δ = 1.17 (t, J = 5.4 Hz, 6H), 1.64 (s, 3H), 2.55-2.67 (m, 4H), 2.84-2.99 (m, 1H), 7.28-7.47 (m, 5H).

^{13}C NMR (125 MHz); δ = 12.8, 13.9, 19.2, 40.1, 42.2, 70.5, 125.6, 127.9, 130.1, 140.7, 173.5.

HPLC (Dialcel Chiralcel OD-H, ^{n}hexane/ ^{i}PrOH = 90/10, flow rate 1.0 mL/min); t_R = 13.7 min (*S*, minor), t_R = 14.4 min (*R*, major).

$[\alpha]_D^{29}$ = + 61.7 (*c* = 0.64, $CHCl_3$).

Ethyl (*R*)-3-hydroxy-3-phenylbutanoate (**7dd**)[38]

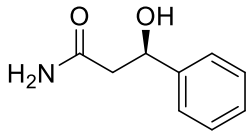

Yellow oil

^{1}H NMR (500 MHz); δ = 2.69-2.73 (m, 2H), 5.20-5.24 (m, 1H), 5.71 (s, 2H), 7.33-7.35 (m, 1H), 7.47-7.50 (m, 2H), 7.54-7.59 (m, 2H).

^{13}C NMR (125 MHz); δ = 46.5, 71.7, 125.7, 128.9, 133.2, 139.7, 176.0.

HPLC (Dialcel Chiralpak AD-H, ^{n}hexane/ ^{i}PrOH = 90/10, flow rate 1.0 mL/min); t_R = 12.4 min (*S*, minor), t_R = 15.9 min (*R*, major).

$[\alpha]_D^{21}$ = + 31.7 (*c* = 1.00, CH_3OH).

(*R*)-3-Hydroxy-3-phenylpropanenitrile (**6ad**)[42]

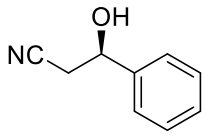

Pale yellow oil

^{1}H NMR (500 MHz); δ = 2.37 (s, 1H), 2.75-2.78 (m, 2H), 5.03 (t, *J* = 3.0 Hz, 1H), 7.34-7.41 (m, 5H).

^{13}C NMR (125 MHz); δ = 27.9, 70.0, 70.5, 125.4, 128.8, 133.2, 141.0.

HPLC (Dialcel Chiralcel OJ-H, ^{n}hexane/ ^{i}PrOH = 90/10, flow rate 1.0 mL/min); t_R = 23.6 min (*S*, minor), t_R = 27.4 min (*R*, major).

$[\alpha]_D^{26}$ = + 55.3 (*c* = 0.84, $CHCl_3$).

(*R*)-3-Hydroxy-3-(4-methylphenyl)propanenitrile[42]

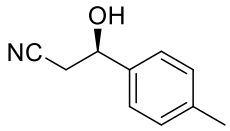

Pale yellow oil

^{1}H NMR (600 MHz); δ = 2.29 (d, *J* = 3.5 Hz, 1H), 2.34 (s, 3H), 2.70-2.78 (m, 2H), 4.99-5.01 (m, 1H), 7.18-7.19 (d, *J* = 7.8 Hz, 2H), 7.26-7.28 (d, *J* = 8.0 Hz, 2H).

^{13}C NMR (150 MHz); δ = 21,1, 27.9, 70.1, 117.3, 125.4, 129.6, 138.1, 138.8.

HPLC (Dialcel Chiralcel OJ-H, ^{n}hexane/ ^{i}PrOH = 90/10, flow rate 1.0 mL/min); t_R = 21.6 min (*S*, minor), t_R = 25.5 min (*R*, major).

$[\alpha]_D^{26}$ = + 25.6 (c = 0.83, $CHCl_3$).

(*R*)-3-(4-Fluorophenyl)-3-hydroxypropanenitrile (**6bd**)[42]

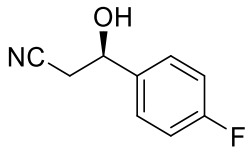

Colorless oil

^{1}H NMR (600 MHz); δ = 2.47 (d, *J* = 3.5 Hz, 1H), 2.72-2.78 (m, 2H), 5.03-5.05 (m, 1H), 7.08 (t, *J* = 8.6 Hz, 2H), 7.37-7.39 (m, 2H).

^{13}C NMR (150 MHz); δ = 28.1, 69.4, 115.8 (d), 117.1, 127.3 (d), 136.9 (d), 162.0 (d).

HPLC (Dialcel Chiralcel OJ-H, ^{n}hexane/ ^{i}PrOH = 90/10, flow rate 1.0 mL/min); t_R = 21.5 min (*S*, minor), t_R = 26.3 min (*R*, major).

$[\alpha]_D^{26}$ = +42.6 (c = 0.88, $CHCl_3$).

(*R*)-3-(Furan-2-yl)-3-hydroxypropanenitrile (**6dd**)[46]

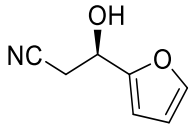

Yellow oil

^{1}H NMR (600 MHz); δ = 2.42 (d, *J* = 5.3 Hz, 1H), 2.89-2.90 (m, 2H), 5.03-5.06 (m, 1H), 6.36-6.40 (m, 2H), 7.39-7.40 (m, 1H).

^{13}C NMR (150 MHz); δ = 24.9, 63.9, 107.5, 110.6, 116.7, 143.0, 152.8.

HPLC (Dialcel Chiralcel OJ-H, ^{n}hexane/ ^{i}PrOH = 90/10, flow rate 1.0 mL/min); t_R = 22.0 min (*S*, minor), t_R = 25.2 min (*R*, major).

$[\alpha]_D^{26}$ = +37.5 (c = 0.82, $CHCl_3$).

(*S*)-3-Hydroxybutanenitrile (**6ed**)[46]

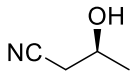

Yellow oil

^{1}H NMR (600 MHz); δ = 1.35 (d, J = 6.2 Hz, 3H), 1.92 (br, 1H), 2.46-2.55 (m, 2H), 4.14-4.17 (m, 1H).

^{13}C NMR (150 MHz); δ = 22.8, 27.5, 64.2, 117.4.

$[\alpha]_D^{26}$ = -2.0 (c = 0.90, $CHCl_3$).

<Determination of the absolute configuration of **6ed**>

(*S*)-3-(Benzyloxy)butanenitrile (**6ef**)[47]

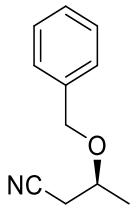

To a mixture of (*S*)-3-Hydroxybutanenitrile **6ed** (57.0 mg, 0.67 mmol), benzyl bromide (229 mg, 1.34 mmol) in dichloromethane (4 mL), Ag_2O (348 mg, 1.5 mmol) was added. Then the reaction was stirred at room temperature in dark (foiled) for 4 h. After filtration, solvent was removed by evaporation and residue was purified by PTLC (^{n}hexane/AcOEt = 10/1) to obtain **6ef** (70.4 mg, 60% yield).

Colorless oil

^{1}H NMR (600 MHz); δ = 1.33 (d, *J* = 6.2 Hz, 3H), 2.49-2.57 (m, 2H), 3.81-3.84 (m, 1H), 4.53-4.60 (dd, *J* = 11.7 Hz, 2H), 7.24-7.34 (m, 5H).

^{13}C NMR (150 MHz); δ = 19.7, 25.1, 70.4, 71.0, 117.5, 127,7, 127.9, 128.5, 137.6.

HPLC (Dialcel Chiralpak AD-H, ^{n}hexane/ ^{i}PrOH = 90/10, flow rate 1.0 mL/min); t_R = 11.1 min (*R*, minor), t_R = 13.0 min (*S*, major).

$[\alpha]_D^{26}$ = +32.1 (c = 0.78, $CHCl_3$).

(*S*)-3-(Benzyloxy)butanamide (**6eg**)[48]

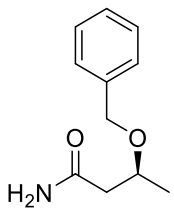

To a solution of (*S*)-3-(benzyloxy)butanenitrile **6ef** (52.6 mg, 0.3 mmol) in AcOH (3 mL), $TiCl_4$ (113.8 mg, 0.6 mmol) and H_2O (16.2 mg, 0.9 mmol) were added successively. Then the reaction was stirred at room temperature for 24 h and poured into water. The mixture was extracted by dichloromethane (20 mL) three times and organic phase was combined, dried by $MgSO_4$ and filtered. After removal of solvent by evaporation, the residue was purified by PTLC (n hexane/AcOEt = 4/1) to give **6eg** (49.3 mg, 85% yield).

Colorless oil.

^{1}H NMR (600 MHz); δ = 1.29 (d, *J* = 6.2 Hz, 3H), 2.41-2.47 (m, 2H), 3.95-3.98 (m, 1H), 4.46 (d, *J* = 11.4 Hz, 1H), 4.61 (d, *J* = 11.4 Hz, 1H), 5.30 (br, 1H), 6.21 (br, 1H), 7.25-7.34 (m, 5H)..

^{13}C NMR (150 MHz); δ = 19.4, 43.3, 70.9, 72.2, 127.7, 127.8, 128.5, 138.0, 173.3.

HPLC (Dialcel Chiralpak AD-H, ^{n}hexane/ ^{i}PrOH = 90/10, flow rate 1.0 mL/min); t_R = 12.4 min (*R*, minor), t_R = 14.2 min (*S*, major).

$[\alpha]_D^{26}$ = +35.6 (c = 0.84, $CHCl_3$).

(*R*, *E*)-4-Hydroxy-6-phenylhex-5-en-2-one (**10bd**)[43]

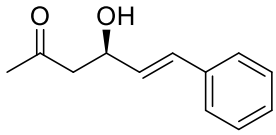

Colorless oil

^{1}H NMR (500 MHz); δ = 2.07-2.13 (m, 3H), 2.75-2.77 (m, 2H), 3.06 (brs, 1H), 4.73-4.77 (m, 1H), 6.21 (d, *J* = 15.1 Hz, 0.98H), 6.64 (d, *J* = 15.1 Hz, 0.98H), 7.29-7.38 (m, 3H), 7.47 (d, *J* = 5.6 Hz, 2H).

^{13}C NMR (125 MHz); δ = 30.6, 49.8, 68.4, 127.2, 128.2, 128.9, 129.4, 130.3, 135.1, 209.4.

HPLC (Dialcel Chiralcel OD-H, ^{n}hexane/ ^{i}PrOH = 85/15, flow rate 1 mL/min); t_R = 18.7 min (*S*, minor), t_R = 22.3 min (*R*, major).

$[\alpha]_D^{25}$ = + 18.3 (*c* = 0.82, $CHCl_3$).

(*R*, *E*)-3-Hydroxy-1,5-diphenylpent-4-en-1-one (**10ad**)[44]

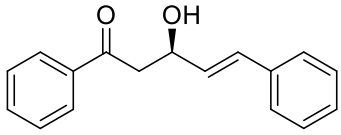

Colorless oil

^{1}H NMR (500 MHz); δ = 2.07-2.13 (m, 3H), 2.77 (m, 2H), 4.73-4.77 (m, 1H), 6.21 (d, *J* = 15.1 Hz, 1H), 6.64 (d, *J* = 15.1 Hz, 1H), 7.29-7.38 (m, 3H), 7.47 (d, *J* = 5.6 Hz, 2H).

^{13}C NMR (125 MHz); δ = 22.4, 25.0, 37.7, 127.2, 128.2, 128.2, 128.9, 128.9, 129.4, 129.4, 135.1, 200.1.

HPLC (Dialcel Chiralcel OD-H, ^{n}hexane/ ^{i}PrOH = 95/5, flow rate 0.5 mL/min); t_R = 19.0 min (*S*, minor), t_R = 22.5 min (*R*, major).

$[\alpha]_D^{21}$ = + 27.9 (*c* = 0.82, $CHCl_3$)

(*R, E*)-Ethyl 3-hydroxy-5-phenylpent-4-enoate (**10fd**)[45]

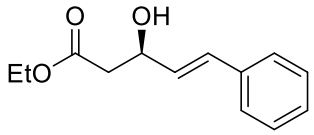

Colorless oil

^{1}H NMR (500 MHz); δ =1.28 (t, *J* = 6.8 Hz, 3H), 2.62-2.68 (m, 2H), 3.13 (s, 1H), 4.19 (dd, *J* = 6.4 Hz, *J* = 8.5 Hz, 2H), 4.73 (s, 1H), 6.22 (dd, *J* = 6.3, 9.8 Hz, 1H), 6.66 (d, *J* = 17.0 Hz), 7.24 (t, *J* = 6.9 Hz, 1H), 7.32 (t, *J* = 7.5 Hz, 2H), 7.38 (d, *J* = 8.0 Hz, 2H).

^{13}C NMR (125 MHz); δ = 14.1, 41.4, 60.8, 68.8, 126.5, 127.8, 128.5, 129.9, 130.7, 136.4, 172.2.

HPLC (Dialcel Chiralcel OD-H, ^{n}hexane/ ^{i}PrOH = 90/10, flow rate 1.0 mL/min); t_R = 14.0 min (*S*, minor), t_R = 20.8 min (*R*, major).

$[\alpha]_D^{21}$ = + 27.9 (*c* = 0.82, $CHCl_3$).

(*R, E*)-4-Hydroxy-4-methyl-6-phenylhex-5-en-2-one (**10cd**)[11]

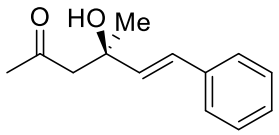

Colorless oil

^{1}H NMR (500 MHz); δ = 1.39 (s, 3H), 2.17 (s, 3H), 2.71 (d, *J* = 17.2 Hz, 1H), 2.84 (d, *J* = 17.2 Hz, 1H), 4.14 (s, 1H), 6.24 (d, *J* = 16.0 Hz, 1H), 6.58 (d, *J* = 16.0 Hz, 1H), 7.20–7.17 (m, 1H), 7.26–7.23 (m, 2H), 7.35 (d, *J* = *7.5* Hz, 2H).

^{13}C NMR (125 MHz); δ = 28.4, 32.1, 53.2, 72.0, 126.4, 127.5, 127.8, 128.6, 135.1, 136.9, 210.0.

HPLC (Dialcel Chiralcel OD-H, ^{n}hexane/ ^{i}PrOH = 95/5, flow rate 1.0 mL/min); t_R = 16.5 min (*S*, minor), t_R = 21.3 min (*R*, major).

$[\alpha]_D^{20}$ = + 19.2 (*c* = 0.61, $CHCl_3$).

(*R*, *E*)-Ethyl 3-hydroxy-3-methyl-5-phenylpent-4-enoate (7ea)[38]

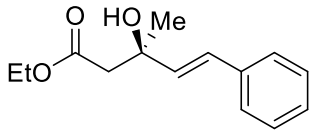

Colorless oil

^{1}H NMR (500 MHz); δ =1.28 (t, *J* = 6.8 Hz, 3H), 2.62-2.68 (m, 2H), 3.13 (s, 1H), 4.19 (dd, *J* = 6.4, 8.5 Hz, 2H), 4.73 (s, 1H), 6.22 (dd, *J* = 6.3, 9.8 Hz, 1H), 6.66 (d, *J* = 17.0 Hz), 7.24 (t, *J* = 6.9 Hz, 1H), 7.32 (t, *J* = 7.5 Hz, 2H), 7.38 (d, *J* = 8.0 Hz, 2H).

^{13}C NMR (125 MHz); δ = 14.1, 28.5, 45.5, 60.8, 71.3, 126.5, 127.5, 127.8, 128.5, 134.7, 136.7, 172.6.

HPLC (Dialcel Chiralcel OD-H, ^{n}hexane/ ^{i}PrOH = 90/10, flow rate 0.7 mL/min); t_R = 12.4 min (*S*, minor), t_R = 15.9 min (*R*, major).

$[\alpha]_D^{21}$ = + 27.9 (*c* = 0.82, $CHCl_3$).

(*R*, *E*)-3-Hydroxy-3-styrylcyclohexanone (**11aad**)

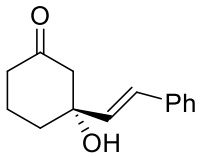

Colorless oil

IR (neat) □ = 1425, 1601, 1701, 3276 cm^{-1}.

^{1}H NMR (500 MHz); δ =0.97 (s, 1H), 2.62-2.68 (m, 2H), 3.13 (s, 1H), 4.19 (dd, *J* = 6.4, 8.5 Hz, 2H), 4.73 (s, 1H), 6.22 (dd, *J* = 6.3, 9.8 Hz, 1H), 6.66 (d, *J* = 17.0 Hz), 7.24 (t, *J* = 6.9 Hz, 1H), 7.32 (t, *J* = 7.5 Hz, 2H), 7.38 (d, *J* = 8.0 Hz, 2H).

^{13}C NMR (125 MHz); δ = 14.1, 28.5, 45.5, 60.8, 71.3, 126.5, 127.5, 127.8, 128.5, 134.7, 136.7, 172.6.

HPLC (Dialcel Chiralcel OD-H, ^{n}hexane/ ^{i}PrOH = 90/10, flow rate 0.7 mL/min); t_R = 12.4 min (*S*, minor), t_R = 15.9 min (*R*, major).

HRMS (ESI) calcd for $C_{14}H_{16}O_2$ $[M+H]^+$ 216.1150, found 216.1154.

$[\alpha]_D^{21}$ = + 19.2 (*c* = 0.96, $CHCl_3$).

(*R*)-3-(2-Hydroxy-2-phenylethyl)cyclohex-2-enone (**11ayd**)

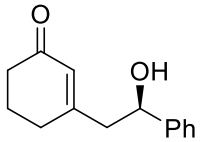

Colorless oil

IR (neat) □ = 1176, 1610, 1662, 3421 cm^{-1}.

^{1}H NMR (500 MHz); δ = 1.85-1.90 (m, 2H), 2.21-2.26 (m, 4H), 2.50 (dd, *J* = 4.6, 9.7 Hz, 1H), 2.60 (dd, *J* = 5.2, 9.2 Hz, 1H), 2.93 (s, 1H), 4.83 (s, 1H), 5.85 (t, *J* = 4.6 Hz, 1H), 7.22-7.30 (m, 5H).

^{13}C NMR (125 MHz); δ = 22.5, 30.0, 37.0, 47.6, 72.3, 125.6, 127.7, 127.8, 128.5, 143.7, 163.0, 200.0.

HPLC (Dialcel Chiralpak AS-H, ^{n}hexane/ ^{i}PrOH = 90/10, flow rate 1.0 mL/min); t_R = 66.5 min (*S*, minor), t_R = 78.3 min (*R*, major).

HRMS (ESI) calcd for $C_{14}H_{16}O_2$ $[M+H]^+$ 216.1150, found 216.1151.

$[\alpha]_D^{20}$ = + 37.3 (*c* = 1.07, $CHCl_3$).

(*R, E*)-3-Hydroxy-3-(2-phenylprop-1-en-1-yl)cyclohexan-1-one (**11od**)

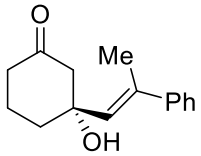

Colorless oil

IR (neat) □ = 1396, 1616, 1697, 3392 cm^{-1}.

^{1}H NMR (500 MHz); δ = 1.37-1.42 (m, 3H), 1.99-2.07 (m, 2H), 2.41-2.56 (m, 4H), 2.77-2.85 (m, 2H), 6.68 (d, *J* = 8.3 Hz), 7.26-7.52 (m, 5H).

^{13}C NMR (125 MHz); δ = 14.1, 18.8, 28.5, 45.5, 60.8, 71.3, 126.2, 127.0, 127.9, 129.1, 137.3, 141.0, 172.6.

HPLC (Dialcel Chiralcel OD-H, ^{n}hexane/ ^{i}PrOH = 90/10, flow rate 0.7 mL/min); t_R = 8.5 min (*S*, minor), t_R = 13.0 min (*R*, major).

HRMS (ESI) calcd for $C_{15}H_{18}O_2$ $[M+H]^+$ 230.1307, found 230.1308.

$[\alpha]_D^{21}$ = + 26.0 (*c* = 0.64, $CHCl_3$).

(*R*)-3-(2-Hydroxy-2-phenylpropyl)cyclohex-2-en-1-one (**11pd**)

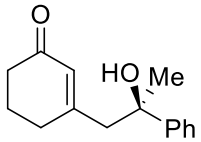

Colorless oil

IR (neat) □ = 1152, 1617, 1657, 3380 cm^{-1}.

^{1}H NMR (500 MHz); δ = 1.79 (s, 3H), 1.92-1.99 (m, 2H), 2.31-2.46 (m, 4H), 2.50 (dd, *J* = 4.6, 9.7 Hz, 1H), 2.60 (dd, *J* = 5.2, 9.2 Hz, 1H), 5.93 (d, *J* = 4.6 Hz, 1H), 7.23-7.36 (m, 5H).

^{13}C NMR (125 MHz); δ = 18.7, 23.1, 30.5, 39.5, 49.2, 74.3, 125.9, 127.8, 128.4, 128.8, 141.3, 159.9, 200.5.

HPLC (Dialcel Chiralpak AS-H, ^{n}hexane/ ^{i}PrOH = 90/10, flow rate 1.0 mL/min); t_R = 55.0 min (*S*, minor), t_R = 64.5 min (*R*, major).

HRMS (ESI) calcd for $C_{15}H_{18}O_2$ $[M+H]^+$ 230.1307, found 230.1304.

$[\alpha]_D^{20}$ = + 31.6 (*c* = 0.98, $CHCl_3$).

<Determination of the absolute configuration of **11ay** and **11pd**>

The absolute configurations of **11ay** and **11pd** were determined to be *R* by comparison of the optical rotation and the HPLC retention time of their derivatives with those of the corresponding compounds synthesized from a literature-known compound.

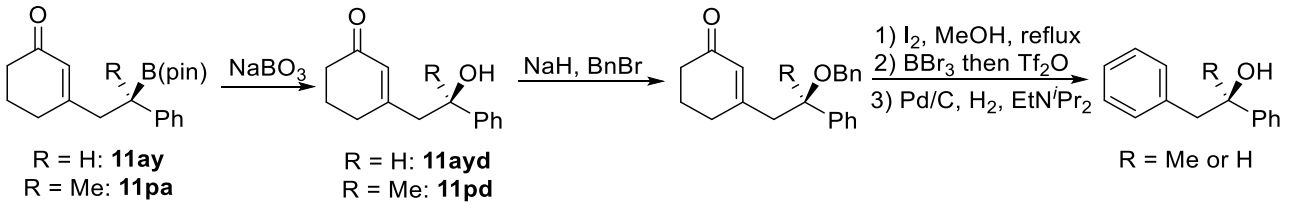

To the solution of the obtained product **11ayd** or **11pd** (0.4 mmol) in DCM (5 mL) were added NaH (1.5 equiv., 0.6 mmol) and BnBr (1.5 equiv., 0.6 mmol) at 0 ºC. After stirred at 0 ºC for 2 h, the reaction solution was quenched with H_2O, extract with AcOEt and washed with 0.1N HCl, H_2O and brine. The crude mixture was purified by flash column chromatography (AcOEt/^{n}hexane = 1/2) to afford the corresponding benzyl ether (1.1812 g, 92% yield).

To the obtained ether (0.37 mmol) in MeOH (5 mL) was added I_2 (2.15 equiv., 0.8 mmol). The reaction mixture was refluxed for 30 min. After completion of the reaction, the resultant solution was concentrated under reduced pressure. The obtained mixture was dissolved in ^{n}hexane and washed with aqueous solution of $Na_2S_2O_3$, sat. $NaHCO_3$ *aq*. and H_2O. The crude was used directly

in the next step without further purification. The crude mixture was dissolved in DCM (5 mL) and BBr_3 (0.62 mL in DCM) was added slowly. The resultant mixture was then warmed gradually up to rt and stirred for another 1.5 h. After quenched with sat. $NaHCO_3$ *aq*. at 0 °C, the reaction solution was extract with AcOEt. The crude mixture was purified by short column chromatography (AcOEt/^{n}hexane = 1/5). To the cold solution in DCM (5 mL) and pyridine (0.4 mmol) was added Tf_2O (0.4 mmol) dropwise at 0 °C. The reaction mixture was stirred for 5 h at rt. After addition of sat. $NaHCO_3$ *aq*., the resultant mixture was extracted with AcOEt and the organic layer was washed with 0.5 N HCl *aq*., H_2O and brine. To 10 mL EtOH solution of the obtained mixture was added 10% Pd/C (40 mg). The reaction mixture was stirred under H_2 for 2 h. The crude mixture was filtered through Celite® and the volatile solvent was evaporated. The residue was purified by PTLC (AcOEt/^{n}hexane = 2/1).

(*R*)-1,2-Diphenylethan-1-ol

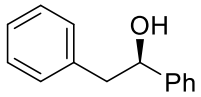

Colorless oil

^{1}H NMR (500 MHz); δ = 2.96-3.01 (m, 2H), 5.22-5.25 (m, 1H), 5.63-5.66 (m, 1H), 6.99-7.33 (m, 10H).

^{13}C NMR (125 MHz); δ = 47.6, 73.2, 126.6, 126.9, 127.6, 127.8, 128.5, 128.7, 138.1, 143.3.

HPLC (Dialcel Chiralcel OD-H, ^{n}hexane/ ^{i}PrOH = 19/1, flow rate 1.0 mL/min); t_R = 18.7 min (*R*, major), t_R = 24.3 min (*S*, minor).

$[\alpha]_D^{27}$ = –37.6 (*c* = 0.86, MeOH).

(*R*)-1,2-Diphenylpropan-2-ol

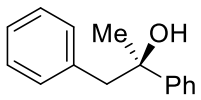

Colorless oil

^{1}H NMR (500 MHz); δ = 1.27 (s, 3H), 2.93-2.98 (m, 2H), 6.99-7.33 (m, 10H).

^{13}C NMR (125 MHz); δ = 21.2, 45.6, 71.2, 125.6, 126.5, 126.6, 127.3, 128.5, 128.7, 138.1, 143.3.

HPLC (Dialcel Chiralpak AD-H, ^{n}hexane/ ^{i}PrOH = 40/1, flow rate 1.0 mL/min); t_R = 22.5 min (*R*,

major), t_R = 29.6 min (*S*, minor).

$[\alpha]_D^{29}$ = –46.6 (*c* = 1.04, MeOH).

(*R*, *E*)-3-Hydroxy-3-styrylcyclopentanone (**11wd**)

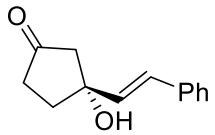

Colorless oil

IR (neat) *v* = 1465, 1622, 1747, 3241 cm^{-1}.

^{1}H NMR (500 MHz); δ =2.06-2.12 (m, 2H), 2.35 (t, *J* = 6.5 Hz, 2H), 2.61 (t, *J* = 6.5 Hz, 2H), 6.07 (s, 1H), 6.87 (d, *J* = 16.1 Hz, 1H), 7.00 (d, *J* = 16.1 Hz, 1H), 7.28-7.38 (m, 3H), 7.48 (d, *J* = 7.5 Hz, 2H).

^{13}C NMR (125 MHz); δ = 22.6, 24.5, 48.2, 71.9, 126.1, 127.9, 128.1, 128.5, 136.5, 157.1, 201.2.

HPLC (Dialcel Chiralcel OD-H, ^{n}hexane/ ^{i}PrOH = 90/10, flow rate 1.0 mL/min); t_R = 20.2 min (*S*, minor), t_R = 28.2 min (*R*, major).

HRMS (ESI) calcd for $C_{13}H_{14}O_2$ $[M+H]^+$ 202.0994, found 202.0985.

$[\alpha]_D^{22}$ = + 21.1 (*c* = 0.31, $CHCl_3$).

(*R*)-3-(2-Hydroxy-2-phenylethyl)cyclopent-2-enone (**11vd**)

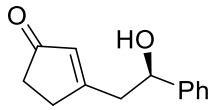

Colorless oil

IR (neat) *v* = 1165, 1616, 1732, 3411 cm^{-1}.

^{1}H NMR (500 MHz); δ = 2.37-2.41 (m, 2H), 2.50 (dd, *J* = 4.6, 9.7 Hz, 1H), 2.50-2.55 (m, 2H), 2.60 (dd, *J* = 5.2, 9.2 Hz, 1H), 2.93 (s, 1H), 4.91 (s, 1H), 5.99 (s, 1H), 7.21-7.34 (m, 5H).

^{13}C NMR (125 MHz); δ = 22.5, 30.0, 37.0, 48.7, 72.3, 125.6, 127.7, 127.8, 128.5, 143.7, 163.0, 200.0.

HPLC (Dialcel Chiralpak AS-H, ^{n}hexane/ ^{i}PrOH = 90/10, flow rate 1.0 mL/min); t_R = 45.5 min (*S*, minor), t_R = 50.6 min (*R*, major).

HRMS (ESI) calcd for $C_{13}H_{14}O_2$ $[M+H]^+$ 202.0994, found 202.0992.

$[\alpha]_D^{20}$ = + 28.1 (*c* = 0.42, $CHCl_3$).

(*R*, *E*)-3-Hydroxy-3-styrylcycloheptanone (**11sd**)

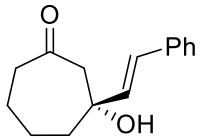

Colorless oil

IR (neat) ν = 1457, 1602, 1703, 3227 cm^{-1}.

^{1}H NMR (500 MHz); δ = 1.66–1.74 (m, 4H), 2.32–2.46 (m, 4H), 2.60-2.63 (m, 1H), 2.69-2.76 (m, 1H), 4.68 (s, 1H), 5.74 (s, 1H), 6.19-6.21 (m, 1H), 6.67-6.68 (m, 1H), 7.24-7.38 (m, 5H).

^{13}C NMR (125 MHz); δ = 24.1, 25.7, 28.5, 43.2, 59.7, 73.3, 125.9, 126.6, 127.0, 128.0, 133.9, 137.1, 207.6.

HPLC (Dialcel Chiralcel OD-H, ^{n}hexane/ ^{i}PrOH = 80/20, flow rate 1.0 mL/min); t_R = 4.9 min (*S*, minor), t_R = 6.5 min (*R*, major).

HRMS (ESI) calcd for $C_{15}H_{18}O_2$ $[M+H]^+$ 230.1307, found 230.1316.

$[\alpha]_D^{21}$ = + 15.9 (*c* = 0.52, $CHCl_3$).

(*R*)-3-(2-Hydroxy-2-phenylethyl)cyclohept-2-enone (**11sd**)

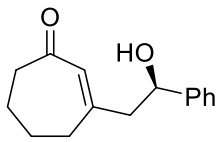

Colorless oil

IR (KBr) ν = 1227, 1601, 1711, 3412 cm^{-1}.

^{1}H NMR (500 MHz); δ = 1.92-2.05 (m, 4H), 2.09-2.19 (m, 2H), 2.46-2.51 (m, 4H), 3.21-3.23 (m, 1H), 4.86-4.89 (m, 1H), 5.89 (d, *J* = 5.6 Hz, 1H), 7.22-7.30 (m, 5H).

^{13}C NMR (125 MHz); δ = 15.6, 23.6, 31.9, 36.8, 49.5, 72.3, 126.7, 127.1, 127.9, 128.2, 142.1, 163.2, 198.5.

HPLC (Dialcel Chiralpak AS-H, ^{n}hexane/ ^{i}PrOH = 90/10, flow rate 1.0 mL/min); t_R = 60.4 min (*S*, minor), t_R = 71.0 min (*R*, major).

HRMS (ESI) calcd for $C_{15}H_{18}O_2$ $[M+H]^+$ 230.1307, found 230.1311.

$[\alpha]_D^{23}$ = + 5.4 (*c* = 0.16, $CHCl_3$).

3-((2*R*)-2-Hydroxy-2-phenylethyl-1-deuterio)cyclohex-2-en-1-one (**11ay-D**)

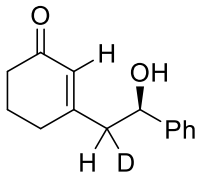

Colorless oil

^{1}H NMR (500 MHz); δ = 1.85-1.90 (m, 2H), 2.21-2.26 (m, 4H), 2.59 (d, *J* = 5.2 Hz, 1H), 2.93 (s, 1H), 4.83 (d, *J* = 4.6 Hz, 1H), 5.85 (s, 1H), 7.22-7.30 (m, 5H).

^{13}C NMR (125 MHz); δ = 22.5, 30.0, 37.0, 47.6, 72.3, 125.6, 127.7, 127.8, 128.5, 143.7, 163.0, 200.0.

HPLC (Dialcel Chiralpak AS-H, ^{n}hexane/ ^{i}PrOH = 90/10, flow rate 1.0 mL/min); t_R = 66.5 min (*S*, minor), t_R = 78.3 min (*R*, major).

HRMS (ESI) calcd for $C_{14}H_{15}DO_2$ $[M+H]^+$ 217.1213, found 217.1212.

$[\alpha]_D^{20}$ = + 35.4 (*c* = 0.65, $CHCl_3$).

(*R*)-3-Hydroxy-3-((1*E*, 3*E*)-4-phenylbuta-1,3-dien-1-yl)cyclohexan-1-one (**11bx**)

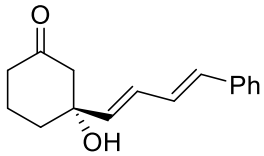

Colorless oil

IR (neat) *ν* = 1412, 1607, 1674, 3457 cm^{-1}.

^{1}H NMR (500 MHz); δ =1.67-1.76 (m, 2H), 2.01-2.08 (m, 2H), 2.30-2.37 (m, 2H), 2.60-2.67 (m, 2H), 4.43 (s, 1H), 5.86 (dd, *J* = 6.3, 9.8 Hz, 1H), 6.39 (d, *J* = 17.0 Hz), 6.54 (d, *J* = 17.0 Hz, 1H), 6.72 (dd, *J* = 6.3, 9.8 Hz, 1H), 7.26-7.40 (m, 5H).

^{13}C NMR (125 MHz); δ = 21.6, 29.4, 46.7, 60.6, 70.8, 126.4, 127.6, 128.3, 128.9, 129.8, 133.4, 136.1, 137.2, 170.9.

HPLC (Dialcel Chiralcel OD-H, ^{n}hexane/ ^{i}PrOH = 90/10, flow rate 0.7 mL/min); t_R = 12.4 min (*S*, minor), t_R = 15.9 min (*R*, major).

HRMS (ESI) calcd for $C_{16}H_{18}O_2$ $[M+H]^+$ 242.1307, found 242.1307.

$[\alpha]_D^{21}$ = + 42.1 (*c* = 0.71, $CHCl_3$).

(*R*, *E*)-3-(2-Hydroxy-4-phenylbut-3-en-1-yl)cyclohex-2-en-1-one (**11by**)

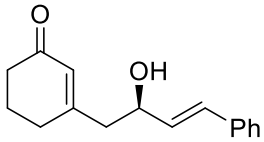

Colorless oil

IR (neat) v = 1362, 1620, 1667, 3369 cm^{-1}.

^{1}H NMR (500 MHz); δ = 1.82-1.90 (m, 2H), 2.20-2.29 (m, 4H), 2.52-2.54 (m, 1H), 2.56-2.60 (m, 1H), 4.89-4.92 (m, 1H), 5.96 (s, 1H), 6.34-6.36 (m, 1H), 6.53-6.56 (m, 1H), 7.22-7.49 (m, 5H).

^{13}C NMR (125 MHz); δ = 27.2, 31.2, 34.3, 42.5, 48.7, 71.4, 125.8, 126.4, 127.0, 128.8, 132.1, 133.4, 141.8, 176.9.

HPLC (Dialcel Chiralpak AS-H, ^{n}hexane/ ^{i}PrOH = 80/20, flow rate 1.0 mL/min); t_R = 26.0 min (*S*, minor), t_R = 31.5 min (*R*, major).

HRMS (ESI) calcd for $C_{16}H_{18}O_2$ $[M+H]^+$ 242.1307, found 242.1310.

$[\alpha]_D^{29}$ = + 36.2 (*c* = 0.55, $CHCl_3$).

(*R*, *E*)-3-(4-Hydroxy-4-phenylbut-1-en-1-yl)cyclohex-2-en-1-one (**11bz**)

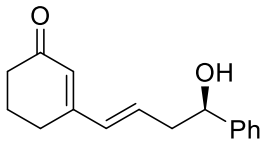

Colorless oil

^{1}H NMR (500 MHz); δ = 1.87-1.93 (m, 2H), 2.29-2.32 (m, 4H), 2.51-2.57 (m, 2H), 3.07 (s, 1H), 4.79-4.82 (m, 1H), 5.74-5.79 (m, 1H), 6.32-6.33 (m, 1H), 6.57-6.58 (m, 1H), 7.22-7.51 (m, 5H).

^{13}C NMR (125 MHz); δ = 21.0, 22.1, 30.1, 38.7, 48.9, 53.8, 60.3, 67.1, 126.9, 127.1, 127.3, 128.5, 134.5, 138.6, 163.0..

HPLC (Dialcel Chiralpak AS-H, ^{n}hexane/ ^{i}PrOH = 90/10, flow rate 1.0 mL/min); t_R = 18.5 min (*S*, minor), t_R = 22.6 min (*R*, major).

HRMS (ESI) calcd for $C_{16}H_{18}O_2$ $[M+H]^+$ 242.1307, found 242.1312.

$[\alpha]_D^{23}$ = + 6.7 (*c* = 0.14, MeOH).

Determination of the absolute configuration of **11bz**:

The absolute configuration of **11bz** was determined to be *R* by comparison of the HPLC retention time of its derivative with those of the corresponding compound synthesized from a literature-known compound.

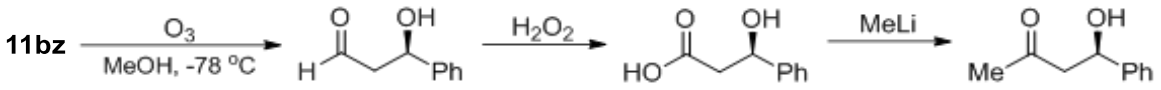

The product **11bz** was dissolved in MeOH (10 mL) and was oxidized by O_3 at –78 °C. The reaction mixture was then bubbled with Ar, and rinsed with H_2O, $Na_2S_2O_3$ aqueous solution and brine. After evaporation of the solvent, 2 mL of EtOH was added to the mixture. 20% H_2O_2 *aq*. (100 □L) was then added and the reaction mixture was stirred for 1h at rt. After addition of 1N NaOH aqueous solution (1 mL), the reaction mixture was washed with Et_2O. After the subsequent addition of 1N HCl (1.5 mL), the mixture was extracted with DCM. After removal of the volatile solvent, to the obtained mixture dissolved in DCM was added MeLi solution slowly under 0 °C. The mixture was stirred for 15 min and quenched with sat. NH_4Cl *aq*. Finally, the mixture was extract with AcOEt and purified by PTLC (AcOEt/^{n}hexane = 1/4) to afford the product (66% yield, 3 steps).

1.1-3 Typical Procedures

<Typical Experimental Procedure for Chiral $Cu(OH)_2$-Catalyzed Enantioselective Boron Conjugate Additions to α,β-Unsaturated Carbonyl Compounds in Water (Table 1.1, Entry 3)>

To an aqueous solution (1 mL) of $Cu(OH)_2$ (2.0 mg, 5 mol%) and chiral 2,2'-bipyridine **L1** (7.9 mg, 6 mol%) was added an acetic acid solution (24 mM, 1 mL). After stirred vigorously for 1 h at room temperature, the resultant mixture was allowed to cool to 5 °C. Chalcone **1a** (81.9 mg, 0.4 mmol) and $B_2(pin)_2$ (121.8 mg, 0.48 mmol) were then added successively at the same temperature. After stirring for 12 h, the reaction mixture was filtered and rinsed with AcOEt. The aqueous layer was extracted with AcOEt (20 mL) three times, and the combined organic layers were dried over anhydrous Na_2SO_4. After concentrated under reduced pressure, the crude mixture was purified by preparative TLC (^{n}hexane/AcOEt = 4/1) to afford the desired product **1aa** (127.9 mg, 95% yield) as a colorless oil.

<Typical Procedure for Turnover Frequency Study>

To an aqueous solution (2 mL) of $Cu(OH)_2$ (0.020 mg, 0.005 mol%) was added chiral 2,2'-bipyridine **L1** (0.079 mg, 0.006 mol%). After stirred vigorously for 15 min at room temperature, the resultant mixture was allowed to cool to 5 ºC. Chalcone **1a** (83.2 mg, 0.4 mmol) and $B_2(pin)_2$ (121.8 mg, 0.48 mmol) were then added successively at the same temperature. After stirring for 15 min, the reaction mixture was filtered and rinsed with THF (3 mL). The excess amount of $NaBO_3 \cdot 4H_2O$ (488 mg) was then added and the mixture was stirred at room temperature for 4 h. The aqueous layer was extracted with AcOEt (20 mL) three times, and the combined organic layers were dried over anhydrous Na_2SO_4. After concentrated under reduced pressure, the crude mixture was purified by preparative TLC (^{n}hexane/AcOEt = 4/1) to afford the desired product **1ad** (48.7 mg, 54 %) as a colorless oil.

<Typical Procedure for Kinetic and KIE Experiments>

[Heterogeneous System]

To an aqueous solution (2 mL) of $Cu(OH)_2$ (2.0 mg, 5 mol%) was added chiral 2,2'-bipyridine L1 (7.9 mg, 6 mol%). After stirred vigorously for 15 min at room temperature, the resultant mixture was allowed to cool to 5 ºC. Chalcone **1a** (83.2 mg, 0.4 mmol) and $B_2(pin)_2$ (121.8 mg, 0.48 mmol) were then added successively at the same temperature. The resultant mixture was stirred for 2, 5, 10, 15, 30 and 60 min, respectively. After stirred, the reaction mixture was filtered and rinsed with THF (3 mL). The excess amount of $NaBO_3 \cdot 4H_2O$ (488 mg) was then added and the mixture was stirred at room temperature for 4 h. The aqueous layer was extracted with AcOEt (20 mL) three times, and the combined organic layers were dried over anhydrous Na_2SO_4. After concentrated under reduced pressure, the crude mixture was purified by preparative TLC (^{n}hexane/AcOEt = 4/1) to afford the desired product **1ad** as a colorless oil. The reaction was conducted 10 times and the result was calculated as an average of 8 experiments after exclusion of two outliers.

< Synthesis of α,β-Unsaturated Imines >

Method A: The corresponding amine (10 mmol), corresponding ketone (10 mmol), montmorillonite K10 (1 g) and molecular sieves 5A (1 g) were stirred in CH_3CN (10 mL) for 16 h at room temperature. The reaction mixture was filtered through celite®, and the product was isolated by distillation.

Method B: A mixture of ketone (10 mmol) and benzylamine (10 mmol) in 20 mL of hexane (freshly

distilled from calcium hydride) was refluxed for 15 h over molecular sieves 5A (1 g). After filtration, the crude oil was crystallized under refrigeration, and recrystallization from THF/^{n}hexane = 1/4.

[Homogeneous System]

To an aqueous solution (2 mL) of $Cu(OAc)_2$ (3.2 mg, 5 mol%) was added chiral 2,2'-bipyridine **L1** (7.9 mg, 6 mol%). After stirred vigorously for 15 min at room temperature, the resultant mixture was allowed to cool to 5 ºC. Chalcone **1a** (83.2 mg, 0.4 mmol) and $B_2(pin)_2$ (121.8 mg, 0.48 mmol) were then added successively at the same temperature. The resultant mixture was stirred for 2, 5, 7, 10, 15, 30 and 60 min, respectively. After stirred, THF (3 mL) was added. The excess amount of $NaBO_3 \cdot 4H_2O$ (488 mg) was then added and the mixture was stirred at room temperature for 4 h. The aqueous layer was extracted with AcOEt (20 mL) three times, and the combined organic layers were dried over anhydrous Na_2SO_4. After concentrated under reduced pressure, the crude mixture was purified by preparative TLC (^{n}hexane/AcOEt = 4/1) to afford the desired product **1ad** as a colorless oil. The reaction was conducted 8 times and the result was calculated as an average of 6 experiments after exclusion of two outliers.

(R)-3-Hydroxy-1,3-diphenyl-2-deuterio-propan-1-one (**1ad-D**)

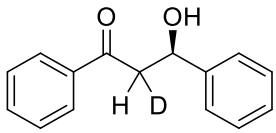

Colorless oil

^{1}H NMR (500 MHz); δ = 3.37 (m, 1H), 3.63 (s, 1H), 5.35 (t, J = 6.0 Hz, 1H), 7.28-7.48 (m, 7H), 7.56-7.59 (m, 1H), 7.96 (d, J = 7.0 Hz, 2H).

^{13}C NMR (125 MHz); δ = 47.4, 70.0, 120.7, 127.5, 128.0, 128.3, 128.4, 133.6, 136.6, 143.0, 200.1.

HPLC (Dialcel Chiralcel OD-H, ^{n}hexane/ ^{i}PrOH = 85/15, flow rate 0.7 mL/min); t_R = 14.4 min (S, minor), t_R = 16.3 min (R, major).

HRMS (ESI) calcd for $C_{15}H_{13}DO_2$ $[M+H]^+$ 227.1057, found 227.1060.

$[\alpha]_D^{29}$ = + 51.3 (c = 1.00, $CHCl_3$).

<Typical Procedure for ESI-MS Analysis>

$Cu(OAc)_2$ (1.7 mg) and chiral 2,2'-bipyridine **L1** (4.0 mg) were dissolved in aqueous tetrahydrofuran (H_2O/THF = 4/1, 2 mL) and stirred at r.t. for 1 hr. To the resultant homogeneous solution was added

chalcone **1a** (20.8 mg) and the mixture was then stirred for another 20 min. Finally $B_2(pin)_2$ (30.3 mg) was added and stirred vigorously for 5 or 15 seconds. The reaction mixture was submitted directly to ESI-MS analysis.

1.1-4 DFT Calculation Results

DFT calculations were utilized to investigate the detailed reaction mechanism of the copper-catalyzed boron conjugate addition. The structures were subjected to geometry optimization using the B3LYP/6-31G* basis set with implicit solvent corrections (COSMO model, H_2O). B3LYP/LanL2DZ was employed for the copper atom. Frequency calculations at the same level of theory have also been performed to identify all of the stationary points as minima (zero imaginary frequencies) or transition states (one imaginary frequency), and to provide free energies at 298.15 K which include entropic contributions by taking into account the vibrational, rotational, and translational motions of the species under consideration.

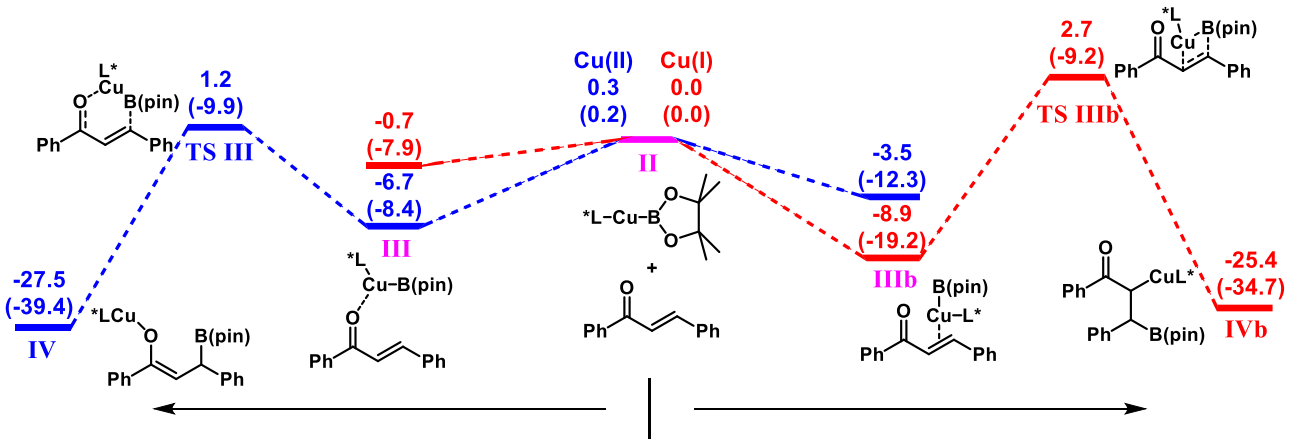

Figure 6.1 Energy profiles calculated for the formation of copper enolates.

a. Colors represent copper species as follows; blue = Cu(II) mediated reaction pathway; red = Cu(I) mediated reaction pathway. L* = **L1**.

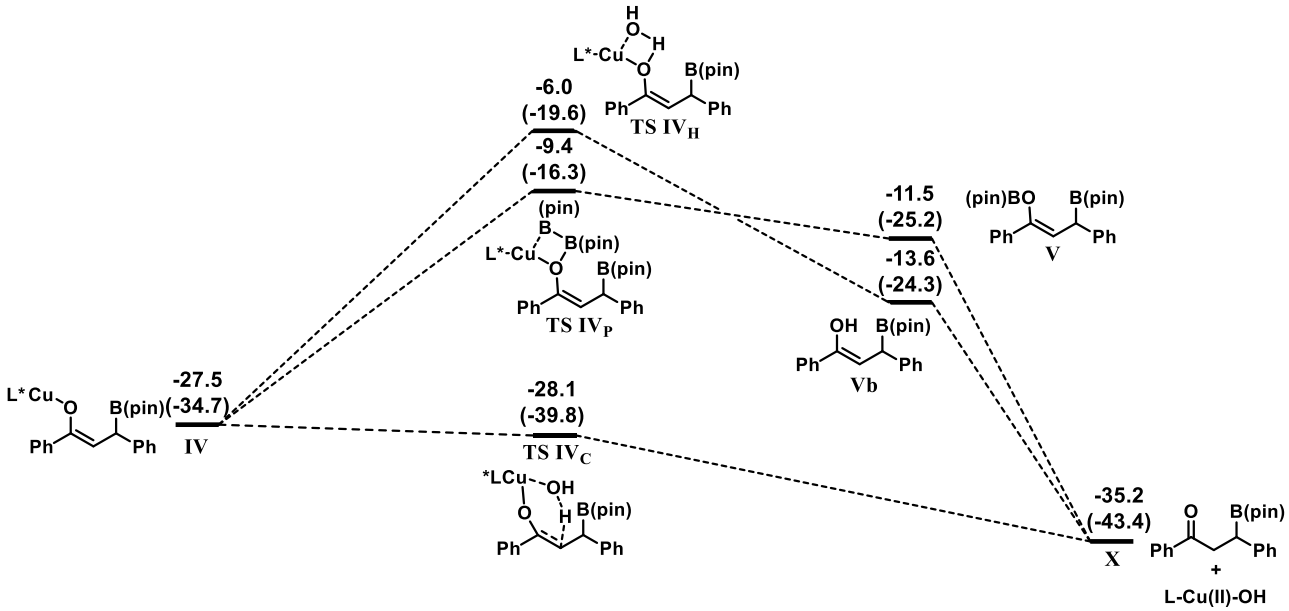

L* = **L1**.

Figure 6.2. Energy profiles calculated for various pathways of Cu(II) catalyst in the final step.

The results are supported by experimental studies.

(1) Kinetic isotope effects were explored with D_2O. The small isotope effect proves that the rate-determining step does not involve the protonation/deuteration of an enolate intermediate at the final stage from **IV-B** back to **I-B**.

Scheme 6.1. Kinetic isotope effect study.

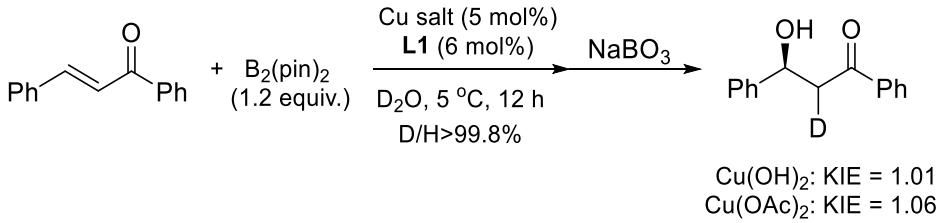

(2) Borylation reactions of styrene with different copper species further confirmed the importance of carbonyl group for Cu(II)-mediated borylation reactions. Cu(I) could still catalyze the borylation of styrene while Cu(II) salts did not catalyze the reaction at all.

Scheme 6.2. Borylation reactions of styrene.

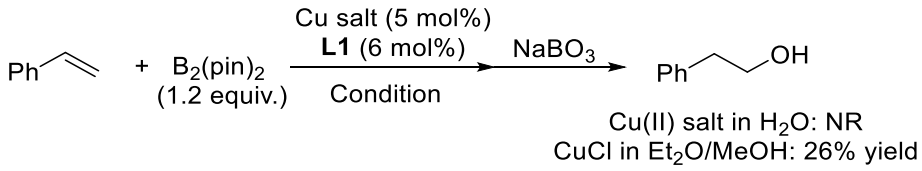

1.1-5 Reference

1 Xu, W. L.; Zhou, Y. G.; Wang, R. M.; Wu, G. T.; Chen, P. *Org. Biomol. Chem.* **2012**, *10*, 367-371.

2 Provencher, B. A.; Bartelson, K. J.; Liu, Y.; Foxman, B. M.; Deng, L. *Angew. Chem. Int. Ed.* **2011**, *50*, 10565-10569.

3 Rana, N. K.; Selvakumar, S.; Singh, V. K. *J. Org. Chem.* **2010**, *75*, 2089-2091.

4 Nishikawa, Y.; Yamamoto, H. *J. Am. Chem. Soc.* **2011**, *133*, 8432-8435.

5 Nolwenn, J. A. M;. Benjamin, L. *J. Am. Chem. Soc.* **2006**, *128*, 13368-13369.

6 Fronza, G.; Fuganti, C.; Serra, S. *Eur. J. Org. Chem.* **2009**, 6160-6171.

7 Watanabe, M.; Hisamatsu, S.; Hotokezaka, H.; Furukawa, S. *Chem. Pharm. Bull.* **1986**, *34*, 2810-2820.

8 Wang, P.; Liu, C. –R.; Sun, X. –L.; Chen, S. –S.; Li, J. –F.; Xie, Z.; Tang, Y. *Chem. Commun.* **2012**, 290-292.

9 Lillya, C. P.; Kluge, A. F. *J. Org. Chem.* **1971**, *36*, 1977-1988.

10 Maj, J.; Morzycki, J. W.; Rárová, L.; Wasilewski, G.; Wojtkielewicz, A. *Tetrahedron Lett.* **2012**, *53*, 5430-5433.

11 Lee, K. S.; Wu, H.; Haeffner, F.; Hoveyda, A. H. *Organometallics* **2012**, *31*, 7823-7826.

12 Crisan, C.; Normant, H. *Bulletin de la Societe Chimique de France* **1957**, 1451-1454.

13 Lasne, M. –C.; Ripoll, J. –L. *Tetrahedron Lett.* **1980**, *21*, 463-464.

14 Staub, K.; Levina, G. A.; Barlow, S.; Kowalczyk, T. C.; Lackritz, H. S.; Barzoukas, M.; Fort, A.; Marder, S. R. *J. Mater. Chem.* **2003**, *13*, 825-833.

15 Tissot, M.; Poggiali, D.; Hénon, H.; Müller, D.; Guénée, M.; Mauduit, M.; Alexakis, A. *Chem. Eur. J.* **2012**, *18*, 8731-8747.

16 Ishiyama, T.; Murata, M.; Ahiko, T.; Miyaura, N. *Org. Synth.* **2000**, *77*, 176-180.

17 Dewar, M. J. S.; Jones, R. *J. Am. Chem. Soc*. **1967**, *89*, 2408-2410.

18 (a) Bolm, C.; Ewald, M.; Felder, M.; Schlingloff, G. *Chem. Ber.* **1992**, *125*, 1169-1190 (b) Ishikawa, S.; Hamada, T.; Manabe, K.; Kobayashi, S. *Synthesis* **2005**, *13*, 2176-2182.

19 Kobayashi, S.; Endo, T.; Ueno, M. *Angew. Chem. Int. Ed.* **2011**, *50*, 12262–12265.

20 Hong, B.; Ma, Y.; Zhao, L.; Duan, W.; He, F.; Song, C. *Tetrahedron: Asymmetry* **2011**, *22*, 1055-1062.

21 Li, H.; Da, C. –S.; Xiao, Y. –H.; Li, X.; Su, Y. –N. *J. Org. Chem.* **2008**, *73*, 7398-7401.
22 Hupe, E.; Marek, I.; Knochel, P. *Org. Lett.* **2002**, *4*, 2861-2863.
23 Yadav, J. S.; Reddy, A. R.; Rao, Y. G.; Narsaiah, A. V.; Reddy, B. V. S. *Synlett* **2007**, 3447-3450.
24 Xu, H. J.; Liu, Y. C.; Fu, Y.; Wu, Y. D. *Org. Lett.* **2006**, *8*, 3449-3451.
25 Ahmad, K.; Koul, S.; Taneja, S. C.; Singh, A. P.; Kapoor, M.; ul-Hassan, R.; Verma, V.; Qazi, G. N. *Tetrahedron Asymmetry* **2004**, *15*, 1685-1692.
26 Trost, B. M.; Ito, H. *J. Am. Chem. Soc.* **2000**, *122*, 12003-12004.
27 Suzuki, T.; Yamagiwa, N.; Matsuo, Y.; Sakamoto, S.; Yamaguchi, K.; Shibasaki, M.; Noyori, R. *Tetrahedron Lett.* **2001**, *42*, 4669-4671.
28 Ghobril, C.; Sabot, C.; Mioskowski, C.; Baati, R. *Eur. J. Org. Chem.* **2008**, 4104-4108.
29 Hara, K.; Akiyama, R.; Sawamura, M. *Org. Lett.* **2005**, *7*, 5621-5623.
30 Aoki, S.; Kotani, S.; Sugiura, M.; Nakajima, M. *Chem. Commun.* **2012**, 5524-5526.
31 Lee, K. –S.; Zhugralin, A. R.; Hoveyda, A. H. *J. Am. Chem. Soc.* **2009**, *131*, 7253-7255.
32 Chen, I. –H.; Yin, L.; Itano, W.; Kanai, M.; Shibasaki, M. *J. Am. Chem. Soc.* **2009**, *131*, 11664-11665.
33 Cossy, J.; Bouzide, A.; Ibhi, S.; Aclinou, P. *Tetrahedron* **1991**, *47*, 7775-7782.
34 Denmark, S. E.; Wynn, T.; Beutner, G. L. *J. Am. Chem. Soc.* **2002**, *124*, 13405-13407.
35 Tang, S.; Jin, R. H.; Zhang, H. S.; Yao, H.; Zhuang, J. L.; Liu, G. H.; Li, H. X. *Chem. Commun.* **2012**, *48*, 6286-6288.
36 Li, W.; Ma, X.; Fan, W.; Tao, X.; Li, X.; Xie, X.; Zhang, Z. *Org. Lett.* **2011**, *13*, 3876-3879.
37 Loubinoux, B.; Sinnes, J. –L.; O'Sullivan, A. C.; Winkler, T. *Tetrahedron* **1995**, *51*, 3549-3558.
38 Lin, N.; Chen, M. –M.; Luo, R. –S.; Deng, Y. –Q.; Lu, G. *Tetrahedron: Asymmetry* **2010**, *21*, 2816-2824.
39 Hirsch-Weil, D.; Abboud, K. A.; Hong, S. *Chem. Commun.* **2010**, 7525-7527.
40 Hlavinka, M. L.; Greco, J. F.; Hagadorn, J. R. *Chem. Commun.* **2005**, 5304-5306.
41 Puterbaugh, W. H.; Hauser, C. R. *J. Am. Chem. Soc.* **1953**, *75*, 2415-2417.
42 Soltani, O.; Ariger, M. A.; Vázquez-Villa, H.; Carreira, E. M. *Org. Lett.* **2010**, *12*, 2893-2895.
43 Abate, A.; Brenna, E.; Costantini, A.; Fuganti, C.; Gatti, F. G.; Malpezzi, L.; Serra, S. *J. Org. Chem.* **2006**, *71*, 5228-5240.
44 Cheon, C. H.; Yamamoto, H. *Org. Lett.* **2010**, *12*, 2476-2479.
45 Wadhwa, K.; Verkade, J. G. *J. Org. Chem.* **2009**, *74*, 4368-4371.
46 Wadhwa, K.; Verkade, J. G. *J. Org. Chem.* **2009**, *74*, 5683-5686.
47 Itoh, T.; Mitsukura, K.; Kanphai, W.; Takagi, Y.; Kihara, H.; Tsukube, H. *J. Org. Chem.* **1997**, *62*, 9165-9172.
48 Ma, D.-Y.; Wang, D.-X.; Pan, J.; Huang, Z.-T.; Wang, M.-X. *J. Org. Chem.* **2008**, *73*, 4087-4091.
49 Dibiase, S. A.; Lipisko, B. A.; Haag, A.; Wolak, R. A.; Gokel, G. W. *J. Org. Chem.* **1979**, *44*, 4640-4649.
50 Jiang, Q.; Guo, T.; Yu, Z. *Chemcatchem* **2015**, *7*, 660-665.

1.2 For Cu(II)-mediated silylation reactions:

1.2-1 <Reagents>

Silyl boron reagents were synthesized using protocols described in literature.

Dimethyl(phenyl)(4,4,5,5-tetramethyl-1,3,2-dioxaborolan-2-yl)silane (**3**)[2]

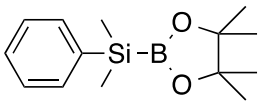

^{1}H NMR (600 MHz); δ = 0.11 (s, 6H), 0.90 (s, 12H), 7.03-7.06 (m, 3H), 7.28-7.30 (m, 2H).

^{13}C NMR (150 MHz); δ = -2.9, 24.8, 25.2, 82.5, 83.6, 127.9, 128.8, 129.7, 133.4, 134.4.

^{11}B NMR (600 MHz); δ = 33.9.

Triethyl(4,4,5,5-tetramethyl-1,3,2-dioxaborolan-2-yl)silane (**3b**)[2]

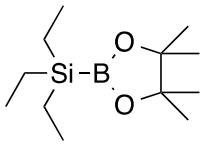

^{1}H NMR (600 MHz); δ = 0.59 (q, J = 9.6 Hz, 6H), 0.96 (t, *J* = 9.6 Hz, 9H), 1.23 (s, 12H).

^{13}C NMR (150 MHz); δ = 4.0, 8.3, 24.5, 83.2.

The reaction using triethyl(4,4,5,5-tetramethyl-1,3,2-dioxaborolan-2-yl)silane instead of **3** did not proceed at all.

1.2-2 Procedure for preparation of chiral Cu(II) complex

$Cu(acac)_2$ (11.1 mg) was dissolved in CH_2Cl_2 (1.5 mL) together with chiral 2,2'-bipyridine ligand **L1** (13.9 mg), warmed to 50 ºC and allowed to cool down to room temperature. The purplish acicular crystal was gradually grown in a thin line from CH_2Cl_2/^{n}hexane system through liquid phase-vapor phase diffusion method. The obtained purplish crystal was fully characterized by several spectrometric methods as shown below. The amount of Cu in the resulting crystal was measured by ICP analysis.

$Cu(acac)_2$-**L1** complex

IR (KBr) = 731, 909, 1267, 1711, 2352, 2826, 2928, 2961, 3067 cm-1.

^{1}H NMR (600 MHz); δ = 0.96 (s, 30H), 4.41 (d, *J* = 19.9 Hz, 4H), 7.21 (d, *J* = 6.9 Hz, 2H), 7.77 (dd, *J* = 6.9, 7.6 Hz, 2H), 8.29 (d, *J* = 7.6 Hz, 2H).

^{13}C NMR (150 MHz); δ = 26.0, 36.4, 80.3, 119.7, 123.1, 136.7, 153.9, 159.4.

Elemental analysis calcd C: 61.05, H: 7.17, N: 4.75; found C: 61.32, H: 7.19, N: 4.87.

HRMS (ESI) calcd for $C_{30}H_{43}N_2O_6Cu$ [$Cu(acac)_2$ + **L1** + H]$^+$: 590.2412; found 590.2405.

Cu content: calcd 10.77; found 10.77.

Typical experimental procedure for enantioselective silyl conjugate additions to α, β-unsaturated acceptors in water

After chiral Cu(II) complex crystal (8.85 mg, 5 mol%) was dispersed into water (2 mL), chalcone (62.5 mg, 0.3 mmol) and $PhMe_2Si$-B(pin) (94.4 mg, 0.36 mmol) was added. After stirring for 24 h, the reaction mixture was extracted with EtOAc (20 mL x 3) and the combined organic layers were dried over anhydrous Na_2SO_4. After concentrated under reduced pressure, the crude mixture was purified by preparative TLC (^{n}hexane/ ^{i}PrOH = 6:1) to afford the desired product **3a** (95.1 mg, 92% yield) as colorless oil.

1.2-3 Analytical Data for Silylated Compounds

The obtained analytical data for literature-known compounds is in full agreement with reported data. The absolute configurations of optically active compounds were determined by comparison of the order of retention time in the chiral HPLC analyses.

1. (*R*)-3-(Dimethyl(phenyl)silyl)-1,3-diphenylpropan-1-one (**1ab**)[3]

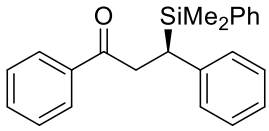

Pale yellow oil

^{1}H NMR (600 MHz); δ = 0.22 (s, 3H), 0.28 (s, 3H), 3.09 (dd, *J* = 10.3, 4.8 Hz, 1H), 3.20 (dd, *J* = 2.0, 4.1 Hz, 1H), 3.48 (dd, *J* = 13.6, 10.3 Hz, 1H), 6.96-6.97 (m, 2H), 7.03-7.06 (m, 1H), 7.14-7.17 (m, 2H), 7.31-7.38 (m, 6H), 7.42-7.43 (m, 1H), 7.47-7.50 (m, 1H), 7.76-7.78 (m, 2H).

^{13}C NMR (150 MHz); δ = –5.2, –3.9, 31.0, 38.9, 124.8, 127.6, 127.7, 127.9, 128.0, 128.4, 129.3, 132.7, 134.1, 136.8, 137.1, 142.3, 199.0.

HPLC (Daicel Chiralpak AD-H, ^{n}hexane/ ^{i}PrOH = 95/5, flow rate 0.8 mL/min); t_R = 9.0 min (*S*, minor), t_R = 15.0 min (*R*, major).

$[\alpha]_D^{20}$ = + 26.4 (*c* = 1.96, $CHCl_3$).

2. (*R*)-3-(Dimethyl(phenyl)silyl)-1-(4-methoxyphenyl)-3-phenylpropan-1-one (**1cb**)

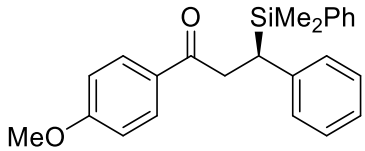

Pale yellow oil.

IR (neat) ν = 810, 976, 1247, 1508, 1685, 1753, 2360 cm^{-1}.

^{1}H NMR (600 MHz); δ = 0.21 (s, 3H), 0.26 (s, 3H), 2.98 (dd, *J* = 10.3, 4.1 Hz, 1H), 3.13 (dd, *J* = 17.2, 4.1 Hz, 1H), 3.36 (dd, *J* = 16.5, 10.3 Hz, 1H), 3.72 (s, 3H), 6.69-6.71 (m, 2H), 6.85-6.88 (m, 2H), 7.30-7.37 (m, 5H), 7.41-7.43 (m, 2H), 7.46-7.49 (m, 1H), 7.74-7.76 (m, 2H).

^{13}C NMR (150 MHz); δ = –5.2, –3.8, 30.1, 39.2, 55.1, 113.6, 127.7, 127.9, 128.4, 128.5, 129.2, 132.7,

134.1, 134.2, 137.0, 137.1, 157.0, 199.3.

HPLC (Daicel Chiralpak AD-H, ^{n}hexane/ ^{i}PrOH = 49/1, flow rate 0.8 mL/min); t_R = 10.0 min (*S*, minor), t_R = 20.4 min (*R*, major).

HRMS (ESI) calcd for $C_{24}H_{27}O_2Si$ $[M+H]^+$: 375.1775, found 375.1778.

$[\alpha]_D^{20}$ = + 23.3 (*c* = 1.14, $CHCl_3$).

3. (*R*)-3-(Dimethyl(phenyl)silyl)-1-phenyl-3-(*p*-tolyl)propan-1-one (**1wb**)

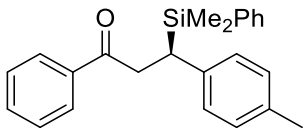

Pale yellow oil.

IR (neat) ν = 980, 1218, 1389, 1507, 1541, 1716, 2360 cm^{-1}.

^{1}H NMR (600 MHz); δ = 0.21 (s, 3H), 0.27 (s, 3H), 2.24 (s, 3H), 3.01 (dd, *J* = 4.1, 10.3 Hz, 1H), 3.13 (dd, *J* = 4.1, 17.2 Hz, 1H), 3.40 (dd, *J* = 10.3, 17.2 Hz, 1H), 6.84-6.86 (m, 2H), 6.95-6.97 (m, 2H), 7.31-7.49 (m, 8H), 7.74-7.77 (m, 2H).

^{13}C NMR (150 MHz); δ = –4.2, –3.9, 20.9, 30.4, 38.7, 127.5, 127.7, 127.9, 128.4, 128.8, 129.4, 132.8, 134.2, 137.0, 139.0, 199.3.

HPLC (Daicel Chiralpak AD-H, ^{n}hexane/ ^{i}PrOH = 98/2, flow rate 0.8 mL/min); t_R = 7.3 min (*S*, minor), t_R = 11.8 min (*R*, major).

HRMS (ESI) calcd for $C_{24}H_{27}OSi$ $[M+H]^+$: 359.1826, found 359.1825.

$[\alpha]_D^{20}$ = + 28.5 (*c* = 0.84, $CHCl_3$).

4. (*R*)-3-(4-Chlorophenyl)-3-(dimethyl(phenyl)silyl)-1-phenylpropan-1-one (**1db**)

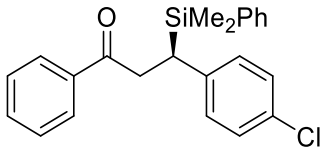

Colorless oil.

IR (neat) ν = 745, 913, 1276, 1420, 1698, 1741, 2360, 2917 cm^{-1}.

^{1}H NMR (600 MHz); δ = 0.23 (s, 3H), 0.27 (s, 3H), 3.03 (dd, *J* = 4.1, 11.1 Hz, 1H), 3.16 (dd, *J* = 4.1, 15.8 Hz, 1H), 3.39 (dd, *J* = 10.3, 11.0 Hz, 1H), 6.86-6.88 (m, 2H), 7.10-7.12 (m, 2H), 7.32-7.42 (m,

7H), 7.49-7.52 (m, 1H), 7.76-7.78 (m, 2H).

^{13}C NMR (150 MHz); δ = –4.0, –5.2, 30.7, 38.7, 127.8, 127.9, 128.2, 128.5, 128.9, 129.5, 130.4, 132.9, 134.1, 136.3, 137.0, 141.0, 198.8.

HPLC (Daicel Chiralpak AD-H, ^{n}hexane/ ^{i}PrOH = 98/2, flow rate 0.8 mL/min); t_R = 8.0 min (*S*, minor), t_R = 14.3 min (*R*, major).

HRMS (ESI) calcd for $C_{23}H_{24}ClOSi$ $[M+H]^+$: 379.1280, found 379.1285.

$[\alpha]_D^{20}$ = + 19.3 (*c* = 0.98, $CHCl_3$).

5. (*R*)-3-(2-Chlorophenyl)-3-(dimethyl(phenyl)silyl)-1-phenylpropan-1-one (**1sb**)

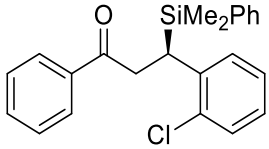

Colorless oil.

IR (neat) ν = 755, 1108, 1247, 1440, 1735, 1863, 2910 cm^{-1}.

^{1}H NMR (600 MHz); δ = 0.25 (s, 3H), 0.31 (s, 3H), 3.17 (dd, *J* = 4.1, 17.2 Hz, 1H), 3.40 (dd, *J* = 10.3, 17.2 Hz, 1H), 3.71 (dd, *J* = 4.1, 10.3 Hz, 1H), 6.89-6.91 (m, 1H), 6.97-7.00 (m, 1H), 7.06-7.09 (m, 1H), 7.28-7.40 (m, 6H), 7.47-7.49 (m, 3H), 7.74-7.76 (m, 2H).

^{13}C NMR (150 MHz); δ = –5.5, –3.6, 31.0, 39.2, 125.8, 126.5, 127.8, 127.9, 128.4, 129.4, 129.6, 132.8, 134.2, 134.6, 140.5, 197.1.

HPLC (Daicel Chiralcel OD-H, ^{n}hexane/ ^{i}PrOH = 98/2, flow rate 0.5 mL/min); t_R = 20.2 min (*S*, minor), t_R = 22.5 min (*R*, major).

HRMS (ESI) calcd for $C_{23}H_{24}ClOSi$ $[M+H]^+$: 379.1280, found 379.1279.

$[\alpha]_D^{20}$ = + 22.8 (*c* = 1.32, $CHCl_3$).

6. (*R*)-3-(Dimethyl(phenyl)silyl)-3-(3-nitrophenyl)-1-phenylpropan-1-one (**1rb**)

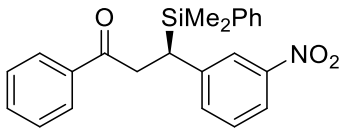

Yellow oil.

IR (neat) ν = 743, 913, 1218, 1364, 1432, 1654, 1718, 1736, 2360, 2969 cm^{-1}.

^{1}H NMR (600 MHz); δ = 0.26 (s, 3H), 0.30 (s, 3H), 3.18 (dd, *J* = 4.1, 11.0 Hz, 1H), 3.25 (dd, *J* = 3.4, 17.2 Hz, 1H), 3.47 (dd, *J* = 10.3, 17.9 Hz, 1H), 7.25-7.41 (m, 9H), 7.50-7.53 (m, 1H), 7.75-7.80 (m, 3H), 7.89-7.94 (m, 1H).

^{13}C NMR (150 MHz); δ = –5.2, –3.8, 31.2, 38.5, 115.2, 124.8, 127.6, 127.7, 128.1, 129.3, 130.2, 130.5, 134.2, 136.9, 142.4, 159.9, 197.9.

HPLC (Daicel Chiralcel OD-H, ^{n}hexane/ ^{i}PrOH = 90/10, flow rate 0.8 mL/min); t_R = 10.4 min (*S*, minor), t_R = 14.6 min (*R*, major).

HRMS (ESI) calcd for $C_{23}H_{24}NO_3Si$ $[M+H]^+$: 390.1520, found 390.1524.

$[\alpha]_D^{20}$ = + 21.1 (*c* = 0.86, $CHCl_3$).

7. (*R*)-3-(2-Chlorophenyl)-3-(dimethyl(phenyl)silyl)-1-(4-fluorophenyl)propan-1-one (**1bb**)

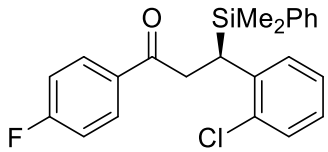

Colorless oil.

IR (neat) ν = 650, 970, 1224, 1264, 1363, 1419, 1715, 2360 cm^{-1}.

^{1}H NMR (600 MHz); δ = 0.26 (s, 3H), 0.31 (s, 3H), 3.17 (dd, *J* = 4.1, 16.5 Hz, 1H), 3.68 (dd, *J* = 4.1, 10.3 Hz, 1H), 4.08 (dd, *J* = 6.9, 14.5 Hz, 1H), 6.89-6.91 (m, 1H), 6.98-7.03 (m, 3H), 7.07-7.10 (m, 1H), 7.29-7.40 (m, 4H), 7.46-7.48 (m, 2H), 7.73-7.76 (m, 2H).

^{13}C NMR (150 MHz); δ = –5.6, –3.6, 26.9, 39.3, 115.4, 115.6, 125.8, 126.5, 127.4, 127.9, 128.3, 128.7, 129.5, 129.6, 130.6, 133.2, 133.8, 134.2, 140.4, 197.1.

HPLC (Daicel Chiralpak AD-H, ^{n}hexane/ ^{i}PrOH = 95/5, flow rate 0.8 mL/min); t_R = 14.6 min (*S*, minor), t_R = 17.9 min (*R*, major).

HRMS (ESI) calcd for $C_{23}H_{23}ClFOSi$ $[M+H]^+$: 397.1185, found 397.1181.

$[\alpha]_D^{20}$ = + 22.7 (*c* = 1.26, $CHCl_3$).

8. (*R*)-3-(Dimethyl(phenyl)silyl)-1-(4-fluorophenyl)-3-(p-tolyl)propan-1-one (**1tb**)

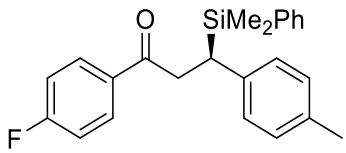

Colorless oil.

IR (neat) ν = 905, 1108, 1247, 1432, 1564, 1698, 1789, 2360 cm^{-1}.

^{1}H NMR (600 MHz); δ = 0.21 (s, 3H), 0.26 (s, 3H), 2.36 (s, 3H), 3.01 (dd, *J* = 4.1, 10.3 Hz, 1H), 3.13 (dd, *J* = 4.1, 17.2 Hz, 1H), 3.35 (dd, *J* = 10.3, 16.5 Hz, 1H), 6.77-6.89 (m, 4H), 7.15-7.17 (m, 2H), 7.31-7.51 (m, 6H), 7.66-7.68 (m, 2H).

^{13}C NMR (150 MHz); δ = –5.2, –4.0, 20.6, 30.3, 39.2, 114.7, 114.9, 127.8, 128.0, 128.8, 129.2, 134.1, 136.4, 143.4, 198.5.

HPLC (Daicel Chiralpak AD-H, ^{n}hexane/ ^{i}PrOH = 90/10, flow rate 0.8 mL/min); t_R = 7.9 min (*S*, minor), t_R = 25.1 min (*R*, major).

HRMS (ESI) calcd for $C_{24}H_{26}FOSi$ $[M+H]^+$: 377.1732, found 377.1736.

$[\alpha]_D^{20}$ = + 15.7 (*c* = 1.96, $CHCl_3$).

9. (*R*)-4-(Dimethyl(phenyl)silyl)-4-phenylbutan-2-one (**1fb**)[4]

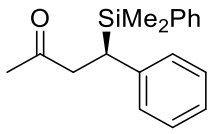

Colorless oil.

^{1}H NMR (600 MHz); δ = 0.19 (s, 3H), 0.22 (s, 3H), 1.92 (s, 3H), 2.62 (m, 1H), 2.84-2.92 (m, 4H), 6.91-6.93 (m, 2H), 7.04-7.09 (m, 1H), 7.15-7.19 (m, 2H), 7.30-7.39 (m, 5H).

^{13}C NMR (150 MHz); δ = –5.4, –4.1, 30.0, 31.4, 43.9, 124.9, 127.5, 127.7, 128.2, 129.3, 134.1, 136.6, 142.0, 208.2.

HPLC (Daicel Chiralcel OD-H, ^{n}hexane/ ^{i}PrOH = 99.9/0.1, flow rate 0.8 mL/min); t_R = 33.6 min (*S*, minor), t_R = 39.2 min (*R*, major).

$[\alpha]_D^{20}$ = + 8.93 (*c* = 0.86, $CHCl_3$).

10. (*R*)-4-(Dimethylphenylsilyl)-4-(4-methoxyphenyl)-2-butan-2-one (**1vb**)[4]

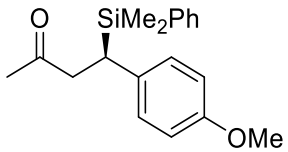

Colorless oil.

^{1}H NMR (600 MHz); δ = 0.21 (s, 3H), 0.23 (s, 3H), 1.94 (s, 3H), 2.57-2.60 (m, 1H), 2.77-2.86 (m, 2H), 3.74 (s, 3H), 6.72 (d, *J* = 8.9 Hz, 2H), 6.82 (d, *J* = 8.9 Hz, 2H), 7.30-7.39 (m, 5H).

^{13}C NMR (150 MHz); δ = –5.4, –4.1, 30.0, 30.4, 44.2, 55.2, 113.6, 127.7, 128.4, 129.3, 133.8, 134.1, 136.7, 157.1, 208.5.

HPLC (Daicel Chiralpak AD-H, ^{n}hexane/ ^{i}PrOH = 98/2, flow rate 0.8 mL/min); t_R = 9.8 min (*S*, minor), t_R = 24.1 min (*R*, major).

$[\alpha]_D^{20}$ = + 5.7 (*c* = 0.60, $CHCl_3$).

11. (*S*)-3-(Dimethyl(phenyl)silyl)-1-phenylbutan-1-one (**1eb**)[5]

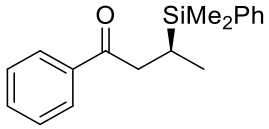

Colorless oil.

^{1}H NMR (600 MHz); δ = 0.32 (s, 3H), 0.34 (s, 3H), 0.98 (d, *J* = 7.2 Hz, 3H), 1.58-1.63 (m, 1H), 2.61 (dd, *J* = 11.0, 15.8 Hz, 1H), 2.96 (dd, *J* = 2.7, 15.8 Hz, 1H), 7.36-7.41 (m, 5H), 7.49-7.53 (m, 3H), 7.80-7.82 (m, 2H).

^{13}C NMR (150 MHz); δ = –5.5, –4.8, 14.5, 15.8, 40.6, 127.8, 128.1, 128.5, 129.1, 132.7, 134.0, 137.1, 137.6, 200.5.

HPLC (Daicel Chiralcel OD-H, ^{n}hexane/ ^{i}PrOH = 99.9/0.1, flow rate 0.8 mL/min); t_R = 21.8 min (*R*, minor), t_R = 27.2 min (*S*, major).

$[\alpha]_D^{20}$ = + 12.4 (*c* = 1.10, $CHCl_3$).

12. (*R*)-3-(Dimethyl(phenyl)silyl)-4,4-dimethyl-1-phenylpentan-1-one (**1gb**)

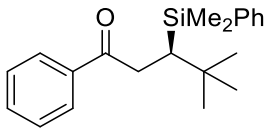

Colorless oil.

IR (neat) ν = 772, 1219, 1551, 1716, 1734, 2414, 2360 cm^{-1}.

^{1}H NMR (600 MHz); δ = 0.30 (s, 3H), 0.37 (s, 3H), 0.88 (s, 9H), 2.09-2.12 (m, 1H), 2.92 (dd, *J* = 5.5, 18.6 Hz, 1H), 3.02 (dd, *J* = 5.5, 18.6 Hz, 1H), 7.26-7.29 (m, 2H), 7.35-7.41 (m, 3H), 7.48-7.54 (m,

3H), 7.81-7.84 (m, 2H).

^{13}C NMR (150 MHz); δ = –1.4, –0.7, 15.0, 30.5, 31.2, 34.2, 65.9, 127.7, 127.8, 128.4, 128.6, 132.7, 134.0, 139.8, 200.3.

HPLC (Daicel Chiralpak AS-H, ^{n}hexane/ ^{i}PrOH = 99.7/0.3, flow rate 0.8 mL/min); t_R = 8.4 min (*R*, major), t_R = 12.0 min (*S*, minor).

HRMS (ESI) calcd for $C_{21}H_{29}OSi$ $[M+H]^+$: 325.1982, found 325.1984.

$[\alpha]_D^{20}$ = + 15.6 (*c* = 1.14, $CHCl_3$).

13. (*R*)-3-(Dimethyl(phenyl)silyl)cyclopentan-1-one (**1ub**)[5]

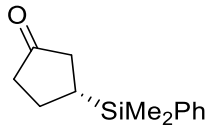

Pale yellow oil.

^{1}H NMR (600 MHz); δ = 0.31 (s, 6H), 1.51-1.56 (m, 1H), 1.62-1.68 (m, 1H), 1.85-1.90 (m, 1H), 2.04-2.12 (m, 2H), 2.17-2.28 (m, 2H), 7.33-7.37 (m, 3H), 7.47-7.50 (m, 2H).

^{13}C NMR (150 MHz); δ = –5.1, –5.0, 23.9, 25.0, 39.3, 40.1, 127.9, 129.3, 133.8, 136.9, 221.0.

HPLC (Daicel Chiralpak AD-H, ^{n}hexane/ ^{i}PrOH = 99/1, flow rate 0.8 mL/min); t_R = 28.3 min (*S*, minor), t_R = 31.7 min (*R*, major).

$[\alpha]_D^{20}$ = + 22.9 (*c* = 1.46, $CHCl_3$).

14. (*R*)-3-(Dimethyl(phenyl)silyl)cyclohexan-1-one (**1hb**)[5]

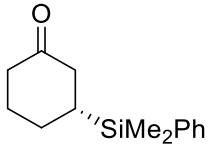

Pale yellow oil.

^{1}H NMR (600 MHz); δ = 0.28 (s, 6H), 1.24-1.29 (m, 1H), 1.36-1.43 (m, 1H), 1.64-1.70 (m, 1H), 1.78-1.80 (m, 1H), 2.05-2.14 (m, 2H), 2.21-2.35 (m, 3H), 7.33-7.37 (m, 3H), 7.44-7.46 (m, 2H).

^{13}C NMR (150 MHz); δ = –5.4, –5.3, 26.0, 27.6, 29.8, 41.9, 42.4, 127.9, 129.3, 133.9, 136.6, 212.7.

HPLC (Daicel Chiralpak AS-3, ^{n}hexane/ ^{i}PrOH = 99.7/0.3, flow rate 0.8 mL/min); t_R = 23.2 min (*R*, major), t_R = 32.0 min (*S*, minor).

$[\alpha]_D^{20}$ = + 15.7 (*c* = 1.48, $CHCl_3$).

15. (*R*)-3-(Dimethyl(phenyl)silyl)-1,3-diphenylbutan-1-one (**1ib**)

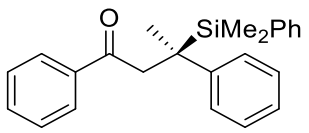

Pale yellow oil.

IR (neat) ν = 832, 910, 1265, 1368, 1545, 1697, 1725, 2235, 2360 cm^{-1}.

^{1}H NMR (600 MHz); δ = 0.22 (s, 3H), 0.28 (s, 3H), 1.58 (s, 3H), 3.15 (d, *J* = 17.2 Hz, 1H), 3.83 (d, *J* = 17.2 Hz, 1H), 6.94-6.96 (m, 2H), 7.02-7.05 (m, 1H), 7.13-7.16 (m, 2H), 7.30-7.39 (m, 7H), 7.47-7.50 (m, 1H), 7.79-7.82 (m, 2H).

^{13}C NMR (150 MHz); δ = –5.8, –5.6, 20.5, 30.0, 43.4, 124.1, 125.9, 127.5, 127.6, 127.7, 128.4, 129.2, 132.6, 134.9, 136.0, 138.1, 145.3, 198.0.

HPLC (Daicel Chiralpak AD-H, ^{n}hexane/ ^{i}PrOH = 99/1, flow rate 0.5 mL/min); t_R = 17.0 min (*S*, minor), t_R = 19.4 min (*R*, major).

HRMS (ESI) calcd for $C_{24}H_{27}OSi$ $[M+H]^+$: 359.1826, found 359.1824.

$[\alpha]_D^{20}$ = +15.8 (*c* = 1.12, $CHCl_3$).

16. Methyl (*R*)-3-(dimethyl(phenyl)silyl)-3-phenylpropanoate (**5ab**)[4]

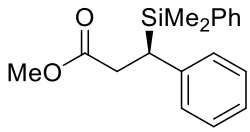

Pale yellow oil.

^{1}H NMR (600 MHz); δ = 0.19 (s, 3H), 0.22 (s, 3H), 2.60-2.64 (m, 1H), 2.70-2.76 (m, 1H), 2.80-2.84 (m, 1H), 3.44 (s, 3H), 6.91-6.93 (m, 2H), 7.06-7.08 (m, 1H), 7.16-7.23 (m, 2H), 7.30-7.39 (m, 5H).

^{13}C NMR (150 MHz); δ = –5.5, –4.1, 32.2, 34.7, 51.5, 125.0, 127.5, 127.7, 128.1, 129.3, 134.1, 136.4, 141.7, 173.4.

HPLC (Daicel Chiralpak AD-H, ^{n}hexane/ ^{i}PrOH = 99.5/0.5, flow rate 0.8 mL/min); t_R = 13.7 min (*S*, minor), t_R = 15.7 min (*R*, major).

$[\alpha]_D^{20}$ = + 6.6 (*c* = 0.68, $CHCl_3$).

17. Ethyl (*R*)-3-(dimethyl(phenyl)silyl)-3-phenylpropanoate (**5bb**)[6]

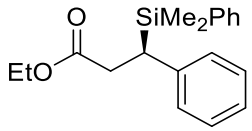

Pale yellow oil.

^{1}H NMR (600 MHz); δ = 0.19 (s, 3H), 0.22 (s, 3H), 1.00-1.03 (m, 3H), 2.58-2.62 (m, 1H), 2.69-2.74 (m, 1H), 2.80-2.84 (m, 1H), 3.84-3.93 (m, 2H), 6.91-6.93 (m, 2H), 7.05-7.08 (m, 1H), 7.15-7.18 (m, 2H), 7.30-7.39 (m, 5H).

^{13}C NMR (150 MHz); δ = –5.5, –4.1, 14.0, 32.3, 34.9, 60.2, 124.9, 127.6, 127.7, 128.0, 129.3, 134.1, 136.5, 141.8, 173.0.

HPLC (Daicel Chiralpak AD-H, ^{n}hexane/ ^{i}PrOH = 99.8/0.2, flow rate 0.8 mL/min); t_R = 8.1 min (*S*, minor), t_R = 11.6 min (*R*, major).

$[\alpha]_D^{20}$ = + 5.7 (*c* = 0.68, $CHCl_3$).

18. Ethyl (R)-3-(dimethyl(phenyl)silyl)-3-(p-tolyl)propanoate (**5fb**)[6]

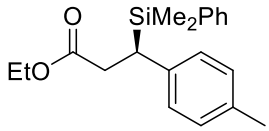

Pale yellow oil.

^{1}H NMR (600 MHz); δ = 0.18 (s, 3H), 0.21 (s, 3H), 1.01-1.04 (m, 3H), 2.25 (s, 3H), 2.55-2.59 (m, 1H), 2.65-2.70 (m, 1H), 2.76-2.79 (m, 1H), 3.85-3.92 (m, 2H), 6.80-6.82 (m, 2H), 6.96-6.98 (m, 2H), 7.30-7.41 (m, 5H).

^{13}C NMR (150 MHz); δ = –5.4, –4.0, 14.2, 21.1, 31.9, 35.1, 60.1, 127.7, 128.0, 128.2, 128.7, 130.3, 134.2, 136.0, 138.7, 140.7, 173.1.

HPLC (Daicel Chiralpak AD-H, ^{n}hexane/ ^{i}PrOH = 99.5/0.5, flow rate 0.8 mL/min); t_R = 8.2 min (*S*, minor), t_R = 10.1 min (*R*, major).

$[\alpha]_D^{20}$ = -5.6 (*c* = 0.64, $CHCl_3$).

19. (*S*)-4-(Dimethyl(phenyl)silyl)dihydrofuran-2(3H)-one (**5gb**)[7]

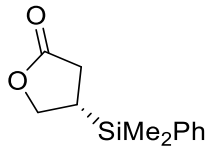

Colorless oil.

^{1}H NMR (600 MHz); δ = 0.33 (t, *J* = 0.75, 6H), 2.01-2.05 (m, 1H), 2.23-2.28 (m, 1H), 2.45 (dd, *J* = 8.8, 17.4 Hz, 1H), 7.35-7.39 (m, 3H), 7.43-7.44 (m, 2H).

^{13}C NMR (150 MHz); δ = –5.1, –4.9, 23.8, 30.3, 70.8, 128.3, 129.9, 133.6, 135.1, 178.0.

HPLC (Daicel Chiralcel OD-H, ^{n}hexane/ ^{i}PrOH = 95/5, flow rate 1.0 mL/min); t_R = 29.6 min (*R*, minor), t_R = 34.3 min (*S*, major).

$[\alpha]_D^{20}$ = + 5.1 (*c* = 1.00, $CHCl_3$).

20. (*R*)-4-(Dimethyl(phenyl)silyl)tetrahydro-2H-pyran-2-one (**5cb**)[8]

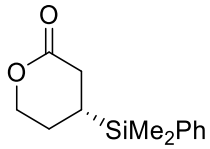

Colorless oil.

^{1}H NMR (600 MHz); δ = 0.32 (d, *J* =1.4, 6H), 1.38-1.40 (m, 1H), 1.58-1.66 (m, 1H), 1.82-1.84 (m, 1H), 2.24-2.29 (m, 1H), 2.53-3.58 (m, 1H), 4.22-4.26 (m, 1H), 4.31-4.34 (m, 1H), 7.37-7.39 (m, 3H), 7.46-7.47 (m, 2H).

^{13}C NMR (150 MHz); δ = –5.73, –5.65, 18.4, 23.7, 30.9, 70.3, 128.1, 129.7, 133.8, 135.5, 171.5.

HPLC (Daicel Chiralcel OD-H, ^{n}hexane/ ^{i}PrOH = 95/5, flow rate 1.0 mL/min); t_R = 29.9 min (*R*, minor), t_R = 34.7 min (*S*, major).

$[\alpha]_D^{20}$ = + 20.6 (*c* = 0.89, $CHCl_3$).

21. (*R*,*E*)-4-(Dimethyl(phenyl)silyl)-6-phenylhex-5-en-2-one (**10bb**)[9]

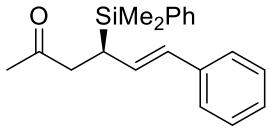

Colorless oil.

^{1}H NMR (600 MHz); δ = 0.32 (d, *J* = 0.8 Hz, 6H), 2.04 (s, 3H), 2.43-2.49 (m, 2H), 2.54-2.56 (m, 1H), 6.02-6.07 (m, 1H), 6.17 (d, *J* = 15.8 Hz, 1H), 7.14-7.17 (m, 1H), 7.23-7.27 (m, 5H), 7.34-7.38

(m, 3H), 7.47-7.48 (m, 2H).

^{13}C NMR (150 MHz); δ = –5.2, –4.4, 29.1, 29.8, 125.7, 126.6, 127.9, 128.3, 128.4, 129.4, 130.4, 134.0, 136.5, 137.8, 208.5.

HPLC (Daicel Chiralcel OD-H, ^{n}hexane/ ^{i}PrOH = 99/1, flow rate 1.0 mL/min); t_R = 11.0 min (*S*, minor), t_R = 12.9 min (*R*, major).

$[\alpha]_D^{20}$ = + 16.0 (*c* = 1.01, $CHCl_3$).

22. (*R*,*E*)-3-(Dimethyl(phenyl)silyl)-1,5-diphenylpent-4-en-1-one (**10ab**)[10]

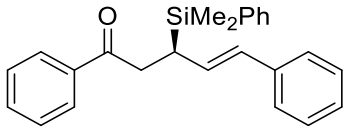

Colorless oil.

^{1}H NMR (600 MHz); δ = 0.39 (d, *J* = 1.4 Hz, 3H), 0.40 (d, *J* = 1.3 Hz, 3H), 2.68-2.69 (m, 1H), 3.07-3.12 (m, 2H), 6.14-6.21 (m, 2H), 7.16-7.17 (m, 1H), 7.22-7.27 (m, 4H), 7.40-7.44 (m, 5H), 7.52-7.57 (m, 3H), 7.82-7.83 (m, 2H).

^{13}C NMR (150 MHz); δ = –5.1, –4.2, 29.1, 38.1, 125.7, 126.5, 127.9, 128.0, 128.3, 128.4, 128.5, 129.4, 130.6, 132.8, 134.1, 136.7, 137.0, 138.0, 199.5.

HPLC (Daicel Chiralcel OD-H, ^{n}hexane/ ^{i}PrOH = 95/5, flow rate 1.0 mL/min); t_R = 5.5 min (*S*, minor), t_R = 6.1 min (*R*, major).

$[\alpha]_D^{20}$ = -15.3 (*c* = 0.95, $CHCl_3$).

23. (*R*)-3-(Dimethyl(phenyl)silyl)-3-phenylpropanenitrile (**6ab**)[5]

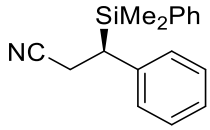

Pale yellow oil.

^{1}H NMR (600 MHz); δ = 0.26 (s, 3H), 0.27 (s, 3H), 2.56-2.67 (m, 3H), 6.92-6.95 (m, 2H), 7.14-7.17 (m, 1H), 7.23-7.26 (m, 2H), 7.33-7.41 (m, 5H).

^{13}C NMR (150 MHz); δ = –5.6, –4.0, 18.8, 33.0, 119.7, 126.0, 127.4, 128.1, 128.6, 129.9, 134.0, 135.2, 139.7.

HPLC (Daicel Chiralcel OJ-H, ^{n}hexane/ ^{i}PrOH = 95/5, flow rate 0.8 mL/min); t_R = 21.7 min (*S*, minor), t_R = 28.1 min (*R*, major).

$[\alpha]_D^{20}$ = -11.4 (*c* = 1.04, $CHCl_3$).

24. (*R*)-3-(Dimethyl(phenyl)silyl)-3-(4-methoxyphenyl)propanenitrile (**6cb**)

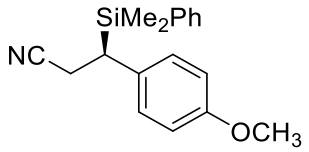

Colorless oil.

IR (neat) ν = 1224, 1265, 1421, 2253, 2986 cm^{-1}.

^{1}H NMR (600 MHz); δ = 0.25 (d, *J* = 2.7 Hz, 6H), 2.50-2.60 (m, 3H), 3.77 (s, 3H), 6.78-6.86 (m, 4H), 7.34-7.39 (m, 5H).

^{13}C NMR (150 MHz); δ = –5.5, –4.0, 19.2, 32.0, 55.2, 114.0, 119.7, 128.0, 128.4, 129.8, 131.6, 134.0, 135.4, 157.8.

HPLC (Daicel Chiralpak AS-H, ^{n}hexane/ ^{i}PrOH = 95/5, flow rate 1.0 mL/min); t_R = 22.3 min (*R*, major), t_R = 34.4 min (*S*, minor).

HRMS (ESI) calcd for $C_{18}H_{22}NOSi$ $[M+H]^+$ 296.1465, found 296.1464.

$[\alpha]_D^{20}$ = -17.2 (*c* = 0.98, $CHCl_3$).

25. (*R*)-3-(Dimethyl(phenyl)silyl)-3-(4-fluorophenyl)propanenitrile (**6bb**)

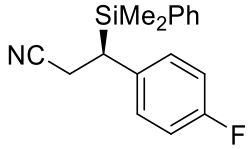

Colorless oil.

IR (neat) ν = 1217, 1364, 1436, 2252, 2968 cm^{-1}.

^{1}H NMR (600 MHz); δ = 0.27 (d, *J* = 3.4 Hz, 6H), 2.56-2.63 (m, 3H), 6.87-6.96 (m, 4H), 7.35-7.40 (m, 5H).

^{13}C NMR (150 MHz); δ = –5.5, –4.2, 19.1, 32.3, 115.4 (d), 119.4, 128.1, 128.7 (d), 130.0, 134.0, 134.8, 135.3, 162.1.

HPLC (Daicel Chiralpak AS-H, ^{n}hexane/ ^{i}PrOH = 9/1, flow rate 1.0 mL/min); t_R = 12.2 min (*R*, major),

t_R = 13.4 min (*S*, minor).

HRMS (ESI) calcd for $C_{17}H_{19}FNSi$ $[M+H]^+$ 284.1265, found 284.1269.

$[\alpha]_D^{20}$ = -15.0 (*c* = 1.03, $CHCl_3$).

26. (*R*)-3-(Dimethyl(phenyl)silyl)-3-(furan-2-yl)propanenitrile (**6db**)

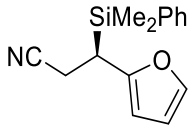

Colorless oil.

IR (neat) ν = 1217, 1228, 1363, 2327, 2969 cm^{-1}.

^1H NMR (600 MHz); δ = 0.32 (s, 3H), 0.36 (s, 3H), 2.50-2.60 (m, 2H), 2.69 (dd, *J* = 4.8, 10.6 Hz, 1H), 5.99 (d, *J* = 3.1 Hz, 1H), 6.30-6.31 (m, 1H), 7.31-7.44 (m, 6H).

^{13}C NMR (150 MHz); δ = –5.2, –3.9, 17.7, 26.5, 105.7, 110.6, 119.3, 128.1, 129.9, 133.8, 135.1, 141.3, 153.5.

HPLC (Daicel Chiralpak AS-H, ^{n}hexane/ ^{i}PrOH = 90/10, flow rate 1.0 mL/min); t_R = 8.7 min (*R*, major), t_R = 12.0 min (*S*, minor).

HRMS (ESI) calcd for $C_{15}H_{18}NOSi$ $[M+H]^+$ 256.1152, found 256.1155.

$[\alpha]_D^{20}$ = -22.8 (*c* = 0.86, $CHCl_3$).

27. (*S*)-3-(Dimethyl(phenyl)silyl)butanenitrile (**6eb**)

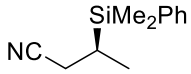

Colorless oil.

IR (neat) ν = 1221, 1363, 2926, 2969 cm^{-1}.

^1H NMR (600 MHz); δ = 0.32 (s, 6H), 1.13 (d, *J* = 7.3 Hz, 3H), 1.22-1.25 (m, 1H), 2.03 (dd, *J* = 10.3, 16.9 Hz, 1H), 2.35 (dd, *J* = 4.3, 16.9 Hz, 1H), 7.35-7.39 (m, 3H), 7.45-7.46 (m, 2H).

^{13}C NMR (150 MHz); δ = –5.7, –5.0, 14.5, 17.3, 20.4, 119.8, 128.1, 129.6, 133.8, 135.9.

HPLC (Daicel Chiralpak AS-H, ^{n}hexane/ ^{i}PrOH = 95/5, flow rate 1.0 mL/min); t_R = 8.7 min (*S*, major), t_R = 9.5 min (*R*, minor).

HRMS (ESI) calcd for $C_{12}H_{18}NSi$ $[M+H]^+$ 204.1203, found 204.1200.

$[\alpha]_D^{20}$ = + 5.6 (*c* = 0.98, $CHCl_3$).

28. (*S*)-Dimethyl(2-nitro-1-phenylethyl)(phenyl)silane (**8ab**)

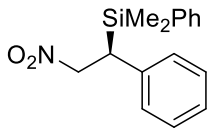

Yellow oil.

IR (neat) ν = 720, 1217, 1364, 1556, 1715, 1737, 2340, 2360 cm^{-1}.

^{1}H NMR (600 MHz); δ = 0.28 (s, 3H), 0.30 (s, 3H), 3.24-3.38 (m, 1H), 4.48-4.52 (m, 1H), 4.79-4.84 (m, 1H), 6.97-6.99 (m, 2H), 7.14-7.17 (m, 1H), 7.22-7.26 (m, 2H), 7.37-7.45 (m, 5H).

^{13}C NMR (150 MHz); δ = –5.5, –4.0, 36.1, 126.1, 127.3, 128.2, 128.6, 130.0, 133.9, 134.8, 137.5.

HPLC (Daicel Chiralcel OJ-H, ^{n}hexane/ ^{i}PrOH = 90/10, flow rate 0.8 mL/min); t_R = 14.9 min (*R*, minor), t_R = 18.4 min (*S*, major).

HRMS (ESI) calcd for $C_{16}H_{20}NO_2Si$ $[M+H]^+$: 286.1258; found 286.1256.

$[\alpha]_D^{20}$ = +6.3 (*c* = 0.86, $CHCl_3$).

The absolute configuration was determined by converting the -$SiMe_2Ph$ group to -OH group, using Fleming-Tamao oxidation reported by the literature.[11] The oxidation was carried out similar to the procedure descried for the conversion of **8ad** below.

(*S*)-2-Nitro-1-phenylethan-1-ol (**8ad**)[12]

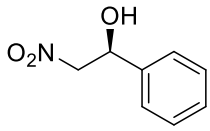

Colorless oil.

^{1}H NMR (600 MHz); δ = 4.48-4.51 (m, 1H), 4.56-4.60 (m, 1H), 5.40-5.46 (dd, *J* = 3.5, 6.9 Hz, 1H), 7.33-7.39 (m, 5H).

^{13}C NMR (150 MHz); δ = 71.0, 81.2, 125.9, 129.0, 138.3.

HPLC (Daicel Chiralcel OD-H, ^{n}hexane/ ^{i}PrOH = 95/5, flow rate 0.5 mL/min); t_R = 17.6 min (*R*, minor), t_R = 20.1 min (*S*, major).

$[\alpha]_D^{20}$ = +8.7 (*c* = 0.6, $CHCl_3$).

29. (*S*)-Dimethyl(2-nitro-1-(p-tolyl)ethyl)(phenyl)silane (**8bb**)

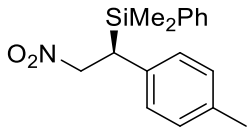

Yellow oil.

IR (neat) ν = 733, 910, 1224, 1363, 1418, 1556, 1714, 2253, 2360 cm^{-1}.

^{1}H NMR (600 MHz); δ = 0.26 (s, 3H), 0.28 (s, 3H), 2.28 (s, 3H), 3.19-3.22 (m, 1H), 4.45-4.48 (m, 1H), 4.74-4.80 (m, 1H), 6.84-6.86 (m, 2H), 7.02-7.04 (m, 2H), 7.35-7.42 (m, 5H).

^{13}C NMR (150 MHz); δ = –5.5, –3.9, 20.9, 35.6, 126.1, 127.2, 128.2, 129.3, 130.0, 133.9, 135.8.

HPLC (Daicel Chiralpak AD-H & Chiralcel OJ-H, ^{n}hexane/ ^{i}PrOH = 99/1, flow rate 0.8 mL/min); t_R = 10.2 min (*R*, minor), t_R = 18.6 min (*S*, major).

HRMS (ESI) calcd for $C_{17}H_{22}NO_2Si$ $[M+H]^+$: 300.1415, found 300.1415.

$[\alpha]_D^{20}$ = +5.8 (*c* = 1.14, $CHCl_3$).

30. (*S*)-(1-(4-Fluorophenyl)-2-nitroethyl)dimethyl(phenyl)silane (**8cb**)

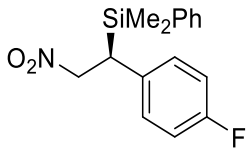

Yellow oil.

IR (neat) = 909, 1121, 1161, 1366, 1466, 2253, 2975, 3398 cm^{-1}.

^{1}H NMR (600 MHz); δ = 0.28 (d, *J* = 0.9 Hz, 6H), 3.20 (dd, *J* = 3.8, 13.4 Hz, 1H), 4.48 (dd, *J* = 3.8, 13.6 Hz, 1H), 4.73 (t, *J* = 13.4 Hz, 1H), 6.89-6.93 (m, 4H), 7.36-7.42 (m, 5H).

^{13}C NMR (150 MHz); δ = –5.4, –4.1, 35.5, 115.4, 115.6, 128.2, 128.6, 128.7, 130.1, 133.9, 134.5.

HPLC (Daicel Chiralpak AD-H & Chiralcel OJ-H, ^{n}hexane/*i*PrOH = 99/1, flow rate 0.8 mL/min); t_R = 18.1 min (*R*, minor), t_R = 20.6 min (*S*, major).

HRMS (ESI) calcd for $C_{16}H_{19}FNO_2Si$ $[M+H]^+$: 304.1164; found 304.1163. $[\alpha]_D^{20}$ = +7.9 (*c* = 1.0, $CHCl_3$).

31. (*S*)-(1-(Furan-3-yl)-2-nitroethyl)dimethyl(phenyl)silane (**8db**)

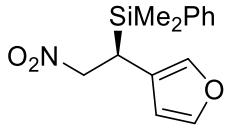

Yellow oil.

IR (neat) ν = 919, 1373, 1459, 1711, 2259, 2975, 3470 cm^{-1}.

^{1}H NMR (600 MHz); δ = 0.32 (d, *J* = 6.3 Hz, 6H), 3.11 (dd, *J* = 3.8, 13.1 Hz, 1H), 4.40 (dd, *J* = 3.7, 13.0 Hz, 1H), 4.52 (t, *J* = 13.1 Hz, 1H), 6.07 (s, 1H), 7.10 (s, 1H), 7.30 (t, *J* = 1.6 Hz, 1H), 7.36-7.44 (m, 5H).

^{13}C NMR (150 MHz); δ = –5.3, –4.1, 26.0, 77.3, 109.9, 121.0, 128.2, 130.1, 133.8, 134.8, 138.7, 143.1.

HPLC (Daicel Chiralpak AD-H & Chiralcel OJ-H, ^{n}hexane/^{i}PrOH = 99/1, flow rate 0.8 mL/min); t_R = 20.1 min (*R*, minor), t_R = 23.9 min (*S*, major).

HRMS (ESI) calcd for $C_{14}H_{18}NO_3Si$ $[M+H]^+$: 276.1050, found 276.1044.

$[\alpha]_D^{20}$ = +5.1 (*c* = 0.6, $CHCl_3$).

32. (*R*)-3-(2-(Dimethyl(phenyl)silyl)-2-phenylethyl)cyclopent-2-en-1-one (**11sz**)

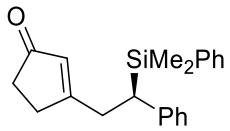

Colorless oil

IR (neat) ν = 738, 1121, 1247, 1373, 1611, 1697, 2259, 2855, 2948 cm^{-1}.

^{1}H NMR (600 MHz); δ = 0.20 (s, 3H), 0.27 (s, 3H), 2.18 (t, *J* = 4.6 Hz, 2H), 2.27-2.31 (m, 2H), 2.55 (dd, *J* = 3.5, 12.4 Hz, 1H), 2.66 (d, *J* = 16.4 Hz, 1H), 2.86 (dd, *J* = 12.5, 16.4 Hz, 1H), 5.73 (s, 1H), 6.88 (d, *J* = 7.6 Hz, 2H), 7.04-7.08 (m, 1H), 7.16 (t, *J* = 7.6 Hz, 2H), 7.33-7.40 (m, 5H).

^{13}C NMR (150 MHz); δ = –5.7, –4.0, 31.3, 33.2, 34.5, 35.2, 125.1, 127.5, 127.8, 129.4, 130.6, 134.1, 136.5, 141.2, 182.5, 210.0.

HPLC (Daicel Chiralcel OD-H, ^{n}hexane/ ^{i}PrOH = 95/5, flow rate 1.0 mL/min); t_R = 11.9 min (*S*, minor), t_R = 16.4 min (*R*, major).

HRMS (ESI) calcd for $C_{21}H_{25}OSi$ $[M+H]^+$: 321.1669; found 321.1675.

$[\alpha]_D^{20}$ = +15.3 (*c* = 0.84, $CHCl_3$).

33. (*R*)-3-(2-(Dimethyl(phenyl)silyl)-2-phenylethyl)cyclohex-2-en-1-one (**11az**)

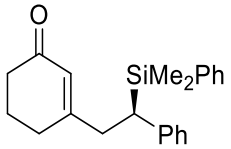

Colorless oil.

IR (neat) ν = 1223, 1265, 1363, 1713, 2987, 3055 cm^{-1}.

^{1}H NMR (600 MHz); δ = 0.17 (s, 3H), 0.26 (s, 3H), 1.72-1.76 (m, 2H), 1.99-2.14 (m, 4H), 2.49-2.63 (m, 3H), 5.69 (s, 1H), 6.87 (d, *J* = 7.9 Hz, 2H), 7.04-7.07 (m, 1H), 7.15 (t, *J* = 7.6 Hz, 2H), 7.31-7.40 (m, 5H).

^{13}C NMR (150 MHz); δ = –5.7, –3.9, 22.5, 29.4, 34.3, 37.2, 37.9, 125.0, 126.9, 127.7, 127.8, 128.2, 129.3, 134.1, 136.8, 141.2, 165.8, 199.8.

HPLC (Daicel Chiralcel OD-H, ^{n}hexane/ ^{i}PrOH = 95/5, flow rate 1.0 mL/min); t_R = 14.8 min (*S*, minor), t_R = 15.9 min (*R*, major).

HRMS (ESI) calcd for $C_{22}H_{26}NaOSi$ $[M+Na]^+$ 357.1651, found 357.1648.

$[\alpha]_D^{20}$ = +25.6 (*c* = 1.10, $CHCl_3$).

The -$SiMe_2Ph$ group was converted into -OH group by Fleming-Tamao oxidation following the literature method.[5] To a solution of (*R*)-3-(2-(dimethyl(phenyl)silyl)- 2-phenylethyl)cyclohex-2-en-1-one (100.4 mg, 0.3 mmol) in MeOH (2 mL), TFA (0.12 mL, 1.5 mmol) and KHF_2 (47.0 mg, 0.6 mmol) were added successively. The reaction mixture was then stirred at room temperature for 12 h. After removal of volatile materials, the residue was dissolved in MeOH/H_2O (v/v 1:1, total 12 mL). To the resultant solution was added 30% H_2O_2 (0.6 mL, 6 mmol), $KHCO_3$ (150 mg, 1.5 mmol). After completion of the reaction within 6 h, the reaction solution was extracted by dichloromethane (20 mL) three times. The combined organic phase was dried over anhydrous $MgSO_4$ and filtered. After concentrated under reduced pressure, the mixture was purified by PTLC to give the corresponding alcohol (48.7 mg, 85% yield) as colorless oil:

(*R*)-3-(2-Hydroxy-2-phenylethyl)cyclohex-2-enone (**11ayd**)[13]

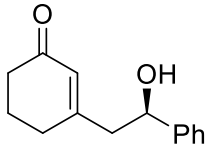

^{1}H NMR (600 MHz); δ = 1.82-1.86 (m, 2H), 2.17- 2.22 (m, 4H), 2.44 (dd, *J* = 5.8, 17.2 Hz, 1H), 2.54 (dd, *J* = 10.5, 17.2 Hz, 1H), 2.88 (br, 1H), 4.77-4.80 (m, 1H), 5.81 (s, 1H), 7.18-7.28 (m, 5H).

^{13}C NMR (150 MHz); δ = 22.5, 30.0, 37.0, 47.6, 72.3, 125.6, 127.7, 127.8, 128.5, 143.7, 163.0, 200.0.

HPLC (Daicel Chiralcel OD-H, ^{n}hexane/ ^{i}PrOH = 90/10, flow rate 1.0 mL/min); t_R = 30.7 min (*S*, minor), t_R = 36.6 min (*R*, major).

$[\alpha]_D^{20}$ = + 35.6 (*c* = 1.00, $CHCl_3$).

1.2-4 Filtration experiment an recovery & reuse of catalyst

I. Filtration experiment

Chiral Cu(II) complex was prepared as an acicular crystal as mentioned above. After chiral Cu(II) complex crystal (8.8 mg, 5 mol%) was dispersed into water (2 mL), chalcone **1a** (62.5 mg, 0.3 mmol) and $PhMe_2Si$-B(pin) (94.4 mg, 0.36 mmol) were added. After vigorous stirring for 24 h following the general experimental procedure, the resultant solution was directly filtered through 0.2 μm PTFE membrane filter (Whatman™ cat. No. 6784-2502) to remove the solid substances. After transferred to test tube, solution was heated at 140 °C to remove solvent and 1 mL of sulfonic acid was then added. When temperature was raised to 200 °C, nitric acid was added dropwise until the mixture to be transparent. After removal of all nitric acid, the solution was allowed to cool down to room temperature. The resulting solution was diluted to 50 mL with pure water using a volumetric flask to prepare ICP sample. The Cu content in the filtrate was thus determined to be less than the detection limit of the ICP equipment (1.4 ppb), which affirms the heterogeneous nature of catalyst.

II. Recovery & reuse of catalyst

After chiral Cu(II) complex crystal (8.8 mg, 5 mol%) was dispersed into water (2 mL), cyclopentenone **1u** (24.6 mg, 0.3 mmol) and $PhMe_2Si$-B(pin) (94.4 mg, 0.36 mmol) were added in a centrifuge tube. After vigorous stirring for 24 h, the reaction mixture was centrifuged (3000 rpm, 10 min) to give three phases composed of both organic and water phase and solid material. The organic phase was removed and purified by preparative TLC (^{n}hexane/^{i}PrOH = 6/1) to afford the desired product **1ub** (59.6 mg, 91% yield) as pale yellow oil with 87% ee. After dispersion of separated solid material in water (2 mL), cyclopentenone (24.6 mg, 0.3 mmol) and $PhMe_2Si$-B(pin) (94.4 mg, 0.36 mmol) were added successively in the second run. After vigorous stirring for 24 h, the reaction mixture was centrifuged (3000 rpm, 10 min) again. The organic phase was removed and purified by preparative TLC (^{n}hexane/^{i}PrOH = 6/1) to afford the desired product **1ub** (52.4 mg, 80% yield) with 82% ee.

1.2-5 Reference

1. Welle, A.; Petrignet, J.; Tinant, B.; Wouters, J.; Riant, O. *Chem. Eur. J.* **2010**, *16*, 10980-10983.
2. Matsumoto, Y.; Hayashi, T.; Ito, Y. *Tetrahedron* **1994**, *50*, 335-346.
3. Kacprzynski, M. A.; Kazane, S. A.; May, T. L.; Hoveyda, A. H. *Org. Lett.* **2007**, *9,* 3187-3190.
4. Lee, K.-S.; Hoveyda, A. M. *J. Am. Chem. Soc.* **2010**, *132*, 2898-2900.
5. Walter, C.; Oestreich, M. *Angew. Chem. Int. Ed.* **2008**, *47*, 3818-3820.
6. Harb, H. Y.; Collins, K. D.; Garcia Altur, J. V.; Bowker, S.; Campbell, L.; Procter, D. J. *Org. Lett.* **2010**, *12*, 5446-5449.
7. O'Brien, J. M.; Hoveyda, A. H. *J. Am. Chem. Soc.* **2011**, *133*, 7712-7715.
8. Lee, K.-S.; Wu, H.; Haeffner, F.; Hoveyda, A. H. *Organometallics* **2012**, *31*, 7823-7826.
9. Shintani, R.; Ichikawa, Y.; Takatsu, K.; Chen, F-X.; Hayashi, T. *J. Org. Chem*. **2009**, *74*, 869-873.
10. Tamao, K.; Ishida, N. *J. Organomet. Chem*. **1984**, *269*, c37-c39.

11. Lai, G. Y.; Wang, S. J.; Wang, Z. Y. *Tetrahedron: Asymmetry* **2008**, *19*, 1813-1819.

12. Kitanosono, T.; Xu, P.; Kobayashi, S. *Chem. Asian J.* **2014**, *9*, 179-188.

Chapter 2: Lewis Acid –Single-Walled Carbon Nanotube Integrated Catalysts

5年以内に雑誌等で刊行予定のため非公開

Chapter 3: Development of New Light-Induced Catalysts and Their Application Toward Hydration Reactions in Water

5年以内に雑誌等で刊行予定のため非公開

Acknowledgement

First and foremost I would like to express sincere and deepest sense of gratitude to my surpervisor Prof. Shū Kobayashi. His overflowing eagerness for being pathfinder, excellent guidance, caring, patience, cultivated and inspired me toward cutting-edge research.

I would like to show my sincere thanks to special assistant professor Dr. Taku Kitanosono. I am very grateful for your edifying instruction, animated discussion, ample patience, and immense supports on my research.

I also want to express my appreciation to Prof. Eiichi Nakamura and Dr. Koji Harano (Department of Chemistry, School of Science, The University of Tokyo) for DLS measurements, to Prof. Shigeo Maruyama and Dr. Shohei Chiashi (Department of Mechanical Engineering, Faculty of Engineering, The University of Tokyo) for Raman analysis and to Mr. Noriaki Kuramitsu for electron microscopic analysis.

I would also like to thank Dr. Masaharu Ueno from Faculty of Science and Technology, Tokushima University, our associate professor Dr. Yasuhiro Yamashita, special associate professor Dr. Haruro Ishitani, assistant professor Dr. Hiroyuki Miyamura, special assistant professor Dr. Woo-jin Yoo, and special assistant professor Dr. Tomohiro Yasukawa, for their exceptional efforts to ensure that my fundamental techniques are flawless, teaching me how to understand, embrace and even implement alternative approaches to answering chemical problems.

To my friends and colleagues, I would like to say thank you for the vital role you have played in my graduate career. I am especially thankful to Mr. Miyo and Ms. Cho for your patience and supports. I would also thanks my friends and colleagues; Mr. Shimizu, Mr. Choo, Mr, Harada, Ms. Sonoyama, and Ms. Okumura for your supports, patience, and discussions.

Finally, I would prefer to pay homage by dedicating my dissertation to my family under whose careful protection and warm encouragement I have been able to enjoy my life.

2017 Pengyu Xu

謝辞

本研究を遂行し、またこの論文を執筆するのにあたり、終始にわたり溢れんばかりの熱意と薫陶を以てご指導、ご鞭撻を賜りました東京大学大学院理学系研究科化学専攻有機合成化学研究室小林修教授に心より感謝申し上げます。

また本研究期間中、直接のご指導並びに数多くの有益な御助言をいただきました特任助教北之園拓博士に深く感謝申し上げます。

本研究を進めるにあたり，DLS 測定を理学系研究科化学専攻元物理有機化学研究室設置の装置を利用しました。中村栄一教授及び准教授・原野幸治博士に深く感謝致します。ラマン分光装置は、工学系研究科機械工学専攻丸山・千足研究室設置の装置を利用しました。丸山茂夫教授及び准教授・千足昇平博士に深く感謝致します。

研究において、実験の手法から論文の執筆に関することまで、あらゆる面でご助言を賜りました徳島大学大学院理工学研究部自然科学系講師・上野雅晴博士、東京大学理学系研究科化学専攻有機合成化学研究室准教授・山下恭弘博士、助教・宮村浩之博士、特任准教授・石谷暖郎博士、特任助教・Yoo　Woo-Jin 博士および安川知宏博士に深く感謝致します。

また、同室に所属し、実験に際して多大な配慮をいただきました三代真澄氏（本学修士課程２年）、Cho Soo-Min 氏（本学修士課程１年）、またその他有機合成化学研究室所属の皆様に深く感謝致します。

研究期間中は、同じ研究室に所属する清水翔太氏、園山亜里紗氏、奥村美樹子氏、Gerald Choo 氏、原田真志氏をはじめ多くの友人の存在に支えられました。ここに深く感謝致します。

最後に、このような研究の機会を与えてくださった家族に、深く感謝致します。

２０１７年
徐　鵬宇